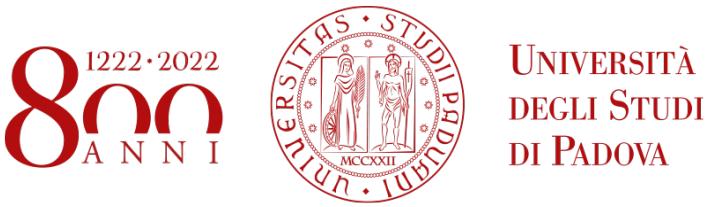

Università degli Studi di Padova

Dipartimento di Ingegneria Industriale DII

Corso di Laurea Magistrale in
Ingegneria dell'Energia Elettrica

Validation of Kalman Filter method for vertical position and speed estimation in the TCV tokamak

Relatore:
Prof. Paolo Bettini

Laureando:
Luca Claude Gino Lebon
1234285

Correlatore:
Prof. Federico Felici (SPC)

Anno Accademico 2021/2022

Dedicato a mia mamma e a mio papà.
E a chi ha creduto in me.

Thesis carried at *Swiss Plasma Center* of *EPFL*, Lausanne, Switzerland

Acknowledgements

Je tiens tout d'abord à remercier le Prof. Paolo Bettini de m'avoir mis en contact avec le team du SPC et d'avoir rendu possible cette expérience extraordinaire. Un merci spécial au Prof. Federico Felici pour sa disponibilité, sa compétence et pour m'avoir initié à l'art de la patience et de la précision. Un grand merci au PhD Stefano Marchioni pour ses précieux conseils et pour le temps qu'il m'a dédié. Enfin, je tiens à remercier Eric Burtschell pour m'avoir accueilli les bras ouverts chez lui parmi sa merveilleuse famille.

Abstract

The main task of this project has been to validate the Kalman filter method in different shots of the **TCV** tokamak, in order to estimate in real-time the position and speed of the plasma. The plasma position and velocity can be retreived from the estimated state of the system. The Kalman filter is a powerful tool for estimation and control goals, since it deals with linear systems which are computationally fast to solve. This permits to estimate plasma quantities in real-time during a plasma shot and fastly recover a control law for plasma stabilization and shape. Indeed, since the Kalman filter is the optimal linear predictor, it can be coupled with a LQR for LQG control. Moreover, it can properly filter noises of the system, once the covariance matrices are properly tuned. The state-space system we deal with derives from a linearization around a plasma-equilibrium point of a non-linear *Forward Evolutive Grad-Shafranov* solver called FGE. In order to properly estimate the desired quantities, particular attention has been put in covariance matrices tuning, to best recover the mismatches due to linearization and the unexpected additional perturbations in the model, which have been modelled as additional noises in the state equation. The Kalman filter design has been firstly performed on an artificial tokamak called **Anamak** and at the end, once the filter behaviour has been validated, it has been used for estimation purposes on **TCV** shots.

In the first Chapter, which gives an introduction of the physics of the problem and of the equilibrium codes used for **TCV**, the *Grad-Shafranov* equation has been derived. It has been introduced the plasma current discretization by means of polynomial basis functions, the *Green* functions mapping for active and vessel currents and their filamentary discretization. An eigenmodes formulation for the vessel currents has been presented too. Then, a description of the linear link between measured quantities (B_m, Ψ_f, I_a) and external currents has been described. After having written down the circuit equation, the main equilibrium codes have been presented. The FGS algorithm and its evolutive extention FGE have been discussed. Finally, defining the external currents as the state, the linearization of FGE around an equilibrium point in the state-space has been performed. Coupling this process equation with the measurement linearization (both in relative or physical frame) the state-space representation has been reached. The Chapter has finished with a qualitative comment around observability and controllability properties of the system.
In the second Chapter the Kalman filter algorithm has been presented. Futhermore, a state-augmented filter has been developed. Finally, a complete description of the covariance matrices design used during the simulations has been provided.
In the third Chapter three statistical tests to be performed onto the innovation residuals have been presented. These rejection tests give a formal instrument in order to check faults in the Kalman filter stochastical behaviour in terms of covariance matrices or in terms of the stochastical hypothesis onto the process or observer noises.

In the fourth Chapter the open-loop results on **Anamak** have been presented. Firstly, using the statistical tests after the imposition of known noises, the performances in the cases of correct, underestimated and oversitimated process covariance matrices, with data retrieved from a linearized FGE run, have been compared. Thus, a comparison in terms of estimated quantities has been set between the case in which measurement data are taken from a run of FGE or from a linearized FGE run. Therefore, a covariance matrix improvement has been developed in order to match the non-linearities of the system. Moreover, using an augmented state filter with data from FGE, an unknown sinusoidal and step perturbation on the first PF coil voltage have been recovered by the filter. Finally, the β_p and the q_A parameters have been estimated after unknowns β_p-ramp and q_A-ramp profiles impositions in the case of contraints state augmentation.
In the last Chapter, the previous simulations have been extended to several **TCV** shots. The plasma position and speed evolutions have been estimated for all these shots and a vertical error analysis has been performed in order to demonstrate the accuracy of the method. Moreover, the open-loop performances of the Kalman Filter observer have been compared to the existing estimates from MGA observer, based on a linear combination of measurements. The control voltages to vertical position transfer functions have been shown and discussed demonstrating that the Kalman filter has a robust phase margin and it is a better alternative to the previous observer also from the frequency point of view.

Contents

Chapter 1

Control oriented modelling of tokamaks

The physical description of the plasma which has been adopted in this work is summarized in this section. It is also shown the link between the control coils, the vessel and the plasma itself by means of *Green functions* and the model discretization for the coils and the vessel filaments. The final model that will be derived will account for the force balance equation given by the *Grad-Shafranov* equation and for the circuit equation linking all the currents of the system. For more details we refer to [2], [4], [5], [17].

1.1 Derivation of Grad-Shafranov equation

Magnetic-fusion plasmas are complex self-organized systems with an extremely wide range of spatial and temporal scales, from the electron-orbit scales ($\sim 10^{-11}\,s$, $\sim 10^{-5}\,m$) to the diffusion time of electrical current through the plasma ($\sim 10^{2}\,s$) and the distance along the magnetic field between two solid surfaces in the region that determines the plasma-wall interactions ($\sim 10^{2}\,m$) [2]. The most straightforward way for describing plasmas would be the microscopic particle approach: solving the equations of motion for the many individual particles (both electrons and ions) that form the plasma in externally imposed electromagnetic fields and in the fields generated by the particles. However, this is computationally impossible to apply to realistic magnetic-fusion plasmas, which typically contain $10^{22}-10^{23}$ particles. The second formalism to describe plasma is the so-called kinetic description. It describes the plasma with a probability density function in the *phase space*[1]. It gives a precise description of the plasma, allowing to describe many nonlinear phenomena and it is programmable using methods such as particle in cell (PIC) hence very promising in the field of theoretical computational physics [2]. Finally, the last approach is the so-called magnetohydrodynamics (MHD) description[2]. It is a fluid description of the plasma combined with the the electromagnetic field evolution. As a fluid description, it also can be obtained from the kinetic description looking at the first moments of the probability function distribution.

[1] In *Hamiltonian Mechanics* it consists of all possible values of position and momentum (q, p).

[2] The time scales of the MHD model are in the order of the *resistive time scale* [2].

Definition 1. *(**Mass bulk fluid velocity**) Given the ion mass bulk velocity* $\mathbf{u_i}$ *and the electron mass bulk velocity* $\mathbf{u_e}$*, i.e.,*

$$\mathbf{u_i} = \frac{1}{N_i}\sum_k \mathbf{u_{ik}}$$
$$\mathbf{u_e} = \frac{1}{N_e}\sum_k \mathbf{u_{ek}}$$

where N_i *and* N_e *are the number of particles of species* i *and* e *in the volume of plasma taken into consideration, we define mass bulk fluid velocity as the quantity*

$$\mathbf{u} = \frac{m_e\, n_e\, \mathbf{u_e} + m_i\, n_i\, \mathbf{u_i}}{m_e\, n_e + m_i\, n_i}$$

where n_k *and* m_k*,* $k = i, e$ *are the number of particles per unit volume and the mass of the species respectively.*

Since $m_i \gg m_e$ we obtain $\mathbf{u} \sim \mathbf{u_i}$, and if we consider the presence only of electrons and ions with a single charge the quasi neutrality condition reads $n = n_e = n_i$.

Definition 2. *(**Plasma current density**) Given the ion mass bulk velocity* $\mathbf{u_i}$ *and the electron mass bulk velocity* $\mathbf{u_e}$*, the number of particles per unit volume of the species and the electron charge* e*, we define plasma current density as the quantity:*

$$\mathbf{j_{pl}} = e\, n_i\, \mathbf{u_i} - e\, n_e\, \mathbf{u_e}$$

If we define the total mass of the plasma $m = m_i + m_e$ and the total plasma pressure $p = p_i + p_e$, the total momentum balance equation is the following:

$$n\, m \left(\frac{\partial \mathbf{u}}{\partial t} + \mathbf{u} \cdot \nabla \mathbf{u} \right) + \nabla p = \mathbf{j_{pl}} \times \mathbf{B}$$

We introduce two important time scales in the system:

Definition 3. *(**Alfvén time**) We define the Alfvén velocity as*

$$v_A = \frac{B}{\sqrt{\mu_0\, n_i\, m_i}}$$

which represents the travelling velocity of typical oscillation of ions (hence the bulk mass of the plasma) in magnetic fields. The Alfvén time τ_A *is the characteristic time of propagation of these waves in the system:*

$$\tau_A = \frac{a}{v_A}$$

where a *is the minor radius of the torus.*

Definition 4. *(**Resistive time**) The characteristic time of momentum transport due to particle collisions is defined as*

$$\tau_R = \frac{\mu_0\, a^2}{\eta}$$

where η *is the plasma resistivity.*

The ratio of the two time scales defines the dimensionless *Lundquist parameter* $S \equiv \frac{\tau_R}{\tau_A}$. In modern fusion experiments $S \sim 10^6 - 10^{12}$ meaning that the propagation of the ions/magnetic field oscillations in the system is much faster than the momentum diffusion from collisions [2]. Since we are interested in phenomena of the order of the resistive time we can use the parameter $\epsilon = S^{-1}$ to look for solutions in which all the time derivatives, velocities, sources of dissipation and the electric field are of order of ϵ i.e:

$$\frac{\partial}{\partial t} \sim \mathbf{u} \sim \eta \sim \mathbf{E} \sim \epsilon \ll 1$$

Therefore we obtain:

$$\epsilon^2 \, n \, m \left(\frac{\partial \mathbf{u}}{\partial t} + \mathbf{u} \cdot \nabla \mathbf{u} \right) + \nabla p = \mathbf{j_{pl}} \times \mathbf{B}$$

and since we are interested in phenomena in the resistive time range we obtain the ideal massless MHD force balance, also called *plasma equilibrium equation*:

$$\mathbf{j_{pl}} \times \mathbf{B} = \nabla p$$

The static free boundary equilibrium problem looks for the magnetic field which satisfies the MHD force balance equation together with *Maxwell's equations* both under the static condition $\frac{\partial}{\partial t} = 0$. The system of equations is then:

$$\begin{cases} \mathbf{j_{pl}} \times \mathbf{B} & = \nabla p \\ \nabla \times \mathbf{B} & = \mu_0 \mathbf{j} \\ \nabla \cdot \mathbf{B} & = 0 \end{cases}$$

where the current density $\mathbf{j}$ is composed of the contribution of both the plasma current density and current densities external to the plasma but present in the domain of validity of the system (poloidal coils[3] and passive structures) i.e. $\mathbf{j} = \mathbf{j_{pl}} + \mathbf{j_e}$ where $\mathbf{j_e} = \mathbf{j_a} + \mathbf{j_v}$ is the sum of contribution from the active coils and the vessel.
Now, as done in [21], if we consider a cylindrical frame (R, Z, φ) in the hypothesis of axisymmetry $\frac{\partial}{\partial \varphi} = 0$ we have that:

$$\begin{aligned} \nabla \cdot \mathbf{B} &= \frac{1}{R}\frac{\partial (R\, B_R)}{\partial R} + \frac{1}{R}\frac{\partial B_\varphi}{\partial \varphi} + \frac{\partial B_Z}{\partial Z} = \\ &= \frac{1}{R}\frac{\partial (R\, B_R)}{\partial R} + \frac{\partial B_Z}{\partial Z} = \frac{1}{R}\frac{\partial (R\, B_R)}{\partial R} + \frac{1}{R}\frac{\partial (R\, B_Z)}{\partial Z} = 0 \end{aligned}$$

Definition 5. *(**Poloidal magnetic flux** [21]) In cylindrical coordinates called R the radius from the geometric centre of the torus, called Z the cylindrical height of the system and identified with $(R, Z)_p$ the toroidal section, is called poloidal magnetic flux Ψ[4] in P, where $P \in (R, Z)_p$ the total flux of $\mathbf{B}$ through the surface S having as its edge the toroidal ring passing through P, i.e.,*

$$\Psi = -\int_S \mathbf{B} \cdot d\mathbf{A} = -2\pi \int_0^{R_P} B_Z \, R \, dR$$

Where R_P is the radius value in P. We have immediatly that

$$R\, B_Z = -\frac{1}{2\pi}\frac{\partial \Psi}{\partial R}$$

[3] We will not consider the toroidal coils currents.
[4] In a simply connected surface we have that $\nabla \times \mathbf{B} = \mathbf{A}$ thus $\Psi = R\, A_\varphi$.

thus

$$\frac{1}{R}\frac{\partial(R\,B_R)}{\partial R}+\frac{1}{R}\frac{\partial(R\,B_Z)}{\partial Z}=\frac{1}{R}\frac{\partial(R\,B_R)}{\partial R}-\frac{1}{2\pi\,R}\frac{\partial\Psi}{\partial Z\partial R}=0$$

from which we get

$$R\,B_R=\frac{1}{2\pi}\frac{\partial\Psi}{\partial Z}$$

We obtain

$$\mathbf{B}=\frac{1}{2\pi R}\frac{\partial\Psi}{\partial Z}\,\mathbf{e_R}-\frac{1}{2\pi R}\frac{\partial\Psi}{\partial R}\,\mathbf{e_Z}+B_\varphi\,\mathbf{e}_\varphi$$

Definition 6. *(**Poloidal magnetic field** [21]) We call poloidal magnetic field the quantity:*

$$\mathbf{B_p}=B_R\,\mathbf{e_R}+B_Z\,\mathbf{e_Z}=\frac{1}{2\pi R}\frac{\partial\Psi}{\partial Z}\,\mathbf{e_R}-\frac{1}{2\pi R}\frac{\partial\Psi}{\partial R}\,\mathbf{e_Z}=\frac{1}{2\pi R}\,\nabla\Psi\times\mathbf{e}_\varphi$$

We deduce that $\mathbf{B}\cdot\nabla\Psi=0$ so field lines lie on iso poloidal flux surfaces.

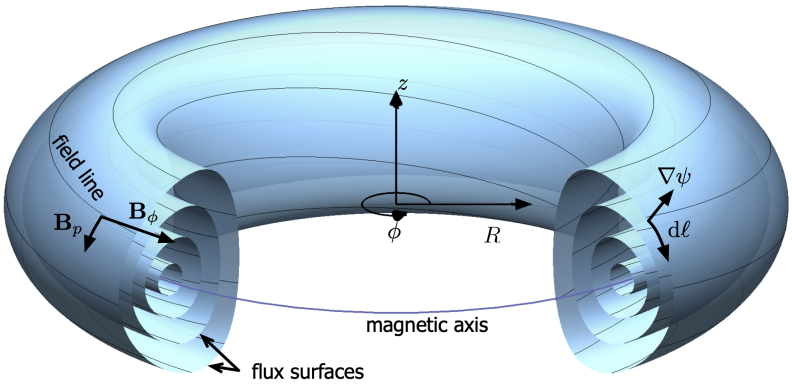

Figure 1.1: Frame of reference, (From [3])

Now, let's consider *Ampère's law* in cylindrical coordinates with the assumption of axisymmetry:

$$\nabla\times\mathbf{B}=\Big(\frac{1}{R}\frac{\partial B_Z}{\partial\varphi}-\frac{\partial B_\varphi}{\partial Z},\frac{1}{R}\Big(\frac{\partial(R\,B_\varphi)}{\partial R}-\frac{\partial B_R}{\partial\varphi}\Big),\frac{\partial B_R}{\partial Z}-\frac{\partial B_Z}{\partial R}\Big)^T=$$
$$=\Big(-\frac{\partial B_\varphi}{\partial Z},\frac{1}{R}\frac{\partial(R\,B_\varphi)}{\partial R},\frac{\partial B_R}{\partial Z}-\frac{\partial B_Z}{\partial R}\Big)^T=\mu_0\mathbf{j}$$

In homogeneous and isotropic conditions we obtain:

$$j_R=-\frac{1}{\mu_0}\frac{\partial B_\varphi}{\partial Z}$$
$$j_Z=\frac{1}{\mu_0\,R}\frac{\partial(R\,B_\varphi)}{\partial R}$$
$$j_\varphi=\frac{1}{\mu_0}\Big(\frac{\partial B_R}{\partial Z}-\frac{\partial B_Z}{\partial R}\Big)=-\frac{1}{2\pi\mu_0 R}\Big(R\frac{\partial}{\partial R}\Big(\frac{\partial\Psi}{R\,\partial R}\Big)+\frac{\partial^2\Psi}{\partial Z^2}\Big)$$

Definition 7. *(**Poloidal current density** [21]) We call poloidal current density the quantity:*

$$\mathbf{j_P}=j_R\,\mathbf{e_R}+j_Z\,\mathbf{e_Z}=-\frac{1}{\mu_0}\frac{\partial B_\varphi}{\partial Z}\,\mathbf{e_R}+\frac{1}{\mu_0\,R}\frac{\partial(R\,B_\varphi)}{\partial R}\,\mathbf{e_Z}=\frac{1}{\mu_0 R}\,\nabla\Big(R\,B_\varphi\Big)\times\mathbf{e}_\varphi$$

Definition 8. *(**Grad-Shafranov operator**) We define the bidimensional elliptical operator:*

$$\Delta^* = R\frac{\partial}{\partial R}\left(\frac{1}{R}\frac{\partial}{\partial R}\right) + \frac{\partial^2}{\partial Z^2}$$

We can now rewrite the last equation:

$$j_\varphi = -\frac{1}{2\pi\mu_0 R}\left(R\frac{\partial}{\partial R}\left(\frac{\partial\Psi}{R\,\partial R}\right) + \frac{\partial^2\Psi}{\partial Z^2}\right) = -\frac{1}{2\pi\mu_0 R}\,\Delta^*\Psi$$

The current density is thereby totally defined by the following equations[5]:

$$\mathbf{j} = \mathbf{j_p} + j_\varphi\,\mathbf{e}_\varphi = \frac{1}{\mu_0 R}\,\nabla\Big(R\,B_\varphi\Big)\times\mathbf{e}_\varphi + j_\varphi\,\mathbf{e}_\varphi$$
$$\Delta^*\Psi = -2\pi\mu_0\,R\,j_\varphi$$

Now, since:

$$\mathbf{B}\cdot(\mathbf{j_{pl}}\times\mathbf{B}) = \mathbf{B}\cdot\nabla p = 0$$

and since we are in axisymmetry and so $p = p(R,Z)$, we have that $\mathbf{B}_\varphi\cdot\nabla p = 0$, thus:

$$\mathbf{B_p}\cdot\nabla p = \frac{1}{2\pi R}\,\nabla\Psi\times\mathbf{e}_\varphi\cdot\nabla p = \frac{1}{2\pi R}\,\mathbf{e}_\varphi\cdot\nabla p\times\nabla\Psi = 0$$

therefore ∇p and $\nabla\Psi$ are parallel vectors, thus $p = p(\Psi)$.
Focusing in a similar way on the plasma current density, since:

$$\mathbf{j_{pl}}\cdot(\mathbf{j_{pl}}\times\mathbf{B}) = \mathbf{j_{pl}}\cdot\nabla p = 0$$

for axisymmetry, we have that:

$$\mathbf{j_p}\cdot\nabla p = \frac{1}{\mu_0 R}\,\nabla\Big(R\,B_\varphi\Big)\times\mathbf{e}_\varphi\cdot\nabla p = \frac{1}{\mu_0 R}\,\mathbf{e}_\varphi\cdot\nabla\Big(R\,B_\varphi\Big)\times\nabla p = 0$$

therefore $\nabla\Big(R\,B_\varphi\Big)$, ∇p and $\nabla\Psi$ are parallel vectors, thus $R\,B_\varphi \equiv T(\Psi)$.
We can finally rewrite the cylindrical *plasma equilibrium equation* in axisymmetry and with isotropic pressure:

$$\mathbf{j_{pl}}\times\mathbf{B} = \Big(\frac{1}{\mu_0 R}\,\nabla\Big(R\,B_\varphi\Big)\times\mathbf{e}_\varphi + j_{pl,\varphi}\,\mathbf{e}_\varphi\Big)\times\Big(\frac{1}{2\pi R}\,\nabla\Psi\times\mathbf{e}_\varphi + B_\varphi\,\mathbf{e}_\varphi\Big) = \nabla p =$$
$$= \Big(\frac{1}{\mu_0 R}\,\frac{dT(\Psi)}{d\Psi}\,\nabla\Psi\times\mathbf{e}_\varphi + j_{pl,\varphi}\,\mathbf{e}_\varphi\Big)\times\Big(\frac{1}{2\pi R}\,\nabla\Psi\times\mathbf{e}_\varphi + \frac{T(\Psi)}{R}\,\mathbf{e}_\varphi\Big) = \frac{dp(\Psi)}{d\Psi}\,\nabla\Psi$$

Now, by performing the vector products and deleting the terms $\nabla\Psi$, we reach the following equation:

$$-\frac{1}{\mu_0 R}\,\frac{dT(\Psi)}{d\Psi}\,\frac{T(\Psi)}{R} + \frac{j_{pl,\varphi}}{2\pi R} = \frac{dp(\Psi)}{d\Psi}$$

If we combine the previous equation with the Poisson's like equation of above and we consider that $\mathbf{j_e} = j_{e,\varphi}\,\mathbf{e}_\varphi$, we obtain the **Grad-Shafranov equation**:

$$\Delta^*\Psi = -4\pi^2\left(\mu_0\,R^2\,\frac{dp(\Psi)}{d\Psi} + T(\Psi)\,\frac{dT(\Psi)}{d\Psi}\right) - 2\pi\mu_0\,R\,j_{e,\varphi} \quad , \quad (R,Z)\in\Omega = (R,Z)_p$$

that is a *Poisson's problem* once we fix the *boundary conditions* [2], [19].

[5]The second equation is similar to a *Poisson's problem* so $\Psi(R,Z)$ is totally defined once we know the source $j_\varphi(R,Z)$ and the boundary conditions.

1.1.1 Boundary conditions

The *Grad-Shafranov* equation is a non-linear 2-dimensional elliptic PDE that gives $\Psi(R,Z)$ once we give $p(\Psi)$, $T(\Psi)$ and the boundary conditions. First of all let's define some poloidal domains [2], [14]:

$\Omega = (R,Z)_p$ - poloidal plane

$\Omega_c \subseteq \Omega$ - computational domain

$\Omega_p \subseteq \Omega_c : j_{pl} \neq 0$ - plasma region

$\Omega_e = \Omega_a \cup \Omega_v \subseteq \Omega$ - active coil and passive vessel region

$\Omega_{vac} = \overline{\Omega_c \cap \Omega_p}$ - vacuum region inside computational domain

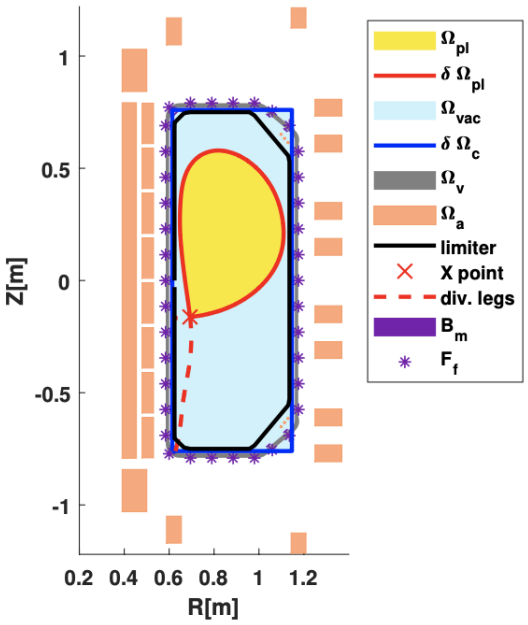

Figure 1.2: Domains, (From [2])

The plasma region Ω_p is contained within the so-called "last closed flux surface" (LCFS) which is the outermost closed surface of the nested flux surfaces at constant Ψ. There are two possible conditions in a tokamak that can define the LCFS [19]. If the plasma touches the limiter then the LCFS is given by the isoflux line at the flux value of the contact point and in these points the flux reaches its maximum value, i.e.

$$\Psi_{\text{LCFS}} = \max_{(R,Z)\in\partial\Omega_L} \Psi$$

In this case we refer to a so-called "*limited*" plasma and with $\partial\Omega_L$ we indicate the limiter contour. In the second case the boundary of the plasma region $\partial\Omega_p$ is defined by the isoflux line at the value of the poloidal flux of the X point, which is a saddle point of the flux map $\Psi(R,Z)$, i.e.

$$\nabla\Psi_{\text{LCFS}} = 0 \ \wedge \ \det \text{Hess}\,(\Psi_{LCFS}) < 0$$

In this case we refer to a so-called "*diverted*" plasma [19].

In figure (1.2) the domains in the poloidal plane of **TCV** are shown. Now we can distinguish two different types of boundary conditions [2], [19]:

- **Fixed BCs**: we prescribe "a priori" *Dirichlet boundary conditions*:

$$\Psi(R,Z) = \Psi_{pl} + \Psi_e = \sum_{i=pl,a,v} \int_{\Omega_i} G(R,Z;R',Z')\, j_i(R',Z')\, dR'dZ' \quad , \quad (R,Z) \in \partial\Omega_c$$

where Ψ_{pl} is produced by current plasma density $j_{pl,\varphi}$ ($j_{pl,\varphi} = 0$ outside $\Omega_p \subseteq \Omega$), Ψ_e is produced by $j_{e,\varphi} = j_{a,\varphi} + j_{v,\varphi}$ and where $G(R,Z;R',Z')$ is the *Green function*

connecting the source point (R', Z') to the target point (R, Z) [6]. Note that only the toroidal component of the current density j_i enters, due to the toroidal symmetry of the tokamak.

- **Free BCs**: determining the plasma boundary is part of the solution of the equilibrium reconstruction and this leads to a non-linear numerical problem. In this case the constraints are:

$$\begin{aligned}
&\Delta^*\Psi = -4\pi^2\left(\mu_0\, R^2\, \frac{dp(\Psi)}{d\Psi} + T(\Psi)\, \frac{dT(\Psi)}{d\Psi}\right) \quad , \quad (R,Z) \in \Omega_p \\
&\Delta^*\Psi = 0 \quad , \quad (R,Z) \in \Omega_{vac} \\
&\Delta^*\Psi = g(\Psi) \quad , \quad (R,Z) \in \Omega_e
\end{aligned}$$

In this work we address to **Free BCs** since the plasma boundary is unknown and is a part of the solution of the problem. The *Dirichlet boundary conditions* holds at every iteration once the plasma region has been determined.

1.2 Model discretization

In order to give a description of the toroidal plasma current $j_{pl,\varphi}$ we need an approximated approach. First of all the 2-dimensional computational domain Ω_c is discretized with a grid of elements of width ΔR and height ΔZ. Also the non-zero plasma current region Ω_p is discretized in the same way[7]. Let's give some definitions to present the *basis function discretization* [19], [6], [17].

Definition 9. *(**Magnetic axis**) We now define with $\Psi_A = \Psi(R_A, Z_A)$ the value of the poloidal flux at the plasma axis as the minumum point of the poloidal flux map $\Psi(R, Z)$, i.e.*

$$\nabla\Psi_A = 0 \ \ \wedge \ \ \det Hess\,(\Psi_{\mathrm{LCFS}}) > 0$$

The point (R_A, Z_A) in the poloidal plane represents the center of the plasma.

Definition 10. *(**Normalized poloidal flux**) We define the normalized poloidal flux as:*

$$\hat{\Psi} = \frac{\Psi(R,Z) - \Psi_A}{\Psi_{\mathrm{LCFS}} - \Psi_A}$$

Definition 11. *(**Poloidal beta**) The poloidal pressure factor β_p is the ratio between the volume-averaged thermal pressure and the volume-averaged poloidal magnetic field pressure:*

$$\beta_p = \frac{\langle p \rangle}{\frac{B_p}{2\,\mu_0}}$$

Definition 12. *(**Total plasma current**) The total plasma current I_p is defined by the flux of the toroidal component of the plasma current density in the poloidal cross-section.*

$$I_p = \int_{\Omega_p} \mathbf{j_{pl}} \cdot d\mathbf{A} = \frac{1}{2\pi} \int_{\Psi_A}^{\Psi_{\mathrm{LCFS}}} d\Psi \oint \frac{\partial\Omega_p}{B_p}$$

[6] For the external current density j_e, instead of continuous distribution in the poloidal plane, we will consider sets of filamentary currents located at the positions (R_i, Z_i) with point-wise sections in the poloidal plane. This is equivalent to consider j_i, as a Dirac distribution $j_i\,\delta(R - R_i, Z - Z_i)$, where (R_i, Z_i) is the location of the filament i.

[7] In our codes we assume at this stage that the plasma current is contained inside a discretized contour $\partial\Omega_p$ where $j_{pl} \neq 0$, hence we do not consider currents in the *scrape off layer* [2].

After an initial ramp-up phase, I_p is maintained stationary and then ramped-down at the end of the experiment. For the proof of the second equivalence in the previous definition we refer to [2].

Definition 13. *(**Safety factor**) If we consider the poloidal cylindrical frame (r, ϑ) and if we call N the number of toroidal turns and M the number of poloidal turns following a field line around the torus, we call safety factor q_A the quantity*[8] *:*

$$q_A = \frac{N}{M} = \frac{\partial \varphi}{\partial \vartheta} = \frac{r}{R}\frac{B_\varphi}{B_p}$$

Definition 14. *(**Basis functions representation of the plasma current distribution**) As a direct consequence of the more fundamental representation of p' and TT' as basis functions, the plasma current is parametrized by a linear combination of polynomial basis functions $g(\Psi(R,Z))$:*

$$j_{pl,\varphi} = 2\pi\Big(R\,\frac{dp(\Psi)}{d\Psi} + \frac{T(\Psi)}{\mu_0 R}\,\frac{dT(\Psi)}{d\Psi}\Big) = \sum_{i_p} \alpha_{i_p}\, R\, g_{i_p}(\Psi(R,Z)) + \sum_{i_T} \alpha_{i_T}\, R^{-1}\, g_{i_T}(\Psi(R,Z))$$

In such a formulation the reconstruction problem consists of finding the coefficients $\alpha_g \equiv \{\alpha_{i_p}, \alpha_{i_T}\}$. The more basis functions are included, the more coefficients are to find but the description of the current will be more precise [14], [19].

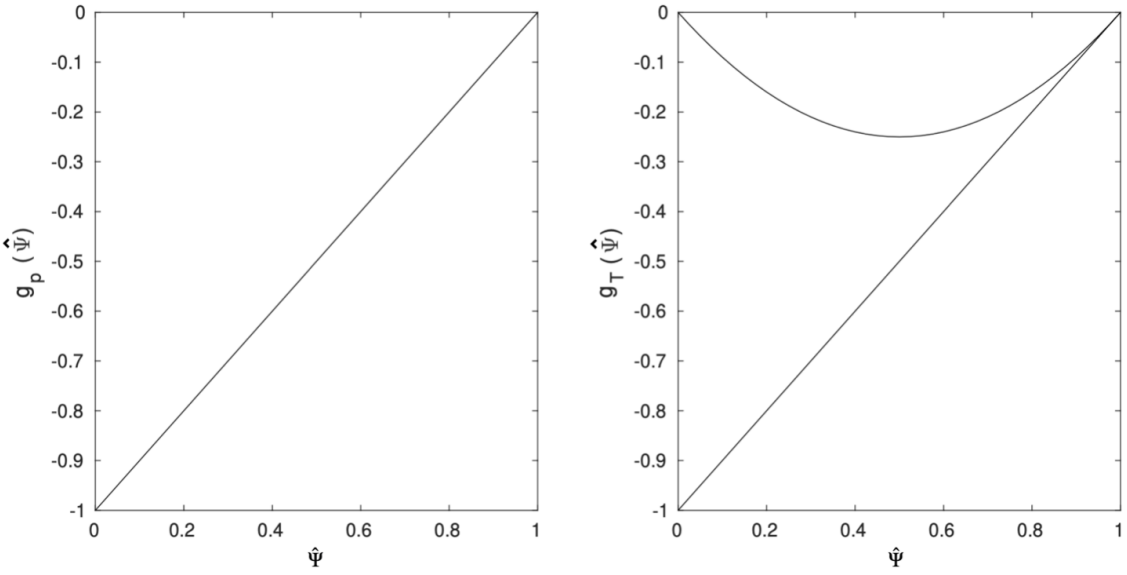

Figure 1.3: Example of basis functions as a function of the normalized poloidal flux $\hat{\Psi}$

As we will see, in FGE-code the number of coefficients α_g will be chosen in order to match exactly the number of parameters in the vector $c = [\beta_p\ I_p\ q_A]^T$ [8].

[8] In conventional tokamaks q_A varies from 1 on axis to $3-4$ on the edge. Since q_A is related to the number of toroidal turns to complete one poloidal revolution of a given magnetic field line lying on a given flux surface, it can be shown that on the isobaric surfaces where $q_A \in \mathbb{Q}$ we have periodicity on the plasma configuration. The q_A-profile is related to plasma instabilities and has become a crucial parameter to be estimated and controlled during plasma operations [2].

1.2.1 Current discretization

1.2.1.1 Active coils

In tokamaks, coils that are used to generate magnetic fields and to control the plasma bulk position have toroidal symmetry. This is done in order to keep the 2-dimensional physical description of the system. We will refer to this set of coils as active, control or poloidal coils. The combination of physical active coils are connected in series[9] to form an active circuit that is labeled a. Each coil is discretized into coil 'winding packs' consisting each one of n_w conductor filamentary windings, since most of the coils in a tokamak are too large to consist of a single conductor (as shown in figure (1.5)). In an independent active coil k, $k \in \{1, ..., n_a\}$ in which each winding is modeled by a filament at (R'_i, Z'_i) , $\forall\, i \in \{1, ..., n_w\}$ and that each one carries the in-series current I_w, the flux generated by all the windings combined is:

$$\Psi_k(R, Z) = \sum_{i=1}^{n_w} M(R, Z; R'_i, Z'_i)\, I_w = M_k(R, Z)\, I_w$$

where the Green function $M_k(R, Z) = \sum_{i=1}^{n_w} M(R, Z; R'_i, Z'_i)$ is the *mutual inductance* between the entire k-coil and the point (R, Z) of the poloidal plane.

1.2.1.2 Vacuum vessel

The tokamak chamber where the plasma is confined is sorrounded by a low resistivity metallic structure called vacuum vessel, in order to slow down the vertical instabilities. Since the vacuum vessel is a metallic structure it has to be accounted that it can carry toroidal electrical currents induced by the time-varying poloidal magnetic field. Morover, since the thickness of the vacuum chamber is little, it is modeled as equidistantly spaced toroidal independent filamentary windings labeled v as in figure (1.4). This filamentary representation of vessels will sometimes also be referred to as passive circuits or passive structures. The combination of the active circuit current and vacuum vessels stacked together will be labeled as e, s.t. the number of external circuits is the sum of the number of independent active circuits and vacuum vessel windings, i.e. $n_e = n_a + n_v$. The contribution of a winding current (active circuit or vessels) to the poloidal flux is given by discretizing the Green function:

$$\Psi^{I_e}(R, Z) = \Psi^{I_a} + \Psi^{I_v} = \sum_{i=1}^{n_a} G(R, Z; R_i, Z_i)\, I_{a,i} + \sum_{j=1}^{n_v} G(R, Z; R_j, Z_j)\, I_{v,j} = M\, I_e$$

where $M \in \mathbb{R}^{n_e}$ is the collection of the Green functions $M_i = G(R, Z, R_i, Z_i)$[10] and $I_e \in \mathbb{R}^{n_e}$ is the external circuit current, both active and passive.

[9] The poloidal coils of **TCV** have independent power supplies. They consists of 32 coils (some of them are connected in series or in anti-series) making up $n_a = 19$ active circuits. In radial position control the coils at the left (inner part of the poloidal cross-section) of the poloidal plane are in series and with opposite sign with respect to the right ones (outer part of the poloidal cross-section) in order to counteract the radial centrifugal force. In vertical position control the coils at the left and at the right of the top of the poloidal cross-section are connected in series and have opposite sign with respect to the left and right coils of the bottom of the poloidal cross-section, in order to counteract the vertical displacement instability.

[10] Because of the symmetry of the Green functions the mutual inductances are symmetric and positive definite matrices.

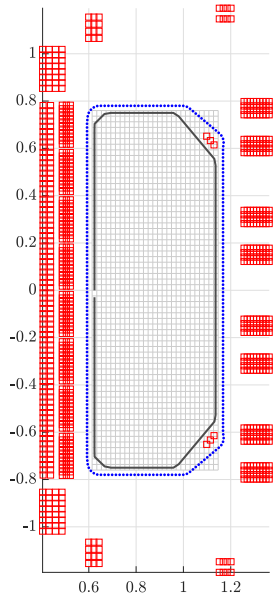

Figure 1.4: Current discretization

If we stack the contribution of the circuit k, $k \in \{a, v\}$ to the flux x, $x \in \{a, v\}$ in the flux vector $\Psi_x^{I_k} \in \mathbb{R}^{n_e}$ the above expression can be written as a linear mapping:

$$\begin{cases} \Psi_a^{I_a} = M_{aa}\, I_a \\ \Psi_a^{I_v} = M_{av}\, I_v \\ \Psi_v^{I_a} = M_{va}\, I_a \\ \Psi_v^{I_v} = M_{vv}\, I_v \end{cases}$$

and in a more compact form:

$$\Psi_e^{I_e} = M_{ee}\, I_e$$

with:

$$M_{ee} = \begin{pmatrix} M_{aa} & M_{av} \\ M_{va} & M_{vv} \end{pmatrix} \in \mathbb{R}^{n_e \times n_e}$$

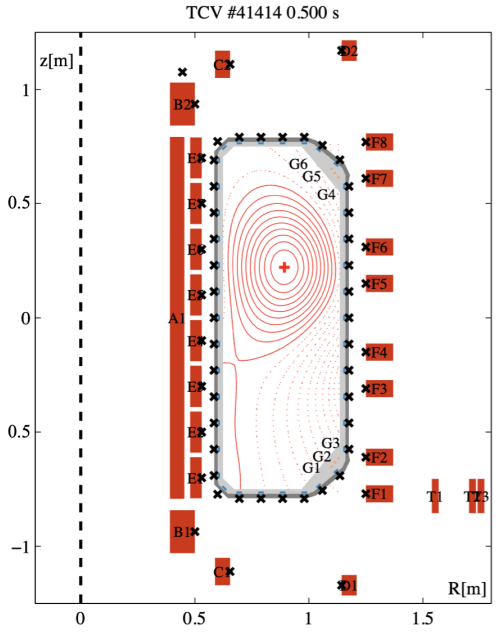

‘Physical’ TCV poloidal coils

- A (72 × 2 windings)
- B1-2 (8 × 4 windings)
- C1-2 (4 × 3 windings)
- D1-2 (2 × 4 windings)
- E1-8: (12 × 3 windings)
- F1-8: (4 × 9 windings)
- G1-6 (1 windings each)
- T1-3: Connectors of TF coils

Active TCV coils

- OH1: A coil
- OH2: B, C, D coils in series
- E1-8: individual
- F1-8: individual
- G: G1-3/G4-6 in antiseries

Figure 1.5: Poloidal coils of **TCV**, (From [4])

1.2.1.3 Plasma current

The plasma toroidal current density is modeled by the computational grid as a rectangular filamentary current of width ΔR and height ΔZ. At each position (R, Z) of the discrete grid Ω_c the filament plasma current is defined as:

$$I_y = j_{pl}(R,Z)\,\Delta R\,\Delta Z = \begin{cases} \sum_{g=i_p,i_T} \alpha_g\, R^{\nu_g}\, g_g(\Psi(R_i,Z_i))\,\Delta R\,\Delta Z & , \text{ if } (R_i,Z_i) \in \Omega_p \\ 0 & , \text{ if } (R_i,Z_i) \in \Omega_c - \Omega_p \end{cases}$$

where $\nu_g = -1$ if $g = i_T$ and $\nu_g = 1$ if $g = i_p$. Morover, since the plasma current is also a source of the poloidal flux we have that the plasma contribution to the flux is:

$$\Psi_e^{I_y} = M_{ey}\, I_y$$

where $M_{ey} \in \mathbb{R}^{n_e \times n_y}$ is the matrix mutual inductance mapping the plasma current to the circuit flux s.t. $M_{ey,ij} = G(R_i, Z_i; R_j, Z_j)$.
Therefore:

$$\Psi_e \equiv \Psi_e^{I_e, I_y} = M_{ee}\, I_e + M_{ey}\, I_y$$

1.2.1.4 Grad-Shafranov operator

The *Grad-Shafranov operator* is discretized by means of the *Finite Difference Method* [19]:

$$\Delta^*\Psi(R_i,Z_j) \approx \Big(\mathbf{D}\,\Psi\Big)_{ij} = \frac{1}{\Delta Z^2}\Big(\Psi_{i,j+1} + \Psi_{i,j-1} + a_i\,\Psi_{i+1,j} + b_i\,\Psi_{i-1,j} - c_i\,\Psi_{i,j}\Big)$$

with:

$$\begin{cases} a_i = \left(\frac{\Delta Z}{\Delta R}\right)^2 \frac{R_i}{R_i + \Delta R_i/2} \\ b_i = \left(\frac{\Delta Z}{\Delta R}\right)^2 \frac{R_i}{R_i - \Delta R_i/2} \\ c_i = 2 + a_i + b_i \end{cases}$$

Therefore, if we stack Ψ in a vector of $\mathbb{R}^{nn}$, where nn is the number of grid nodes of Ω_c [11], the differential operation becomes a linear matrix multiplication:

$$\Delta^*\Psi \approx \mathbf{D}\,\Psi$$

where $\Psi = [\Psi_{11}\ \Psi_{12}\ ...\ \Psi_{21}\ \Psi_{22}\ ...\ \Psi_{nn}]^T$ and $\mathbf{D}$ is a matrix formed of 5 diagonals. Since $a_i \neq b_i$ the matrix $\mathbf{D}$ is not symmetric. The *discretized Grad-Shafranov equation* is then:

$$\mathbf{D}\,\Psi_y = -2\pi\mu_0 \frac{R_y}{\Delta R \Delta Z}\, I_y(\alpha_g, \Psi_y) - 2\pi\mu_0\, R_y\, I_e$$

where R_y is the radial coordinate in the poloidal plane computed in $(R_y, Z_y) \in \Omega_p$. This equation can be solved by means of the *iterative Picard method*[12] once we impose the boundary condition:

$$\Psi_o = M_{oa}\, I_a + M_{ov}\, I_v + M_{oy}\, I_y \quad , (R,Z) \in \partial\Omega_c$$

where Ψ_o is the discretized flux on the discretized boundary domain $\partial\Omega_c$, $\{I_a, I_v, I_y\}$ are respectively the discretized control coil, vessel and plasma currents vectors, and $M_{ox} = G(R_o, Z_o; R_x, Z_x) \in \mathbb{R}^{n_o \times n_x}$, $x \in \{a, v, y\}$ are the discretized Green functions linking the source points (R_x, Z_x) to the boundary points $(R_o, Z_o) \in \partial\Omega_c$.

For more details, we refer to [2], [4], [8], [19].

[11] In this example the computational domain has $n \times n$ nodes spaced ΔR along R and ΔZ along Z.

[12] The *iterative Picard method* is used in reconstruction codes such as LIUQE where the solution is found iteratively from measurements in a least square sense once we impose the boundary conditions and we fix the first iteration of p' and TT' (i.e., we impose the first iteration coefficients α_g). But since the *Picard method* presents instability to vertical displacement events the reconstruction problem has been recast into a zero-finding problem and solved by means of the *Jacobian free Newton-Krylov method* [2], [8].

1.2.2 Circuit equation

The evolution of the active and passive circuits follows the *Ohm-Faraday law*:

$$\frac{d\Psi_e}{dt} = V_e - R_{ee}\, I_e$$

where $V_e = [V_a\ \underline{0}]^T$ is the voltage applied to the circuit (only the PF coils have a voltage source), $R_{ee} \in \mathbb{R}^{n_e \times n_e}$ is a diagonal matrix with entries the resistances of each of the conducting structure elements [4], [14]. Now, since:

$$\Psi_e = M_{ee}\, I_e + M_{ey}\, I_y$$

and since M_{ee} and M_{ey} are assumed constant in time, we get:

$$M_{ee}\, \dot{I}_e + M_{ey}\, \dot{I}_y - V_e + R_{ee}\, I_e = \underline{0}$$

1.2.2.1 Vacuum vessel eigenmodes decomposition

Instead of looking at the vessel as a filamentary discretization it is often useful to change the frame basis and describe the vessel according to its reaction speed to perturbations. If we consider the linear ODE associated with the PF circuits, the vessel currents and the plasma currents we get the following linear system [4]:

$$\begin{pmatrix} V_a \\ \underline{0} \\ \underline{0} \end{pmatrix} = \begin{pmatrix} M_{aa} & M_{av} & M_{ay} \\ M_{va} & M_{vv} & M_{vy} \\ M_{ya} & M_{yv} & L_p \end{pmatrix} \begin{pmatrix} \dot{I}_a \\ \dot{I}_v \\ \dot{I}_y \end{pmatrix} + \begin{pmatrix} R_{aa} & \mathbb{O} & \mathbb{O} \\ \mathbb{O} & R_{vv} & \mathbb{O} \\ \mathbb{O} & \mathbb{O} & R_p \end{pmatrix} \begin{pmatrix} I_a \\ I_v \\ I_y \end{pmatrix}$$

Since from reconstruction codes we know iteratively the plasma boundary $\partial\Omega_p$, we can know the value of the total toroidal plasma current I_p and stack the values of the inner rectangles into a distribution vector I_y s.t. the self inductance of the plasma is defined as [2]:

$$L_p = \frac{I_y^T\, M_{yy}\, I_y}{I_p}$$

The plasma resistance $R_p \in \mathbb{R}^{n_y \times n_y}$ is a diagonal matrix collecting the resistances of all the plasma elements (R_p is usually defined externally). Now if we consider the second equation of the system we obtain:

$$\underline{0} = M_{va}\, \dot{I}_a + M_{vv}\, \dot{I}_v + M_{vy}\, \dot{I}_y + R_{vv}\, I_v$$

Let's pack the external factors as an input such that:

$$\underline{0} = M_{vv}\, \dot{I}_v + R_{vv}\, I_v + U$$

Solving the homogeneous equation and since the mutual inductance matrix is symmetric and positive definite and thus invertible we get the continuous linear system:

$$\dot{I}_v = -M_{vv}^{-1}\, R_{vv}\, I_v$$

Now, since M_{vv}^{-1} and R_{vv} are symmetric and positive definite then $-M_{vv}^{-1}\, R_{vv}$ is symmetric and negative definite thus, from the *spectral theorem*, diagonalizable in $\mathbb{R}$ such that:

$$-M_{vv}^{-1}\, R_{vv} = T\, \Lambda\, T^T$$

where the orthogonal matrix T and the diagonal matrix Λ are made such as Λ has decreasing diagonal elements. Now, if we define:

$$I_u = T^T I_v$$

we have that:

$$\dot{I}_v = T\,\Lambda\,T^T I_v \implies T^T \dot{I}_v = \Lambda\,T^T I_v \implies \dot{I}_u = \Lambda\,I_u$$

The solution of the linear system is therefore:

$$I_v(t) = \sum_{i=1}^{n_v} v_i\,\alpha_i\,\exp(\lambda_i t)$$

where $v_i \in \mathbb{R}^{n_v}$ are the eigenvectors of $-M_{vv}^{-1}\,R_{vv}$ (i.e., the columns of T), λ_i are the eigenvalues of $-M_{vv}^{-1}\,R_{vv}$ and $\alpha_i \in \mathbb{R}\ \forall\, i$ are determined by imposing the initial conditions:

$$T\,[\alpha_1\ ...\ \alpha_{n_v}]^T = [v_1\ ...\ v_{n_v}]\,[\alpha_1\ ...\ \alpha_{n_v}]^T = I_v(0)$$

Instead of considering all the modes, the fastest decaying ones could be omitted. This would allow simplifying a lot the system while keeping an accurate description.
Let's now find the vessel circuit equation with this new frame instead of the filamentary description. The vessel circuit equation in *Laplace domain* becomes:

$$\begin{aligned}
\underline{0} = \mathcal{L}\left(\underline{0}\right) &= \mathcal{L}\left(M_{va}\,\dot{I}_a + M_{vv}\,\dot{I}_v + M_{vy}\,\dot{I}_y + R_{vv}\,I_v\right) = \\
&= \left(R_{vv} + s\,M_{vv}\right) I_v + s\,M_{va}\,I_a + s\,M_{vy}\,I_y = \\
&= R_{vv}\left(\mathcal{I} + s\,R_{vv}^{-1}\,M_{vv}\right) I_v + s\,M_{va}\,I_a + s\,M_{vy}\,I_y = \\
&= R_{vv}\left(\mathcal{I} - s\,T\,\Lambda^{-1}\,T^T\right) I_v + s\,M_{va}\,I_a + s\,M_{vy}\,I_y = \\
&= R_{vv}\,T\left(\mathcal{I} - s\,\Lambda^{-1}\right) T^T I_v + s\,M_{va}\,I_a + s\,M_{vy}\,I_y = \\
&= \frac{R_{vv}}{r_u}\,T\left(r_u\,\mathcal{I} - s\,r_u\,\Lambda^{-1}\right) T^T I_v + s\,M_{va}\,I_a + s\,M_{vy}\,I_y = \\
&= \frac{R_{vv}}{r_u}\,T\left(r_u\,\mathcal{I} + s\,D\right) T^T I_v + s\,M_{va}\,I_a + s\,M_{vy}\,I_y = \\
&= \frac{R_{vv}}{r_u}\,T\left(r_u\,\mathcal{I} + s\,D\right) T^T I_v + s\,M_{va}\,I_a + s\,M_{vy}\,I_y
\end{aligned}$$

where r_u is a positive resistance like term (arbitrary chosen) to give a resistive form to the diagonalized expression, and $D = -r_u\,\Lambda^{-1}$ is a positive definite matrix with deacreasing diagonal elements. If we multiply the last equation for $\left(\frac{R_{vv}}{r_u}\,T\right)^{-1}$ we obtain:

$$\begin{aligned}
\underline{0} &= \left(r_u\,\mathcal{I} + s\,D\right) I_u + s\,T^T\left(\frac{R_{vv}}{r_u}\right)^{-1} M_{va}\,I_a + s\,T^T\left(\frac{R_{vv}}{r_u}\right)^{-1} M_{vy}\,I_y = \\
&= \left(R_{uu} + s\,M_{uu}\right) I_u + s\,M_{ua}\,I_a + s\,M_{uy}\,I_y
\end{aligned}$$

The last equation is the corresponding circuit equation in the basis of vessel eigenmodes in frequency domain. If we define $T_{uv} \equiv \left(\frac{R_{vv}}{r_u}\,T\right)^{-1} = T^T\left(\frac{R_{vv}}{r_u}\right)^{-1}$ we obtain the following

linear tranformations:

$$\begin{cases} I_v = T_{vu}\, I_u \\ I_u = T_{vu}^T\, I_v \\ R_{uu} = T_{uv}\, R_{vv}\, T_{vu} \\ M_{uu} = T_{uv}\, M_{vv}\, T_{vu} \\ M_{ua} = T_{uv}\, M_{va} \\ M_{uy} = T_{uv}\, M_{vy} \end{cases}$$

where $T_{vu} \neq T_{uv}^T$, $T_{uv}^{-1} \neq T_{uv}^T$ and $T_{vu}^{-1} = T_{vu}^T$. The number of eigenmodes will be hereafter defined as $n_u \leq n_v$ [14].

1.3 Measurements

Reconstruction codes apply also for RFP machines[13] but in this work the vessel currents of the **TCV** tokamak fusion reactor[14] are estimated [11]. The Kalman filter method has been already used in a previous work on a more basic simulated tokamak reactor called **Anamak** [5], [14].

> **Anamak** (analytical-tokamak) is a numerical tokamak developed at SPC that can be configured to produce a circular stable shot (without vertical displacement event) as well as elongated unstable shots. Anamak consists of $n_a = 8$ control coils, each one corresponding to an active circuit, $n_f = 16$ flux loops and $n_m = 16$ magnetic probes. Additionally the vessels are described by $n_v = 200$ equally spaced toroidal filaments.

In comparison,

> **TCV** accounts for 32 control coils (some of them are connected in series or in anti-series) making up $n_a = 19$ active circuits, 38 flux loops, and 38 magnetic probes. The D-shaped chamber is allowing to produce elongated plasmas. The vessels are described by $n_v = 256$ equally spaced toroidal filaments that reduces to n_u [15] most significant modes (the slowest ones) in the eigenmode description.

An example of a stable shot is given in circular **Anamak** in figure (1.6) on the left while, on the right, an unstable elongated and limited shot (66872) of **TCV** is presented.

In **TCV** plasma parameters[16], currents, electric and magnetic fields, flux values and its variations are measured by means of wires and coils[17] set all around the tokamak, poloidally and toroidally. Imposing the force balance equation represented in the poloidal plane by the Grad-Shafranov equation we can solve the problem of reconstruction of the Ψ-surfaces in a least square sense using the basis functions. The constant terms of the equations are the measures of the $\mathbf{\Psi}$ values, the $\mathbf{B}$ values and the active coil currents I_a [5].
The active coils currents are measured and the filamentary discretization has already been explained so the link between coil currents and measurements is trivially given by:

$$I_a = \mathcal{I}\, I_a$$

A flux loop is a wire mounted on the vacuum vessel connected to a voltmeter. Since the

[13] Such as at *Consorzio RFX* in Padua, Italy.
[14] At *SPC-EPFL* in Lausanne, Switzerland.
[15] The choice on n_u depends on the specific application.
[16] For example: *poloidal beta* β_p, *total plasma current* I_p, *internal inductance* l_i, *safety factor* q_A [24].
[17] For example: *Rogowski coil*, flux loop, diamagnetic loop, poloidal field probes, *Mirnov coils* [24].

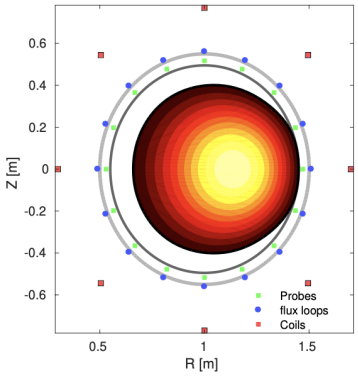

(a) Anamak circular shot 1, $t = 0\,\mathrm{s}$. In the rest of the work the measurement devices will be numbered as follow : starting from the most right and counting in a trigonometric direction. There are $n_a = 8$ actives circuits (that we sometimes refer simply as coils), $n_m = 16$ magnetic probes and $n_f = 16$ flux loops.

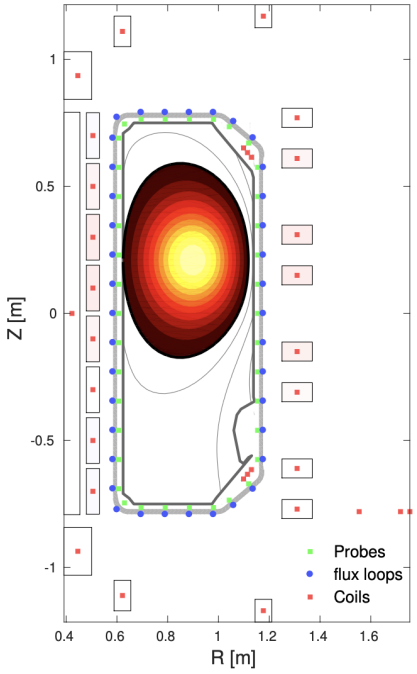

(b) TCV elongated shot 66872, $t = 0.7\,\mathrm{s}$

Figure 1.6: (From [14])

voltage is given by $V_f = \dot{\Psi}$ it's necessary to use an integrator (using operational amplifiers) to obtain the magnetic poloidal flux:

$$\Psi(t) = \int_0^t V_f(\tau)\, d\tau$$

A magnetic probe consists of a small winding with several turns s.t. the magnetic field is homogeneous inside of it. Coupled to a voltmeter it provides a direct measurement of the magnetic field time derivative amplitude, i.e. $V_m = NS\dot{B}$, where N is the number of windings, S is the area of the probe. Using again an integrator we obtain a measure of the magnetic field:

$$B(t) = \frac{1}{NS} \int_0^t V_m(\tau)\, d\tau$$

The linear mapping between currents and poloidal flux and magnetic field is made as usual by Green functions:

$$\begin{cases} B_m = B_{ma}\, I_a + B_{mv}\, I_v + B_{my}\, I_y \\ \Psi_f = M_{fa}\, I_a + M_{fv}\, I_v + M_{fy}\, I_y \end{cases}$$

where $B_{mx} \in \mathbb{R}^{n_m \times n_x}$, $x \in \{a, v, y\}$ is a Green function made modifying the mutual inductance matrix M_{mx} simply dividing by NS.

One possible reconstruction of the plasma and external currents from the measurements devices diagnostics is given solving in a least square sense the system:

$$\|Ax - y\|_2^2$$

where the matrix A represents the linear link between the vector of measurements $y = [I_a\ B_m\ \Psi_f\ I_s]^T$ and $x = [I_e\ I_y\ I_s\ \alpha_g]^T \in \mathbb{R}^{n_e+n_y+n_f+n_{\alpha_g}}$ [18]. The result can be used to determine the plasma domain and solve the *discretized Grad-Shafranov equation* previously presented. Unfortunately this approach is not feasible since to have an accurate solution in flux surfaces reconstruction it is necessary to have a large number of plasma current filaments. On the other hand another approach, that is used in post-shot equilibrium reconstruction code developed on **TCV**, should be to define a new state $x = [I_e\ \alpha_g]^T$ in order to find the basis function coefficients and then solve for the plasma current I_y in a further step [5], [14], [19].

1.4 Equilibrium codes

A MATLAB-based library of codes called MEQ has been developed at SPC in order to solve various equilibrium problems. The main codes of such a library are:

- **LIUQE**:
  Inputs: magnetic measurements y
  Outputs: $\{I_a,\ I_v,\ \frac{dp}{d\Psi},\ T\,\frac{dT}{d\Psi},\ \Psi(R,Z)\}$
  It solves MER [19] using least squares estimation by finding the optimals α_g coefficients. It is used for post-discharge and real time analysis [19].

- **FBT**:
  Inputs: $\{\frac{dp}{d\Psi},\ T\,\frac{dT}{d\Psi},\ \partial\Omega_p\}$
  Outputs: $\{I_a,\ \Psi(R,Z)\}$
  It solves the LIUQE inverse problem i.e. for a given plasma shape and contraints on the Ψ-functions p' and TT' it finds the active coils current I_a to achieve the desired equilibrium. It is used for shot preparation and feedforward $I_a(t)$ for **TCV** operations [12].

- **FGS**:
  Inputs: $\{\frac{dp}{d\Psi},\ T\,\frac{dT}{d\Psi},\ I_a,\ I_v\}$
  Outputs: $\{\Psi(R,Z)\}$
  It is the *Forward Static Grad-Shafranov* solver, it solves a free boundary static problem for given contraints on the α_g-coefficients. The main differences with respect to LIUQE are that in FGS I_a is assumed known and there are no measurements. Moreover the algorithm of FGS is based on a root-finding problem [2], [8].

- **FGE**:
  Inputs: $\{I_p(t),\ \beta_p(t),\ q_A(t),\ l_i(t),\ V_a(t)\}$
  Outputs: $\{I_a(t),\ I_v(t),\ \Psi(R,Z,t)\}$
  It is a dynamical solver: for a given initial time condition on the outputs and a set c of constraints on plasma quantities to constrain α_g, it solves Grad-Shafranov equations coupled with circuit equations. As we will see in the next Chapters, the code can be used as a simulator for pre-shot preparation and a local linearization of this system of equations around an equilibrium can be derived and used for linear plasma position controller and observer design [2], [8].

Since the pourpose of this work is to design a state observer for the vessel current estima-

[18] The current vector I_s represents the vessel currents in the positions of the poloidal flux loops and can be defined as $I_s = -\frac{\dot{\Psi}_f}{R_s}$ where R_s is the local vessel resistances matrix.

[19] Magnetic equilibrium reconstruction.

tion, the FGS solver will be explained more in detail. Some details concerning the other codes can be found in [2], [8], [12], [19].

1.4.1 FGE - Forward Evolutive Grad-Shafranov solver

FGE is a free boundary dynamical Grad-Shafranov solver. It is based on the time-step iteration of FGS coupled to time-step dynamical circuit equation. Let's introduce first the principle of free boundary Grad-Shafranov equation: given $\nu = \{I_a,\, I_v,\, c\}$ where for example $c = \{I_p(t),\, \beta_p(t),\, q_A(t)\}$[20] is a set of fixed constraints, we aim to find $x = \{I_y,\, \alpha_g\}$ where α_g is the coefficients vector of the polynomial function expansion of p' and TT'. The problem is cast as a root-finding problem[21]:

$$G_{k+1}(x,\nu) = \begin{pmatrix} \epsilon_{y_{k+1}} \\ \epsilon_{c_{k+1}} \end{pmatrix} \xrightarrow{k\to\infty} \begin{pmatrix} \underline{0} \\ \underline{0} \end{pmatrix} \in \mathbb{R}^{n_y+n_{\alpha_g}}$$

The function G is now only function of I_y and α_g since ν is fixed. The Grad-Shafranov equation gives n_y equations and the constraints equations give n_{a_g} equations. The iterative-step residuals must converge to zero. The plasma current residual is defined as:

$$\epsilon_{y_{k+1}} = I_y^k - I_y^{k+1}$$

where I_y^{k+1} is computed from:

$$\begin{aligned} \Psi_o^k &= M_{oe} I_e + M_{oy} I_y^k \quad , \quad (R,Z) \in \partial\Omega_c \\ \mathbf{D}\,\Psi_y^k &= -2\pi\mu_0 \frac{R_y^k}{\Delta R \Delta Z}\, I_y^k - 2\pi\mu_0\, R_y^k\, I_e \end{aligned}$$

And finally, once the plasma domain Ω_p^k is known from $\Psi_x^k,\ x \in \{a,\, v,\, y\}$ we obtain:

$$I_y^{k+1} = \begin{cases} \sum_g \alpha_g^k\, R^{\nu_g^k}\, g_g(\Psi_y^k(R_i,Z_i))\, \Delta R\, \Delta Z & , \quad (R_i,Z_i) \in \Omega_p^k \\ 0 \quad , \quad (R_i,Z_i) \in \Omega_c - \Omega_p^k \end{cases}$$

where $\nu_g = -1$ if $g = i_T$ and $\nu_g = 1$ if $g = i_p$.
Moreover, concerning the constraints residual $\epsilon_{c_{k+1}}$ if $c = [c_1\ ...\ c_{n_{\alpha_g}}]^T$ is the vector of constraints and $c_i\,,\ i \in 1, ..., n_{\alpha_g}$ is a scalar, there exists a linear map

$$A : \alpha_g \mapsto c$$

linking the α_g-coefficients to the contraints, i.e. $A_j(\alpha_1\ ...\ \alpha_{n_{\alpha_g}}) = c_j$. For example let's take as scalar constraint the total plasma current at time t, i.e. $c_i = I_p$. At the k-th iteration (referring of course to the same time instant) we have that:

$$I_p^k = \sum_{y\in\Omega_p^k} I_y^k = \sum_{y\in\Omega_p^k} \sum_g \alpha_g^k\, R^{\nu_g^k}\, g_g(\Psi_y^k(R_i,Z_i))\, \Delta R\, \Delta Z = A_{pg}^k\, \alpha_g^k$$

In this case we have that $\epsilon_{c_{k+1}} = A_{pg}^{k+1}\, \alpha_g^{k+1} - I_p$.
Since the problem is non-linear the solution is not necessary unique and the method might not converge. FGS is a static solver that allows computing equilibrium plasma flux surfaces

[20] If we consider the polynomial functions described in this work we have that $n_{\alpha_g} = 3$ since we take a linear function for g_{i_p} and a combination of a linear and parabolic function for g_{i_T}.
[21] It is solved using *Newton-Krylov method*.

and toroidal plasma current distribution at time t, assuming known conductor currents I_e. In reality, the currents are a result of the circuit equations (as it was presented in a previous subsection), which are ODEs that involve also the movement of the plasma. Therefore a dynamic solver is needed. FGE is a dynamical solver, based on FGS, that includes the circuit equations to express the time evolution of the poloidal flux Ψ combined with the evolution of the conductor currents. We indicate with $\nu^t = \{I_a^t,\, I_v^t,\, c^t\}$[22] the external currents vector and the constraints vector at time instant t while we indicate the vector of unknowns at time t with $x^t = \{I_y^t,\, \alpha_g^t,\, I_e^t\}$ since overall I_e^t is unknown (only I_a is known from measurements in specific time instants). The active coils voltages $V_a(t)$ are provided at each time-iteration. The problem is cast as a root-finding problem just as in FGS:

$$F(x^{t+1}) = \begin{pmatrix} \frac{\Psi_e^{t+1} - \Psi_e^t}{\Delta t} - V_a^{t+1} + R_e I_e^{t+1} \\ \Psi_e^{t+1} - M_{ee} I_e^{t+1} - M_{ey} I_y^{t+1} \\ G_{t+1}(x, \nu) \end{pmatrix} \xrightarrow{N\to\infty} \begin{pmatrix} \underline{0} \\ \underline{0} \\ \underline{0} \end{pmatrix} \in \mathbb{R}^{2n_e + n_y + n_{\alpha_g}}$$

where index $t+1$ means that the quantity is computed at time $t+\Delta t$, with user defined time step Δt. Hence if we call N the total number of time-steps and T the entire time interval of interest we have $T = N\Delta t$. G-function has already been defined in FGS. Once we know all the quantities at time t, the constraints at time $t+1$ and also the controller action on the poloidal coils V_a^{t+1}, the solution x^{t+1} can be found. Therefore the problem is solved once we fix the initial conditions x^{t_0}, ν^{t_0}, $V_a^{t_0}$ and we know the values of the constraints and input voltages step-by-step. The circuit equation has been treated as a DAE[23] : the general method to solve numerically DAEs is called θ-method. In this particular case $\theta = 1$ and the method is then called *implicit Euler's*[24] . A typical run of FGE requires firstly to obtain an initial active coil and vessel configuration for a wanted plasma shape using FBT. The initial plasma current and poloidal flux could then be obtained using FGS. Once the initial conditions have been obtained it is possible to run FGE to simulate a plasma evolution. This procedure is very useful to control design and tuning. For the linearization procedures we adopted the formalism of [8] and [14].

1.4.1.1 FGE linearization

In this section the linearization of F-function is performed along an equilibrium plasma trajectory for FGE, which means a trajectory of I_e for which the equilibirum is kept fixed while inducing the plasma current with external coils [8]. The linearization is computed assuming a fixed I_p current[25] . The linearization of the F-function simplifies the formalism of the current circuit equation and allows to write the problem in state-space. In this way it is described the evolution of the circuit currents (both active and passive structures) around a nominal point $x_0 = [I_{y,0}\ I_{e,0}\ \alpha_{g,0}\ c_0]^T$ that is solution of the operator F:

$$F(x_0) = \underline{0}$$

The output equation is obtained instead from the linearization of the measurements, and will be treated in the next section. We can expand $G(x_0+\delta x)$ in Taylor series and truncate to the first order and furthermore we aim to find small δx perturbations s.t. $G(x_0+\delta x)$ is zero at first order:

$$G(x_0 + \delta x) = G(x_0) + \nabla_x G\big|_{x=x_0} \delta x + \mathcal{O}(\delta x^2)$$

[22] In our work $c^t = \{I_p(t),\, \beta_p(t),\, q_A(t)\}$.

[23] *Differential algebraic equation.*

[24] It can be proved that the method is asymptotically stable if $\theta \leq \frac{1}{2}$.

[25] The case of a *current diffusion equation*, valid during the stationary phase, is presented in [2]. In this case the basis function coefficients must be such that I_p matches the I_p computed by the *CDE* [8].

where $\nabla_x G\big|_{x=x_0}$ is the Jacobian of G evaluated in x_0. With our hypothesis on small perturbations we get $\nabla_x G\big|_{x=x_0}\delta x = 0$, i.e. $\delta x \in \ker \nabla_x G\big|_{x=x_0}$.
Since $G(x) = [G_y(x)\ G_g(x)]^T \in \mathbb{R}^{n_y+n_{\alpha_g}}$ we can rewrite the previous equation in the following way:

$$\begin{pmatrix} \nabla_{I_y} G_y\big|_{x=x_0} & \nabla_{I_e} G_y\big|_{x=x_0} & \nabla_{\alpha_g} G_y\big|_{x=x_0} & \underline{0} \\ \nabla_{I_y} G_g\big|_{x=x_0} & \nabla_{I_e} G_g\big|_{x=x_0} & \nabla_{\alpha_g} G_g\big|_{x=x_0} & \nabla_c G_g\big|_{x=x_0} \end{pmatrix} \begin{pmatrix} \delta I_y \\ \delta I_e \\ \delta \alpha_g \\ \delta c \end{pmatrix} = \underline{0}$$

where $\dim \nabla_{I_y} G_y = n_y \times n_y$, $\dim \nabla_{I_e} G_y = n_y \times n_e$ and so on. Since the constraits vector c doesn't appear directly in G_y we have that $\nabla_c G_y = \underline{0}\ \forall x$. If $c \in \mathbb{R}^{n_{\alpha_g}}$, i.e. there are as many constraint equations as basis function coefficients, the matrix $\nabla_{\alpha_g} G_g$ has full rank and so it can be inverted. From the second line of the system is then possible to isolate the unknown $\delta\alpha_g$:

$$\delta\alpha_g = -(\nabla_{\alpha_g} G_g\big|_{x=x_0})^{-1}\left[\nabla_{I_y} G_g\big|_{x=x_0}\,\delta I_y + \nabla_{I_e} G_g\big|_{x=x_0}\,\delta I_e + \nabla_c G_g\big|_{x=x_0}\,\delta c\right]$$

Therefore, by replacing it into the first line of the system we obtain:

$$Z_1\,\delta I_y + Z_2\,\delta c + Z_3\,\delta I_e = 0$$

with:

$$\begin{cases} Z_1 \equiv [\nabla_{I_y} G_y\big|_{x=x_0} + \nabla_{\alpha_g} G_y\big|_{x=x_0}(-(\nabla_{\alpha_g} G_g\big|_{x=x_0})^{-1}\nabla_{I_y} G_g\big|_{x=x_0})] \\ Z_2 \equiv [\nabla_{\alpha_g} G_y\big|_{x=x_0}(-(\nabla_{\alpha_g} G_g\big|_{x=x_0})^{-1}\nabla_c G_g\big|_{x=x_0})] \\ Z_3 \equiv [\nabla_{I_e} G_y\big|_{x=x_0} + \nabla_{\alpha_g} G_y\big|_{x=x_0}(-(\nabla_{\alpha_g} G_g\big|_{x=x_0})^{-1}\nabla_{I_e} G_g\big|_{x=x_0})] \end{cases}$$

We can then isolate the unknown δI_y:

$$\delta I_y = D_c^{I_y}\,\delta c + D_{I_e}^{I_y}\,\delta I_e$$

with:

$$\begin{cases} D_c^{I_y} = -Z_1^{-1}\,Z_2 \\ D_{I_e}^{I_y} = -Z_1^{-1}\,Z_3 \end{cases}$$

δI_y is now a function only of δc and δI_e. Replacing δI_y into $\delta\alpha_g$ we obtain:

$$\delta\alpha_g = D_c^{\alpha_g}\,\delta c + D_{I_e}^{\alpha_g}\,\delta I_e$$

with:

$$\begin{cases} D_c^{\alpha_g} = -(\nabla_{\alpha_g} G_g\big|_{x=x_0})^{-1}[\nabla_{I_y} G_g\big|_{x=x_0}\,D_c^{I_y} + \nabla_c G_g\big|_{x=x_0}] \\ D_{I_e}^{\alpha_g} = -(\nabla_{\alpha_g} G_g\big|_{x=x_0})^{-1}[\nabla_{I_y} G_g\big|_{x=x_0}\,D_{I_e}^{I_y} + \nabla_{I_e} G_g\big|_{x=x_0}] \end{cases}$$

Now since both $\delta\alpha_g$ and δI_y are functions of only δc and δI_e we can write:

$$\begin{cases} D_c^{\alpha_g} = \nabla_c\,\alpha_g\big|_{x=x_0} \\ D_{I_e}^{\alpha_g} = \nabla_{I_e}\alpha_g\big|_{x=x_0} \\ D_c^{I_y} = \nabla_c\,I_y\big|_{x=x_0} \\ D_{I_e}^{I_y} = \nabla_{I_e} I_y\big|_{x=x_0} \end{cases}$$

Now let's consider the first two equations in the definition of the F-function:

$$\begin{cases} \dot{\Psi}_e = V_a - R_e I_e \\ \Psi_e = M_{ee} I_e + M_{ey} I_y \end{cases}$$

Collecting them together and recalling that the mutual inductances are time-invariant, we obtain:

$$M_{ee}\dot{I}_e + M_{ey}\dot{I}_y = V_a - R_e I_e$$

Since we are linearizing around the fixed nominal point x_0 we have that:

$$\begin{cases} I_e(t) = I_{e,0} + \delta I_e(t) \\ I_y(t) = I_{y,0} + \delta I_y(t) \\ c(t) = c_0 + \delta c(t) \end{cases}$$

Thus:

$$\begin{cases} \dot{I}_e = \delta \dot{I}_e \\ \dot{I}_y = \delta \dot{I}_y \end{cases}$$

Once again, since the we have linearized around an equilibrium point, the matrices $D_c^{I_y}$ and $D_{I_e}^{I_y}$ are assumed time-invariant. Therefore, substituting δI_y we obtain another set of equation that are functions only of δc and δI_e:

$$\begin{aligned} V_a - R_e I_e &= M_{ee}\dot{I}_e + M_{ey}\dot{I}_y = \\ &= M_{ee}\delta\dot{I}_e + M_{ey}\delta\dot{I}_y = \\ &= \left(M_{ee} + M_{ey}D_{I_e}^{I_y}\right)\delta\dot{I}_e + M_{ey}D_c^{I_y}\,\delta\dot{c} \end{aligned}$$

The linearized evolution of I_e can be written as:

$$M_1\,\dot{I}_e = M_2\,I_e + M_3\,\dot{c} + V_a$$

with:

$$\begin{cases} M_1 = M_{ee} + M_{ey}D_{I_e}^{I_y} \\ M_2 = -R_e \\ M_3 = -M_{ey}D_c^{I_y} \end{cases}$$

Finally, since c is assumed constant in time[26] and M_1 is invertible [27], we obtain the **continuous LTI state-space representation** for the state I_e:

$$\dot{I}_e = A\,I_e + B\,V_a$$

with:

$$\begin{cases} A = M_1^{-1}M_2 \\ B = M_1^{-1} \end{cases}$$

In order to implement a *Kalman filter* the previous continuous LTI model must be converted into a discrete one. Using an *implicit Euler's* scheme we obtain:

$$M_1\,\frac{I_e^{t+1} - I_e^t}{\Delta t} = M_2\,I_e^{t+1} + V_a^{t+1} + M_3\,\frac{\Delta c^{t+1}}{\Delta t}$$

where $\Delta c^{t+1} = c^{t+1} - c^t$ and V_a^{t+1} are supposed to be known at the next time step $t+1 = t + \Delta t$. Therefore:

$$I_e^{t+1} = (M_1 - \Delta t M_2)^{-1}\left[M_1\,I_e^t + \Delta t\,V_a^{t+1} + M_3\,\Delta c^{t+1}\right]$$

[26] If the constraints are not constant in time they can be considered as exogenous inputs in the state equations.

[27] M_{ee} (and M_{ey}) is invertible since in a magnetic system the energy is defined as $W_{ee} = I_e^T\,M_{ee}\,I_e$ and so M_{ee} (and M_{ey}) is positive definite. Thus M_1 is invertible since it is the sum of invertible matrices.

In the end we obtain the following **discrete LTI state-space representation**:

$$I_e^{t+1} = A\, I_e^t + B\, u^{t+1}$$

with:

$$\begin{cases} A \equiv (M_1 - \Delta t M_2)^{-1}\, M_1 \in \mathbb{R}^{n_e \times n_e} \\ B = [B_1\ B_2] \equiv (M_1 - \Delta t M_2)^{-1}\, [\Delta t\, \mathcal{I}_{n_e}\ \ M_3] \in \mathbb{R}^{n_e \times (n_e + n_{\alpha_g})} \\ u^{t+1} = [V^{t+1}\ \Delta c^{t+1}]^T \in \mathbb{R}^{n_e + n_{\alpha_g}} \end{cases}$$

since $V^{t+1} = [V_a^{t+1}\ V_v^{t+1}]^T = [V_a^{t+1}\ \underline{0}]^T \in \mathbb{R}^{n_e = n_a + n_v}$.

1.4.1.2 Measurements linearization

The output equation is obtained from the linearization of the measurements relations between $\{I_a,\ B_m,\ \Psi_f\}$ and $\{I_e,\ I_y\}$, around a nominal equilibrium point $x_0 = [I_{y,0}\ I_{e,0}\ \alpha_{g,0}\ c_0]^T$. Since we have proven that $I_y = I_y(I_e, c)$ and $\alpha_g = \alpha_g(I_e, c)$ the equilibrium point[28] reduces to $[I_{e,0}\ c_0]^T$. If we consider a generic measurement at time step t we can write:

$$y^t = y^t(I_y(I_e, c),\ I_e,\ \alpha_g(I_e, c),\ c) = y^t(I_e, c)$$

Linearizing around the equilibrium point $y_0 = y(I_{e,0}\ c_0)$ and remembering that no measurement depends explicitly on α_g or c we get:

$$y^t = y(I_{e,0}\ c_0) + \nabla_{I_e} y(I_{e,0}\ c_0)\, \delta I_e^t + \nabla_{I_y} y(I_{e,0}\ c_0)\, \delta I_y^t$$

Now remembering that:

$$\delta I_y = D_c^{I_y}\, \delta c + D_{I_e}^{I_y}\, \delta I_e$$

we obtain:

$$y^t = y(I_{e,0}\ c_0) + \nabla_{I_e} y(I_{e,0}\ c_0)\, \delta I_e^t + \nabla_{I_y} y(I_{e,0}\ c_0)\, D_{I_e}^{I_y}\, \delta I_e^t + \nabla_{I_y} y(I_{e,0}\ c_0)\, D_c^{I_y}\, \delta c^t$$

Assuming constant contraints, i.e. $\delta c^t \simeq \Delta c^t \approx \underline{0}$ [29], the equation takes the following form:

$$y^t = y(I_{e,0}\ c_0) + \left(\nabla_{I_e} y(I_{e,0}\ c_0) + \nabla_{I_y} y(I_{e,0}\ c_0)\, D_{I_e}^{I_y}\right) \delta I_e^t$$

that can be written in compact form:

$$\delta y^t = y^t - y(I_{e,0}\ c_0) = \left(\nabla_{I_e} y(I_{e,0}\ c_0) + \nabla_{I_y} y(I_{e,0}\ c_0)\, D_{I_e}^{I_y}\right) \delta I_e^t = C\, \delta I_e^t$$

So, together with the state equation, we reach the following **state-space description**:

$$\begin{cases} I_e^{t+1} = A\, I_e^t + B\, u^{t+1} \\ \delta y^t = C\, \delta I_e^t \end{cases}$$

Otherwise, if the constraits are time-varying (such as in the general form of the state equation presented at the end of the FGE linearization), the observer equation is given by:

$$\delta y^t = C\, \delta I_e^t + D\, \Delta c^t$$

with:

$$D = \nabla_{I_y} y(I_{e,0}\ c_0)\, D_c^{I_y} = \nabla_{I_y} y(I_{e,0}\ c_0)\, \nabla_c I_y(I_{e,0}\ c_0)$$

[28] An equilibrium point x_0 and an initial condition point x^0 are different concepts that, at steady-state, are linked together by a linear relation. For details see [25].

[29] In this assertion the passage between continuous and discrete formulation is implicit.

In the case of constant constraints, the magnetic probes relation is:

$$B_m = B_{me}\, I_e + B_{my}\, I_y$$

thus, linearizing around x_0 we obtain:

$$B_m^t = B_{m,0} + \left(B_{me} + B_{my}\, D_{I_e}^{I_y}\right)\delta I_e^t$$

therefore:

$$\delta B_m^t = \left(B_{me} + B_{my}\, D_{I_e}^{I_y}\right)\delta I_e^t$$

where $B_{m,0} = B_{me}\, I_{e,0} + B_{my}\, I_{y,0}$ is the value at the linearization point.
Similarly, the relation for the flux loops is:

$$\delta \Psi_f^t = \left(M_{fe} + M_{fy}\, D_{I_e}^{I_y}\right)\delta I_e^t$$

And for the active coils, remembering that $\delta I_e^t = [\delta I_a^t \ \delta I_v^t]^T$, we obtain trivially:

$$\delta I_a^t = [\,\mathcal{I}_{n_a} \ \ \underline{0}\,]\,\delta I_e^t$$

1.4.1.3 Choice of the frame in the observer equation

In the state-space representation with previously defined matrices A, B, C, D:

$$\begin{cases} I_e^{t+1} = A\, I_e^t + B\, u^{t+1} \\ \delta y^t = C\, \delta I_e^t + D\, \Delta c^t \end{cases}$$

the state equation of the model is described in a physical frame whereas the output equation is described in a relative frame with respect to the linearization point. It is possible to change coordinates and skip to a measurement equation in physical frame:

$$\begin{aligned} \delta y^t &= C\, \delta I_e^t + D\, \Delta c^t \\ y^t &= C\, I_e^t + D\, c^t + \tilde{D}\, \nu^t \end{aligned}$$

with:

$$\begin{cases} \tilde{D} \equiv \begin{bmatrix} -C & -D & \mathcal{I}_{n_y} \end{bmatrix} \\ \nu^t \equiv [I_{e,0} \ c_0 \ y_0]^T \in \mathbb{R}^{n_e + n_y + n_{\alpha_g}} \end{cases}$$

As a matter of fact, our transformation is based on the assumption that the total trajectory of I_e does not change the equilibrium[30], i.e. $\frac{\partial I_y}{\partial I_e}\, I_e$ is close to zero on the trajectory $I_e(t)$. This transformation holds at steady-state condition and close to the linearization point. Its validity decreases if is the plasma boundary is changing. Since the estimator is thought to be coupled to a controller, we will assume that the plasma will be close to its equilibrium. Otherwise, it is always possible to change coordinates in real time imposing non-constant nominal trajectories equations to switch from the relative formulation to the physical one. In this cases the transformation is less trivial but still well defined.
More details about this topic can be found in [25].

[30] *Weak definition*: Equilibrium is defined as the electrical condition on external currents for which forces are balanced and plasma is stabilized to a certain shape and average current I_p.

1.4.1.4 About Controllability and Observability of the system

In order to get structural informations on the previous system we have considered not varying constraints and we have analyzed two different shots in **Anamak**: the first stable with limiter plasma and the other unstable with diverted plasma. Since the dimensions of the system are big ($A \in \mathbb{R}^{208\times208}$, $B \in \mathbb{R}^{208\times8}$, $C \in \mathbb{R}^{40\times208}$) it has been performed a *singular value decomposition* of the Gramians of Controllability and Observability. A similar procedure was used in [7].

Theorem 1. *The n-state discrete LTI system* $x^{t+1} = A\,x^t + B\,u^{t+1}$ *is controllable iff the* ***Controllability Gramian****:*

$$W_c(k) = \sum_{i=0}^{k} A^{k-i}\,B\,B^T\,(A^T)^{k-i} \in \mathbb{R}^{n\times n}$$

is positive definite for some $k < \infty$*. In this case* W_c *is the positive definite solution of the* ***Lyapunov equation****:*

$$W_c(k) = A\,W_c\,A^T + B\,B^T$$

Theorem 2. *The n-state discrete LTI system:*

$$\begin{cases} x^{t+1} = A\,x^t + B\,u^{t+1} \\ y^t = C\,x^t \end{cases}$$

is observable iff the ***Observability Gramian****:*

$$W_o(k) = \sum_{i=0}^{k} (A^T)^i\,C^T\,C\,(A)^i \in \mathbb{R}^{n\times n}$$

is positive definite for some $k < \infty$*. In this case* W_o *is the positive definite solution of the* ***Lyapunov equation****:*

$$W_o = A^T\,W_c\,A + C^T\,C$$

In the stable shot, if we look at the 2-norm induced *condition number* $\kappa = \frac{\sigma_{\max}}{\sigma_{\min}}$ we can see that both Gramians are very ill-conditioned, indeed $\kappa_o = \kappa(W_o) = 1.7279 \cdot 10^{19}$ and $\kappa_c = \kappa(W_c) = 4.2787 \cdot 10^{21}$. Furthermore, we can see that all the eigenvalues of A have absolute value minor than one and so, even if the Gramians are singular (as we can see from SVD), the system is both stabilizable and detectable. In the unstable shot there is an eigenvalue of A which has absolute value major than one. This eigenvalue represents the vertical instability and it is always present in vertically elongated plasma profiles.

In any case the unstable subsystem is both controllable and observable since there exist a non singular input actuator and a non singular state-observer for this subsystem. To check this we have verified that this unstable eigenvalue is not in the null spaces of the Observability and Controllability Gramians, therefore also in the unstable case we have a stabilizable and detectable system.

Finally, since we are in the hypothesis of the *general DRE convergence theorem*, we can use for these systems both *adaptative* or *asymptotic* Kalman filters. The results are shown in the following figures (1.7).

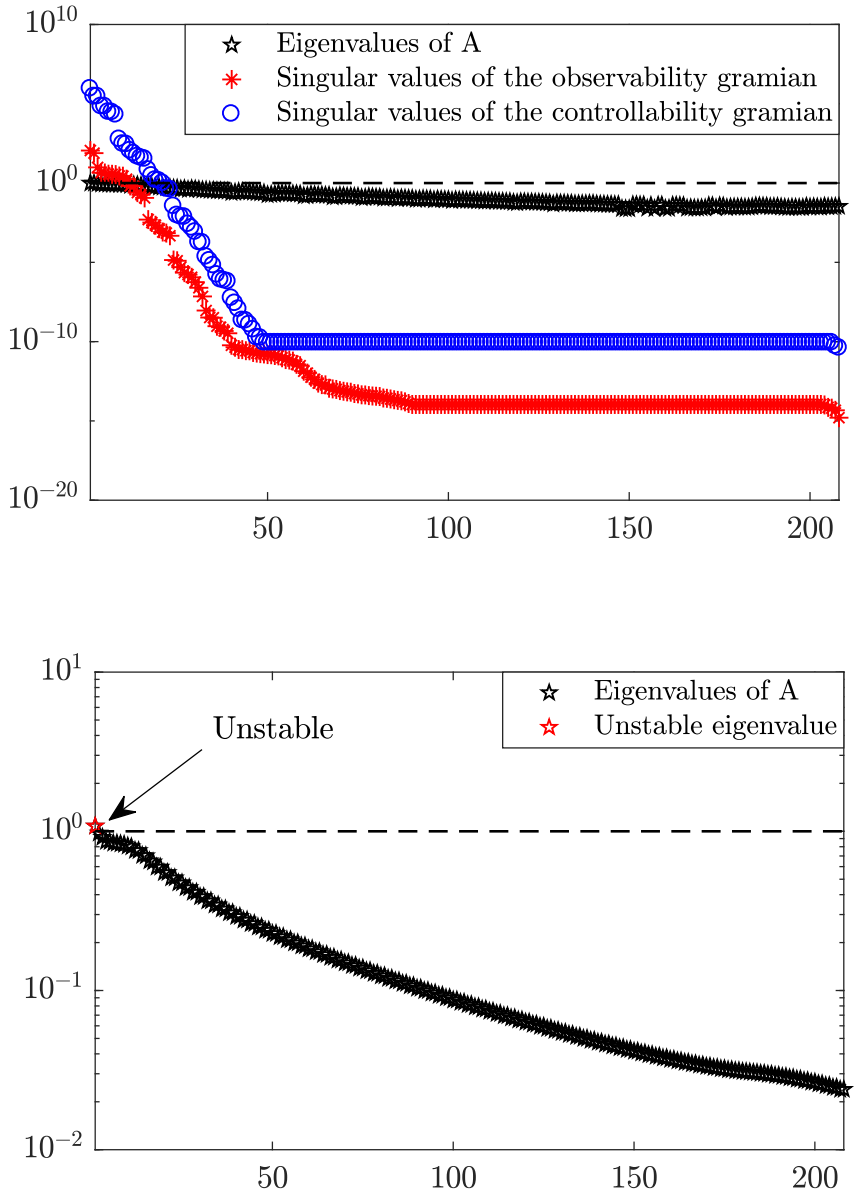

Figure 1.7: Stable limiter plasma shot (higher) and unstable diverted plasma shot (lower)

Chapter 2

State observer design

In control theory, a state observer is a dynamical system that provides an estimate of the internal state of a given real system, from measurements of the input and output of the real system and using a model of the system. Knowing the system state is necessary to solve many control theory problems for example, stabilizing a system using state feedback. In many practical cases, the physical state of the system cannot be determined by direct observation. Instead, indirect effects of the internal state are observed by means of the system's outputs. In our work the building of a state observer is required since the vessel currents, taking part of the state, are difficult to measure. Vessels currents have great influence on the plasma behaviour, since they participate, together with active coil currents and plasma current, to the poloidal flux evolution. Tokamak vessels are also of paramount importance as their induced currents slow down vertical displacement events [6]. Vessel currents vector I_v is not readily available but can be modeled with a certain degree of uncertainty. An observer would aim to best estimate I_v and this will be done in TCV by means of a real-time *Kalman filter*. Moreover, the observer based on Kalman filter is the optimal linear estimator [1] and it is of foundamental importance in LQG control [2].
Since we have already introduced our state-space model, the notation for the Kalman filter's parameters will follow the one of the model in exam.

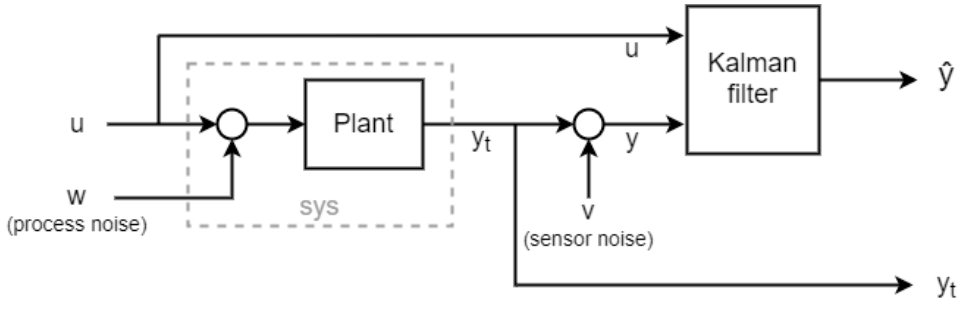

Figure 2.1: Kalman filter block diagram, (From [16])

[1] If the noises are white and uncorrelated or if the covariances of the noises are known exactly.
[2] Thanks to *Separation Principle* on LQR and LQE.

2.1 Kalman Filter for state estimation

In this section, we will develop the observer of the active coils and vessel currents using a *Kalman filter* algorithm. Before starting writing the equations of our specific work let's refresh what a Kalman filter does and which formulation has been adopted.

Let's consider the following discrete dynamical system:

$$\begin{cases} x(t+1) &= F(t)\,x(t) + G(t)\,u(t) + w(t) \\ y(t) &= H(t)\,x(t) + v(t) \quad , \qquad t \in \mathbb{Z} \end{cases}$$

where, if $\delta(t)$ indicates the Kronecker delta and the white noises w and v are uncorrelated:

$$\begin{aligned} &\mathbb{E}\left[w(t)\right] = 0 \ , \ \forall\, t \\ &\mathbb{E}\left[v(t)\right] = 0 \ , \ \forall\, t \\ &\mathbb{E}\left[w(t_1)\,w^T(t_2)\right] = Q(t_1)\,\delta(t_2 - t_1) \\ &\mathbb{E}\left[v(t_1)\,v^T(t_2)\right] = R(t_1)\,\delta(t_2 - t_1) \\ &\mathbb{E}\left[w(t_k)\,v^T(t_j)\right] = 0 \end{aligned}$$

As we can see in the Appendix (A.3.2.2 , A.3.3), the equations for the *Kalman one-step predictor* are the following:

$$\begin{cases} \hat{x}(N+1 \mid N) &= F(N)\,\hat{x}(N \mid N-1) + G(N)\,u(N) + K(N)\,e(N) \\ \hat{y}(N+1 \mid N) &= H(N)\,\hat{x}(N+1 \mid N) \\ e(N) &= y(N) - \hat{y}(N \mid N-1) \end{cases}$$

where e is the *innovation* and $K(N)$ is the *Kalman predictor gain*:

$$K(N) = \left[F\,P(N)\,H^T\right]\left[H\,P(N)\,H^T + R(N)\right]^{-1}$$

with covariance matrix of the state predictor error:

$$P(N) = \mathbb{E}\left[\,\nu(N)\,\nu(N)\right]^T] = Var\left[\nu(N)\right]$$

solving the DRE. Moreover, we performed the equations of the filter too:

$$\hat{x}(N \mid N) = \hat{x}(N \mid N-1) + K_0(N)\,e(N)$$

where $K_0(N)$ is the *Kalman filter gain*:

$$K_0(N) = P(N)\,H^T]\left[H\,P(N)\,H^T + R(N)\right]^{-1}$$

In order to give a coherent and consistent formulation to the problem, accordingly to the previous works around Kalman filters applications in **TCV** [14], let's rename some of the main quantities:

Definition 1. *(**"a priori" estimate**) Given a set of $N-1$ measurements $y^{N-1} = [y(N-1)^T \dots y(t_0)^T]^T = [y(N-1)^T \dots y(1)^T]^T$, where the output at time t is s.t. $y(t) = y_t \in \mathbb{R}^p$, $k \in \{1, ..., N-1\}$ we call **"a priori" estimate** of the state $x(t) \in \mathbb{R}^n$ the quantity:*

$$\hat{x}_N^- = \hat{x}(N \mid N-1) = \mathbb{E}\left[x\,(N) \mid y(N-1)\,,\,\dots\,,\,y(1)\right]$$

Definition 2. *(**"a posteriori" estimate**) Given a set of N measurements $y^N = [y(N)^T \dots y(t_0)^T]^T = [y(N)^T \dots y(1)^T]^T$, where the output at time t is s.t. $y(t) = y_t \in \mathbb{R}^p$, $k \in \{1, ..., N\}$ we call **"a posteriori" estimate** of the state $x(t) \in \mathbb{R}^n$ the quantity:*

$$\hat{x}_N^+ = \hat{x}(N \mid N) = \mathbb{E}\left[x\,(N) \mid y(N)\,,\,\dots\,,\,y(1)\right]$$

Definition 3. *(**"a priori" estimation error covariance**) Given the state prediction error also called "a priori" estimation error:*

$$\epsilon_N^- = \nu(N) = x(N) - \hat{x}(N \mid N-1) = x(N) - \hat{x}_N^-$$

*we call **"a priori" estimation error covariance** the already defined **variance matrix of state predictor error**:*

$$P_N^- = P(N) = Var[\nu(N)] = \mathbb{E}\left[[x(N) - \hat{x}_N^-]\,[x(N) - \hat{x}_N^-]^T\right]$$

Definition 4. *(**"a posteriori" estimation error covariance**) Given the state filter error also called "a posteriori" estimation error:*

$$\epsilon_N^+ = x(N) - \hat{x}(N \mid N) = x(N) - \hat{x}_N^+$$

*we call **"a posteriori" estimation error covariance** the already defined **variance matrix of filter error**:*

$$P_N^+ = Var[x(N) - \hat{x}_N^+] = \mathbb{E}\left[[x(N) - \hat{x}_N^+]\,[x(N) - \hat{x}_N^+]^T\right]$$

The covariance matrices of the state and the observer equations will be renamed with Q and R. With the above replacements it is now possible to recast the *Kalman filter algorithm* presented in the Appendix into a computationally more convenient set of equations based on time-update and measurement-update[3] . In order to avoid overloading the notation we will use x^t instead of $x(t)$.

2.1.1 Time-update and measurement-update formulation

We will now develop the filter equations that will be used in the numerical code. The results are developed in the relative frame and matrices are supposed fixed, nevertheless the results are the same if we replace X with X_t, $X \in \{A, B, C\}$. In our specific work the measurement vector at time t can be expressed both in a physical or relative frame, i.e. $y^t = y(t)$ or $\delta y^t = \delta y(t)$. We referred to [22] (in particular p. 85 and ch. 5-7).

Theorem 1. *If we consider the n-state discrete LTI system:*

$$\begin{cases} x^{t+1} = A\,x^t + B\,u^t + G\,w^t \\ y^t = C\,x^t + v^t \end{cases}$$

*with u^t deterministic input, $w^t \sim (\underline{0}, Q_w^t)$ [4] and $v^t \sim (\underline{0}, R^t)$ zero-mean uncorrelated noises with symmetric and positive definite covariance matrices $\forall\, t$, the **linear**[5] **adaptative**[6] **unbiased miniumum variance estimator** is the one who is retrieved by the following*

[3] The equivalence between the *one-step Kalman predictor/filter* formulation and the time/measurement-update equations is described in [22].

[4] G is the matrix connecting the input noise to the state. For example, if x is a current and w is a voltage noise, then G is a conductance.

[5] If the noises are Gaussian then it will be the *minimum variance estimator*. In this work the noises will be supposed normally distributed.

[6] If we are in the hypothesis of the *general DRE convergence theorem* it is possible to compute the steady-state gain of the filter without iterations.

set of equations[7] *:*

$$
\begin{aligned}
P_t^- &= A\,P_{t-1}^+\,A^T + Q^t \\
K_t &= P_t^-\,C^T\,[\,C\,P_t^-\,C^T + R^t\,]^{-1} \\
\hat{x}_t^- &= A\,\hat{x}_{t-1}^+ + B\,u^{t-1} \\
\hat{x}_t^+ &= \hat{x}_t^- + K_t\,e_t = \hat{x}_t^- + K_t\,[\,y^t - C\,\hat{x}_t^-\,] \\
P_t^+ &= [\,\mathcal{I} - K_t\,C\,]\,P_t^-\,[\,\mathcal{I} - K_t\,C\,]^T + K_t\,R^t\,K_t^T
\end{aligned}
$$

where e_t is the ***innovation*** *and $Q^t = G\,Q_w^t\,G^T$, and where the equations for $\hat{x}_t^-$ and P_t^- are the* ***time-update equations*** *for $\hat{x}$ and P, whereas the equations for $\hat{x}_t^+$ and P_t^+ are the* ***measurement-update equations*** *for $\hat{x}$ and P.*

Proof. Given the set of measurements $Y^t \equiv \{y^1, ..., y^t\}$ from time $t_0 = 1$ to time t, we look at the linear estimate of the state $\hat{x}_t$ which fulfills $\forall\, t$ the following conditions:

- $\mathbb{E}\,[x^t - \hat{x}_t] = \underline{0}$ Unbiased condition
- $\hat{x}_t = \arg\min_{\hat{x}_t} \mathbb{E}\,[\|x^t - \hat{x}_t\|_2^2]$ Minimum square error condition

Since we do not have any measurement avaible to estimate $x(0)$ since the first measurement is taken at time $t_0 = 1$, it is reasonable to initialize the algorithm imposing $\hat{x}_0^+$ as the expected value of the initial state $x_0 = x(0)$ [8] :

$$
\hat{x}(0 \mid 0) = \hat{x}_0^+ = \mathbb{E}\,[x_0] \qquad\qquad P_0^+ = \mathbb{E}\,[[x_0 - \hat{x}_0^+]\,[x_0 - \hat{x}_0^+]^T]
$$

Therefore, supposing to know the "a posteriori" estimate of the state $\hat{x}_t^+$ at time t, the "a priori" estimate at time $t+1$ given Y^t is, by induction:

$$
\begin{aligned}
\hat{x}_{t+1}^- &= \mathbb{E}\,[x^{t+1} \mid Y^t] = \mathbb{E}\,[A\,x^t + B\,u^t + G\,w^t \mid Y^t] = \\
&= A\,\mathbb{E}\,[x^t \mid Y^t] + B\,u^t + G\,\mathbb{E}\,[w^t \mid Y^t] = A\,\hat{x}_t^+ + B\,u^t
\end{aligned}
$$

Moreover, if we suppose the "a posteriori" estimate of the state $\hat{x}_t^+$ to be unbiased, i.e. $\mathbb{E}\,[\hat{x}_t^+] = \mathbb{E}\,[x^t]$, then also $\hat{x}_{t+1}^-$ will be unbiased:

$$
\begin{aligned}
\mathbb{E}\,[\hat{x}_{t+1}^-] &= \mathbb{E}\,[A\,\hat{x}_t^+] + B\,u^t = \\
&= \mathbb{E}\,[A\,x^t] + B\,u^t = \\
&= \mathbb{E}\,[A\,\hat{x}_t^+ + B\,u^t] = \mathbb{E}\,[x^{t+1}]
\end{aligned}
$$

The "a priori" estimation error covariance is therefore given by:

$$
\begin{aligned}
P_{t+1}^- &= \mathbb{E}\,[[x^{t+1} - \hat{x}_{t+1}^-]\,[x^{t+1} - \hat{x}_{t+1}^-]^T] = \\
&= A\,\mathbb{E}\,[[x^t - \hat{x}_t^+]\,[x^t - \hat{x}_t^+]^T]\,A^T + G\,\mathbb{E}\,[[w^t]\,[w^t]^T]\,G^T = \\
&= A\,P_t^+\,A^T + G\,Q_w^t\,G^T = A\,P_t^+\,A^T + Q^t
\end{aligned}
$$

Since we know $\hat{x}_{t+1}^-$ and P_{t+1}^- if we suppose to get a new measurement y^{t+1} we write our "a posteriori" estimate as a weighted sum of the prediction and the new observation. We aim to find the gain matrices L_{t+1} and K_{t+1} s.t.:

$$
\hat{x}_{t+1}^+ = L_{t+1}\,\hat{x}_{t+1}^- + K_{t+1}\,y^{t+1}
$$

[7] If we use the physical frame, we must add into the innovation at third equation $\hat{D}\,\nu^t$ (1.4.1.3) too.

[8] Otherwise, we can initialize the algorithm at time $t_0 = 1$ starting from an "a priori" guess, i.e.:

$$
\hat{x}(1 \mid 0) = \hat{x}_1^- = x(1) \qquad\qquad P(1) = P_1^- = \mathbb{E}\,[[x(1) - \hat{x}_1^-]\,[x(1) - \hat{x}_1^-]^T]
$$

.

with $\hat{x}_{t+1}^{+}$ satisfying the unbiased condition and minimizing the conditional square error. If we take the mean of the "a posteriori" estimate and we use the condition that the "a priori" estimate is unbiased, we obtain:

$$\begin{aligned}\mathbb{E}\left[\hat{x}_{t+1}^{+}\right] &= \mathbb{E}\left[L_{t+1}\,\hat{x}_{t+1}^{-} + K_{t+1}\,y^{t+1}\right] = \\ &= \mathbb{E}\left[L_{t+1}\,\hat{x}_{t+1}^{-} + K_{t+1}\,C\,x^{t+1} + K_{t+1}\,v^{t}\right] = \\ &= L_{t+1}\,\mathbb{E}\left[\hat{x}_{t+1}^{-}\right] + K_{t+1}\,C\,\mathbb{E}\left[x^{t+1}\right] = \left[L_{t+1} + K_{t+1}\,C\right]\mathbb{E}\left[x^{t+1}\right]\end{aligned}$$

To obtain the "a posteriori" estimate unbiased we must impose that:

$$L_{t+1} + K_{t+1}\,C = \mathcal{I} \;\;\Rightarrow\;\; L_{t+1} = \mathcal{I} - K_{t+1}\,C$$

Thus:

$$\begin{aligned}\hat{x}_{t+1}^{+} &= L_{t+1}\,\hat{x}_{t+1}^{-} + K_{t+1}\,y^{t+1} = \\ &= \left[\mathcal{I} - K_{t+1}\,C\right]\hat{x}_{t+1}^{-} + K_{t+1}\,y^{t+1} = \\ &= \hat{x}_{t+1}^{-} + K_{t+1}\left[y^{t+1} - C\,\hat{x}_{t+1}^{-}\right] = \hat{x}_{t+1}^{-} + K_{t+1}\,e_{t+1}\end{aligned}$$

The "a posteriori" estimation error covariance is therefore given by:

$$\begin{aligned}&P_{t+1}^{+} = \mathbb{E}\left[\left[x^{t+1} - \hat{x}_{t+1}^{+}\right]\left[x^{t+1} - \hat{x}_{t+1}^{+}\right]^{T}\right] = \\ &= \mathbb{E}\left[\left[x^{t+1} - \left[\mathcal{I} - K_{t+1}\,C\right]\hat{x}_{t+1}^{-} - K_{t+1}\,y^{t+1}\right]\left[x^{t+1} - \left[\mathcal{I} - K_{t+1}\,C\right]\hat{x}_{t+1}^{-} - K_{t+1}\,y^{t+1}\right]^{T}\right] = \\ &= \mathbb{E}\left[\left[x^{t+1} - \left[\mathcal{I} - K_{t+1}C\right]\hat{x}_{t+1}^{-} - K_{t+1}[Cx^{t+1} + v^{t+1}]\right]\left[x^{t+1} - \left[\mathcal{I} - K_{t+1}C\right]\hat{x}_{t+1}^{-} - K_{t+1}[Cx^{t+1} + v^{t+1}]\right]^{T}\right] \\ &= \mathbb{E}\left[\left[\left[\mathcal{I} - K_{t+1}C\right][x^{t+1} - \hat{x}_{t+1}^{-}] - K_{t+1}v^{t+1}\right]\left[\left[\mathcal{I} - K_{t+1}C\right][x^{t+1} - \hat{x}_{t+1}^{-}] - K_{t+1}v^{t+1}\right]^{T}\right] = \\ &= \left[\mathcal{I} - K_{t+1}C\right]P_{t+1}^{-}\left[\mathcal{I} - K_{t+1}C\right]^{T} - \left[\mathcal{I} - K_{t+1}C\right]\mathbb{E}\left[\left[x^{t+1} - \hat{x}_{t+1}^{-}\right]\left[v^{t+1}\right]^{T}\right]K_{t+1}^{T} - \\ &- K_{t+1}\,\mathbb{E}\left[\left[v^{t+1}\right]\left[x^{t+1} - \hat{x}_{t+1}^{-}\right]^{T}\right]\left[\mathcal{I} - K_{t+1}C\right]^{T} + K_{t+1}\,\mathbb{E}\left[\left[v^{t+1}\right]\left[v^{t+1}\right]^{T}\right]K_{t+1}^{T}\end{aligned}$$

Using the properties of the noise v^{t+1} and since the "a priori" estimation error $x^{t+1} - \hat{x}_{t+1}^{-}$ is independent of v^{t+1}, i.e. $\mathbb{E}\left[v^{t+1}\left[x^{t+1} - \hat{x}_{t+1}^{-}\right]^{T}\right] = \mathbb{E}\left[v^{t+1}\right]\mathbb{E}\left[x^{t+1} - \hat{x}_{t+1}^{-}\right] = 0$, we obtain:

$$P_{t+1}^{+} = \left[\mathcal{I} - K_{t+1}C\right]P_{t+1}^{-}\left[\mathcal{I} - K_{t+1}C\right]^{T} + K_{t+1}\,R^{t+1}\,K_{t+1}^{T}$$

Finally, using the assumption of minimum square error if we define as cost functional:

$$\begin{aligned}J_{t+1} &= \mathbb{E}\left[\|x^{t+1} - \hat{x}_{t+1}\|_2^2\right] = \\ &= \mathbb{E}\left[\left[x^{t+1} - \hat{x}_{t+1}^{+}\right]^{T}\left[x^{t+1} - \hat{x}_{t+1}^{+}\right]\right] = \\ &= \mathbb{E}\left[\,\mathrm{Tr}\left(\left[x^{t+1} - \hat{x}_{t+1}^{+}\right]\left[x^{t+1} - \hat{x}_{t+1}^{+}\right]^{T}\right)\right] = \\ &= \mathrm{Tr}\,\mathbb{E}\left[\left[x^{t+1} - \hat{x}_{t+1}^{+}\right]\left[x^{t+1} - \hat{x}_{t+1}^{+}\right]^{T}\right] = \mathrm{Tr}\,P_{t+1}^{+}\end{aligned}$$

Then:

$$K_{t+1}^{opt} = \arg\min_{K_{t+1}} J_{t+1}$$

Recalling that, if P is symmetric:

$$\frac{\partial}{\partial K}\Big(\mathrm{Tr}\left(K\,P\,K^{T}\right)\Big) = 2\,K\,P$$

then:

$$\frac{\partial J_{t+1}}{\partial K_{t+1}} = 2\left(\mathcal{I} - K_{t+1}\,C\right)P_{t+1}^{-}\left(-C^{T}\right) + 2\,K_{t+1}\,R^{t+1} = \mathbb{O}$$

and since both P^-_{t+1} and R^{t+1} are symmetric and positive definite we can find the optimal gain of the filter by matrix inversion:

$$K_{t+1} \equiv K^{opt}_{t+1} = P^-_{t+1}\, C^T\, [\, C\, P^-_{t+1}\, C^T + R^{t+1}\,]^{-1}$$

□

Particular attention has to be set in the covariance matrices design and in the filter initialization. In our work we handled with time-invariant covariance matrices $Q^t = Q$ and $R^t = R$. A common choice in adapltive filtering has been to set $P^-_1 = 10\, Q$, like in [14], since we maintain a degree of incertitude on the initial condition.

2.2 Filter augmented state

In this subsection will be detailed the stochastic behavior of the system in order to develop our *Kalman filter* [14]. In our model Gaussianity for the noises will be assumed. Diagnostic noise in the the observer equation is represented with an additive white noise $v^t = v(t) \sim \mathcal{N}(0, R(t))$ with covariance matrix $R_t = R(t)$. This noise aims to model the measurement inaccurancies. The value of the covariance matrix R^t can be obtained from the standard deviation taken from devices references [18]. Adding noise v^t on the diagnostics has the same effect on a relative or physical frame description since:

$$(y^t + v^t) - y^0 = \delta y^t + v^t$$

On the other hand uncertainties on the active coil and vessel current model are described by an additive white noise in the state equation $w^t_x = w_x(t) \sim \mathcal{N}(0, Q^x(t))$ with covariance matrix $Q^x_t = Q^x(t)$ where the state update is the vector $x^{t+1} = I^{t+1}_e$.

Moreover we add an offset unknown disturbance vector in the state equation $\xi^t = \xi(t) \in \mathbb{R}^{n_\xi}$, $n_\xi \leq n_e$. These disturbances are assumed to be constant on average with white noise $w^t_\xi = w_\xi(t) \sim \mathcal{N}(0, Q^\xi(t))$ with covariance matrix $Q^\xi_t = Q^\xi(t)$ added to the evolution equation of these disturbances.

Finally, the state is augmented to account for time-varying constraint vector c [9] since it is never the case that the parameters used as constraints are constant during the shot and so we want the observer to be able to estimate them too. We consider the discrete-time derivative of the constraint to be constant on average, i.e. $\mathbb{E}[\Delta c^{t+1}] = \mathbb{E}[\Delta c^t]$, where $\Delta c^t \equiv c^t - c^{t-1}$. Again a white noise $w^t_{\Delta c} = w_{\Delta c}(t) \sim \mathcal{N}(0, Q^{\Delta c}(t))$ with covariance matrix $Q^{\Delta c}_t = Q^{\Delta c}(t)$ added to the evolution equation of these time derivatives. Another white noise $w^t_c = w_c(t) \sim \mathcal{N}(0, Q^c(t))$ with covariance matrix $Q^c_t = Q^c(t)$ is added as well to the evolution equation of the vector c, i.e. $c^{t+1} = c^t + \Delta c^t + w^t_c$.

Furthermore, the state can be augmented also to estimate the input voltage increment δV^t assuming a constant on average evolution of the voltage $V^t = [V^t_a\ V^t_v]^T = [V^{t+1}_a\ \underline{0}]^T \in \mathbb{R}^{n_e = n_a + n_v}$ s.t. $V^t = V^t_{\texttt{known}} + \delta V^t$ and adding a white noise $w^t_{\delta V} = w_{\delta V}(t) \sim \mathcal{N}(0, Q^{\delta V}(t))$ with covariance matrix $Q^{\delta V}_t = Q^{\delta V}(t)$ to the evolution equation of δV^t.

We obtain the following state-space set of equations:

[9] FGE code is built in a way assuming constraints on some of the internal parameters such as I_p, β_p, l_i or q_A s.t. $\dim c = \dim \alpha_g$.

$$\begin{cases} I_e^{t+1} = A\, I_e^t + B\, u^{t+1} + \xi^t + G\, w_x^t \\ \xi^{t+1} = \xi^t + w_\xi^t \\ \Delta c^{t+1} = \Delta c^t + w_{\Delta c}^t \\ c^{t+1} = c^t + \Delta c^t + w_c^t \\ \delta V^{t+1} = \delta V^t + w_{\delta V}^t \\ \delta y^t = C\, \delta I_e^t + D\, \Delta c^t + v^t \end{cases}$$

Matrices A, B, C, D [10] have already been defined in FGE linearization in Chapter 1 (1.4.1.1). As we will see the input vector $u^{t+1} = [V^{t+1}\ \Delta c^{t+1}]^T \in \mathbb{R}^{n_e+n_{\alpha g}}$ will be reduced only to the voltage since the contraints will be part of the state to be estimated. Matrix G accounts for the fact that process noise may enter in a different form than the state (the external currents). For example if the process noise appears in the input voltage, we take $G = R_e^{-1}$.
Let's gradually augment the state $x = I_e = [I_a\ I_v]^T \in \mathbb{R}^{n_e}$:

Constant disturbance: Assuming a constant disturbance $\xi_i \in \mathbb{R}$ on the state component $x_i \in \mathbb{R}$ evolution equation, with process noise w_ξ. The disturbances are stacked in a vector $\xi \in \mathbb{R}^{n_\xi}$. The disturbance can be added to each elements of the state or to selected parts of x in which case $n_\xi \leq n_e$. The state evolution at index i and time t is:

$$\begin{aligned} x_j^{t+1} &= A_j\, x^t + \xi_j^t + B_{1j}\, V^{t+1} \\ x_i^{t+1} &= A_i\, x^t + B_{1i}\, V^{t+1} \\ \xi_j &= \xi_j \end{aligned}$$

where A_j is the *j-th* line of A. In a matrix formulation we obtain:

$$\begin{pmatrix} x^{t+1} \\ \xi^{t+1} \end{pmatrix} = \begin{pmatrix} A & A_\xi \\ \mathbb{O}_{n_\xi \times n_e} & \mathcal{I}_{n_\xi \times n_\xi} \end{pmatrix} \begin{pmatrix} x^t \\ \xi^t \end{pmatrix} + \begin{pmatrix} B_1 \\ \mathbb{O}_{n_\xi \times n_a} \end{pmatrix} V^{t+1}$$

where the lines of the matrix A_ξ are non-zero only corresponding to the index on which the disturbance is added. For example, if we consider $n_e = 4$ and $n_\xi = 2$ and we add disturbances on x_1 and x_3 we obtain:

$$A_\xi = \begin{pmatrix} 1 & 0 \\ 0 & 0 \\ 0 & 1 \\ 0 & 0 \end{pmatrix}$$

The observer equation is not affected by these disturbances so:

$$\delta y^t = \begin{pmatrix} C & \mathbb{O}_{n_y \times n_\xi} \end{pmatrix} \begin{pmatrix} x^t \\ \xi^t \end{pmatrix}$$

In this way it is possible to account for constant disturbances on the state currents only in specific coils. By the way in the simulations on **TCV** shots, since the perturbation is unknown and can affect every coil, we have set $A_\xi = \mathcal{I}_{n_\xi \times n_\xi}$, with $n_\xi = n_e$.

[10] D matrix has not been introduced in the previous theorem (written in relative frame) since the stochastic part of the measurement equation is carried by the vector v^t. If we had considered D matrix the innovation would have been different, taking into account for the Δc^t deterministic input. But since Δc^t can be considered as a part of an augmented state of the system, the variables used for the statement are consistent.

Constraints: If we define the augmented state as $x^t = [I_e^t\ \Delta c^t\ c^t]^T \in \mathbb{R}^{n_e+2n_{\alpha_g}}$ the state space equations assume a different form with respect to the ones derived after FGE linearization[11] but keep the same physical meaning. We add the two state update equations:

$$\Delta c^{t+1} = \Delta c^t$$
$$c^{t+1} = c^t + (c^{t+1} - c^t) = c^t + \Delta c^{t+1} = c^t + \Delta c^t$$

Hence in matrix form we obtain:

$$\begin{pmatrix} x^{t+1} \\ \Delta c^{t+1} \\ c^{t+1} \end{pmatrix} = \begin{pmatrix} A & B_2 & \mathbb{O}_{n_e \times n_{\alpha_g}} \\ \mathbb{O}_{n_{\alpha_g} \times n_e} & \mathcal{I}_{n_{\alpha_g} \times n_{\alpha_g}} & \mathbb{O}_{n_{\alpha_g} \times n_{\alpha_g}} \\ \mathbb{O}_{n_{\alpha_g} \times n_e} & \mathcal{I}_{n_{\alpha_g} \times n_{\alpha_g}} & \mathcal{I}_{n_{\alpha_g} \times n_{\alpha_g}} \end{pmatrix} \begin{pmatrix} x^t \\ \Delta c^t \\ c^t \end{pmatrix} + \begin{pmatrix} B_1 \\ \mathbb{O}_{2n_{\alpha_g} \times n_a} \end{pmatrix} V^{t+1}$$

$$\delta y^t = \begin{pmatrix} C & D & \mathbb{O}_{n_y \times n_{\alpha_g}} \end{pmatrix} \begin{pmatrix} x^t \\ \Delta c^t \\ c^t \end{pmatrix}$$

where B_1 and B_2 are defined inside B matrix in the *FGE linearization section* around the nominal point $[I_{y,0}\ I_{e,0}\ \alpha_{g,0}\ c_0]^T$.

Constant input voltage perturbation: If we suppose the known input voltage $V^t_{\texttt{known}}$ over or underestimated by a factor $\delta V \in \mathbb{R}^{n_a}$ we can define the augmented state as $x^t = [I_e^t\ \delta V^t]^T \in \mathbb{R}^{n_e+n_a}$. In this case the disturbance is carried directly by the voltages: the effect is similar to the one induced by the *constant disturbances*, the main difference is that it is possible to augment the degree of freedom in the covariance matrix design if we assume a probability distribution on coils voltage errors. We obtain:

$$\begin{pmatrix} x^{t+1} \\ \delta V^{t+1} \end{pmatrix} = \begin{pmatrix} A & B_1 \\ \mathbb{O}_{n_a \times n_e} & \mathcal{I}_{n_a \times n_a} \end{pmatrix} \begin{pmatrix} x^t \\ \delta V^t \end{pmatrix} + \begin{pmatrix} B_1 \\ \mathbb{O}_{n_a \times n_a} \end{pmatrix} V^{t+1}_{\texttt{known}}$$

$$\delta y^t = \begin{pmatrix} C & \mathbb{O}_{n_y \times n_a} \end{pmatrix} \begin{pmatrix} x^t \\ \delta V^t \end{pmatrix}$$

General case: If we define the **augmented state** [12] as:

$$X^t \equiv [x^t\ \xi^t\ \Delta c^t\ c^t\ \delta V^t]^T$$

with $x^t = I_e^t$ and the vector of process disturbances as:

$$w^t \equiv [w_x^t\ w_\xi^t\ w_{\Delta c}^t\ w_c^t\ w_{\delta V}^t]^T$$

then the following state-space representation is reached:

$$\begin{cases} X^{t+1} = \mathbb{A}\, X^t + \mathbb{B}\, V^{t+1}_{\texttt{known}} + \mathbb{G}\, w^t \\ \delta y^t = \mathbb{C}\, \delta X^t + v^t \end{cases}$$

[11] In that case the constraints, if present, were interpreted as inputs into the state-equation.
[12] Since the measurements are fixed, if we augment the state we could loose degrees of observability [14].

with matrices:

$$\mathbb{A} = \begin{pmatrix} A & A_\xi & B_2 & \mathbb{O} & B_1 \\ \mathbb{O} & \mathcal{I} & \mathbb{O} & \mathbb{O} & \mathbb{O} \\ \mathbb{O} & \mathbb{O} & \mathcal{I} & \mathbb{O} & \mathbb{O} \\ \mathbb{O} & \mathbb{O} & \mathcal{I} & \mathcal{I} & \mathbb{O} \\ \mathbb{O} & \mathbb{O} & \mathbb{O} & \mathbb{O} & \mathcal{I} \end{pmatrix}$$

$$\mathbb{B} = \begin{pmatrix} B_1 \\ \mathbb{O} \\ \mathbb{O} \\ \mathbb{O} \\ \mathbb{O} \end{pmatrix}$$

$$\mathbb{C} = \begin{pmatrix} C & \mathbb{O} & D & \mathbb{O} & \mathbb{O} \end{pmatrix}$$

$$\mathbb{G} = \begin{pmatrix} G & \mathbb{O} & \mathbb{O} & \mathbb{O} & \mathbb{O} \\ \mathbb{O} & \mathcal{I} & \mathbb{O} & \mathbb{O} & \mathbb{O} \\ \mathbb{O} & \mathbb{O} & \mathcal{I} & \mathbb{O} & \mathbb{O} \\ \mathbb{O} & \mathbb{O} & \mathbb{O} & \mathcal{I} & \mathbb{O} \\ \mathbb{O} & \mathbb{O} & \mathbb{O} & \mathbb{O} & \mathcal{I} \end{pmatrix}$$

The state estimation problem of this LTI system can be solved using the *time-update* and *measurement-update* equations of the *Kalman filter* previously presented in (2.1.1) [13] , once we design the covariance matrices of the disturbances, that in our work will be assumed fixed in time. In this work we will also assume the noises on the state and the noises on the observer uncorrelated. A MATLAB function called KALSASS.M has been implemented to recover all state augmented combinations and it is discussed in (4.4).

2.3 Covariance matrix design

In this work we have considered time-invariant covariance matrices both for the process and the observer's errors.

First of all, we fix the covariance of the measurements errors: the matrix R is a block-diagonal matrix where each block is a diagonal matrix collecting the standard deviations of the diagnostics, respectively of the active currents, of the magnetic fiels and of the fluxes, i.e.: $\sigma_a = \omega_a^2 \mathcal{I}_{n_a} \in \mathbb{R}^{n_a}$, $\sigma_m = \omega_m^2 \mathcal{I}_{n_m} \in \mathbb{R}^{n_m}$, $\sigma_f = \omega_f^2 \mathcal{I}_{n_f} \in \mathbb{R}^{n_f}$, where $\{\omega_a, \omega_m, \omega_f\} = \{100\,\mathrm{A}, 10^{-3}\,\mathrm{T}, 10^{-3}\,\mathrm{Wb}\}$ s.t.:

$$R = \begin{pmatrix} \sigma_a & & \mathbb{O} \\ & \sigma_m & \\ \mathbb{O} & & \sigma_f \end{pmatrix}$$

The process covariance matrix Q has a block-diagonal structure too i.e.:

$$Q = \begin{pmatrix} Q_a & & \mathbb{O} \\ & Q_v & \\ \mathbb{O} & & Q_c \end{pmatrix}$$

where Q_a is the covariance matrix of the active currents, Q_v is the covariance matrix of the vessel currents and Q_c is the covariance matrix of the constraints.

[13] The matrices of the system are assumed time-invariant around the linearization point.

Since the active coils of **TCV** have independent power supplies the active currents are assumed independent, so $Q_a \in \mathbb{R}^{n_a}$ is diagonal. A practical and well performing choice of the diagonal terms is to take $Q_a = (\sigma_a)^{1/2} = \omega_a \mathcal{I}_{n_a}$.

In the other hand, since the vessel is modelled with discretized filaments sorrounding the cross-section, the vessel current are assumed correraled with each others with degree of correlation decreasing linearly with the distance. The idea has been to give $Q_v \in \mathbb{R}^{n_v}$ the structure of a *Toeplitz matrix*[14] . Moreover, since the vessel cross-section has a circular profile, the covariance between filaments k and $k+j$ should be the same between filaments k and $k-j$ and so, giving the filaments an increasing numbering from 1 to n_v, then $Cov_{12} = Q_v(1,2) = Cov_{1n_v} = Q_v(1,n_v)$. In particular two different Toeplitz matrices have been designed: one with continuous decreasing correlation between contiguous filaments and another one in which the correlation decreases linearly until a certain quantity of filaments, out of them the vessel currents are assumed uncorrelated. The limit distance between filaments in order to assume uncorrelation introduces a matrix gap between diagonals[15] and can be fixed manually. Degrees of freedom of such a matrix are then the gaps and the coefficients of the principal diagonal: a possible choice should be to take $Q_v(i,i) = \frac{1}{10} Q_a(k,k), i \in \{1,...,n_v\}, k \in \{1,...,n_a\}$. Moreover, if we use the eigenmode representation of the vessel the matrix Q_v will transform into Q_u in the following way:

$$Q_u = T_i \, Q_v \, T_i^T$$

where $T_i = T^{-1}$ is s.t. $I_v = T \, I_u$ with I_v filamentary vessel currents vector and I_u vessel eigencurrents vector. If we adopt a model reduction in order to take into account only a reduced relevant subset of slow eigenmodes, then $T_i = T^+$ is the *pseudoinverse* of T.

Finally, the matrix block $Q_c \in \mathbb{R}^{n_{\alpha_g}} = \mathbb{R}^3$ can be chosen diagonal supposing the constraints independent. The values of the optimal combination of coefficients varies with the shot that is considered: in order to tune properly this block, several shots of **TCV** have been performed with different covariances and compared to LIUQE results. In the Results Chapter (4.4) are reported several combinations of covariance matrices: the estimation behavior changes if we use a diagonal matrix or a not-sparse matrix Q_c counting for correlations between contraints errors.

If the filter is extended to account for δV and Δc quantities, their covariance matrices should be tuned properly for each shot. If c vector is no longer assumed constant in the time interval of operations so that the state is augmented to estimate the Δc contraint variation vector, it is possible to design a coupled block covariance matrix $Q_{c,\Delta c} \in \mathbb{R}^{2n_{\alpha_g}}$ (a possible design for it can be found in [14] and will be used in the β_p-ramp testcase (4.4.4.1)).

Finally, if the state is augmented to estimate constant perturbations, the simplest possibility is to define another block matrix $Q_\xi \in \mathbb{R}^{n_\xi}$, $n_\xi \leq n_e$ to fix into $Q \in \mathbb{R}^{n_x+n_\xi}$ and furthermore to choose diagonal this block (i.e. assuming the constant disturbances errors independent).

In the Results Chapter it will be shown that even if we make this assumption the constant disturbances are very well recovered by the filter even if the diagonals terms of Q_ξ are chosen small. However, in the restricted case of constant perturbations added only to the active coils currents (i.e. $n_\xi = n_a$) it has been assumed correlation only between the active

[14] i.e.: square matrix with constant decreasing diagonals from the principal one.

[15] We call gap the fixed number of contiguous vessel filaments that present correlation.

currents errors and the errors of the constant perturbations referring to the same coils (4.4.2.1). If we consider a coil i, with $i \in \{1, ..., n_a\}$, we have imposed that[16] :

$$Cov_{i_a i_\xi} = Q(i, i + n_a + n_u) = Q(i + n_a + n_u, i) = Cov_{i_\xi i_a} = \sqrt{Q_a(i,i)\, Q_\xi(i,i)}$$

In this case the matrix Q is no longer block diagonal.

In the pictures below the spectra of the vessel Toeplitz matrices in filamentary decomposition are shown both in the cases continuous and with gap. Finally, it is shown the spectrum of the process covariance matrix in previuously presented state augmented case with correlation. The pictures in figure 2.2 refers to **Anamak** and the vessel is described by its $n_u = 8$ slowest eigencurrents.

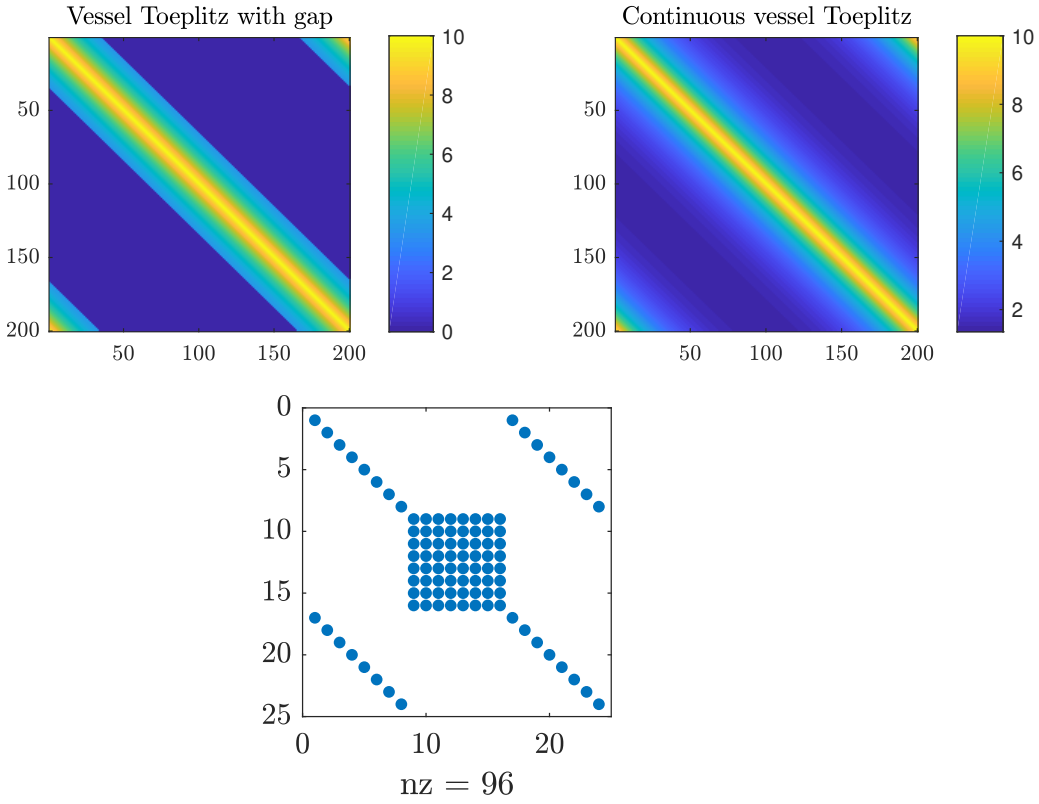

Figure 2.2: Sparsity pattern of Q with correlation, $n_a = n_u = n_\xi = 8 \wedge \ n_c = n_{\Delta\xi} = n_{\Delta c} = n_{\delta V} = 0$

[16] In this experience we have not estimated the constraints so we do not have the block Q_c.

Chapter 3

Filter validation

In this Chapter we discuss three analythical tests that have been implemented in order to verify the optimality of the filter and the assumptions of Gaussianity of the noises. All these tests are performed on the *innovation residuals* e_t (1 , 1) , [14], [7]. Before presenting the following statement (1), we rememeber that this result will remain consistent even if we consider the relative or the physical frame description, as discussed in (1.4.1.3).

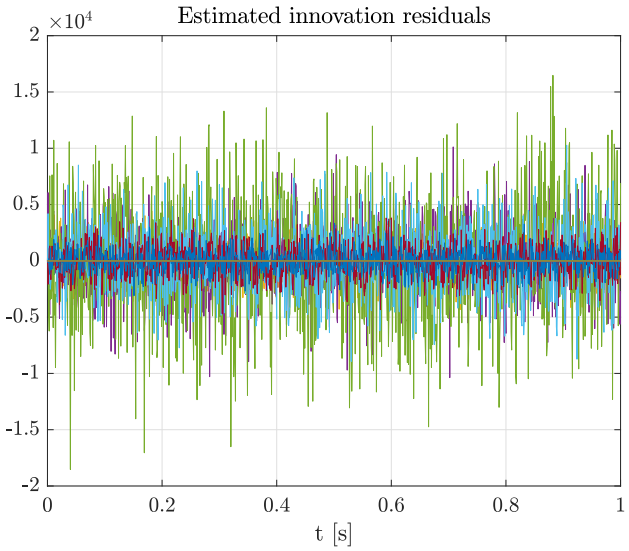

Figure 3.1: Typical innovation residuals dynamics along a simulation

3.1 Innovation as a white noise process

Proposition 1. *If we consider the innovation residuals at time t defined as:*

$$\begin{aligned} e_t &= \delta y - \delta \hat{y}_t^- = \delta y - C\,\delta \hat{x}_t^- = \\ &= y - \hat{y}_t^- = y - (C\,\hat{x}_t^- + \bar{D}\,\nu^t) = \\ &= (C\,x^t + \bar{D}\,\nu^t + v^t) - (C\,\hat{x}_t^- + \bar{D}\,\nu^t) = C\,\epsilon_t^- + v^t \end{aligned}$$

and iff we use the optimal Kalman gain in the filter equations, then the innovation residuals are uncorrelated in time and follow a centered Gaussian distribution of covariance matrix

$S_t = C\,P_t^-\,C^T + R^t \in \mathbb{R}^{n_y \times n_y}$, *i.e.:*

$$e_t \sim \mathcal{N}(\underline{0}, S_t)$$

Proof. Since the "a priori" estimate is unbiased then $\mathbb{E}[\epsilon_t^-] = \underline{0}$ and since v^t is white then:

$$\mathbb{E}[e_t] = C\,\mathbb{E}[\epsilon_t^-]\,C^T + \mathbb{E}[v^t] = \underline{0}$$

Therefore the covariance matrix is given by:

$$\begin{aligned} S_t &= \mathbb{E}[e_t\,e_t^T] = \mathbb{E}[[C\,\epsilon_t^- + v^t]\,[C\,\epsilon_t^- + v^t]^T] = \\ &= C\,\mathbb{E}[[\epsilon_t^-]\,[\epsilon_t^-]^T]\,C^T + C\,\mathbb{E}[[\epsilon_t^-]\,[v^t]^T] + \mathbb{E}[[v^t]\,[\epsilon_t^-]^T]\,C^T + \mathbb{E}[[v^t]\,[v^t]^T] = \\ &= C\,\mathbb{E}[[\epsilon_t^-]\,[\epsilon_t^-]^T]\,C^T + \mathbb{E}[[v^t]\,[v^t]^T] = C\,P_t^-\,C^T + R^t \end{aligned}$$

In order to prove that there is not cross-correlation in the innovation residuals let's consider a time instant $k < t$, thus:

$$\begin{aligned} \mathbb{E}[e_t\,e_k^T] &= C\,\mathbb{E}[[\epsilon_t^-]\,[\epsilon_k^-]^T]\,C^T + C\,\mathbb{E}[[\epsilon_t^-]\,[v^k]^T] + \mathbb{E}[[v^t]\,[\epsilon_k^-]^T]\,C^T + \mathbb{E}[[v^t]\,[v^k]^T] = \\ &= C\,\mathbb{E}[[\epsilon_t^-]\,[\epsilon_k^-]^T]\,C^T + C\,\mathbb{E}[[\epsilon_t^-]\,[v^k]^T] \end{aligned}$$

since the v^t are uncorrelated in time and since the state estimation is independent of future output noises. Let's obtain now the recursive equation of the state estimate error using Kalman filter equations:

$$\begin{aligned} \epsilon_{t+1}^- &= x^{t+1} - x_{t+1}^- = A\,x^t + B\,u^t + G\,w^t - A\,x_t^+ - B\,u^t = \\ &= A\,x^t + G\,w^t - A\,([\mathcal{I} - K_t\,C]\,x_t^- + K_t\,y^t) = \\ &= A\,x^t + G\,w^t - A\,([\mathcal{I} - K_t\,C]\,x_t^- + K_t\,C\,x^t + K_t\,v^t) = \\ &= A\,(x^t - x_t^-) - A\,K_t\,C\,(x^t - x_t^-) + G\,w^t - A\,K_t\,v^t = \\ &= A\,[\mathcal{I} - K_t\,C]\,\epsilon_t^- + (G\,w^t - A\,K_t\,v^t) = \Phi_t\,\epsilon_t^- + \tilde{v}^t \end{aligned}$$

Therefore, starting from initial condition ϵ_k^-, with $k < t$, then the free and forced evolutions become[1]:

$$\epsilon_t^- = \Phi_{t,k}\,\epsilon_k^- + \sum_{i=k}^{t-1} \Phi_{t,i+1}\,\tilde{v}^i$$

where:

$$\Phi_{t,k} = \begin{cases} \prod_{i=k}^{t} \Phi_i & , \quad t > k \\ \mathcal{I} & , \quad t = k \end{cases}$$

Now, since the forced term is zero mean we can then assert that:

$$\mathbb{E}[[\epsilon_t^-]\,[\epsilon_k^-]^T] = \Phi_{t,k}\,\mathbb{E}[[\epsilon_k^-]\,[\epsilon_k^-]^T] = \Phi_{t,k}\,P_k^-$$

Moreover $\mathbb{E}[[\epsilon_k^-]\,[v^k]^T] = \mathbb{O}$: the "a priori" state error estimate ϵ_k^- is indeed uncorrelated to the observer noise. Therefore, since $\mathbb{E}[[\tilde{v}^i]\,[v^k]^T] = \mathbb{O}$ if $k < i \leq t-1$, and since w^k and

[1] If the gain $K_t = K$ is constant $\forall\, t$, then $\Phi_t = \Phi$ is constant and we can rewrite the evolution of ϵ_t^- as:

$$\epsilon_t^- = \Phi^{t-k}\,\epsilon_k^- + \sum_{i=k}^{t-1} \Phi^{t-i-1}\,\tilde{v}^i$$

v^k are uncorrelated:

$$\begin{aligned}\mathbb{E}\left[[\epsilon_t^-]\,[v^k]^T\right] &= \mathbb{E}\left[\left(\Phi_{t,k}\,\epsilon_k^- + \sum_{i=k}^{t-1}\Phi_{t,i+1}\,\tilde{v}^i\right)[v^k]^T\right] = \\ &= \mathbb{E}\left[\left(\sum_{i=k}^{t-1}\Phi_{t,i+1}\,\tilde{v}^i\right)[v^k]^T\right] = \mathbb{E}\left[[\Phi_{t,k+1}\,\tilde{v}^k]\,[v^k]^T\right] = \\ &= \mathbb{E}\left[[\Phi_{t,k+1}\,(G\,w^k - A\,K_k\,v^k)]\,[v^k]^T\right] = -\Phi_{t,k+1}\,A\,K_k\,R^k\end{aligned}$$

Since $\Phi_{t,k} = \Phi_{t,k+1}\,\Phi_k$ we can now rewrite the previous cross-correlation equation for the innovation residuals as follows:

$$\begin{aligned}\mathbb{E}\left[e_t\,e_k^T\right] &= C\,\mathbb{E}\left[[\epsilon_t^-]\,[\epsilon_k^-]^T\right]C^T + C\,\mathbb{E}\left[[\epsilon_t^-]\,[v^k]^T\right] = \\ &= C\,\Phi_{t,k+1}\left[\Phi_k\,P_k^-\,C^T - A\,K_k\,R^k\right] = \\ &= C\,\Phi_{t,k+1}\left[A\left[\mathcal{I} - K_k\,C\right]P_k^-\,C^T - A\,K_k\,R^k\right] = \\ &= C\,\Phi_{t,k+1}\left[A\,P_k^-\,C^T - A\,K_k\,C\,P_k^-\,C^T - A\,K_k\,R^k\right] = \\ &= C\,\Phi_{t,k+1}\left[A\,P_k^-\,C^T - A\,K_k\,(C\,P_k^-\,C^T + R^k)\right]\end{aligned}$$

Finally, iff we use the *optimal Kalman gain* $K_k \equiv K_k^{opt} = P_k^-\,C^T\,[\,C\,P_k^-\,C^T + R^k\,]^{-1}$ we remove the cross-correlation in the innovation residuals, i.e.:

$$\mathbb{E}\left[e_t\,e_k^T\right] = C\,\Phi_{t,k+1}\left[A\,P_k^-\,C^T - A\,K_k\,(C\,P_k^-\,C^T + R^k)\right] = C\,\Phi_{t,k+1}\left[A\,P_k^-\,C^T - A\,P_k^-\,C^T\right] = \mathbb{O}$$

□

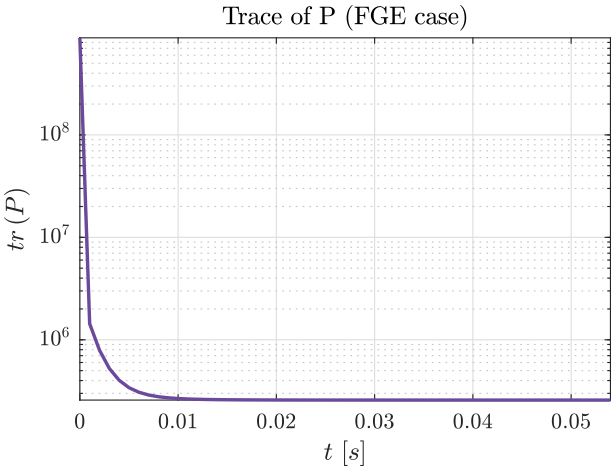

Figure 3.2: Trace of P_t^+ in **Anamak**, measurements taken from FGE, indexes from 1 to l with tolerance $\delta = 0.1$

In order to consistently evaluate the stochastic behaviour of the innovation residuals it should be necessary in principle to perform many runs of filter. We can instead assume the innovation residuals to be an *ergodic process*[2] [14] that after many time steps is statistically converging and thus perform the tests after each single run of the simulation. The tests presented below are indeed performed assuming that the filter has converged, i.e. that the

[2]A stochastic process $\{e_t\}_t$ is said to be ergodic if its statistical properties can be deduced from a single, sufficiently long, random sample of the process.

Frobenius norm[3] of the difference of the "a posteriori" estimation error covariance between two time steps is less than a user-defined tolerance δ. If n_t is the total number of time instants then the total amount of time-steps to perform the tests will be $N = n_t - l + 1$, with index $j = l$ s.t:

$$l = \arg\max_j \|P^+_{t(j)} - P^+_{t(j-1)}\|_F < \delta$$

The convergence is usually very fastly recovered as we can see in figure (3.2).

3.1.1 Test n^o 1 - 1σ gate test

For this test we have partitioned the innovation of the measurements at each time-step t in this way:

$$e_t = [e_{t,a}\ e_{t,m}\ e_{t,f}]^T \in \mathbb{R}^{n_y} = \mathbb{R}^{n_a+n_m+n_f}$$

In order to verify if the residuals follow the distribution $\mathcal{N}(\underline{0}, S_t)$ as proven in (1), instead of looking at all the covariance elements of S_t the check has been done only on the diagonal terms of S_t with respect to the diagonal elements of the estimator defined below:

$$\hat{q} = \frac{1}{N}\sum_{t=l}^{n_t} e_t\, e_t^T \in \mathbb{R}^{n_y \times n_y}$$

The mean in time of the e_t components defines the center of the 1σ gate, where σ is defined as the distance between the mean in time (from $t(l)$ to $t(n_t)$) of the standard deviations of each innovation (i.e. the mean of the square roots of the diagonal elements of S_t) from the mean in time of the innovations..

If the innovations follow a normal distribution, the 68% of each innovation index will stand inside the 1σ gate after the running time of the test simulation. We will see in the Results Chapter 4 (4.1) how this test performs in **Anamak**. The previous estimator can be implemented in real time too. Supposing to know $\hat{q}_k = \frac{1}{k}\sum_{t=1}^{k} e_t\, e_t^T$ at time k we can achieve recursively the estimator at the next time step:

$$\hat{q}_{k+1} = \frac{1}{k+1}\sum_{t=1}^{k+1} e_t\, e_t^T = \frac{1}{k+1}\sum_{t=1}^{k}\Big(e_t\, e_t^T + e_{k+1}\, e_{k+1}^T\Big) = \frac{k}{k+1}\,\hat{q}_k + \frac{e_{k+1}\, e_{k+1}^T}{k+1}$$

3.1.2 Test n^o 2 - Cross-correlation test

With this test we aim to prove that the estimated cross-correlation of the innovation residuals is zero or close to zero, as proven in (1). The estimator we performed is the following:

$$\hat{r} = \frac{1}{N-\tau}\sum_{t=l}^{n_t-\tau} e_t\, e_{t+\tau}^T \in \mathbb{R}^{n_y \times n_y} \quad , \quad \forall\, \tau = \{0,\ 1,\ 2,\ ...,\ 100\}$$

However, in order to have a scalar function of the discrete time index τ we performed the trace of the above estimator, i.e.:

$$\tilde{r} = \frac{1}{N-\tau}\sum_{t=l}^{n_t-\tau} e_t^T\, e_{t+\tau} = \mathrm{Tr}\,\hat{r} \ \in \mathbb{R} \quad , \quad \forall\, \tau = \{0,\ 1,\ 2,\ ...,\ 100\}$$

[3] If $A \in \mathbb{K}^{m\times n}$ then $\|A\|_F = \sqrt{\sum_{i=1}^{m}\sum_{j=1}^{n}|a_{ij}|^2} = \sqrt{\mathrm{Tr}\,A\,A^\dagger} = \sqrt{\mathrm{Tr}\,A^\dagger\,A} = \sqrt{\sum_{i=1}^{\min\{m,n\}}\sigma_i^2}$, where σ_i is the *i-th* singular value of A. If $A \in \mathbb{R}^{m\times n}$ then $A^\dagger = A^T$.

If the innovation residuals are uncorrelated in time then it should be:

$$\tilde{r} = \begin{cases} 1 \ , & \tau = 0 \\ 0 \ , & \tau \geq 1 \end{cases}$$

We can see that if $\tau = 0$ we are computing the trace of the first estimator $\hat{q}$: dividing this trace by the mean of the diagonal elements of $\hat{q}$ we reach the normalized unitary value, which shows that the innovation (if Gaussian) can be correlated only at the same time instants (4.1).

3.1.3 Test n^o 3 - χ^2 test

Let's first of all introduce the following Theorem:

Theorem 1. *If $e_t \sim \mathcal{N}(\underline{0}, S_t)$, with $S_t = C\,P_t^- C^T + R^t \in \mathbb{R}^{n_y \times n_y}$, then $e_t^T\, S_t^{-1} e_t \sim \chi^2_{n_y}\ \forall\, t$, where the quadratic form $e_t^T\, S_t^{-1} e_t$ is called the* ***normalized innovation****.*

Proof. If $\{\gamma_i(t)\}_{\substack{i=1,...,n \\ t=1,...,n_t}}$ are independent, *standard* normal aleatory variables s.t. $\forall\, t$, $\forall\, i$ $\gamma_i(t) \sim \mathcal{N}(0, 1)$, then the sum of their squares Γ_t follow a chi-squared distribution with n degrees of freedom $\forall\, t = 1, ..., n_t$:

$$\Gamma_t = \sum_{i=1}^{n} \gamma_i^2(t) \ \sim\ \chi^2_n \quad \forall\, t = 1, ..., n_t$$

Moreover, thanks to the *additivity property*:

$$\Gamma = \sum_{t=1}^{n_t} \Gamma_t = \sum_{t=1}^{n_t} \sum_{i=1}^{n} \gamma_i^2(t) \ \sim\ \chi^2_{n \times n_t}$$

Now, since S_t is a covariance matrix it is symmetric positive definite and so its inverse S_t^{-1} is well defined and it is symmetric positive definite too. By *Spectral Theorem* S_t and S_t^{-1} are both diagonalizable with orthogonal change of basis matrices:

$$S_t = V\,\Lambda_t\,V^T \ \Leftrightarrow\ \Lambda_t = V^T S_t\, V$$
$$S_t^{-1} = (V\,\Lambda_t\,V^T)^{-1} = V\,\Lambda_t^{-1} V^T \ \Leftrightarrow\ \Lambda_t^{-1} = V^T S_t^{-1}\, V$$

Hence we obtain:

$$e_t^T\, S_t^{-1} e_t = e_t^T V\,\Lambda_t^{-1} V^T e_t = y_t^T \Lambda_t^{-1} y_t = $$
$$= \sum_{i=1}^{n_y} y_{t,i}\,(\lambda_{t,i})^{-1} y_{i,t} = \sum_{i=1}^{n_y} \Big(\frac{y_{t,i}}{\sqrt{\lambda_{t,i}}}\Big)^2$$

where in the last step we used the fact that $S_t > 0 \wedge S_t^{-1} > 0$ an so their eigenvalues are always positive, i.e. $\lambda_{t,i} > 0\ \forall\, i = 1, ..., n_y$. Moreover, using the property of Gaussianity conservation under linear transformations[4] if $e_t \sim \mathcal{N}(\underline{0}, S_t)$ then $y_t = V^T e_t \sim \mathcal{N}(\underline{0}, V^T S_t\, V) = \mathcal{N}(\underline{0}, \Lambda_t)$. Therefore, $\forall\, i = 1, ..., n_y$ we have that:

$$y_{t,i} \sim \mathcal{N}(0, \lambda_{t,i}) \ \Leftrightarrow\ \frac{y_{t,i}}{\sqrt{\lambda_{t,i}}} \sim \mathcal{N}(0, 1) \ \Rightarrow\ e_t^T\, S_t^{-1} e_t \sim \chi^2_{n_y}\ \forall\, t = 1, ..., n_t$$

[4] See *Theorem 3* of Appendix (3).

Finally, we obtain that:

$$\sum_{t=1}^{n_t} e_t^T \, S_t^{-1} e_t = \sum_{t=1}^{n_t} \sum_{i=1}^{n_y} \Big(\frac{y_{t,i}}{\sqrt{\lambda_{t,i}}} \Big)^2 \sim \chi^2_{n_y \times n_t}$$

□

For this test we have defined the following normalized estimator:

$$\hat{s} = \frac{1}{N} \sum_{t=l}^{n_t} e_t^T \, S_t^{-1} e_t$$

where l-index and the total amount of time-steps $N = n_t - l + 1$ has already been discussed.

The estimator $\hat{s}$ is the *sample mean* of the normalized innovations: we aim to show that $N\hat{s} \sim \chi^2_{n_y \times N}$ in order not to refuse the hypothesis of $e_t \sim \mathcal{N}(\underline{0}, S_t)$ which arises from the optimality of the filter.
We defined indeed the null hypothesis H^o as the hypothesis that the normalized estimator $N\hat{s}$ follow a $\chi^2_{n_y \times N}$ distribution with probability $1 - \alpha$, and *significance level* $\alpha = 0.05$ [5].
We defined the confidence interval s.t.:

$$[r_1, \, r_2] = \Big[\chi^2_{n_y \times N}(\alpha/2), \, \chi^2_{n_y \times N}(1 - \alpha/2) \Big] \; \mid \; P\left(N\hat{s} \in [r_1, \, r_2] \mid H^o \right) = 1 - \alpha$$

If the estimator is not within this interval the null hypothesis can be rejected and we can assert with $1 - \alpha$ confidence that the normalized residuals are not following a $\chi^2_{n_y}$ distribution, which in turns means that the filter is not performing optimally. Otherwise, if the estimator is within the confidence interval it doesn't mean that the normalized residuals are following a $\chi^2_{n_y}$ distribution. In order to show that the residuals are following a $\chi^2_{n_y}$ distribution we should define a null hypothesis saying that the residuals are not following the distribution and then reject this null hypothesis. Details on the computation of the χ^2 inverse cumulative distribution function can be found in [15].

However, these tests have been performed only to check faults in the filter, which may arise from various reasons: first of all the noise level included in the model may be wrong. Moreover, in the Kalman filter derivation, white noises on the process and measurements equations have been assumed and it is not necessarily the case.

If those tests fail, we ensure the filter is not following the good statistics while otherwise, if they are successful, they do not give certainty on the probability distributions of the innovation residuals. In this sense they are properly called *rejection tests* rather than *validation tests* [14]. By the way these tests give a powerful instrument to best tune the covariance matrices in order to ensure the innovation residuals not to follow the wrong statistics. The outcomes of these tests are shown in the Results Chapter 4 (4.1).

[5] For the sake of completeness: if the p-value is less than the level significance level, then the null hypothesis is rejected. The lower the p-value is, the more significant will be the result. In our case we aim just not to reject the null hypothesis, and so the results of this test will not give us statistical informations. Otherwise if the null hypothesis is rejected (and the statistical significance increases if the p-value decreases with respect to α) we can conclude that the filter is not optimal.

Chapter 4

Anamak results

A good orientation for this chapter was following what has been done in [14] where the statistical tests have been used with typical induced perturbations. Starting from this, in this work an augmented state Kalman filter has been implemented by means of KALSASS.M function that permits changements in the filter design with respect to the encoutered problems. In the next Chapter this full augmented state Kalman filter, designed on **Anamak**, is then tested on existing **TCV** shots and a comparison with the previous implemented MGA observer is detailed in the frequency domain (5.2). For the filter's design, in this Chapter all the tests have been run on a stable shot of **Anamak** (similar to the one in the left in figure 1.6) where $n_a = 8$, $n_v = 200$, $n_m = 16$ and $n_f = 16$. The simulation run-time has been set from $0\,s$ to $1\,s$ with equally spaced time-steps of $T_s = 1\,ms$. For test performances comparison, eigenmodes decomposition of vessel currents has been set with $n_u = 20$, whereas for FGE vs linearized FGE comparison as well for the sinusoidal PF001 voltage and β_p-ramp perturbation it has been set $n_u = 8$.

4.1 Test performances

In this section the performances of the filter with different process covariance matrices are discussed. The measurements are taken from a simulation of linearized FGE afer known perturburbations in the model. In the observer equation white noises have been added to the measurements with amplitudes matching exactly their standard deviations. The diagnostics covariance matrix R is therefore kept constant during the simulations. In the linear model equations the only source of perturbation has been set onto the active coil voltages, adding a known white noise disturbance. Moreover, we have assumed the constraints to be time-invariant i.e. $\Delta c^t = 0 \;\; \forall\, t$ and for filter's design pourposes the state has been limited only to the external currents, i.e. $x^t = I_e^t \;\; \forall\, t$.
The process equation is the following:

$$I_e^{t+1} = A\, I_e^t + B_1\, \tilde{V}_a^{t+1}$$

with:

$$\tilde{V}_a^t = V_a^t + w_V^t \in \mathbb{R}^{n_a}$$

where $w_V^t \sim \mathcal{N}\,(\,V_{a,err}, \tilde{Q}_V\,)$, $V_a^t = V_{\texttt{known}}^t$ and $\tilde{Q}_V = V_{a,err}^2\, \mathcal{I}_{n_a \times n_a}$. We have set $V_{a,err} = 10\,V$. Therefore, the correct process covariance matrix of the system is:

$$Q_V = B_1\, \tilde{Q}_V\, B_1^T \in \mathbb{R}^{n_a + n_u}$$

We have compared the three tests (3.1.1 , 3.1.2 , 3.1.3) using:

1. A correct process covariance matrix, i.e. $Q = Q_V$
2. An underestimated process covariance matrix by a factor 10, i.e. $Q = 0.1\, Q_V$
3. A overestimated process covariance matrix by a factor 10, i.e. $Q = 10\, Q_V$

4.1.1 Correct process covariance matrix

The 1σ gate test is presented in the following figures (4.1). For each measurement, we can see that the innovation residuals stay inside their theoretical averaged standard deviations with probability of 68 %, like in perfect normal distributions (4.2).

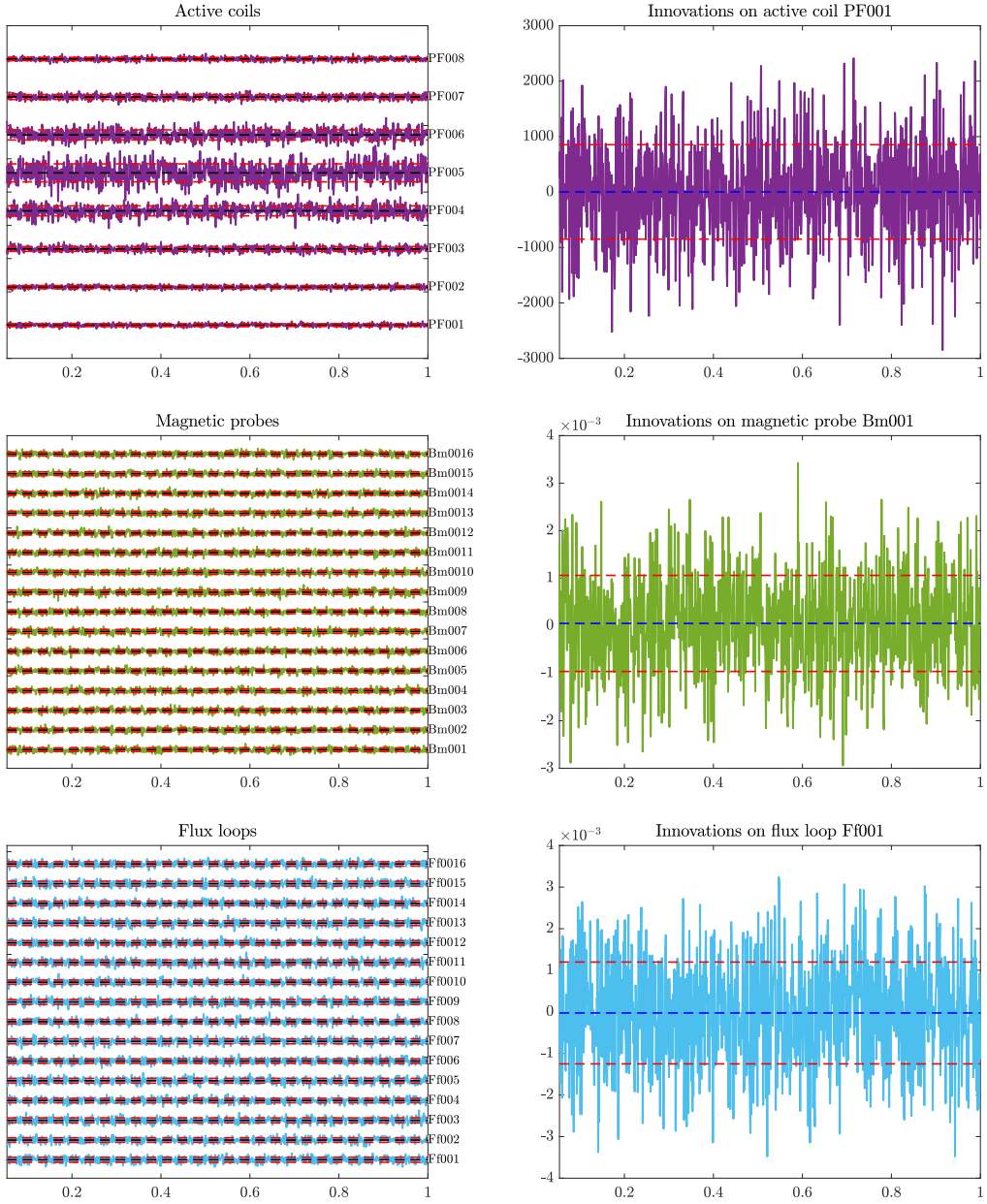

Figure 4.1: 1σ gate test for all the innovations $Q = Q_V$

In the following pictures are also presented the cross-correlation test and the χ^2 test (4.3 , 4.4). We can see that in the case 1. the statistical behaviour of the innovations is well respected, since we have set the correct covariance matrix matching exactly the covariances of the imposed noises on the system. In all these tests the filter's statistical assumptions cannot be rejected, as expected.

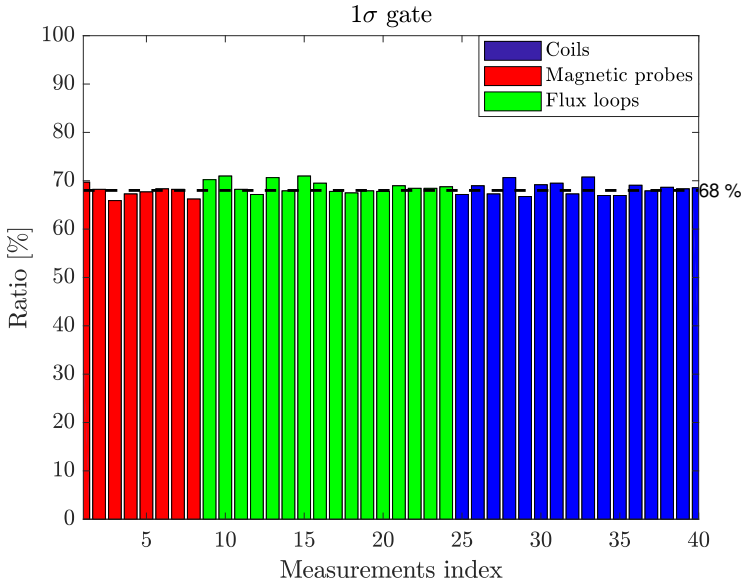

Figure 4.2: Computing of the percentage of innovations which belong to the 1σ gate

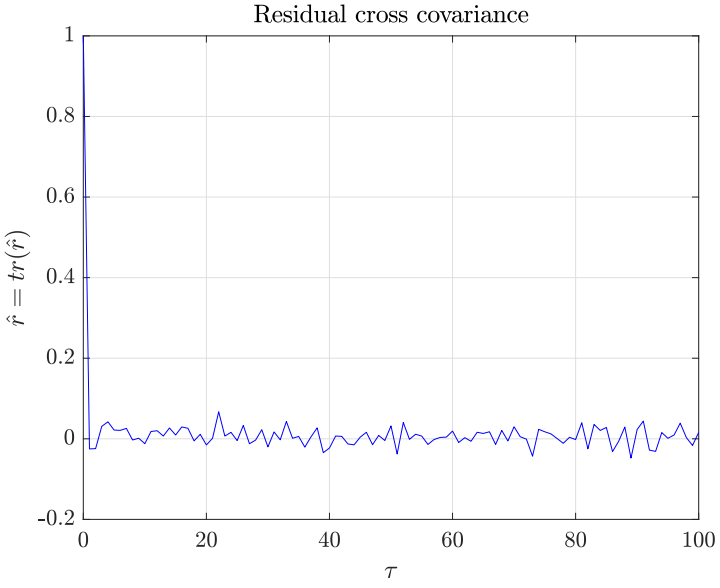

Figure 4.3: Residual cross-covariance test: we can see that only for $\tau = 0$ we have $\hat{r} = 1$, while for all other time instants $\hat{r} = 0$ as expected with Gaussian innovations (3.1.3)

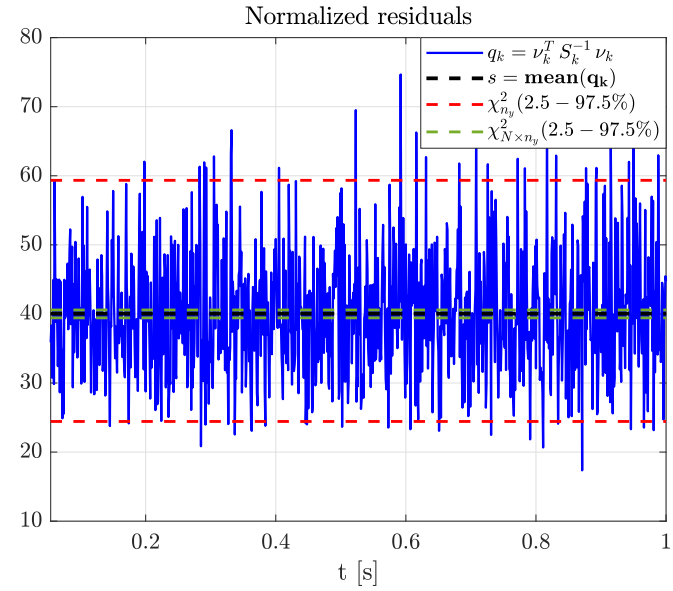

Figure 4.4: χ^2-test to check the Gaussianity on e_t *pdf*

Finally the state estimates are shown, in comparison to the linearized FGE results: the sum of active currents estimates is shown in figure (4.5), while in figure (4.6) and in figure (4.7) the slowest and the fastest eingencurrents estimates are shown respectively.

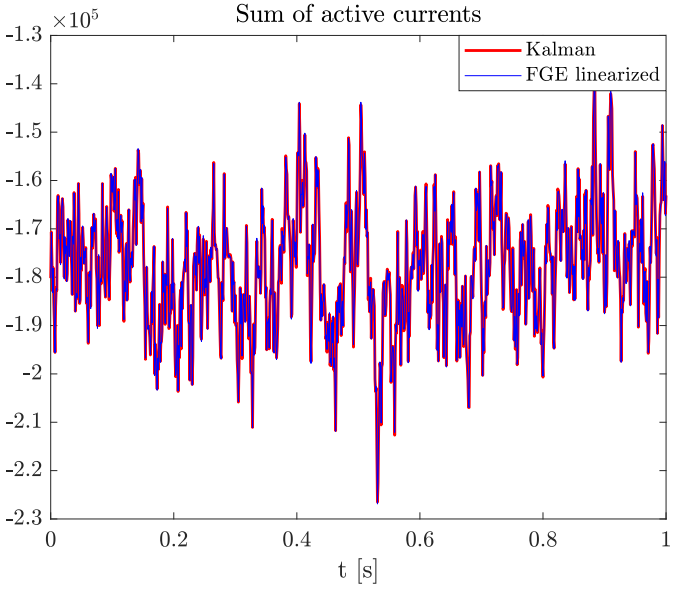

Figure 4.5: Sum of active currents, $Q = Q_V$

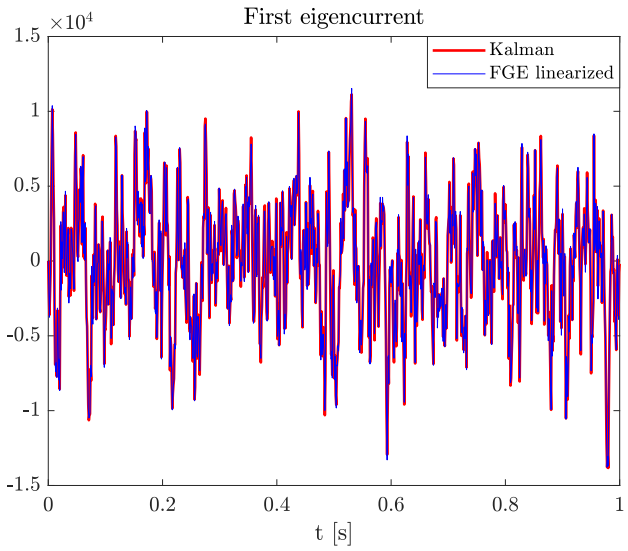

Figure 4.6: 1st eigencurrent, $Q = Q_V$

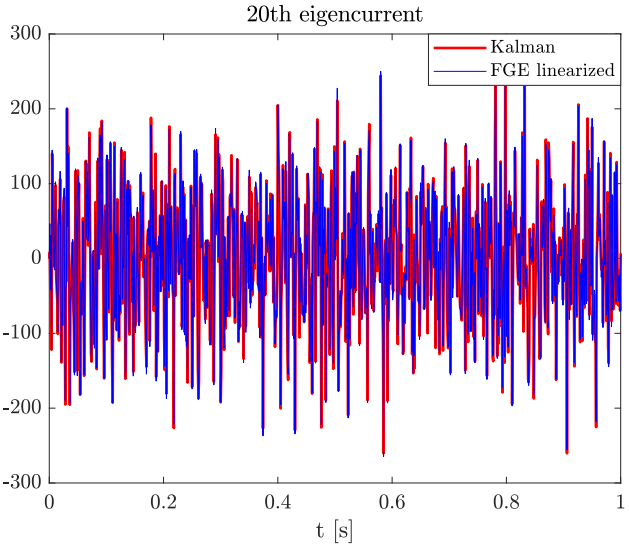

Figure 4.7: 20th eigencurrent, $Q = Q_V$

4.1.2 Underestimated process covariance matrix

We present now in figures (4.8 , 4.9 , 4.10 , 4.11) the three tests in the underestimated case. First of all, for instance, only the plot of the 1σ gate of the Active coils innovations is displayed (4.8) since all the innovations follow approximately the same behaviour. The 1σ test and the χ^2 test fail (4.9 , 4.11) as expected even if the cross-covariance (4.10) remains around zero for each time step except $\tau = 0$. Since the filter is putting a lot of trust in the model with respect to measurements, it is missing up some informations from the measurements. This leads to higher values on the residuals, as we can see in the normalized residual distribution plot (4.11). Once again the state estimates have been computed, in comparison to the linearized FGE results but, since the estimates are really well performed by the filter, as in figure (4.7), even in the underestimated or in the overestimated case the plots are not shown, since they don't give additional informations to the reader.

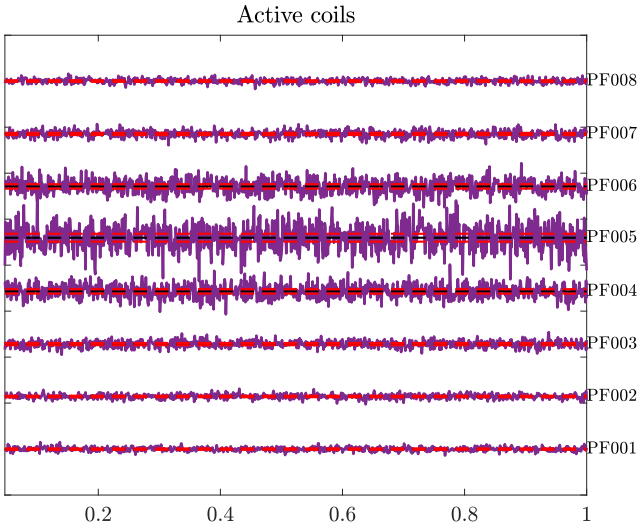

Figure 4.8: 1σ gate test for the Active coils innovations with $Q = 0.1\, Q_V$

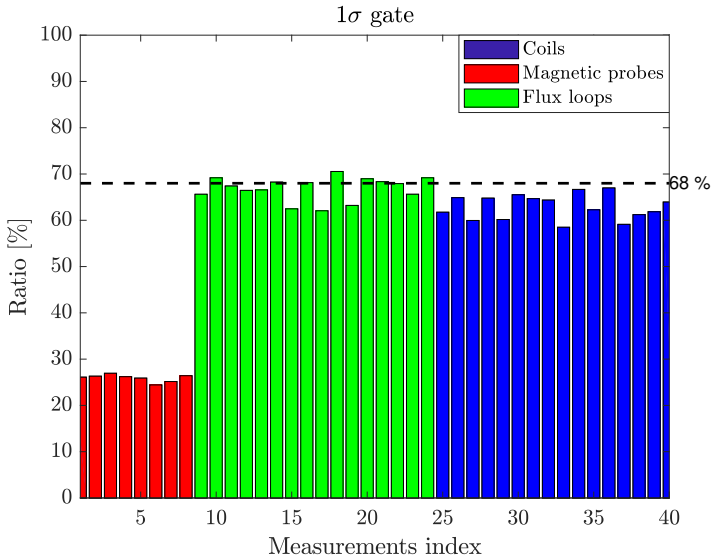

Figure 4.9: Computing of the percentage of innovations which belong to the 1σ gate

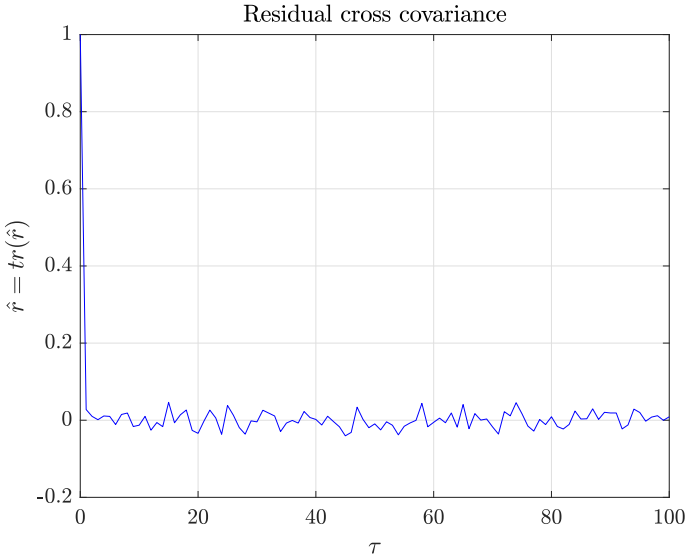

Figure 4.10: Residual cross-covariance test: we can see that only for $\tau = 0$ we have $\hat{r} = 1$, while for all other time instants $\hat{r} = 0$ as expected with innovations uncorrelated in time

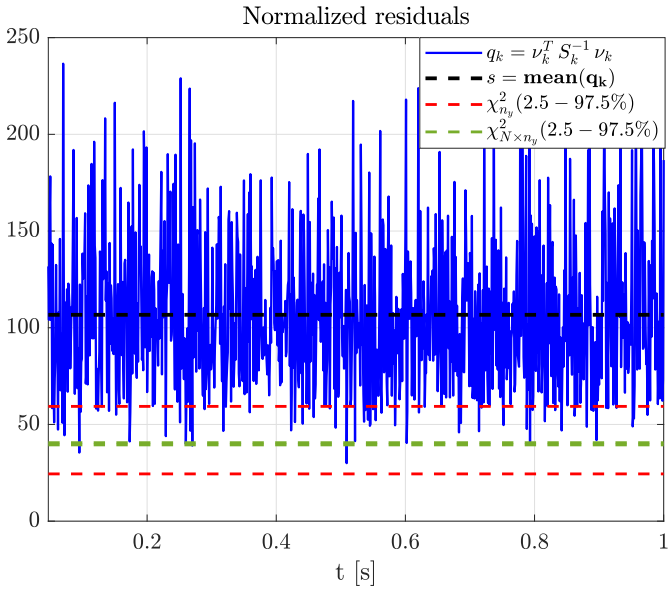

Figure 4.11: χ^2-test to check the Gaussianity on e_t *pdf*

4.1.3 Overestimated process covariance matrix

Finally, we present the three tests in the overestimated case in figures (4.12 , 4.13 , 4.14 , 4.15). The 1σ test and the χ^2 test fail (4.13 , 4.15) as expected even if, one more time, the cross-covariance remains around zero for each time step except $\tau = 0$ (4.14). In this case too many residuals are within the 1σ gate and the normalized innovations are too low. Therefore in this case, like in the underestimated one, the innovations are no longer white noises with covariance matrix $S_t \; \forall \, t = t(l), ..., t(n_t)$. One more time the state estimates are computed, in comparison to the linearized FGE and the estimates are well retrieved by the filter despite the overestimation on Q.

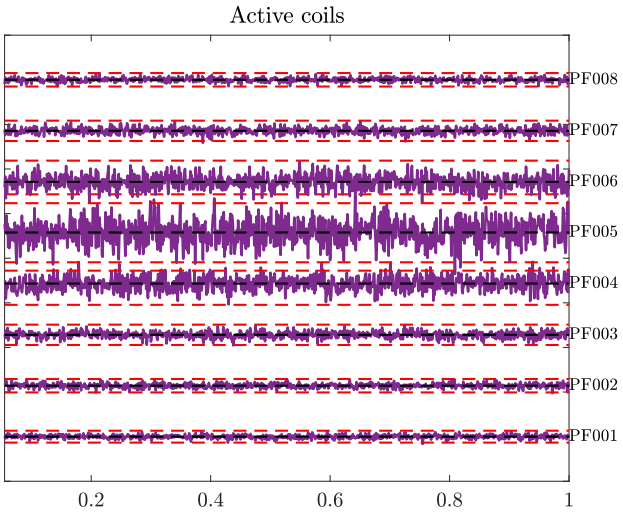

Figure 4.12: 1σ gate test for the Active coils innovations with $Q = 10\, Q_V$

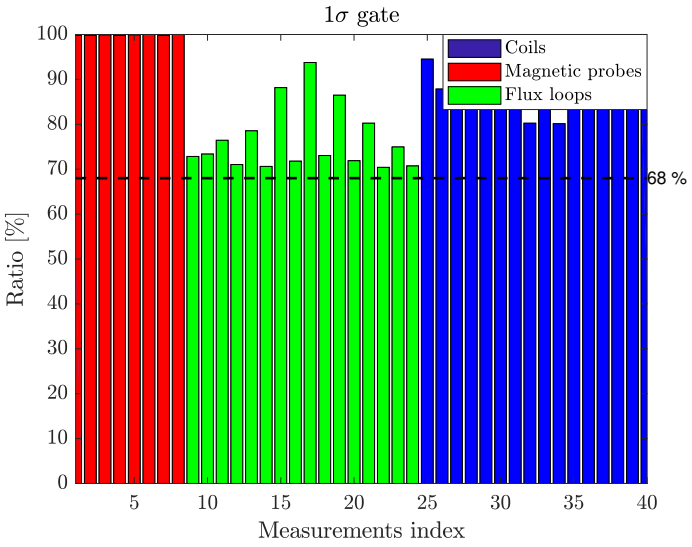

Figure 4.13: Computing of the percentage of innovations which belong to the 1σ gate

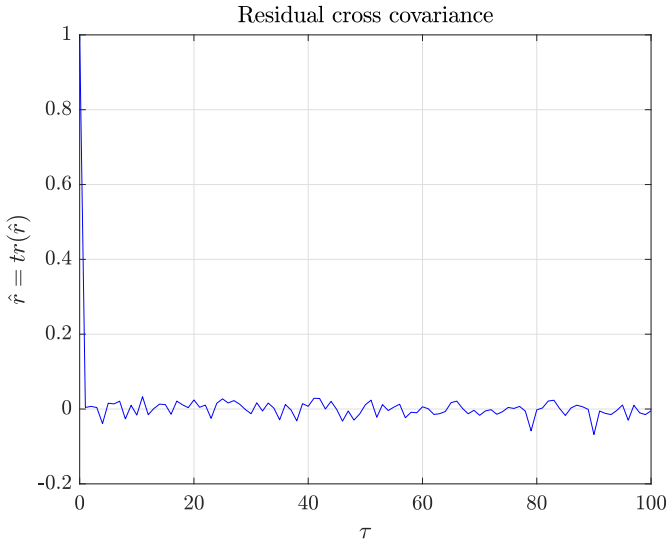

Figure 4.14: Residual cross-covariance test: we can see that only for $\tau = 0$ we have $\hat{r} = 1$, while for all other time instants $\hat{r} = 0$ as expected with innovations uncorrelated in time

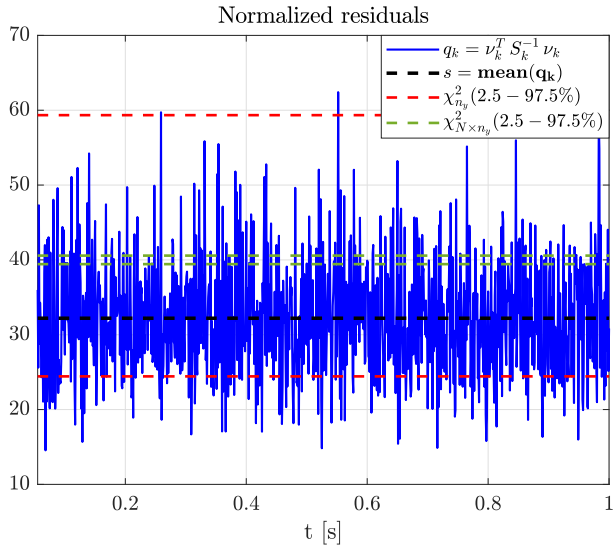

Figure 4.15: χ^2-test to check the Gaussianity on e_t *pdf*

In both the three situations the estimates match with the measurements. This is due to the fact that, in **Anamak**, measurements are directly provided by linearized FGE, which is the state space-model we adopted. Moreover, the measurement noise has been assumed "a priori" known and therefore the only fault has been in the guess on Q. In any case, in this particular and very limited case, the wrong choice on Q doesn't affect too much the estimation performances.

4.2 Comparison between linearized FGE and non-linear FGE

In this Section the same tests as before have been performed. The model is still the linearization around an equilibrium point in the state-space of the FGE equations. The divergence of the measurements evolution in the linearized case with respect to non-linear FGE is shown in figures (4.16).

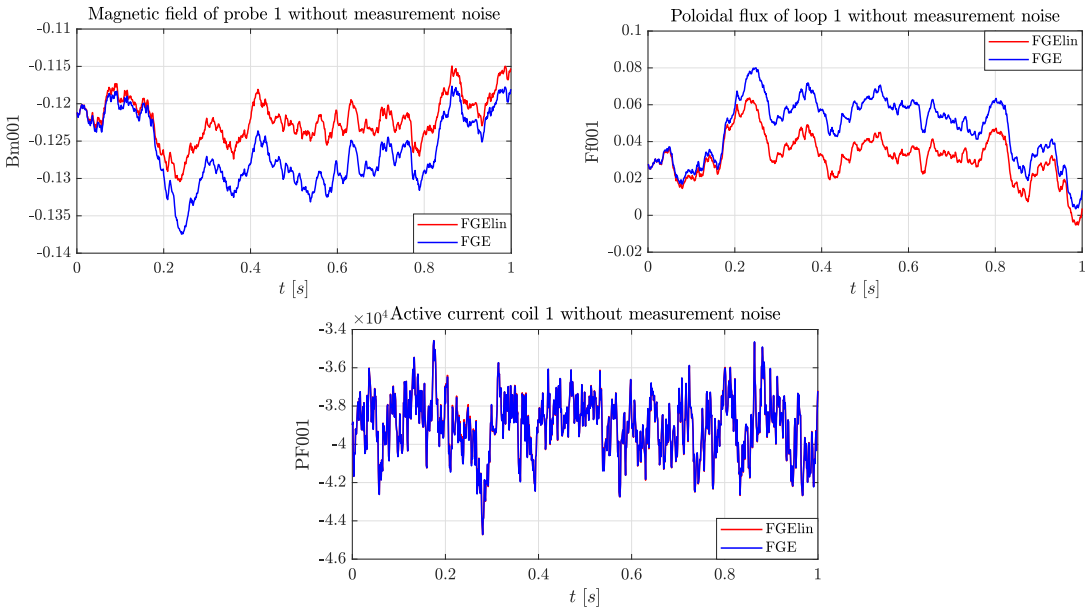

Figure 4.16: Divergence from the equilibrium point between FGE and linearized FGE

Test validations and estimation performances are compared in the cases in which measurements are taken from the linearized version of FGE (as before) or in which they are taken directly from a run of the non-linear FGE solver. The process covariance matrix Q has been chosen equal to Q_V in order to match exactly the imposed voltage perturbation. Finally, the noises on the observer equation have been assumed "a priori" known and so the R matrix is well defined and time-invariant. All the tests are shown in figures (4.17 , 4.18 , 4.19). We can see that in the non-linear case we loose the hypothesis of white innovations. This is due to the fact that we should have modelled the non-linearity as an additional noise and we should have taken it into account in the Q-design. Contrary to the linearized case, the disturbance does not have the structure associated with one particular input, therefore it cannot be classified as an input disturbance but as a structural disturbance arising from a modeling error [7]. The χ^2 test and the 1σ gate test give the confirmation of such a behaviour since their failures are similar to the ones of the previous underestimated case (4.9 , 4.11 , 4.19). Nevertheless, the cross-correlation tests give almost the same results in both cases as we can see in (4.19). In figures (4.20 , 4.21) the main estimates are compared in the two cases.

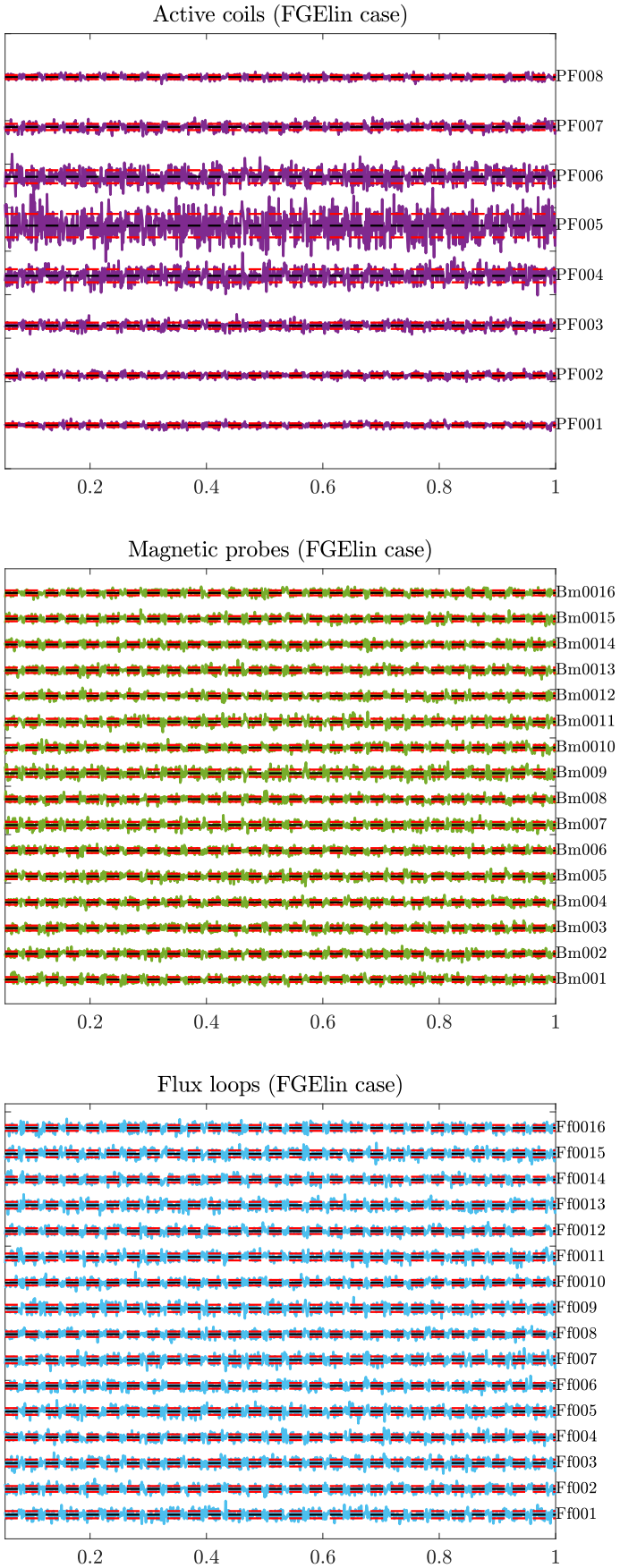

Figure 4.17: 1σ gate test, diagnostics from linearized FGE

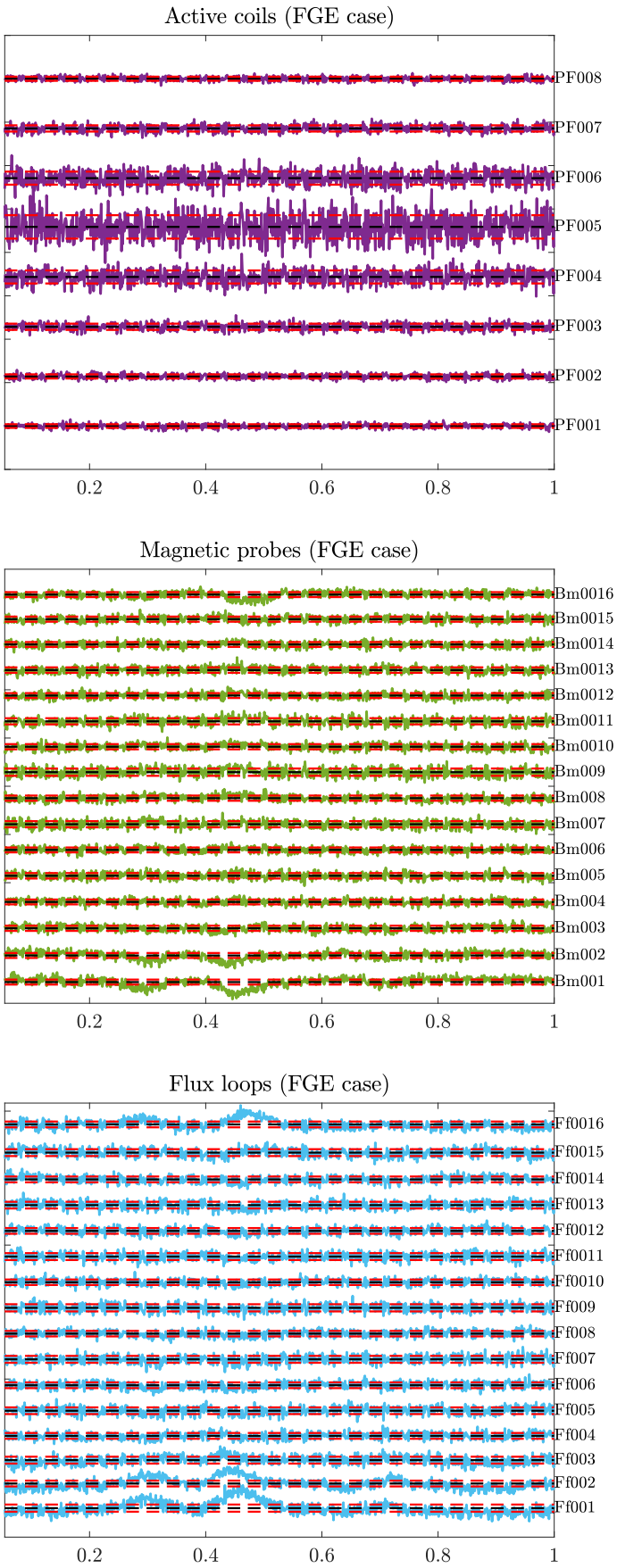

Figure 4.18: 1σ gate test, diagnostics from non-linear FGE: we can see some perturbations on the magnetic probes and flux loops innovations due to the amplification of the voltage perturbation in the non-linear model

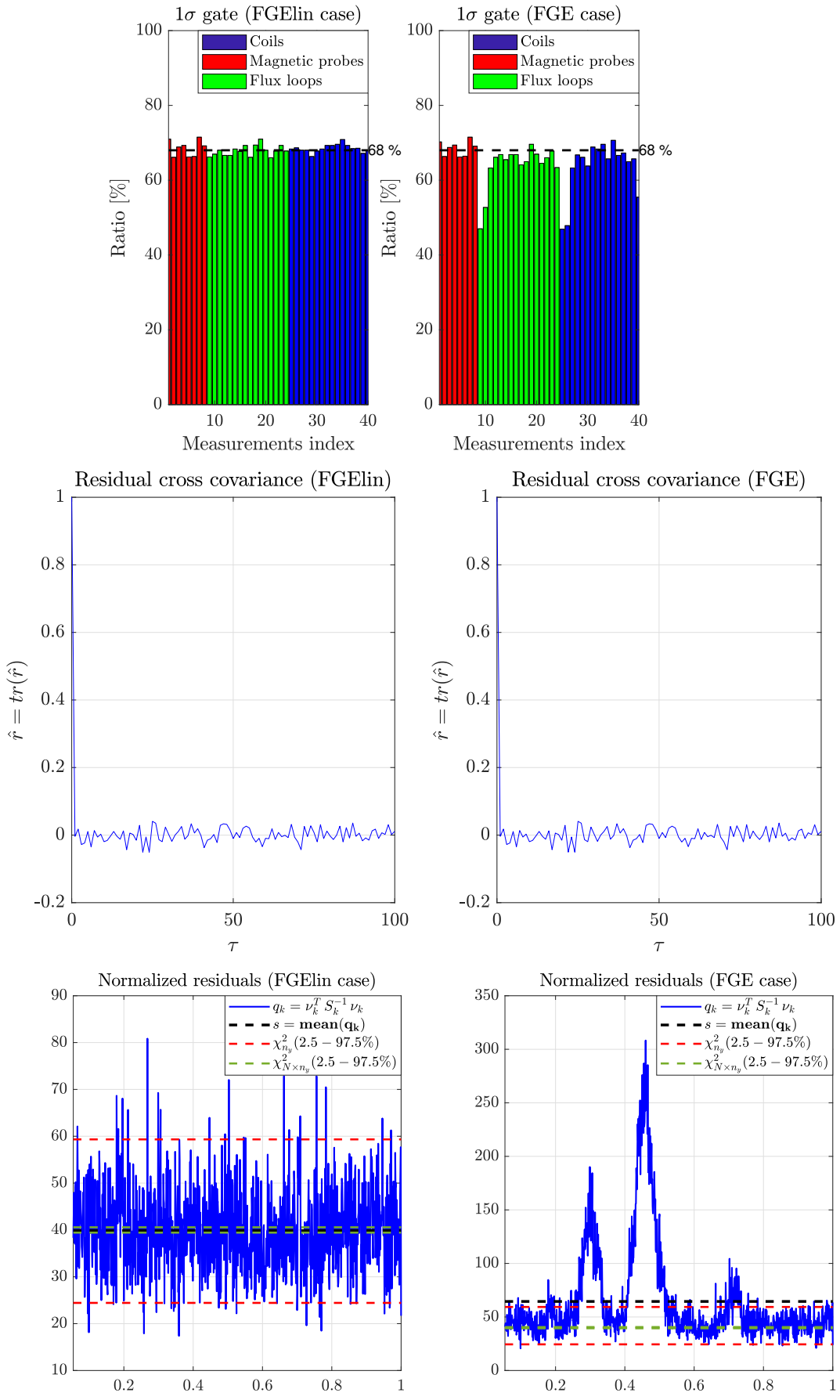

Figure 4.19: 1σ gate test, cross-correlation test, χ^2 test comparison between the cases of measures taken from linearized FGE and from non-linear FGE

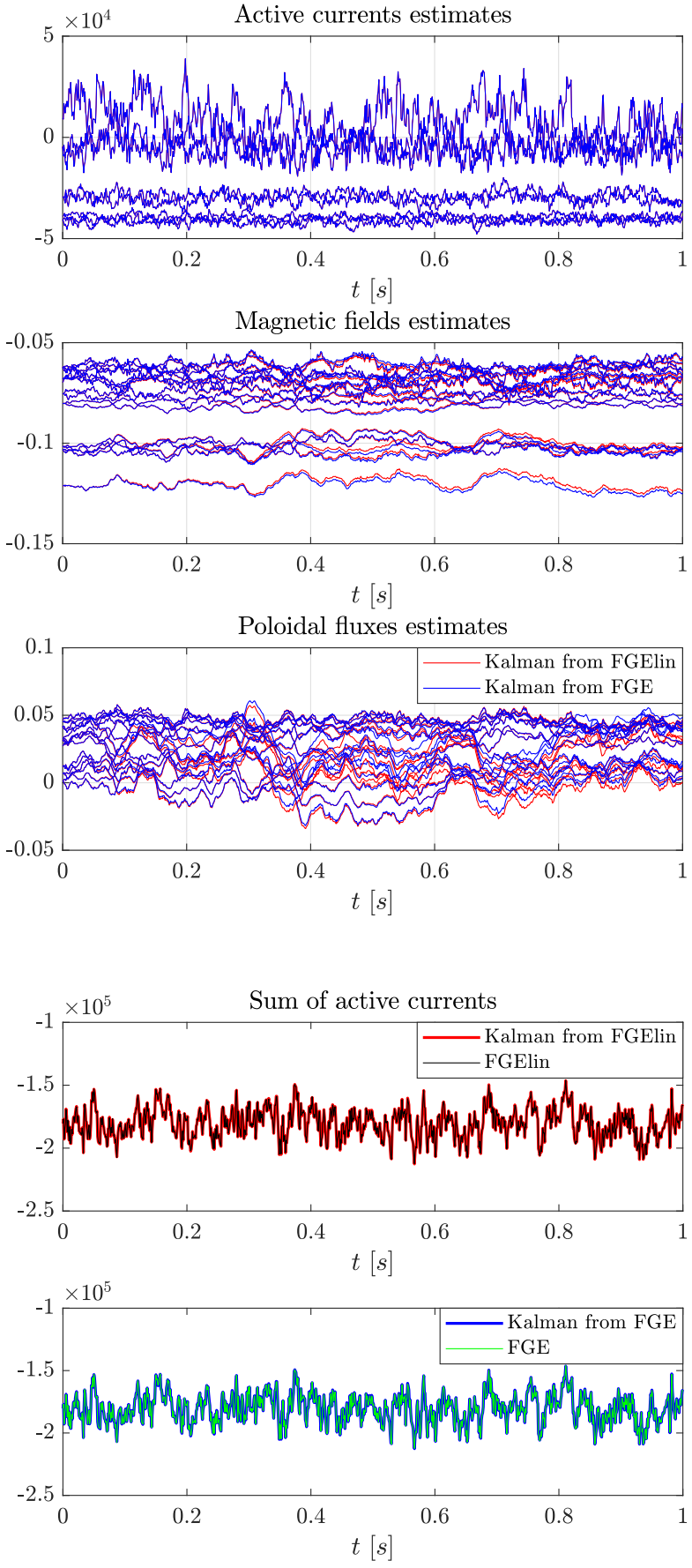

Figure 4.20: Post-processing measurements estimations and sum of active currents comparison using data from linearized FGE and from non-linear FGE

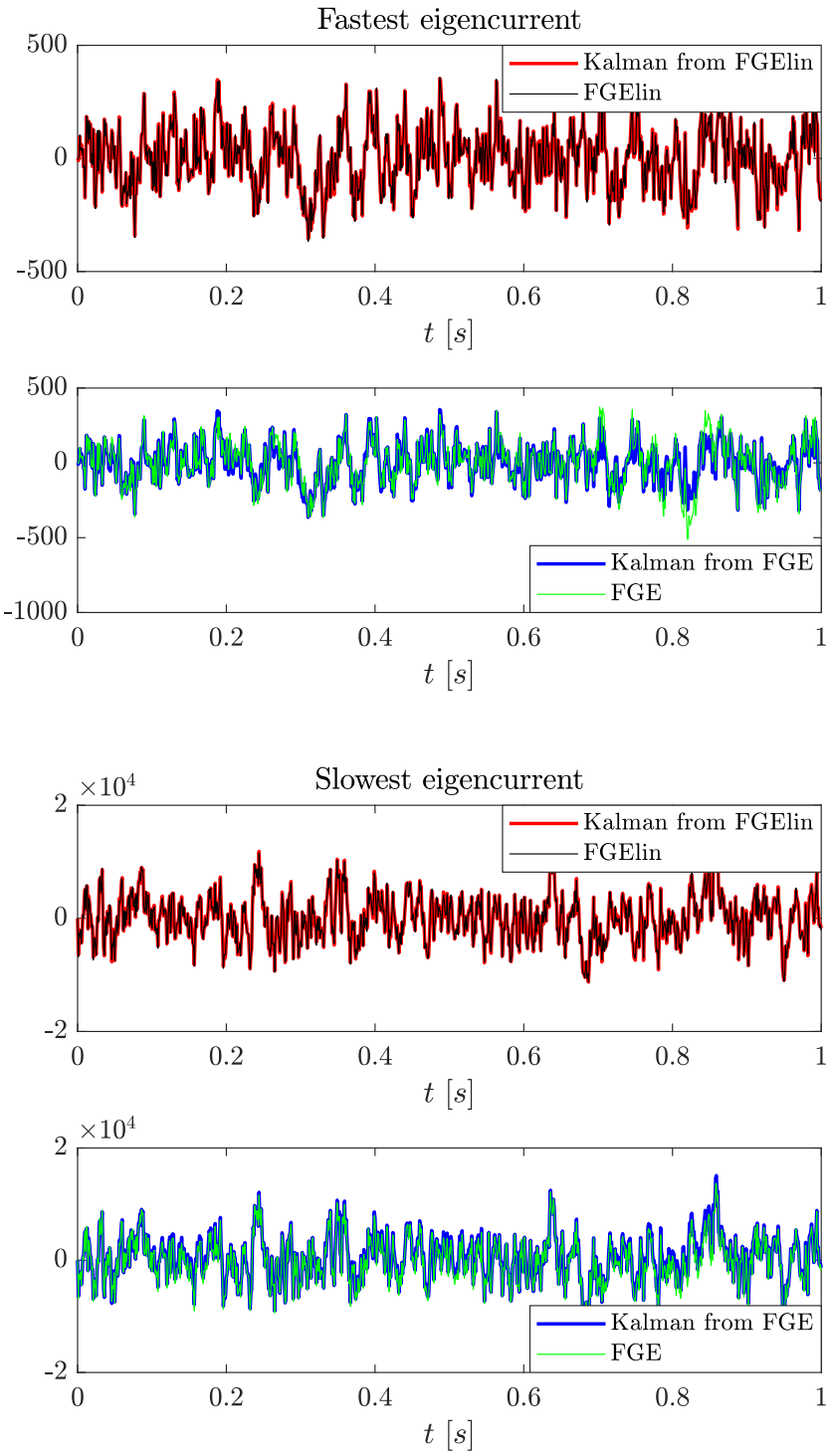

Figure 4.21: 8st and 1th eigenmodes comparison using data from linearized FGE and from non-linear FGE

4.3 Covariance matrix tuning for non-linear FGE

In this Section we have performed the Kalman filtering on the same perturbed system as before, but trying to account also for the non-linearities of the system in the design of the process covariance matrix Q. We can distinguish three main cases:

1. $Q = Q_V$
2. $Q = Q_x$
3. $Q = Q_V + Q_x$

where Q_x is the block diagonal matrix presented in Chapter 2 (2.3), with a diagonal block for the active currents and a *Toeplitz* block for the vessel currents.

4.3.1 Case $Q = Q_V$

As we have already anticipated in the previous section, if we impose:

$$Q = Q_V = B_1 \tilde{Q}_V B_1^T = V_{a,err}^2 B_1 B_1^T$$

in the non-linear FGE, there will be a lack in the estimation performance and a fault in the tests since we are missing the non-linearities of the system, which should be modelled as additionals noises. Let's see the tests (4.22):

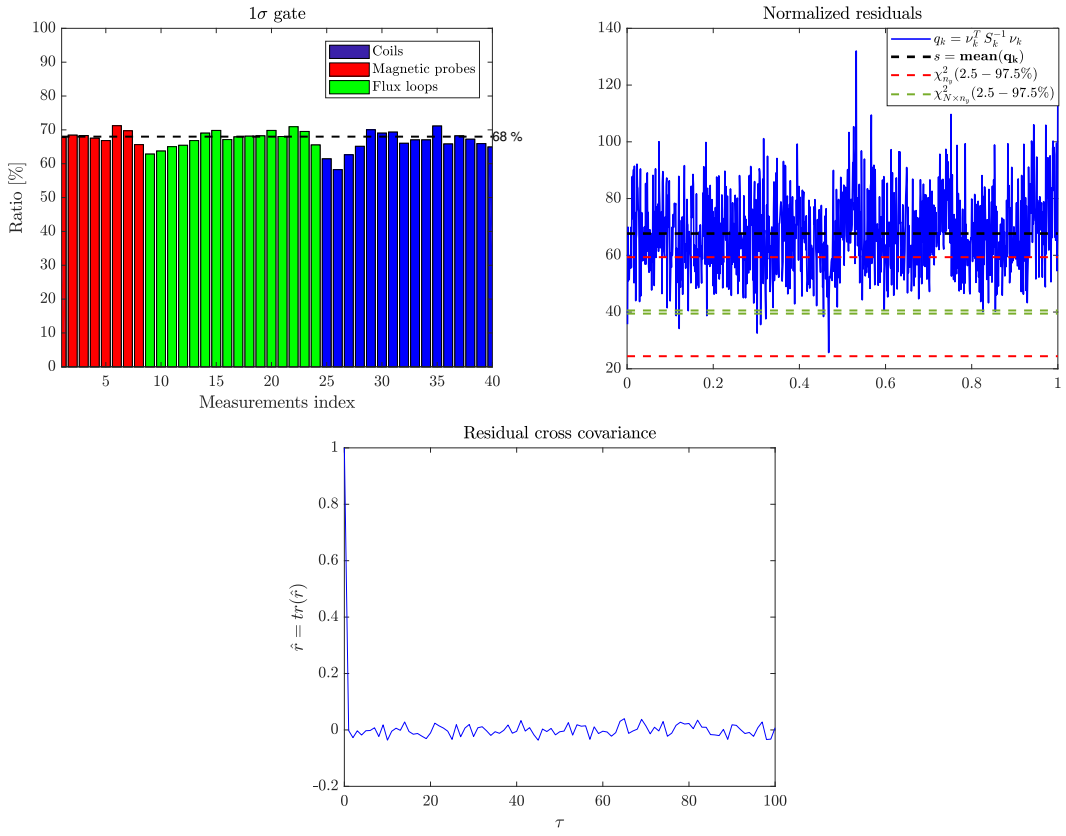

Figure 4.22: As we have already stressed, the main faults affect the 1σ gate test and the χ^2 test. We can see big spikes in the normalized residuals distribution and an underestimated process covariance matrix behaviour

4.3.2 Case $Q = Q_x$

We introduce now a block diagonal matrix in order to properly account for non-linearities in the system. The structure of such a matrix has already been presented in (2.3). Let's see in (4.23) the test performances, perturbing the system with the same voltage noise.

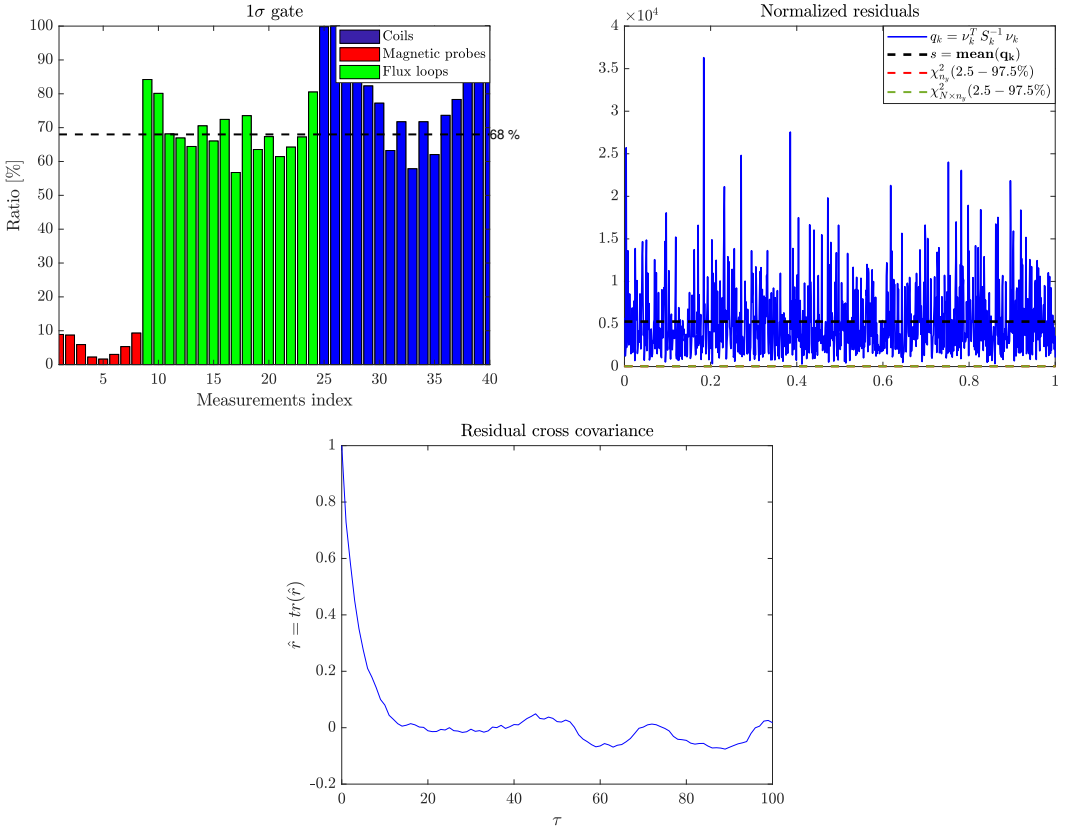

Figure 4.23: Of course all the tests fail: we have indeed imposed a voltage noise that we didn't account for in the design of the process covariance matrix. An intuitive solution is to combine the information around input voltage noise from the Q_V matrix with the covariance matrix Q_x which models the random contributions in the state equation due to linearization and external currents additional perturbations

4.3.3 Case $Q = Q_V + Q_x$

If we suppose that the noise due to voltage perturbation and the noises due to external currents perturbations and non-linearities in the system are independent, we can define the covariance matrix of their sum as the sum of their covariance matrices, i.e. $Q = Q_V + Q_x$. Since the cross-correlation test gives a value around $0 \; \forall \tau \neq 0$, we have presented here below only the 1σ gate test and the χ^2 test (4.24 , 4.25). As we can see, even if the tests are not perfectly performed, in the χ^2 test the averaged value of the sample mean of the normalized residuals has decreased since the spikes in their distribution have disappeared. Moreover, in the 1σ gate test we are no more in a underestimated situation.
Finally, the time evolutions of the state estimates in all the different cases are shown in figures (4.26 , 4.27).

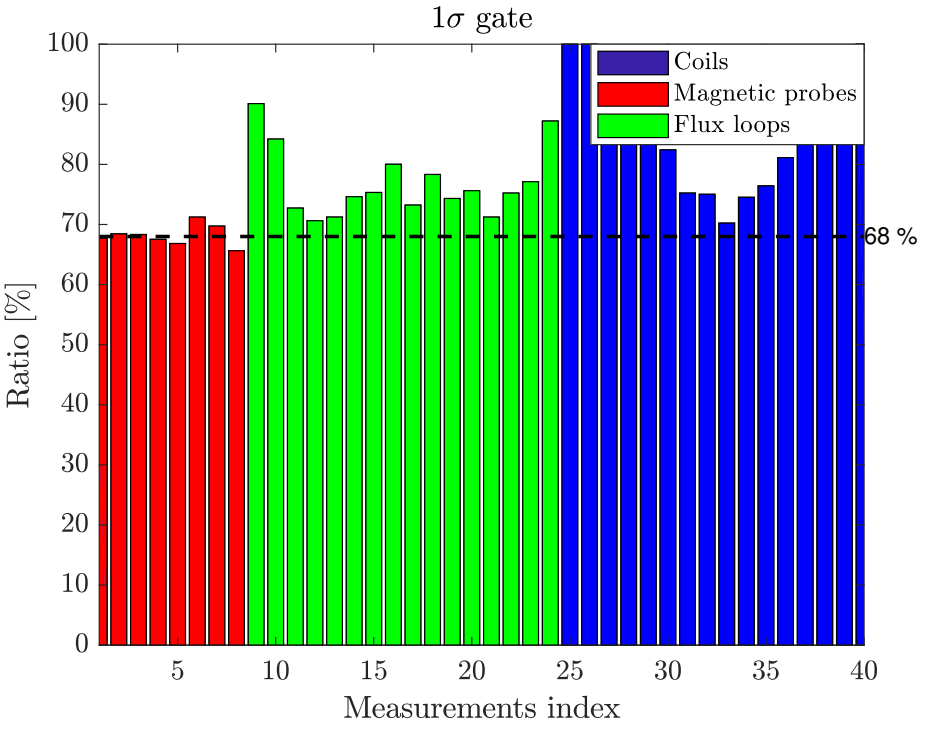

Figure 4.24: 1σ gate test with $Q = Q_V + Q_x$

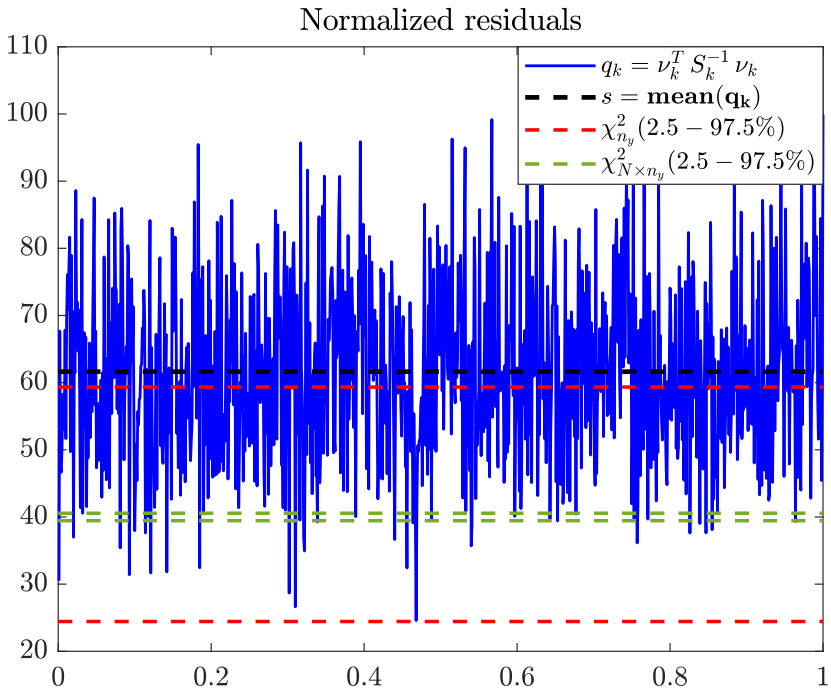

Figure 4.25: χ^2 test with $Q = Q_V + Q_x$

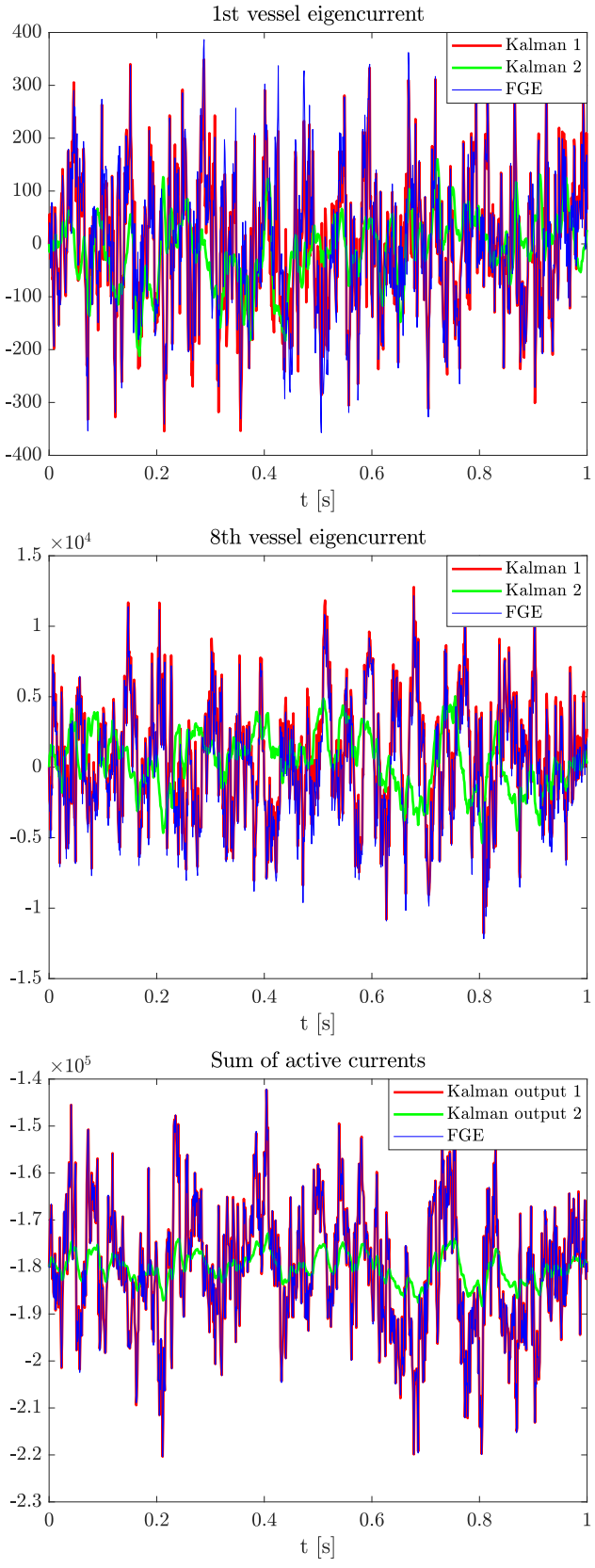

Figure 4.26: Kalman 1 : $Q = Q_V$; Kalman 2 : $Q = Q_x$

As we can see in figure (4.26) the slowest and fastest eigencurrents and the sum of active currents are computed in the cases of $Q = Q_V$ and $Q = Q_x$. We can see that the estimation given by $Q = Q_x$ doesn't follow the right dynamics since the perturbation is given essentially by an external voltage noise. We must take into account this behaviour in our filter design, since in real-time applications, there should exist a voiltage noise in the system. Considering $Q = Q_V$ we can see that the difference with respect to FGE is less significant.

In figure (4.27) the slowest and fastest eigencurrents and the sum of active currents are computed in the cases of $Q = Q_V$ and $Q = Q_V + Q_x$. The introduction of $Q_x + Q_V$ with respect to only Q_V is giving a significant improvement to the filter in the statistical level and in the estimates dynamics of the slowest eigencurrent. The other quantities are well estimated in both cases since the voltage perturbation is the principal cause of perturbation and both noises due to linearization and external currents perturbations are almost negligible with respect to it.

As a conclusion, in real-applications we should always account for white noise in the voltages adding to the covariance matrix of the process a diagonal covariance matrix with user defined diagonal elements or, to avoid the hypothesis of independence between state errors, account for a voltage covariance block matrix using an augmented state Kalman filter. This topic will be discussed in detail in the next section.

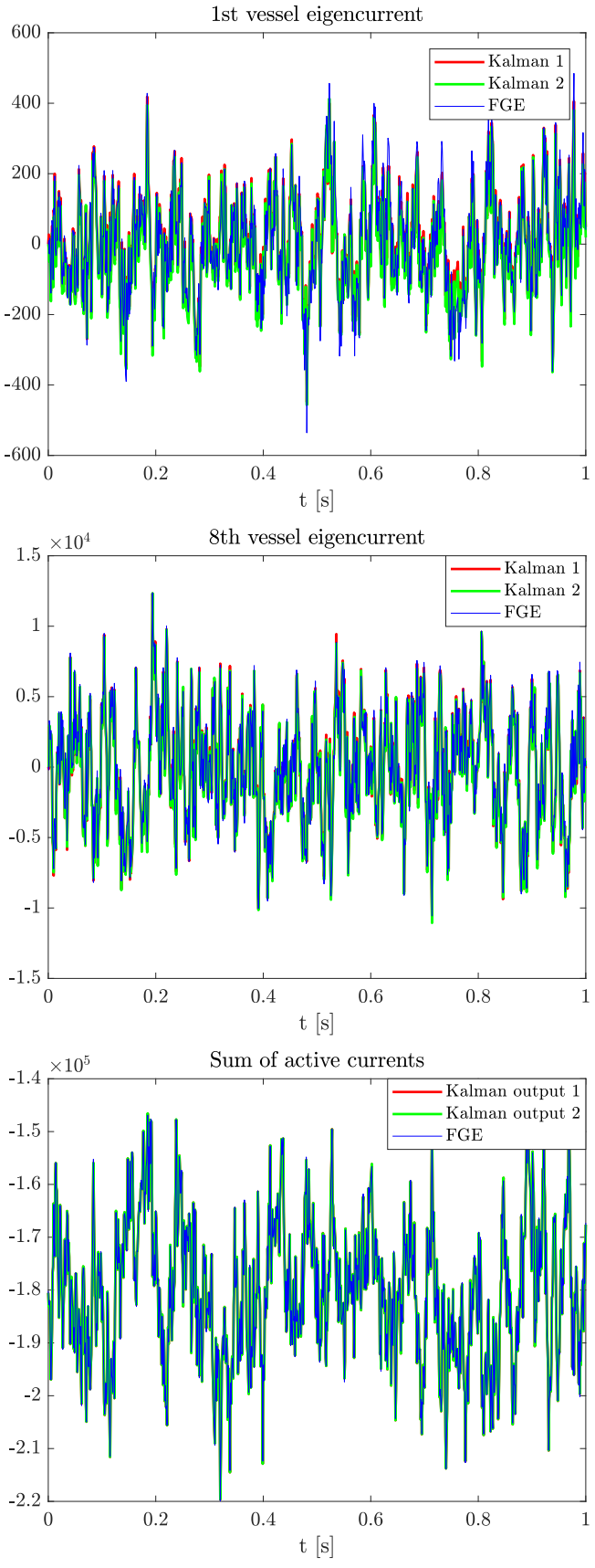

Figure 4.27: Kalman 1 : $Q = Q_V$; Kalman 2 : $Q = Q_V + Q_x$

4.4 Filter augmented state for non-linear FGE

In this Section we present the situation in which the system is perturbed without giving this information to the Kalman filter. In order to recover this unknown perturbation one strategy was to augment the process covariance matrix in order to improve the contribution of the measurements giving less faith to the model. The problem in this case is that the estimate is very noisy, even if it follows the correct unknown perturbation profile. In order to tackle this issue, a filter with augmented state has been implemented.
In some particular simulations n_ξ additionals state components have been added to all the components of the previous external current state vector, s.t. $n_\xi = n_e = n_a + n_u$. Therefore, the augmented state has doubled its dimension: for large state-space systems, like in **TCV** with filamentary vessel currents, the state augmentation could cause a lack in observability since the measurements could no longer be sufficient to recover all the components of the state vector. By the way in the next Chapter we have checked that this doesn't happen for the **TCV** shots taken into account but we have noted a decrease on estimation performance due to state dimensionality, as we can see in figure (5.27)). In the sinusoidal case two different covariance matrices for the additional disturbances are discussed: the first with correlation with active currents and the second one uncorrelated with active currents. In this particular cases the number of additional states has been set equal to the number of active currents, i.e. $n_\xi = n_a$.

4.4.1 KALSASS.M function

The MATLAB function **kalsass.m** providing all possible state augmented Kalman filter's linear state spaces, following what described in (2.2), has been implemented and has been called into the environmental MATLAB script **kal_stateaugmented.m** accounting for different testcases, each one with its particular state extention and properly designed covariance matrices. The KALSASS.M function requires as inputs: the simulation time t, the linearization structure given by the FGEL.M function, the linear state space model (with state: I_e, inputs: $\{V_a,\, c,\, \frac{dc}{dt}\}$ [1] and outputs: $\{I_a,\, B_m,\, F_f\}$) given by FGESS.M and then six logical entries which can characterise all the state's components combinations of the Kalman Filter. Furthermore an extra logical input defines if the state space will be in *continuous time* or in *discrete time*[2] . The KALSASS.M function gives as output the extended state space structure *kalsass*. If $\delta V^t = \Delta V^t$ the generalized n_e equations for the external currents are:

$$
\begin{aligned}
I_e^{t+1} &= A\, I_e^t + A_\xi\, \xi^t + O_c\, c^t + A_{\Delta\xi}\, \Delta\xi^t + B_2\, \Delta c^t + B_1\, (V_{\texttt{known}}^t + \Delta V^t) + G\, w_{I_e}^t = \\
&= A\, I_e^t + \begin{pmatrix} A_\xi & O_c \end{pmatrix} \begin{pmatrix} \xi^t \\ c^t \end{pmatrix} + \begin{pmatrix} A_{\Delta\xi} & B_2 & B_1 \end{pmatrix} \begin{pmatrix} \Delta\xi^t \\ \Delta c^t \\ \Delta V^t \end{pmatrix} + B_1\, V_{\texttt{known}}^t + G\, w_{I_e}^t = \\
&= A\, I_e^t + Z_1\, \varphi^t + Z_2\, \Delta\Phi^t + B_1\, V_{\texttt{known}}^t + G\, w_{I_e}^t
\end{aligned}
$$

where we have introduced the vectors $\varphi^t = [\xi^t\ c^t]^T$ with $\dim \varphi^t = n_\varphi = n_\xi + n_c\ \forall\, t$ and $\Delta\Phi^t = [\Delta\xi^t\ \Delta c^t\ \Delta V^t]^T$ with $\dim \Delta\Phi^t = n_{\Delta\Phi} = n_{\Delta\xi} + n_{\Delta c} + n_{\Delta V}\ \forall\, t$. Since $n_{\Delta V} = n_V = n_a$, if we impose for exemple $A_\xi = \mathcal{I}_{n_e \times n_e}$ and $n_{\Delta\xi} = n_\xi = n_e$ we have $n_\xi = n_e = n_a + n_u$, therefore $n_\varphi = n_a + n_u + n_c$ and $n_{\Delta\Phi} = 2n_a + n_u + n_c$, whereas if $n_{\Delta\xi} = 0\ \wedge\ n_\xi = n_e$ then

[1] If we consider simulations with regular time stepping $\Delta t = T_s$ we have that $\Delta c = \frac{dc}{dt}\, T_s$. The model can be easily written taking into account Δc^t or $\frac{dc^t}{dt}$ simply by multiplying or dividing the related matrix blocks by T_s.

[2] In this work *discrete time* formulation has always been adopted.

$n_\varphi = n_a + n_u + n_c$ and $n_{\Delta\Phi} = n_a + n_c$. The matrices we imposed are defined here below:

$$Z_1 = \begin{pmatrix} A_\xi & O_c \end{pmatrix} = \begin{pmatrix} \mathcal{I}_{n_e \times n_e} & \mathbb{O}_{n_e \times n_c} \end{pmatrix}$$
$$Z_2 = \begin{pmatrix} A_{\Delta\xi} & B_2 & B_1 \end{pmatrix} = \begin{pmatrix} \mathbb{O}_{n_e \times n_{\Delta\xi}} & B_2 & B_1 \end{pmatrix}$$

Now imposing an averaged constant behaviour for ξ^t and ΔV^t and a linear track for c^t we obtain that $n_c \equiv n_{\Delta c}$ and the following $n_\xi + 2n_c + n_V$ equations:

$$\xi^{t+1} = \xi^t + w_\xi^t$$
$$c^{t+1} = c^t + \Delta c^t + w_c^t$$
$$\Delta c^{t+1} = \Delta c^t + w_{\Delta c}^t$$
$$\Delta V^{t+1} = \Delta V^t + w_{\Delta V}^t$$

that have been rearranged into the following $n_\varphi + n_{\Delta\Phi}$ equations:

$$\varphi^{t+1} = Z_3\,\varphi^t + Z_4\,\Delta\Phi^t + Q_\varphi\,w_\varphi^t$$
$$\Delta\Phi^{t+1} = Z_5\,\Delta\Phi^t + Q_{\Delta\Phi}\,w_{\Delta\Phi}^t$$

with white noise vectors $w_\varphi^t = [w_\xi^t\ w_c^t]^T$ and $w_{\Delta\Phi}^t = [w_{\Delta\xi}^t\ w_{\Delta c}^t\ w_{\Delta V}^t]^T$ and matrices defined here below:

$$Z_3 = \begin{pmatrix} \mathcal{I}_{n_\xi \times n_\xi} & \mathbb{O}_{n_\xi \times n_c} \\ \mathbb{O}_{n_c \times n_\xi} & \mathcal{I}_{n_c \times n_c} \end{pmatrix}$$
$$Z_4 = \begin{pmatrix} Z_4^\xi & \mathbb{O}_{n_\xi \times n_c} & \mathbb{O}_{n_\xi \times n_V} \\ \mathbb{O}_{n_c \times n_{\Delta\xi}} & \mathcal{I}_{n_c \times n_c} & \mathbb{O}_{n_c \times n_V} \end{pmatrix} = \begin{pmatrix} \mathbb{O}_{n_\xi \times n_{\Delta\xi}} & \mathbb{O}_{n_\xi \times n_c} & \mathbb{O}_{n_\xi \times n_V} \\ \mathbb{O}_{n_c \times n_{\Delta\xi}} & \mathcal{I}_{n_c \times n_c} & \mathbb{O}_{n_c \times n_V} \end{pmatrix}$$
$$Z_5 = \begin{pmatrix} Z_5^{\Delta\xi} & \mathbb{O}_{n_{\Delta\xi} \times n_c} & \mathbb{O}_{n_{\Delta\xi} \times n_V} \\ \mathbb{O}_{n_c \times n_{\Delta\xi}} & \mathcal{I}_{n_c \times n_c} & \mathbb{O}_{n_c \times n_V} \\ \mathbb{O}_{n_V \times n_{\Delta\xi}} & \mathbb{O}_{n_V \times n_c} & \mathcal{I}_{n_V \times n_V} \end{pmatrix} = \begin{pmatrix} \mathbb{O}_{n_{\Delta\xi} \times n_{\Delta\xi}} & \mathbb{O}_{n_{\Delta\xi} \times n_c} & \mathbb{O}_{n_{\Delta\xi} \times n_V} \\ \mathbb{O}_{n_c \times n_{\Delta\xi}} & \mathcal{I}_{n_c \times n_c} & \mathbb{O}_{n_c \times n_V} \\ \mathbb{O}_{n_V \times n_{\Delta\xi}} & \mathbb{O}_{n_V \times n_c} & \mathcal{I}_{n_V \times n_V} \end{pmatrix}$$

If we want to impose a linear track for ξ it is sufficient to set $Z_4^\xi = Z_5^{\Delta\xi} = \mathcal{I}_{n_\xi \times n_\xi}$ and in this case $n_\xi \equiv n_{\Delta\xi}$. If we didn't deal with $\Delta\xi^t$ the matrices Q_φ and $Q_{\Delta\Phi}$ are simply:

$$Q_\varphi = \begin{pmatrix} \mathcal{I}_{n_\xi \times n_\xi} & \mathbb{O}_{n_\xi \times n_c} \\ \mathbb{O}_{n_c \times n_\xi} & \mathcal{I}_{n_c \times n_c} \end{pmatrix}$$
$$Q_{\Delta\Phi} = \begin{pmatrix} \mathbb{O}_{n_\xi \times n_\xi} & \mathbb{O}_{n_\xi \times n_c} & \mathbb{O}_{n_\xi \times n_V} \\ \mathbb{O}_{n_c \times n_\xi} & \mathcal{I}_{n_c \times n_c} & \mathbb{O}_{n_c \times n_V} \\ \mathbb{O}_{n_V \times n_\xi} & \mathbb{O}_{n_V \times n_c} & \mathcal{I}_{n_V \times n_V} \end{pmatrix}$$

Once defined the **augmented state** [3] as $x^t = [I_e^t\ \varphi^t\ \Delta\Phi^t]^T$, with $\dim x^t = n_e + n_\varphi + n_{\Delta\Phi}$ we have obtained the following *generalized state space model*:

$$x^{t+1} = A_{\mathtt{au}}\,x^t + B_{\mathtt{au}}\,V_{\mathtt{known}}^t + Q_x\,w_x^t =$$
$$= \begin{pmatrix} I_e^{t+1} \\ \varphi^{t+1} \\ \Delta\Phi^{t+1} \end{pmatrix} = \begin{pmatrix} A & Z_1 & Z_2 \\ \mathbb{O} & Z_3 & Z_4 \\ \mathbb{O} & \mathbb{O} & Z_5 \end{pmatrix} \begin{pmatrix} I_e^t \\ \varphi^t \\ \Delta\Phi^t \end{pmatrix} + \begin{pmatrix} B_1 \\ \mathbb{O}_{n_\varphi \times n_a} \\ \mathbb{O}_{n_{\Delta\Phi} \times n_a} \end{pmatrix} V_{\mathtt{known}}^t + \begin{pmatrix} G & \mathbb{O} & \mathbb{O} \\ \mathbb{O} & Q_\varphi & \mathbb{O} \\ \mathbb{O} & \mathbb{O} & Q_{\Delta\Phi} \end{pmatrix} w_x^t$$

[3] The filter behaviour has been validated with the previous *rejection tests* considering only the external currents as state vector components: i.e. with $n_\varphi = 0\ \wedge\ n_{\Delta\Phi} = 0$.

with white noise vector $w_x^t = [w_{I_e}^t \; w_\varphi^t \; w_{\Delta\Phi}^t]^T$ [4]. The KALSASS.M function computes also the matrices which appear into the *generalized observer equation*. In physical frame, if we define the equilibrium state as $x_{eq} = [I_{e,eq} \; c_{eq}]^T$ we get:

$$\begin{cases} y^t = C_1\, I_e^t + C_2\, c^t + C_3\, \Delta c^t + y_o \\ y_o = \tilde{D}\, U = \tilde{D} \begin{pmatrix} x_{eq} \\ y_{eq} \end{pmatrix} \end{cases}$$

Since $\xi_{eq} = \Delta\xi_{eq} = \Delta c_{eq} = \Delta V_{eq} = \underline{0}$, then $U = [I_{e,eq} \; c_{eq} \; y_{eq}]^T$, thus:

$$\tilde{D} = \begin{pmatrix} -C_1 & -C_2 & \mathcal{I}_{n_y \times n_y} \end{pmatrix} = \begin{pmatrix} -C & -D & \mathcal{I}_{n_y \times n_y} \end{pmatrix}$$

with $n_y = n_a + n_m + n_f = \dim y^t$. We therefore obtain:

$$\begin{aligned} y^t &= C_{\mathtt{au}}\, x^t + \tilde{D}\, U = \\ &= \begin{pmatrix} I_a^t \\ B_m^t \\ F_f^t \end{pmatrix} = \begin{pmatrix} C_1 & M & N \end{pmatrix} \begin{pmatrix} I_e^t \\ \varphi^t \\ \Delta\Phi^t \end{pmatrix} + \begin{pmatrix} -C_1 & -C_2 & \mathcal{I}_{n_y \times n_y} \end{pmatrix} \begin{pmatrix} I_{e,eq} \\ c_{eq} \\ y_{eq} \end{pmatrix} \end{aligned}$$

with matrices:

$$\begin{aligned} M &= \begin{pmatrix} \mathbb{O}_{n_y \times n_\xi} & C_2 \end{pmatrix} = \begin{pmatrix} \mathbb{O}_{n_y \times n_\xi} & D \end{pmatrix} \\ N &= \begin{pmatrix} \mathbb{O}_{n_y \times n_{\Delta\xi}} & C_3 & \mathbb{O}_{n_y \times n_V} \end{pmatrix} = \begin{pmatrix} \mathbb{O}_{n_y \times n_{\Delta\xi}} & \mathbb{O}_{n_y \times n_{\Delta c}} & \mathbb{O}_{n_y \times n_V} \end{pmatrix} \end{aligned}$$

4.4.2 Sinusoidal perturbation

A sinusoidal perturbation has been added to the first PF coil voltage V_{a1}:

$$\tilde{V}_{a1}^t = V_{a1}^t + x_1^t + w_1^t$$

where $V_{a1} < 0$ is the constant voltage of the first PF coil after an unperturbed run of FGE, x_1 is the sinusoidal disturbance defined by:

$$x_1^t = -k\sqrt{2}\, V_{a1,RMS}\, \sin(2\pi f t)$$

with $k = 0.01$, $V_{a1,RMS} = |V_{a1}|$ and $f = \frac{1}{T} = \frac{1}{t(n_t) - t(1)} = 1\, Hz$ since $T = 1\, s$.
We added to this perturbation a white noise w_1 too, with amplitude $V_{a1,err} = 0.2\, V$. Finally, a global white noise of amplitude k has been added to all the voltage components. For the covariance matrix design the active currents block Q_a has been chosen diagonal with diagonal elements equal to $Q_a(i,i) = 100$. For the vessel block Q_v it has been implemented a continuous *Toeplitz* algorithm with main diagonal elements equals to $Q_v(i,i) = 10$. A change of basis then sent Q_v to Q_u since we adopted the eigenmode representation with $n_u = 8$. Finally, the process covariance matrix has been set block diagonal with blocks Q_a and Q_u.

In order to show that an increasing process covariance matrix improves the estimation of unknown perturbations in the system, both cases Q and $10\, Q$ have been considered. In the state augmented case we assumed that the additional state components enters in all the components of the external current state. The initial condition of these perturbations has been fixed to zero and their stochastic dynamics is driven by the sum of an additional

[4] In any case the stochastic addendum $Q_x\, w_x^t$ is not computed by KALSASS.M since for Kalman Filters models the predictive equation takes only the deterministic contributions.

unitary white noise. Therefore, the block $Q_\xi \in \mathbb{R}^{n_\xi} = \mathbb{R}^{n_a+n_u}$ has been chosen diagonal with diagonal elements $Q_\xi(i,i) = 1$. Since we have assumed the external currents to be independent of the $\xi_i \ \forall\, i = 1, ..., n_\xi$, the global state augmented process covariance matrix is the block diagonal matrix of blocks Q and Q_ξ. In figures (4.28 , 4.29 , 4.30 , 4.31) the estimation performances of the fastest and slowest eigencurrents estimates, the sum of the active currents estimates and the first PF coil current are depicted, in the cases of process covariance matrices Q and $10\,Q$ or in the augmented state case. As we can see, we can recover the unknown perturbations simply by augmenting the process covariance matrix. However, this increases a lot the quantity of measurement noise in the system. In the state augmented case the tracking is more accurate and not very noisy.

Referring to the KALSASS.M function, we have compared the simplest state with $n_\varphi = 0 \ \wedge \ n_{\Delta\Phi} = 0$ with the simple augmented state with $n_\varphi = n_\xi = n_e \ \wedge \ n_{\Delta\Phi} = 0$. We can see in figure (4.32), the normalized *Power Density Spectrum* of the ξ disturbances. This plot has been implemented first of all computing the **FFT** [5] of the ξ_i and then multiplying each transformed component with its complex conjugate. We can see that most of the ξ_i-disturbances have an high amplitude in the Fourier space at $1\,Hz$, which is the frequency at which the first PF coil has been perturbed.

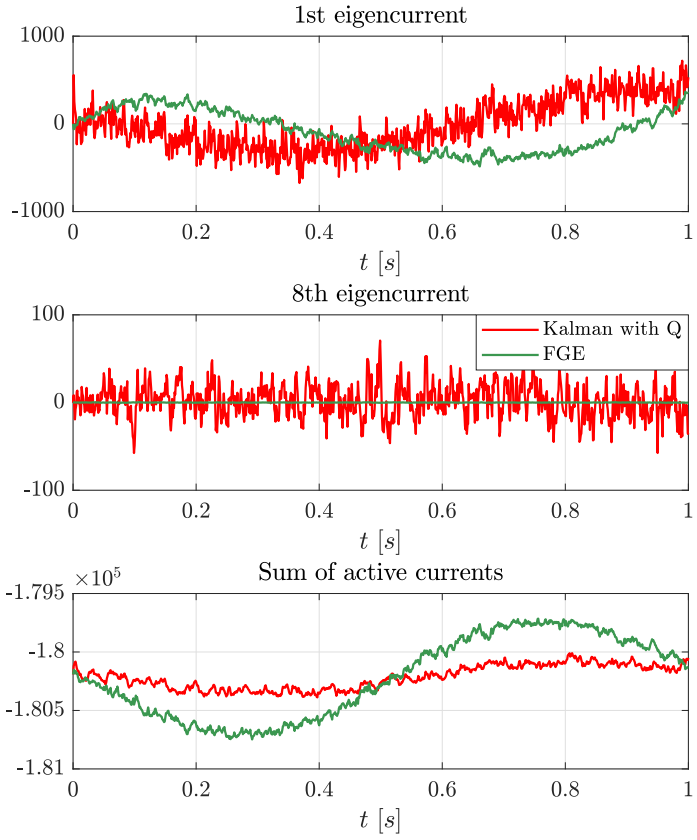

Figure 4.28: $1st$ and $8th$ eigencurrents, sum of active currents with Q, $n_\varphi = n_{\Delta\Phi} = 0$

[5] *Fast Fourier Transform*: $\mathcal{F}_d\,(\xi_i) = \sum_{k=1}^{n_t} \xi_i(k)\, \exp(-\jmath\, \frac{2\pi}{n_t}\, k\, t) \ , \ \ t = 1, ..., n_t, \ \ \forall\, i = 1, ..., n_\xi.$

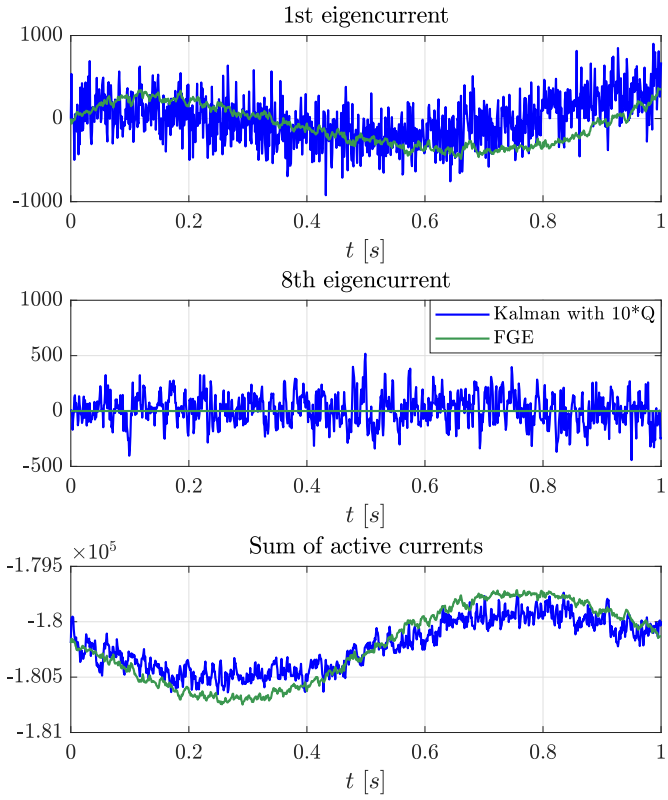

Figure 4.29: $1st$ and $8th$ eigencurrents, sum of active currents with $10\,Q$, $n_\varphi = n_{\Delta\Phi} = 0$

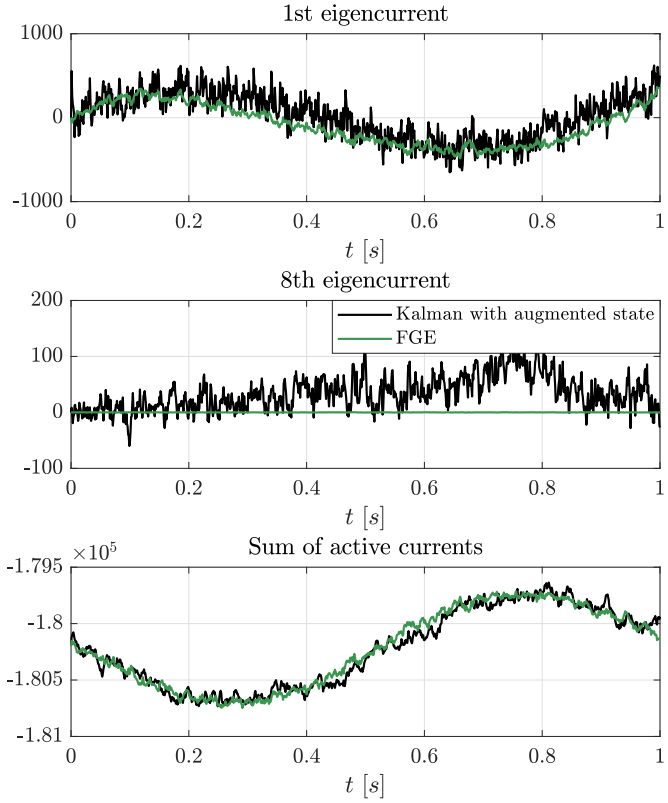

Figure 4.30: $1st$ and $8th$ eigencurrents, sum of active currents with augmented state Q, $n_\varphi = n_\xi = n_e \ \wedge \ n_{\Delta\Phi} = 0$

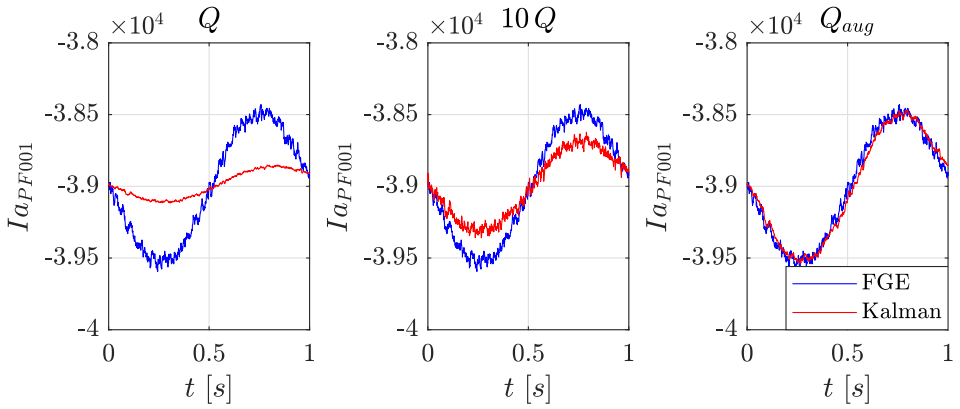

Figure 4.31: First coil current estimates comparison with sinusoidal unknown perturbation

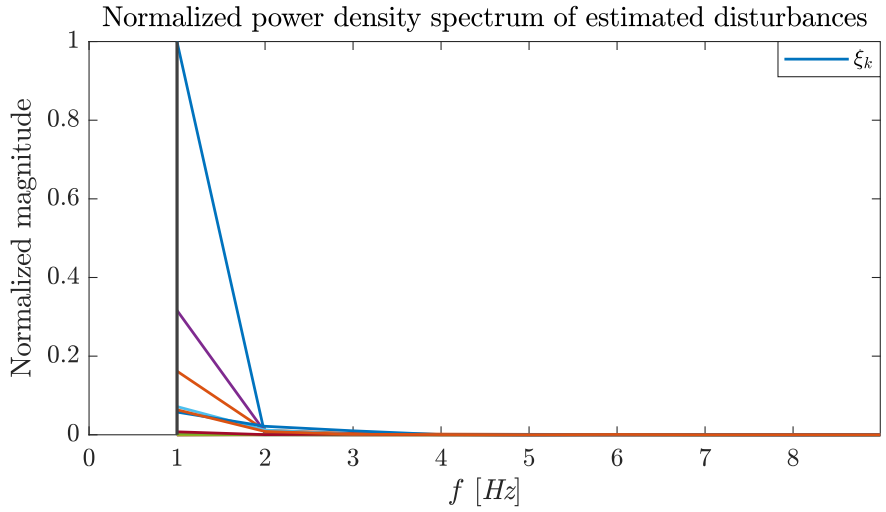

Figure 4.32: Normalized *Power Density Spectrum* of the ξ disturbances

Finally, we presented the augmented state case in which $n_\varphi = n_\xi = n_e \ \wedge \ n_{\Delta\Phi} = n_V = n_a$, with covariance matrix block $Q_{\delta V}$ of the $\delta V \in \mathbb{R}^{n_a}$ state component, matching exactly the input white noise imposed in all the coils, i.e. $Q_{\delta V} = k^2\, \mathcal{I}_{n_a \times n_a}$. In this way the filter is able to predict the state taking into account multiple sources of perturbation (in this case constant disturbances on the currents and on the input voltages, with random evolutions driven by the *measurement-update* equations) that participate to the state evolution. We obtained a further improvement in the estimation performance since in this case the signal is closer to the sinusoidal input even though it is a bit more noisy. In figures (4.33 , 4.34 , 4.35) the first poloidal coil currents are compared together with the sparsity patterns of the covariance matrices Q in all the three situations.

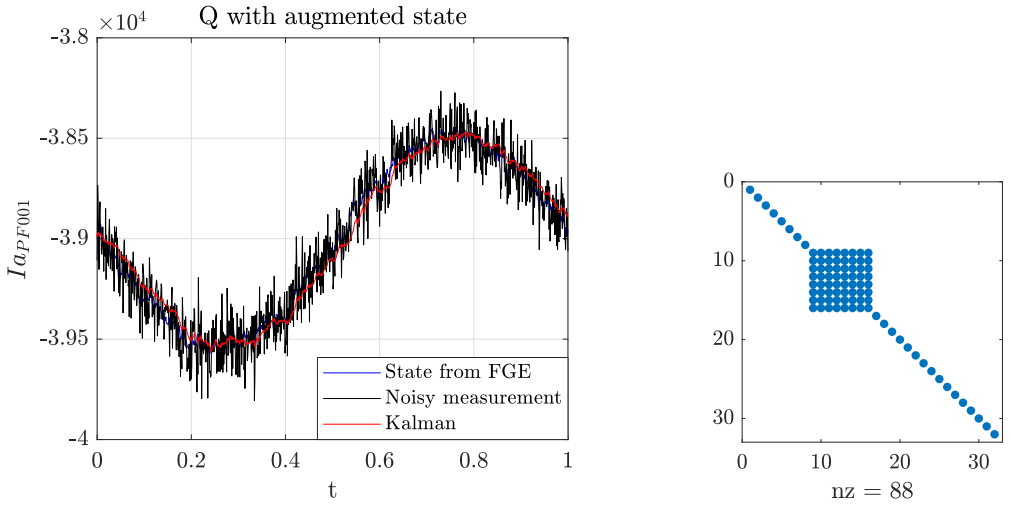

Figure 4.33: $n_\varphi = n_\xi = n_e \ \wedge \ n_{\Delta\Phi} = 0$

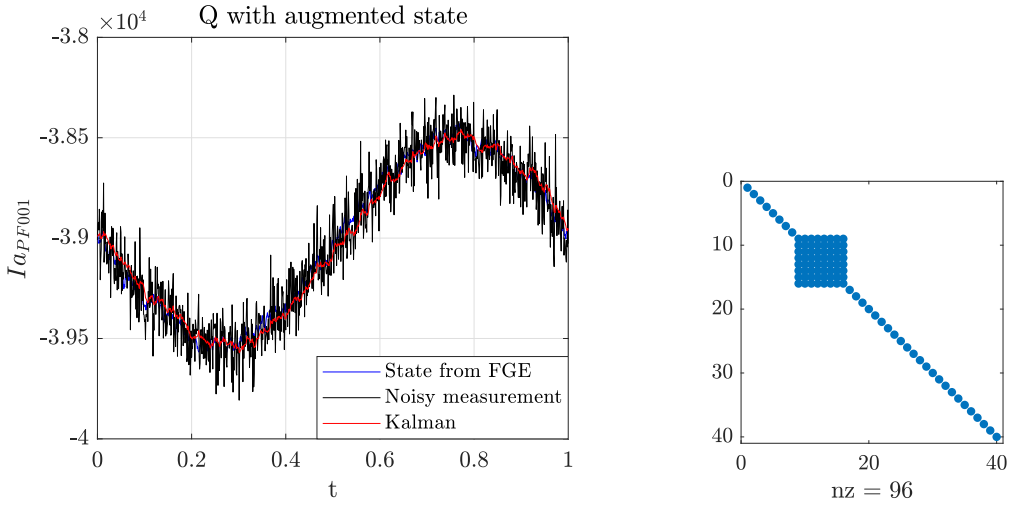

Figure 4.34: $n_\varphi = n_\xi = n_e, \wedge n_{\Delta\Phi} = n_{\Delta V} = n_a$

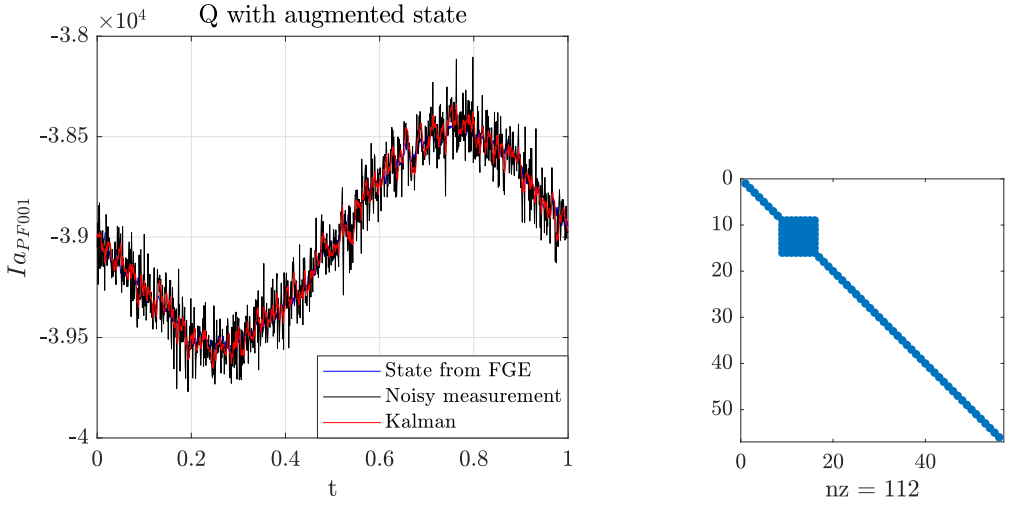

Figure 4.35: $n_\varphi = n_\xi = n_e \ \wedge \ n_{\Delta\Phi} = n_{\Delta\xi} + n_{\Delta V} = n_e + n_a = 2n_a + n_u$

4.4.2.1 Correlated and uncorrelated comparison

So far we have not considered correlation between the noises on ξ_i and the noises on the active currents. In this subsection we have fixed $n_\varphi = n_\xi = n_a \ \wedge \ n_{\Delta\Phi} = 0$ and we have tried to study, by imposing correlation between perturbation noises and active current noises of the same index, whether there would have been estimation improvements with respect to the previous uncorrelated state augmented case. The cross-covariances have already been defined in the Chapter 2 (2.3) and have been chosen as the *geometric mean* of the covariances of the i-th noises of ξ and I_a.

Like before the main estimated quantities are presented in both cases in figures (4.38). With this specific perturbation the performances are almost the same, except for the very initial time-steps of the estimation, as we can see looking at the first coil current estimation in figure (4.36).

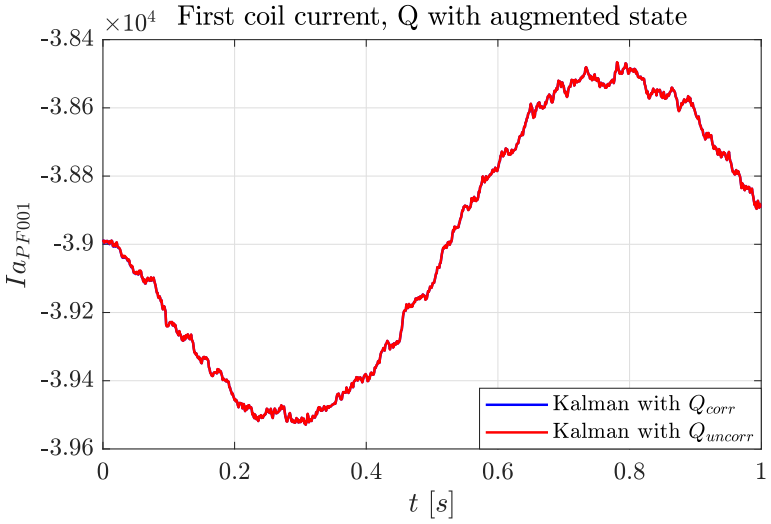

Figure 4.36: Correlated and uncorrelated comparison for first coil current estimation

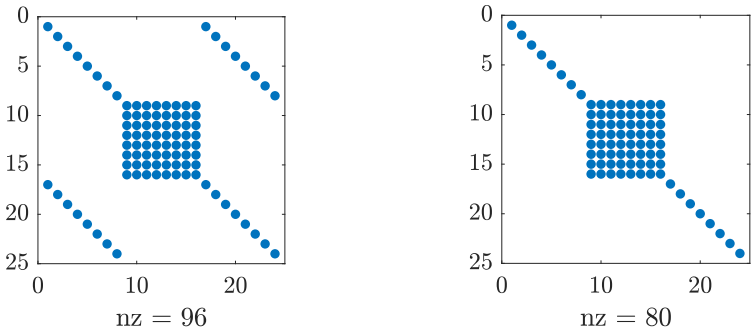

Figure 4.37: Correlated and uncorrelated global process covariance matrices sparsity patterns

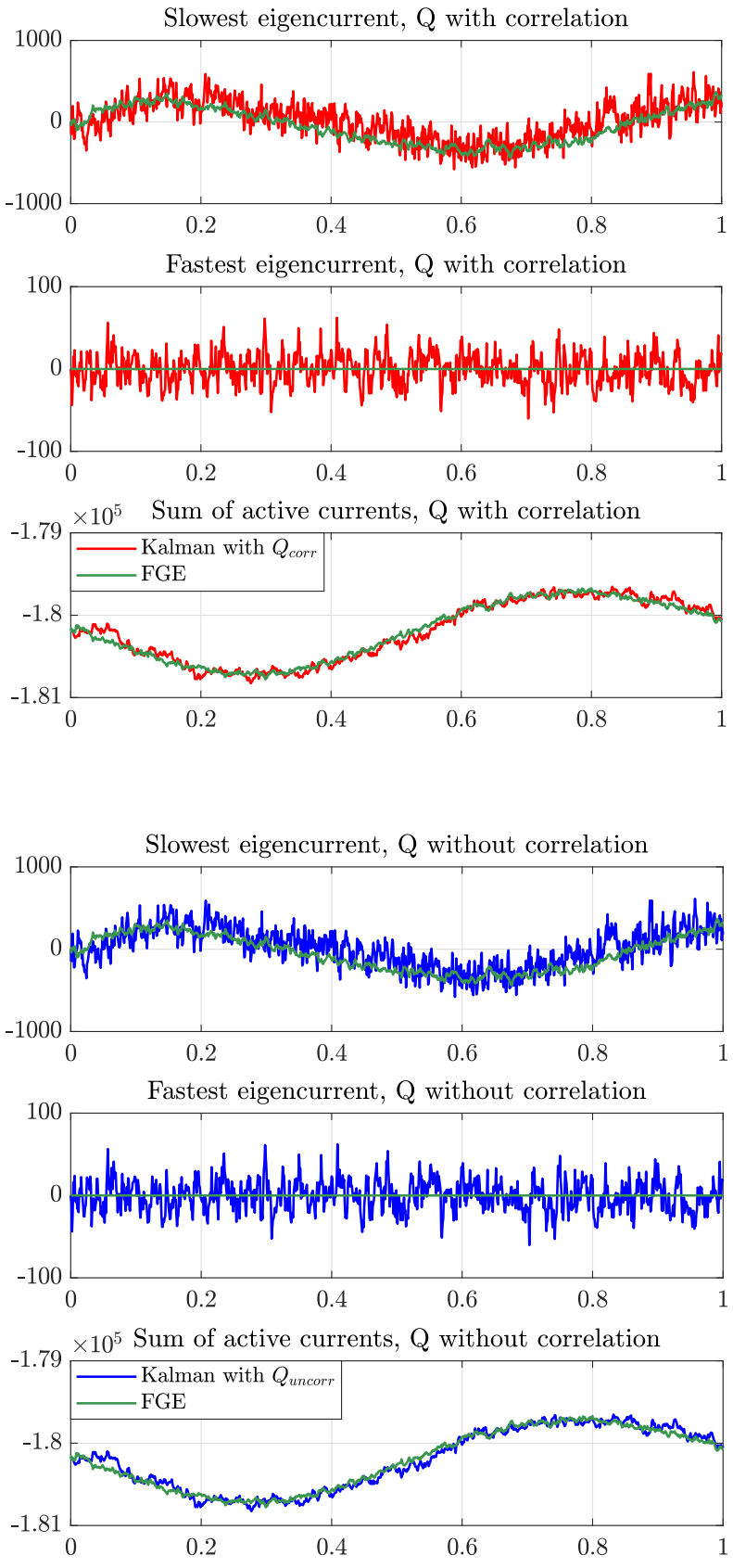

Figure 4.38: Slowest and fastest eigencurrent, sum of active currents with correlation (red) and without correlation (blue): as we can see the performances are almost the same in both cases

4.4.3 Step perturbation

In this subsection a noisy step perturbation affects one more time the first PF coil voltage V_{a1}:

$$\tilde{V}_{a1}^t = V_{a1}^t + x_1^t + w_1^t$$

where $V_{a1} < 0$ is the constant voltage of the first PF coil after an unperturbed run of FGE and where x_1 is the step disturbance from $0.4\,s$ to $0.6\,s$ defined by:

$$x_1^t = \text{rect}\left(\frac{t - 0.5}{5}\right)$$

i.e. the unitary rectangle centered in $t = 0.5\,s$ and with length of $0.1\,s$. Moreover, w_1 is a white noise over all the time domain with amplitude $k = 0.01$ (4.40). Finally, a global white noise of amplitude k has been added to all the voltage components. For the process covariance matrix design we adopted the same approach of the sinusoidal case. In figures (4.39 , 4.41 , 4.42 , 4.43) are exposed the differences between the main estimated quantities both with Q, $10\,Q$ and in the augmented state case with $n_\xi = n_a + n_u$. Referring to the KALSASS.M function, we have compared the simplest state with $n_\varphi = 0 \ \wedge \ n_{\Delta\Phi} = 0$ with the simple augmented state with $n_\varphi = n_\xi = n_e \ \wedge \ n_{\Delta\Phi} = 0$.

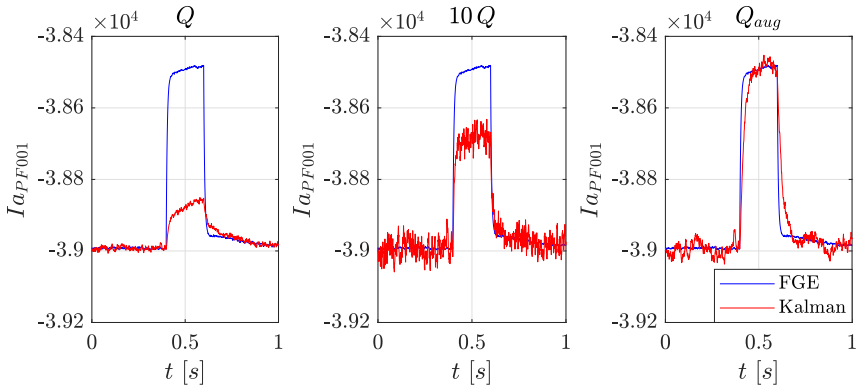

Figure 4.39: Active current estimates of the first PF coil

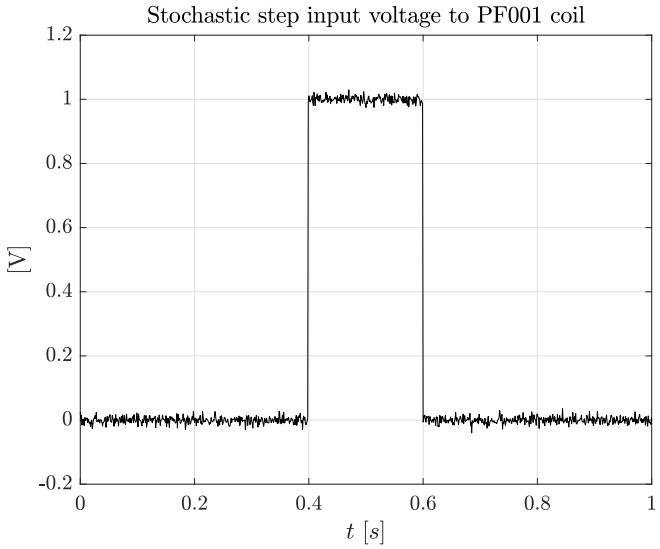

Figure 4.40: Stochastic step input voltage perturbation of the first PF coil

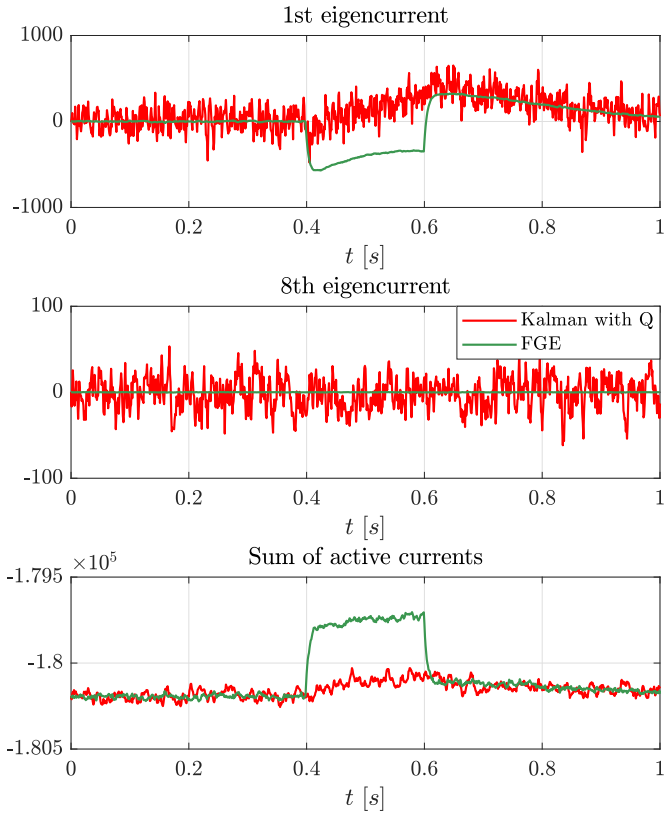

Figure 4.41: 1*st* and 8*th* vessel eigencurrents, sum of active currents with Q

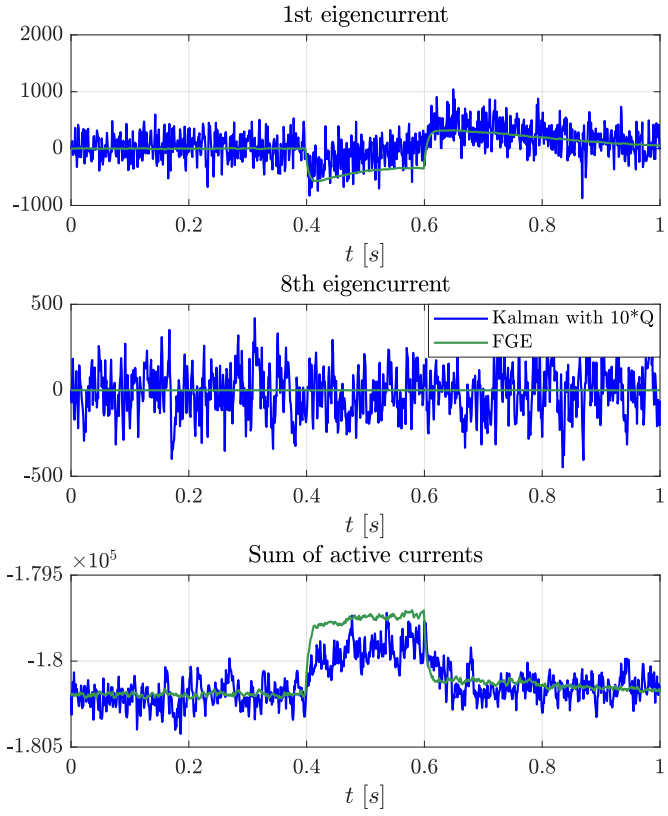

Figure 4.42: 1*st* and 8*th* vessel eigencurrents, sum of active currents with $10\,Q$

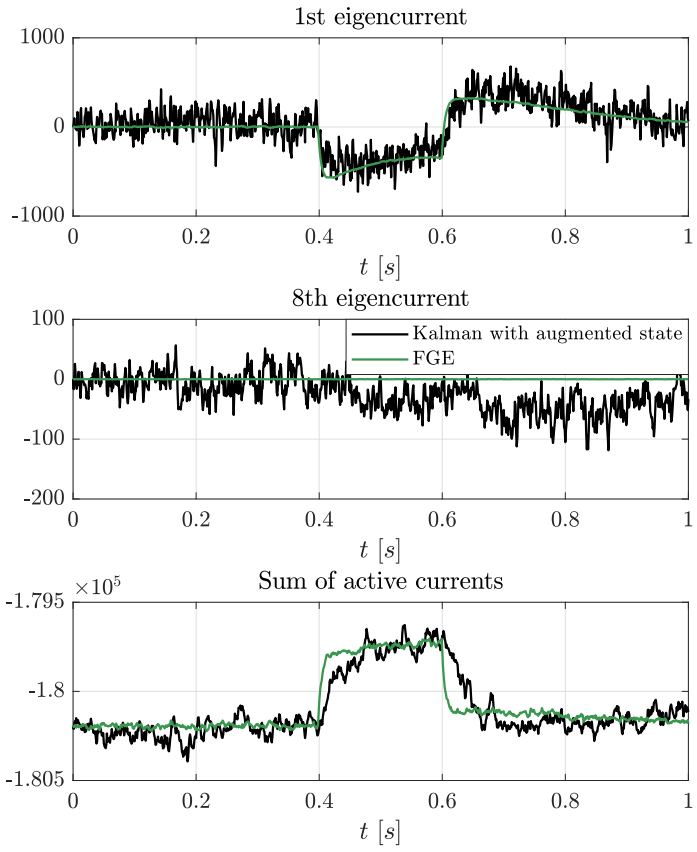

Figure 4.43: 1*st* and 8*th* vessel eigencurrents, sum of active currents with Kalman filter augmented state

As we can see, we can recover the unknown perturbations simply by augmenting the process covariance matrix but, once more, this increases the quantity of measurement noise in the system. In the state augmented case the tracking is improved allowing to estimate more accurately while remaining less sensitive to noise, compared to the case without state augmentation. This can be ascertained looking at the active current estimates of the first PF coil in all the three cases (4.39).

4.4.4 Constraints estimation

In this subsection we have extended the state in order to estimate the internal plasma constraints evolution $\beta_p(t)$ and $q_A(t)$ after an unknown perturbation of their derivatives. In particular we have performed the estimations in these two cases:

- Monotonically increasing q_A-ramp
- Monotonically decreasing and increasing β_p-ramp with $\frac{d\beta_p}{dt}$ discontinuity

For both cases we extended the state in order to impose $n_\varphi = n_c \ \wedge \ n_{\Delta\Phi} = n_{\Delta c} = n_c$.

4.4.4.1 q_A-ramp

First of all we have perturbed the system introducing a monotonically increasing q_A-ramp which has been computed by integrating its time derivative $\frac{dq_A}{dt}$ which is a 0.2 constant with an extra white noise perturbation of amplitude $k = 0.5 \cdot 10^{-6}$. Then we add a tiny amount of white noise to all the voltages in order to let the dynamics of the system been excited essentially by the q_A-perturbation. We set for **Anamak** the **TCV** standard measurement noises $\{\omega_a, \omega_m, \omega_f\} = \{100\,A,\, 10^{-3}\,T,\, 10^{-3}\,Wb\}$ and then we reattempted the estimation with a 10-times lower measurement noises. We set initial condition of the estimation error covariance matrix $P_0 = 10\,Q$ and we imposed Q_c, $Q_{\Delta c}$ submatrices as diagonal uncorrelated blocks. The process covariance matrix is varying with time-step Δt and it is equal to:

$$Q = \begin{pmatrix} Q_e & \mathbb{O} & \mathbb{O} \\ \mathbb{O} & Q_c & \mathbb{O} \\ \mathbb{O} & \mathbb{O} & Q_{\Delta c} \end{pmatrix}$$

with:

$$\begin{pmatrix} Q_c & \mathbb{O} \\ \mathbb{O} & Q_{\Delta c} \end{pmatrix} = \begin{pmatrix} \Delta t\,\sigma_{I_p} & 0 & 0 & 0 & 0 & 0 \\ 0 & \Delta t\,\sigma_{\beta_p} & 0 & 0 & 0 & 0 \\ 0 & 0 & \Delta t\,\sigma_{q_A} & 0 & 0 & 0 \\ 0 & 0 & 0 & \frac{1}{3}\Delta t^3\,\sigma_{\Delta I_p} & 0 & 0 \\ 0 & 0 & 0 & 0 & \frac{1}{3}\Delta t^3\,\sigma_{\Delta \beta_p} & 0 \\ 0 & 0 & 0 & 0 & 0 & \frac{1}{3}\Delta t^3\,\sigma_{\Delta q_A} \end{pmatrix}$$

In the simultation t ranges from 0 to 1 s with $\Delta t = 10^{-3}$. We have chosen $\{\sigma_{I_p},\, \sigma_{\beta_p},\, \sigma_{q_A}\} = \{10^6,\, 1,\, 10^{-5}\}$ and $\{\sigma_{\Delta I_p},\, \sigma_{\Delta \beta_p},\, \sigma_{\Delta q_A}\} = \{10^6,\, 1,\, 10^{-2}\}$ and we imposed the right initial condition on $\frac{dq_A}{dt}$. At the end of the subsection the estimations of $\{q_A,\, \beta_p\}$-ramps and their derivatives are presented both with standard and reduced measurement noises (4.45 , 4.46).

4.4.4.2 β_p-ramp

First of all we have perturbed the system introducing a monotonically increasing β_p-ramp from $t \in [0,\, 0.5]\,s$ and a monotonically decreasing β_p-ramp from $t \in [0.5,\, 1]\,s$, which has been computed by integrating its time derivative $\frac{d\beta_p}{dt}$ which presents a discontinuity at $t = 0.5\,s$ and a symmetrical jump of amplitude $8{\cdot}10^{-5}$. Then we add a tiny amount of white noise to all the voltages in order to let the dynamics of the system been excited essentially by the β_p-perturbation. We set, in a first moment **TCV** standard measurement noises $\{\omega_a, \omega_m, \omega_f\} = \{100\,A,\, 10^{-3}\,T,\, 10^{-3}\,Wb\}$ and then we retrieved the simulation with a lesser measurement noise i.e. $\{\omega_a, \omega_m, \omega_f\} = \{10\,A,\, 10^{-4}\,T,\, 10^{-4}\,Wb\}$. We have seen that the tracking is less oscillating if there is less measurement noise. In any case the estimation of β_p is really hard to recover with high precision since the initial condition over $\frac{d\beta_p}{dt}$ is given wrong and equal to 0. In order to increase the estimation performances a big initial condition onto the estimation error covariance matrix has been set, i.e. $P_0 = 200\,Q$. Like in the q_A-ramp case we have imposed Q_c, $Q_{\Delta c}$ submatrices as diagonals without introducing correlation between these two blocks. In a further step we have tried to introduce some correlation through a new block $Q_{c,\Delta c}$ but without seeing great improvements in the results. The process covariance matrix is varying with time-step Δt and it is equal to:

$$Q = \begin{pmatrix} Q_e & \mathbb{O} & \mathbb{O} \\ \mathbb{O} & Q_c & Q_{c,\Delta c} \\ \mathbb{O} & Q_{c,\Delta c} & Q_{\Delta c} \end{pmatrix}$$

with:

$$\begin{pmatrix} Q_c & Q_{c,\Delta c} \\ Q_{c,\Delta c} & Q_{\Delta c} \end{pmatrix} = \begin{pmatrix} \Delta t\,\sigma_{I_p} & 0 & 0 & 0 & 0 & 0 \\ 0 & \Delta t\,\sigma_{\beta_p} & 0 & 0 & 0 & 0 \\ 0 & 0 & \Delta t\,\sigma_{q_A} & 0 & 0 & 0 \\ 0 & 0 & 0 & \frac{1}{3}\Delta t^3\,\sigma_{\Delta I_p} & 0 & 0 \\ 0 & 0 & 0 & 0 & \frac{1}{3}\Delta t^3\,\sigma_{\Delta\beta_p} & 0 \\ 0 & 0 & 0 & 0 & 0 & \frac{1}{3}\Delta t^3\,\sigma_{\Delta q_A} \end{pmatrix}$$

or, if there is correlation, it is equal to [14]:

$$\begin{pmatrix} Q_c & Q_{c,\Delta c} \\ Q_{c,\Delta c} & Q_{\Delta c} \end{pmatrix} = \begin{pmatrix} \Delta t\,\sigma_{I_p} & 0 & 0 & \frac{1}{2}\Delta t^2\,\sigma_{I_p} & 0 & 0 \\ 0 & \Delta t\,\sigma_{\beta_p} & 0 & 0 & \frac{1}{2}\Delta t^2\,\sigma_{\beta_p} & 0 \\ 0 & 0 & \Delta t\,\sigma_{q_A} & 0 & 0 & \frac{1}{2}\Delta t^2\,\sigma_{q_A} \\ \frac{1}{2}\Delta t^2\,\sigma_{I_p} & 0 & 0 & \frac{1}{3}\Delta t^3\,\sigma_{\Delta I_p} & 0 & 0 \\ 0 & \frac{1}{2}\Delta t^2\,\sigma_{\beta_p} & 0 & 0 & \frac{1}{3}\Delta t^3\,\sigma_{\Delta\beta_p} & 0 \\ 0 & 0 & \frac{1}{2}\Delta t^2\,\sigma_{q_A} & 0 & 0 & \frac{1}{3}\Delta t^3\,\sigma_{\Delta q_A} \end{pmatrix}$$

In the simultation t ranges from 0 to 1 s with $\Delta t = 10^{-3}$. We have chosen $\{\sigma_{I_p}, \sigma_{\beta_p}, \sigma_{q_A}\} = \{10^6, 7 \cdot 10^{-6}, 10^{-6}\}$ and $\{\sigma_{\Delta I_p}, \sigma_{\Delta\beta_p}, \sigma_{\Delta q_A}\} = \{10^6, 10^5, 10^{-6}\}$.

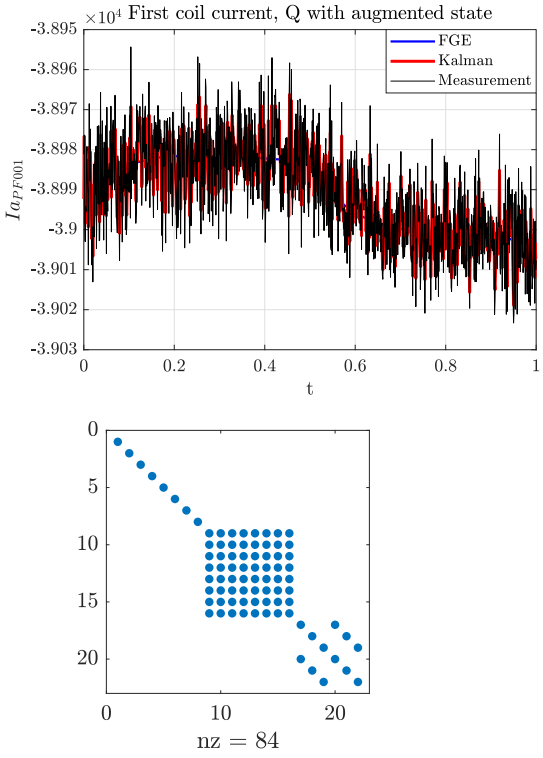

Figure 4.44: First coil current after β_p-ramp perturbation; sparsity pattern of covariance matrix Q, with c-Δc correlation but without I_e-c correlation

If the measurement noise is set low it is possible to select a higher process covariance matrix (with respect to measurements covariance matrix R) so that the filter will be able to easily adapt to quick changes such as a discontinuity in the time derivative of a component of its state. On the other hand, if the measurement noise is set high, keeping the process covariance high as well all the measurement noise will enter in the estimates (4.47 , 4.48). Therefore in this case it is necessary to lower the process covariance matrix, renouncing to the possibility of recovering fast changes of the parameters. An intersting estimation improvement would be to analyze in depth the relationships between the parameters and the active and vessel currents. In order to do so it will be necessary to reduce the perturbation on the voltages letting the state evolution being a direct consequence of β_p-perturbation. An intersting further covariance matrix design improvement would be to fill some correlations between the errors of β_p, the first vessel eigenmodes (the slowest ones) errors and the active coils errors. The estimated first coil current after β_p-ramp perturbation and the sparsity pattern of Q introducing correlation between c and Δc are shown in figure (4.44). We can see that the estimation of first coil I_a retrieved by the Kalman filter follows the FGE profile and reduces the noises of the measurements.

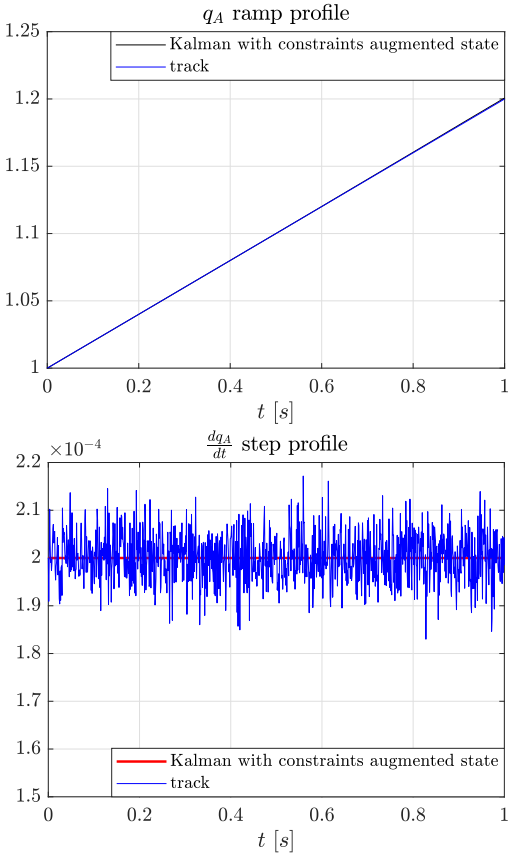

Figure 4.45: Tracking of q_A-ramp and $\frac{dq_A}{dt}$-step with $\{\omega_a, \omega_m, \omega_f\} = \{100\,A,\ 10^{-3}\,T,\ 10^{-3}\,Wb\}$

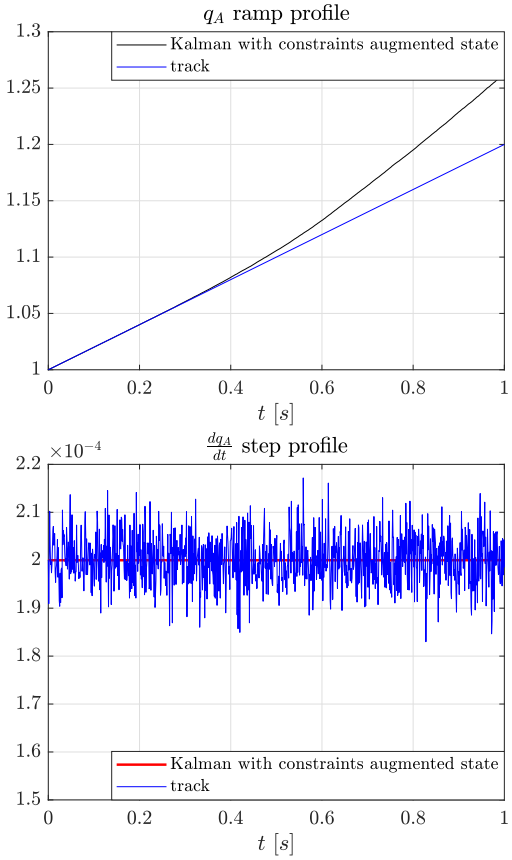

Figure 4.46: Tracking of q_A-ramp and $\frac{dq_A}{dt}$-step with $\{\omega_a, \omega_m, \omega_f\} = 0.1 \cdot \{100\,A,\ 10^{-3}\,T,\ 10^{-3}\,Wb\}$

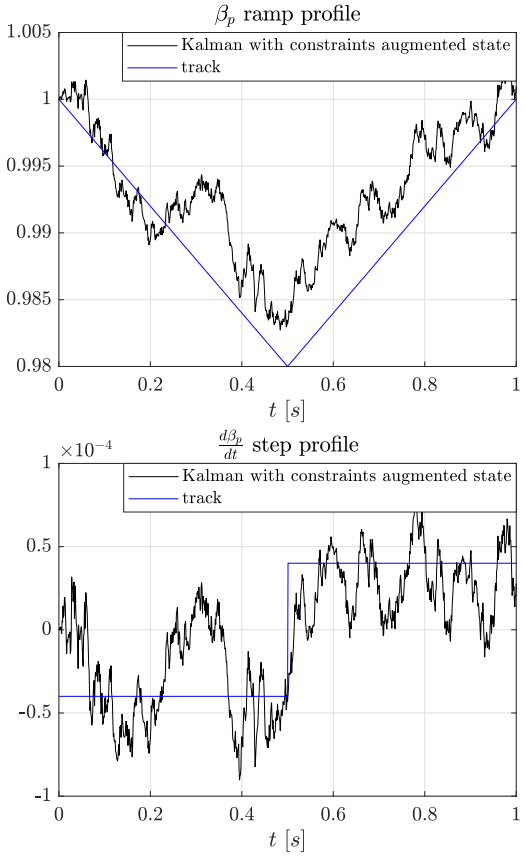

Figure 4.47: Tracking of β_p-ramp and $\frac{d\beta_p}{dt}$-step with $\{\omega_a, \omega_m, \omega_f\} = \{100\,A,\, 10^{-3}\,T,\, 10^{-3}\,Wb\}$

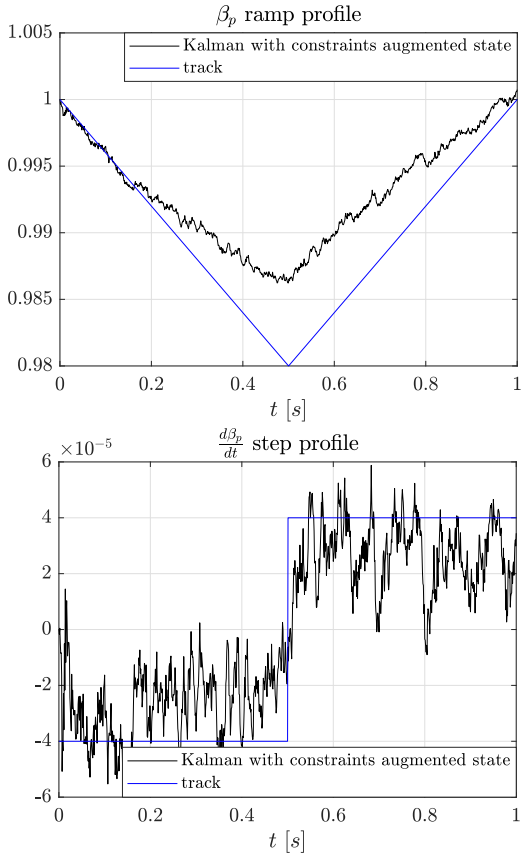

Figure 4.48: Tracking of β_p-ramp and $\frac{d\beta_p}{dt}$-step with $\{\omega_a, \omega_m, \omega_f\} = 0.1 \cdot \{100\,A,\, 10^{-3}\,T,\, 10^{-3}\,Wb\}$

4.4.5 Plasma position estimation

In this subsection the post-processing plasma vertical and radial position estimates are presented. The position of plasma is computed directly from the estimated state and the measured total plasma current[6]. We will see in the next Chapter (5.2) that it is possible to compute the baricentral positions rI_p and zI_p of the plasma by multiplying the state x of the system (I_e or $[\, I_e \; c]^T$) by $\frac{\partial rI_p}{\partial x}$ and $\frac{\partial zI_p}{\partial x}$ (see block diagrams in 5.19 , 5.20). The radial and vertical positions are then computed by multiplying these quantities by I_p.

In figures (4.49 , 4.50 , 4.51 , 4.52 , 4.53) the radial and vertical plasma positon evolutions are computed in a stable circular shot of **Anamak** over a 1 s time window of simulation. The following perturbations have been used:

1. Sinusoidal voltage perturbation (first coil)
2. Step voltage perturbation (first coil)
3. White noise voltage perturbation
4. q_A-ramp constraint perturbation
5. β_p-ramp constraint perturbation

In the case 3. the white noise has been injected with amplitude of $4\,V$ to all the n_a voltages, whereas for the other cases the disturbance is the same as that presented in the previous subsections.

Several combinations of the state augmentation have been set using the KALSASS.M function which have given some improvements in the plasma position estimation. In any case, even if we set $n_\varphi = n_{\Delta\Phi} = 0$ and we refer to the simplest state accounting only for the external currents, neglecting the constraints contributions and using a reduced substate that takes into account only the slowest $n_u = 8$ vessel eigencurrents, the plasma position is still well recovered in **Anamak** for all these induced perturbations test-cases.

In the first part of the next Chapter (5.1) the full augmented state design of the Kalman filter is maintained and tested on several shots of **TCV**. The stress has been put in the evaluation of the plasma position estimation, like it was done this Section with induced perturbations. Moreover, in Section (5.1.4) the z-error with respect to a plasma reconstruction solver (in that case LIUQE) has been compared for different typical **TCV** shots.

[6] It is possible to estimate I_p too and make the computation with all estimated quantities.

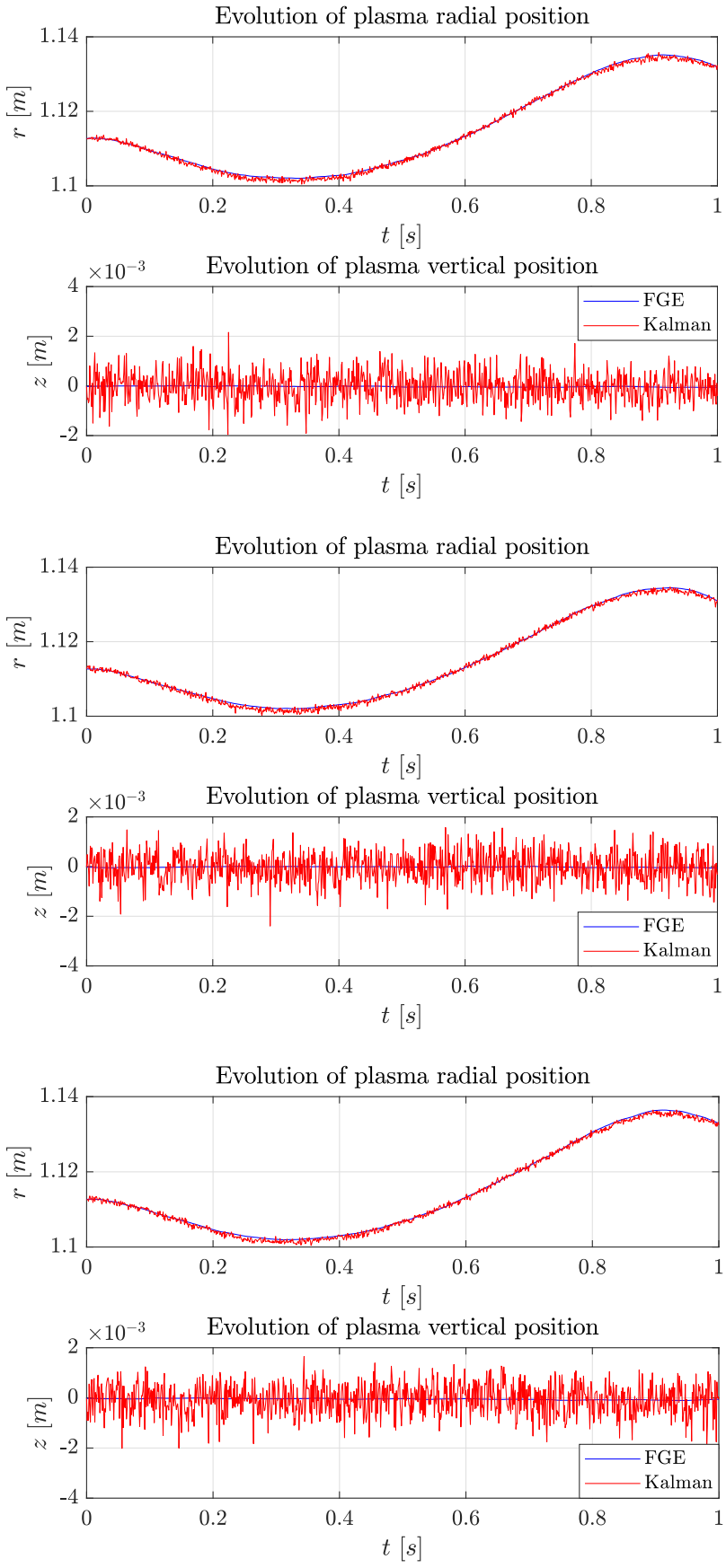

Figure 4.49: Case 1.: from top to bottom (1) – (3): (1) $n_\varphi = n_\xi \ \wedge \ n_{\Delta\Phi} = 0$, (2) $n_\varphi = n_\xi \ \wedge \ n_{\Delta\Phi} = n_{\Delta\xi}$, (3) $n_\varphi = n_\xi \ \wedge \ n_{\Delta\Phi} = n_{\Delta\xi} + n_{\Delta V}$

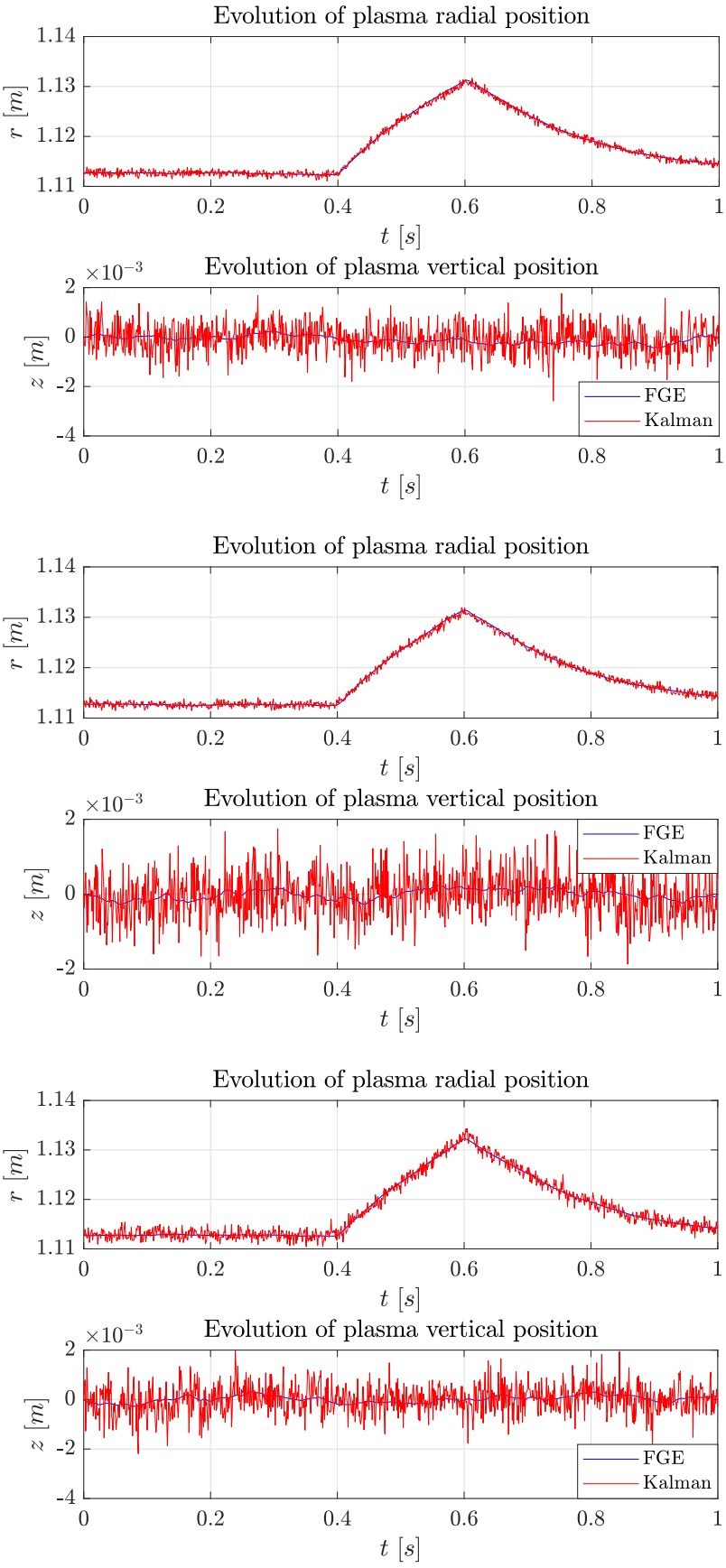

Figure 4.50: Case 2.: from top to bottom $(1)-(3)$: $(1)\ \ n_{\varphi}=0\ \wedge\ n_{\Delta\Phi}=0$, $(2)\ \ n_{\varphi}=n_{\xi}\ \wedge\ n_{\Delta\Phi}=0$, $(3)\ \ n_{\varphi}=n_{\xi}+n_{c}\ \wedge\ n_{\Delta\Phi}=n_{\Delta\xi}+n_{\Delta c}+n_{\Delta V}$

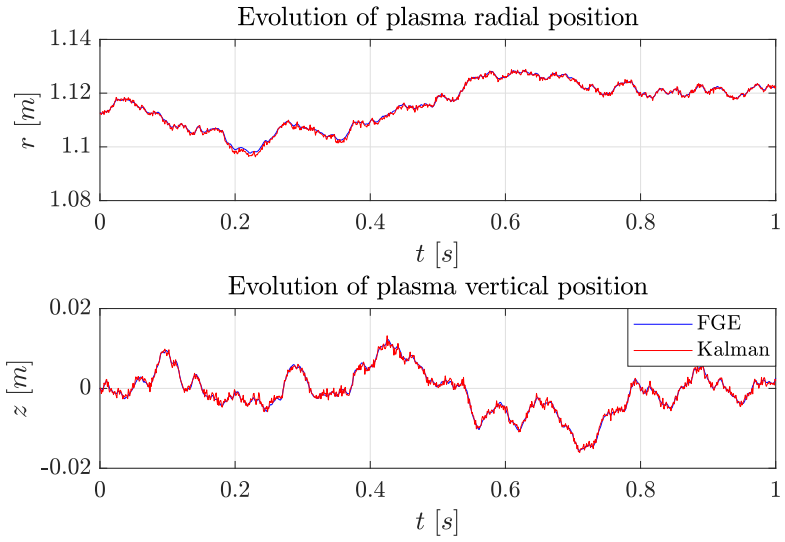

Figure 4.51: Case 3.: $n_\varphi = 0 \ \wedge \ n_{\Delta\Phi} = n_{\Delta V}$

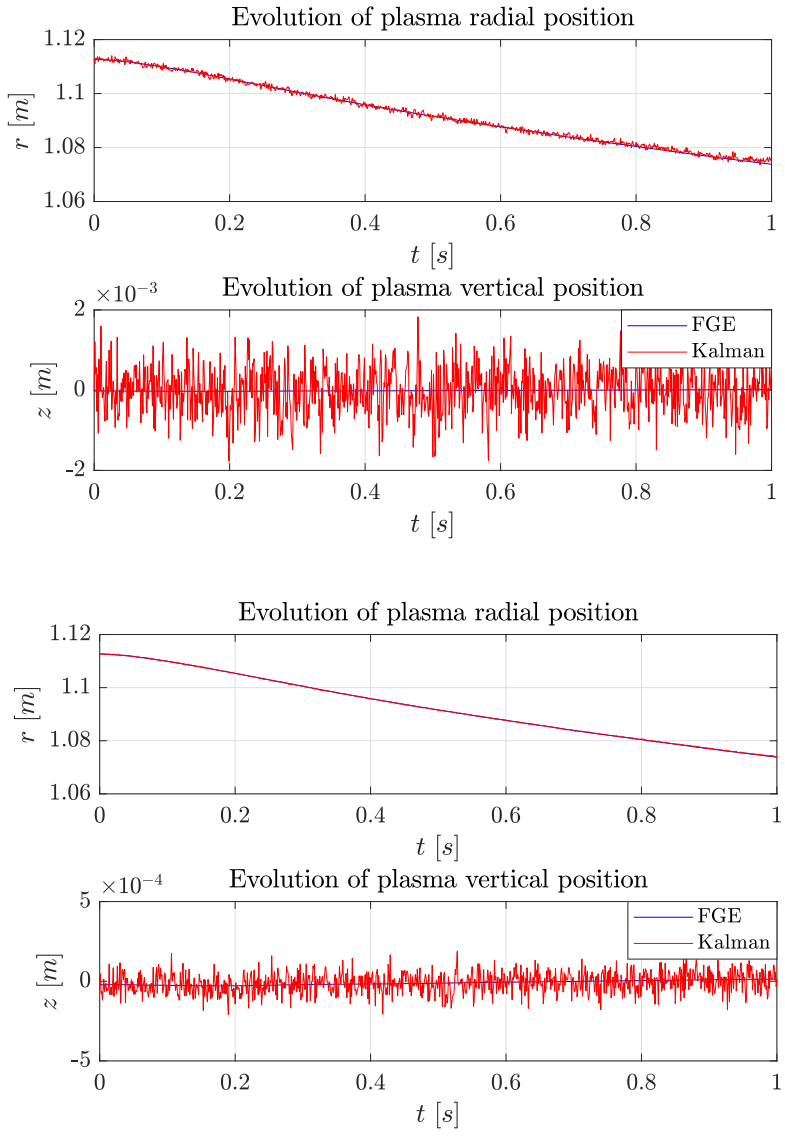

Figure 4.52: Case 4.: from top to bottom (1) – (2) with $n_\varphi = n_c \ \wedge \ n_{\Delta\Phi} = n_{\Delta c}$:
(1) $\{\omega_a, \omega_m, \omega_f\} = 0.1 \cdot \{100\,A,\ 10^{-3}\,T,\ 10^{-3}\,Wb\}$,
(2) $\{\omega_a, \omega_m, \omega_f\} = \{100\,A,\ 10^{-3}\,T,\ 10^{-3}\,Wb\}$

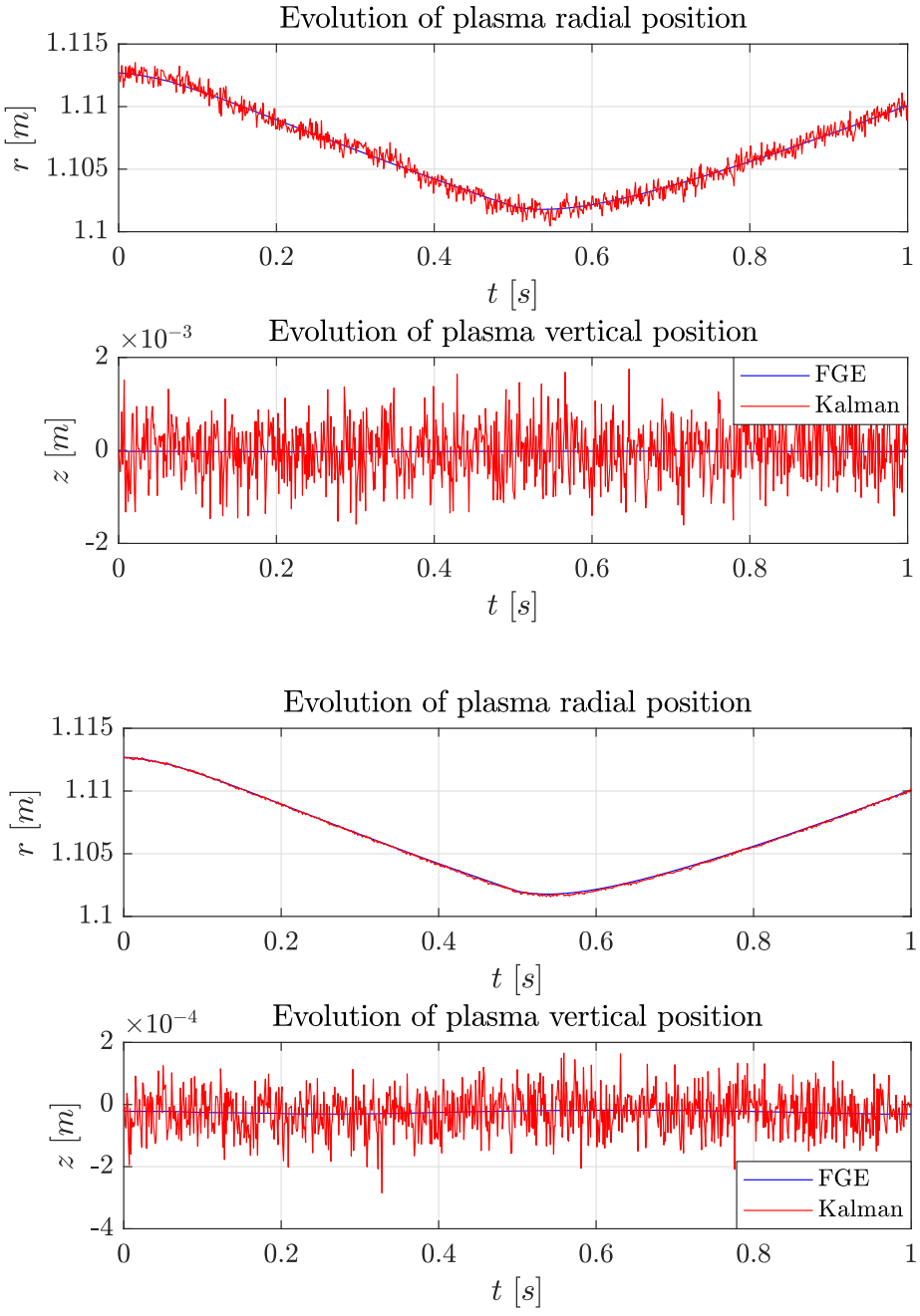

Figure 4.53: Case 5.: from top to bottom (1) – (2) with $n_\varphi = n_c \ \wedge \ n_{\Delta\Phi} = n_{\Delta c}$:
(1) $\{\omega_a, \omega_m, \omega_f\} = 0.1 \cdot \{100\,A,\, 10^{-3}\,T,\, 10^{-3}\,Wb\}$,
(2) $\{\omega_a, \omega_m, \omega_f\} = \{100\,A,\, 10^{-3}\,T,\, 10^{-3}\,Wb\}$

Chapter 5

TCV results

In this Chapter the filter performs in the **TCV** framework with $n_a = 19$, $n_v = 256$, $n_m = 38$ and $n_f = 38$. The measurements are taken from the plasma reconstruction code LIUQE (we refer to 1.4 and to [19] for further details) and the vessels are described by their slowest $n_u = 20$ eigenmodes. Moreover, to account for three unreliable flux loops sensors[1] , a mask has been imposed to reduce n_f to 35. As a remark, all these simultations are achieved in an open-loop while, during real working operations, the observer is assumed to be implemented onto a controlled closed-loop network.

5.1 Simulations

In this subsection the filter has been tested onto experimental data from several **TCV** shots with various typical configurations. The shots presented are numbers: 61400 (*diverted*), 69293 (*limited*), and 69393 (*negative triangularity*). The linearization of FGE has been set at the beginning of the flat-top zones[2] . In order to recover all the plasma profiles as well as possible, a unique filter has been implemented for all these tests. The full extended state has been used and particular attention has been put in covariance matrix tuning. The choices adopted for the augmented blocks are the following:

$$
\begin{aligned}
Q_\xi &= \kappa\, \mathcal{I}_{n_\xi} \\
Q_c &= diag\left(T_s\, [10^{10}\ 10^{9}\ 10^{8}]^T \right) \\
Q_{\Delta\xi} &= Q_\xi \\
Q_{\Delta c} &= diag\left(\frac{T_s^3}{3}\, [10^{-1}\ 10^{-1}\ 10^{-1}]^T \right) \\
Q_{\delta V} &= V_{a,err}^2\, \mathcal{I}_{n_a}
\end{aligned}
$$

with $n_\xi = n_e = n_a + n_u = 39$ and where $\kappa = V_{a,err} = 1\ [V]$ and $T_s = 10^{-3}\ [s]$.

5.1.1 Shot 61400 - Diverted

In this particular shot two different linearizations have been set at the beginning of two flat-top zones. The ending part of the first flat-top is affected by a fast increase of β_p

[1] Ψ_{f10}, Ψ_{f11}, Ψ_{f12}.

[2] The filter performs less good in the ramp-up since the hypothesis of constant I_p is no longer valid. A solution should be to add a *CDE* and perform several closer FGE linearizations.

while in the beginning of the second flat-top there are fast variations both on β_p and in q_A.

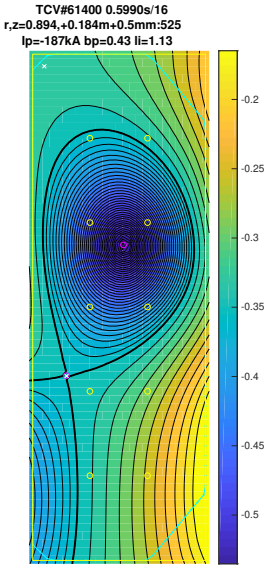

The shape of plasma is shown in figure (5.1) at time $t \approx 0.6\,s$ among the first interval of simulation. The full interval of simulation of shot 61400 started at time $t = 0.1\,s$ and ended at $t = 2\,s$. Hereafter the linearization criterium has been shown in a plot dividing the two subintervals of simulation (5.2). Moreover, using the augmented state Kalman Filter, the estimation plots of the main quantities are shown: the estimated plasma position, the most significant estimated currents and the estimated constraints are compared to the ones retrieved by LIUQE code.

Figure 5.1: **TCV** 61400 shot, time $0.5990\,s$

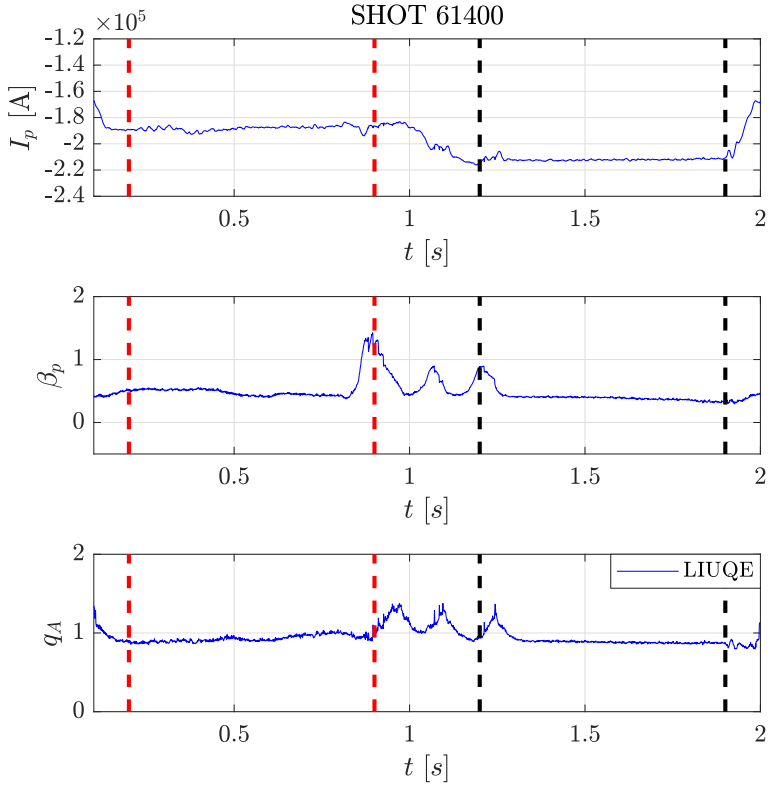

Figure 5.2: Full interval of magnetic reconstruction of shot 61400

5.1.1.1 First flat-top

The first observer simulation has been set in the first flat-top, from time $t = 0.2\,s$ to time $t = 0.9\,s$. The FGE linearization has been set at time $t = 0.2\,s$. In figures (5.3 , 5.4) we can see that, with this particular choice of the covariance matrices of the process, the most critical remarks can be set on β_p, q_A and the fastest eigencurrent trackings which diverge approximately at the middle of the simulation. Moreover, the first eigencurrent estimate is affected by a amplification of its oscillating behaviour. The sum of active currents, the radial and vertical position estimations are performed very well by the filter (an analytical description will be carried in subsection (5.1.4)). However, even though some estimates are not fully precise the results are very satisfactory since the state-space model retrieved from the linearization of FGE carries the vertical instability of the system. This means that thanks to the *measurement-update* equations the filter reaches the good information from the measurements to handle its inbuilt unstability. Moreover in all these simulations we have considered only $n_u = 20$, and we will see in Section (5.2) that the Kalman filter has an higher phase margin if we increase the number of vessel eigenmodes. Improvements can be achieved also reducing the sample time T_s.

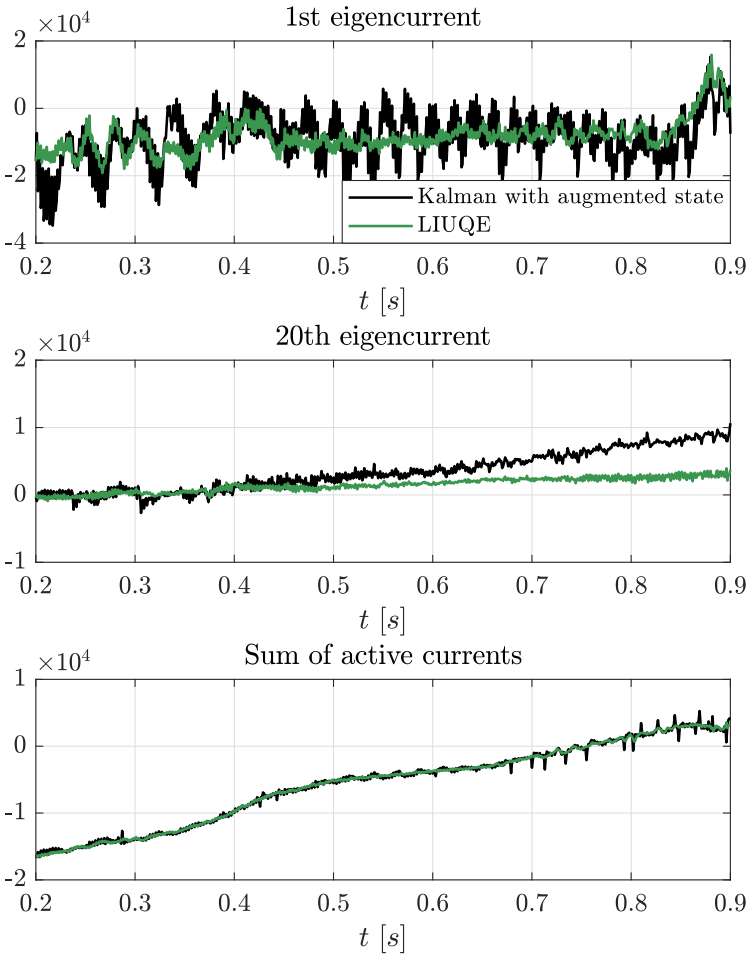

Figure 5.3: From top to bottom (1)-(3): slowest (1) and fastest (2) eigencurrents, sum of active currents (3)

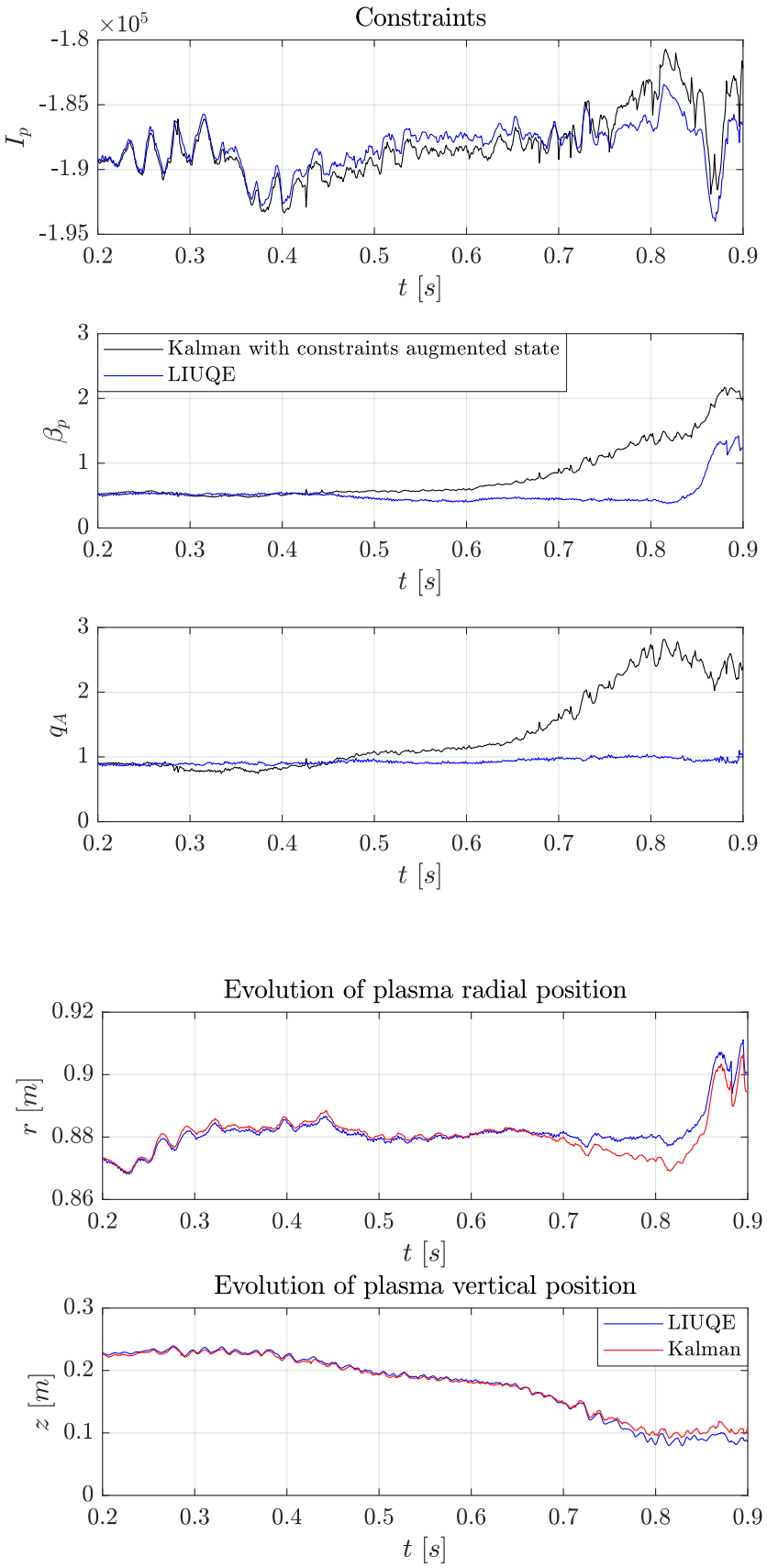

Figure 5.4: From top to bottom (1)-(5): I_p (1), β_p (2), q_A (3), radial (4) and vertical (5) plasma position

5.1.1.2 Second flat-top

The second observer simulation has been set in the second flat-top, from time $t = 1.2\,s$ to time $t = 1.9\,s$. In this case the FGE linearization has been set at time $t = 1.2\,s$. In figures (5.5 , 5.6) we can see that, with this particular choice of the covariance matrices of the process, the most critical remarks can be set on β_p, q_A and the fastest eigencurrent trackings. In this case the constraints results are affected by some offsets which are tiny for I_p and impact basically on β_p and q_A evolutions. The $20th$ eigencurrent estimate starts at a wrong working point and then converges to the correct values after $\Delta t \approx 0.25\,s$. The sum of active currents and, most of all, the vertical position estimation are very close to the reconstructed ones (the difference is in the order of mm or lesser (5.1.4)).

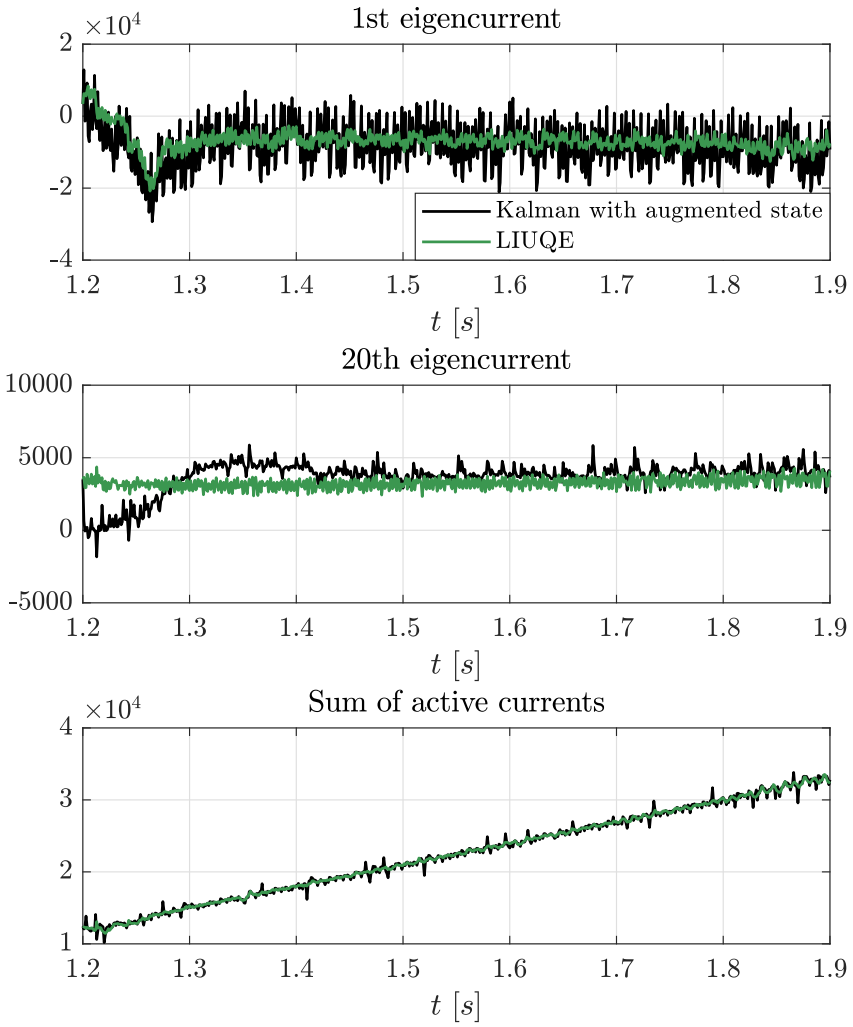

Figure 5.5: From top to bottom (1)-(3): slowest (1) and fastest (2) eigencurrents, sum of active currents (3)

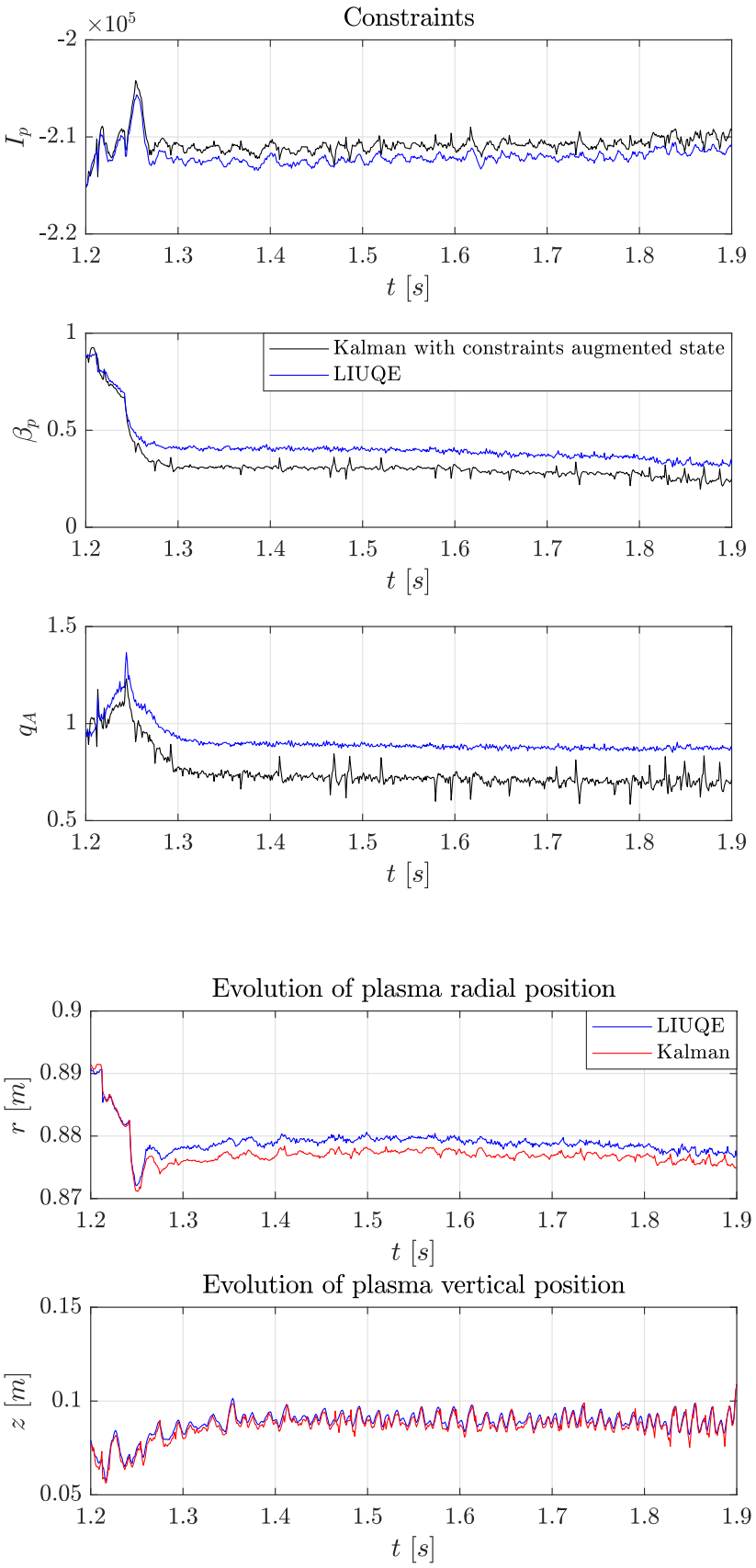

Figure 5.6: From top to bottom (1)-(5): I_p (1), β_p (2), q_A (3), radial (4) and vertical (5) plasma position

5.1.2 Shot 69293 - Limited

The observer simulation has been set during flat-top, from time $t = 0.5\,s$ to time $t = 1.6\,s$. This time region presents slow-varying constraints.

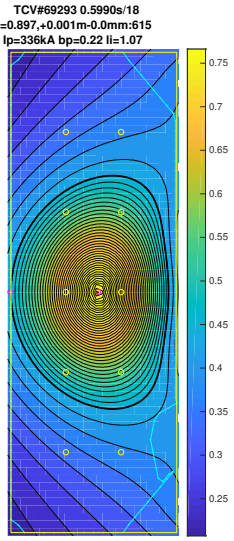

The shape of plasma is shown in figure (5.7) at time $t \approx 0.6\,s$. The full interval of simulation of shot 69293 started at time $t = 0.1\,s$ and ended at $t = 1.8\,s$. In figure (5.8) the linearization criterium has been shown in a graph that identifies the range of the simulation. Moreover, using the augmented state Kalman Filter, the estimation plots of the main quantities are shown: the estimated plasma position, the most significant estimated currents and the estimated constraints are compared to the ones retrieved by LIUQE code.

Figure 5.7: **TCV** 69293 shot, time 0.5990 s

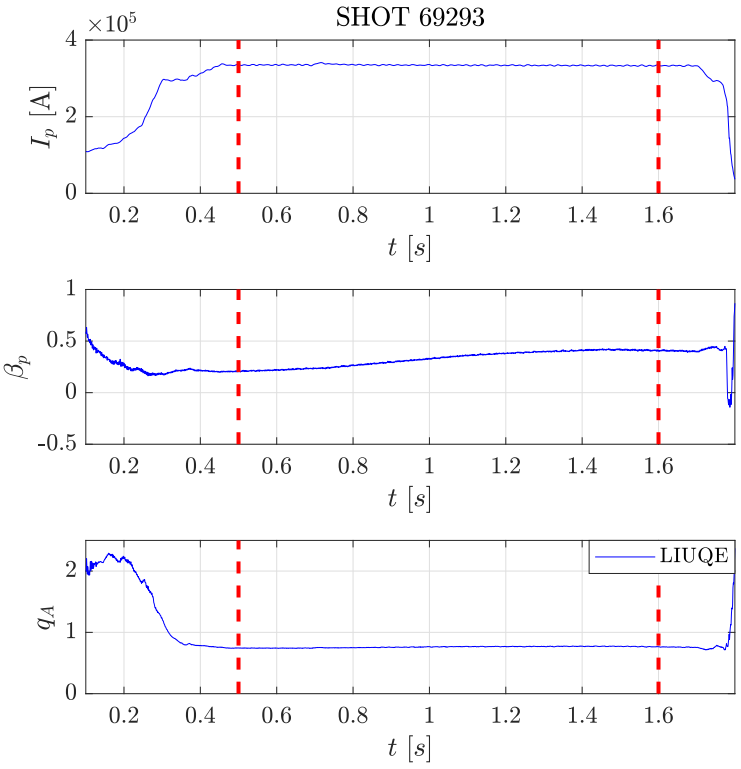

Figure 5.8: Full interval of magnetic reconstruction of shot 69293

As already said, the simulation has been set in the flat-top region, from time $t = 0.5\,s$ to time $t = 1.6\,s$. In this case the FGE linearization has been set at time $t = 0.5\,s$. In figures (5.9 , 5.10) we can see that, with this particular choice of the covariance matrices of the process, the most critical remarks can be set on q_A and the fastest eigencurrent trackings. In this case the q_A estimation evolution is affected by both offsets and uncorrect slope. The $20th$ eigencurrent estimate starts at a wrong working point and then converges to the correct values after $\Delta t \approx 0.25\,s$. All the other estimation quantities are performed very close to the reconstructed ones. We will see in (5.1.4) that for this shot we have the best z-error performances, since the plasma is less vertically elongated and the constraints are varying slowly. This implies that the divergence from equilibrium is less significative with respect to the other shots taken into account.

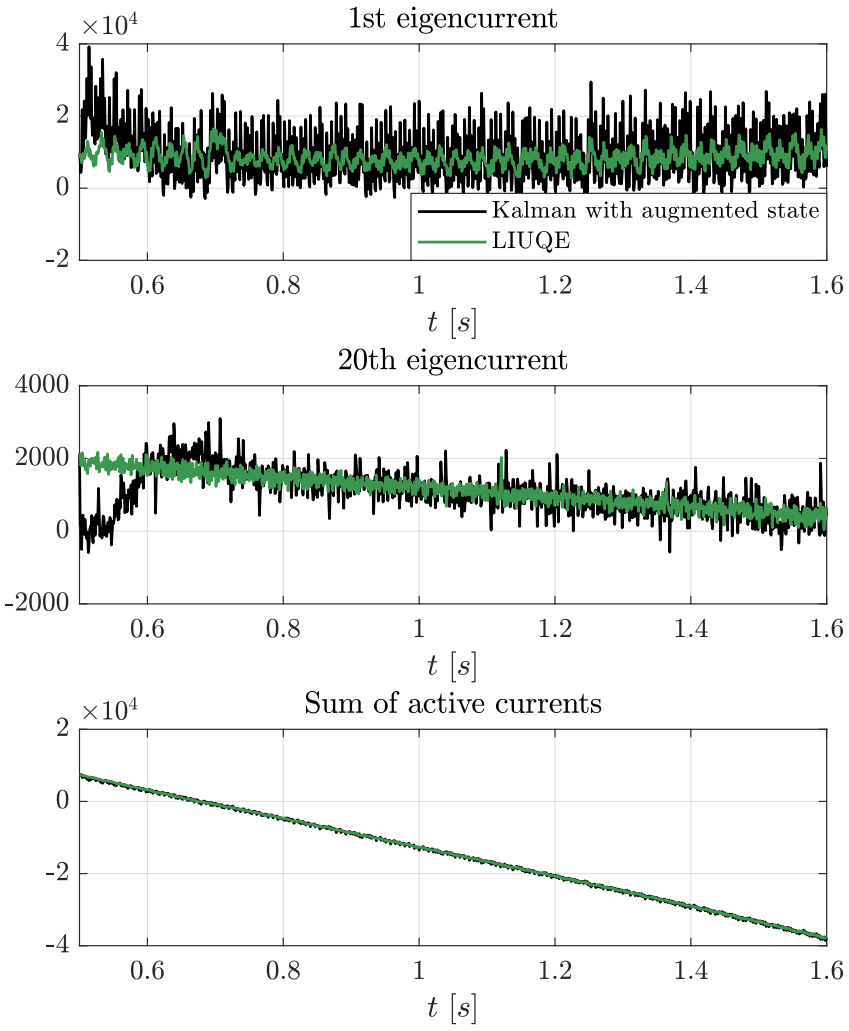

Figure 5.9: From top to bottom (1)-(3): slowest (1) and fastest (2) eigencurrents, sum of active currents (3)

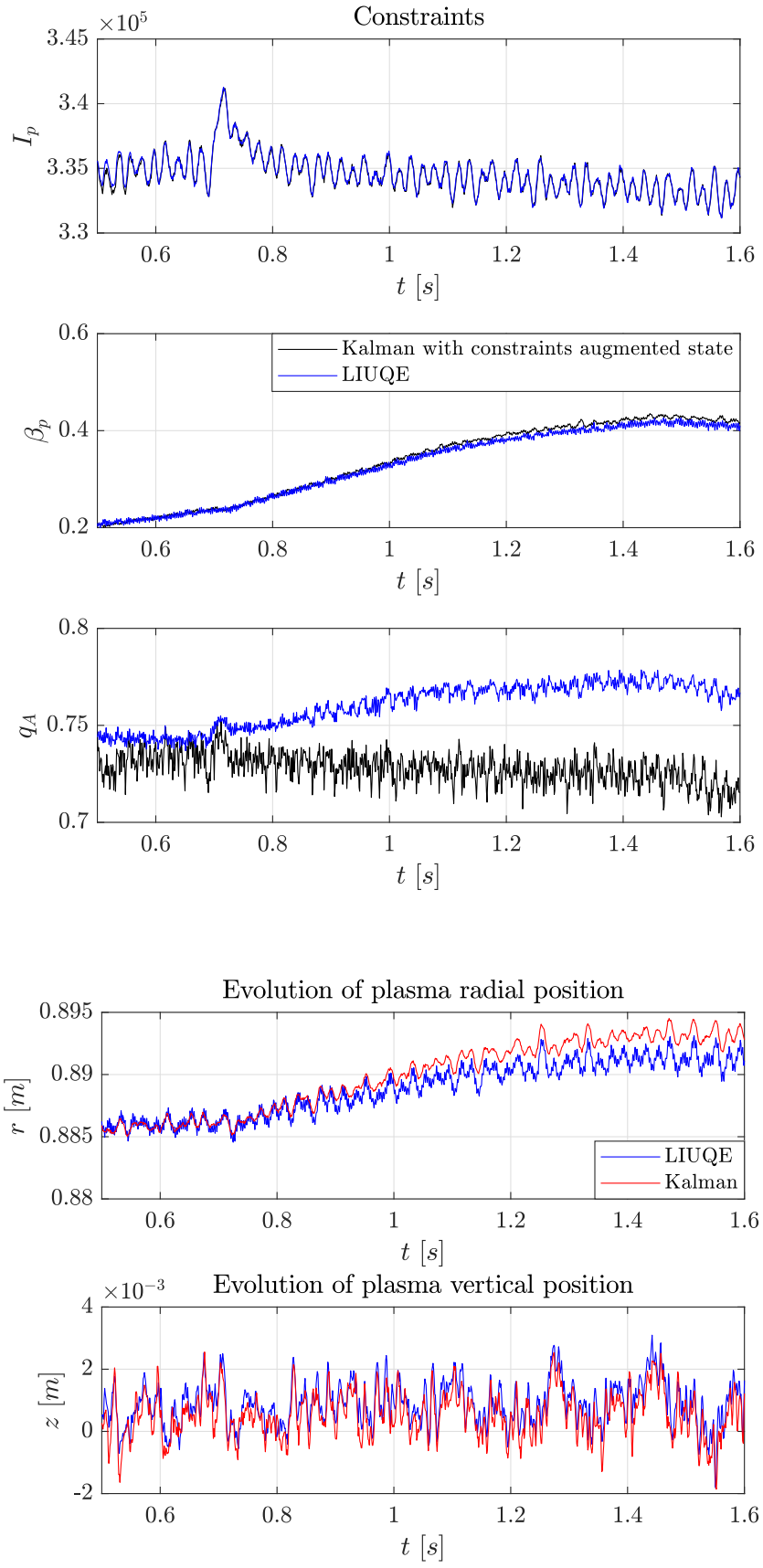

Figure 5.10: From top to bottom (1)-(5): I_p (1), β_p (2), q_A (3), radial (4) and vertical (5) plasma position

5.1.3 Shot 69393 - Negative triangularity

The observer simulation has been set during flat-top, from time $t = 0.9\,s$ to time $t = 1.5\,s$. This time interval presents slow-varying constraints since the negative triangularity is imposed by the sorrounding magnetic configuration around instant $t \approx 0.3\,s$.

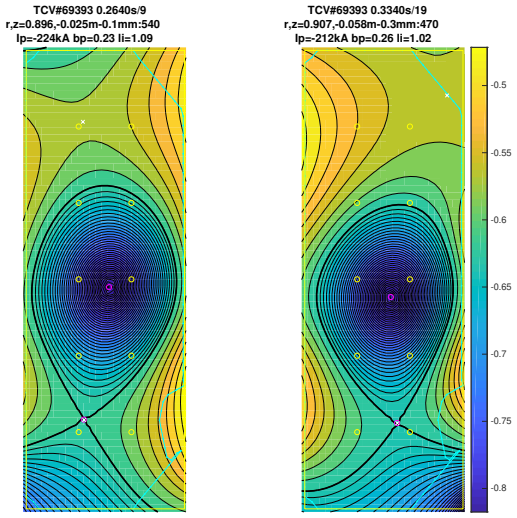

Figure 5.11: **TCV** 69293 shot, times $0.2640\,s$ and $0.3340\,s$

The shape of plasma is shown in figure (5.11) at times $t \approx 0.3\,s$, just before and after the change of triangularity. The full interval of simulation of shot 69293 started at time $t = 0.2\,s$ and ended at $t = 1.6\,s$. In figure (5.12) the linearization criterium has been shown in a graph that identifies the range of the simulation. Moreover, using the augmented state Kalman Filter, the estimation plots of the main quantities are shown: the estimated plasma position, the most significant estimated currents and the estimated constraints are compared to the ones retrieved by LIUQE code.

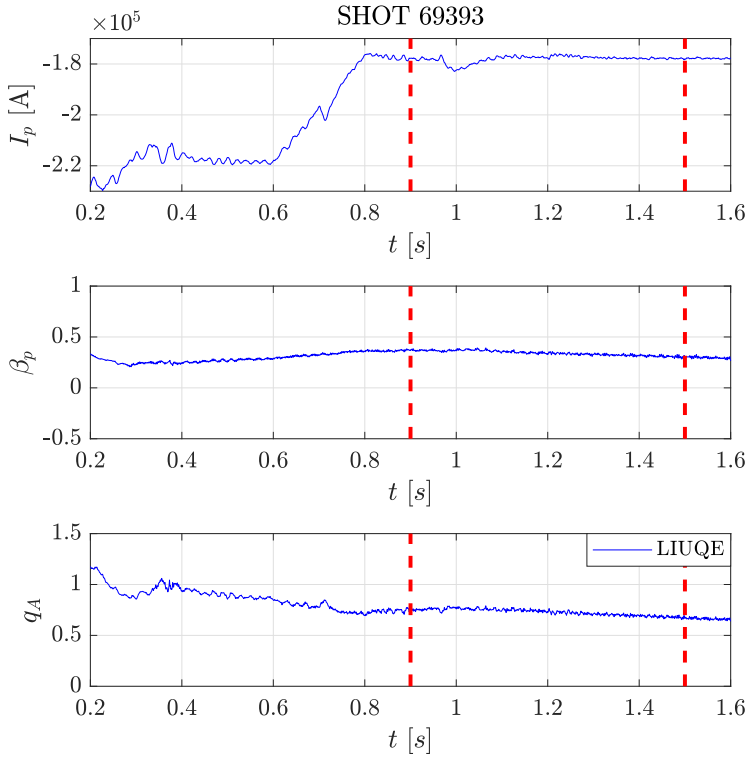

Figure 5.12: Full interval of simulation of shot 69393

As already said, the observer simulation has been set in the flat-top region, from time $t = 0.9\,s$ to time $t = 1.5\,s$. In this case the FGE linearization has been set at time $t = 0.9\,s$. In figures (5.13 , 5.14) we can see that, with this particular choice of the covariance matrices of the process, the most critical remarks can be set on β_p, q_A and the fastest eigencurrent trackings. In this case the β_p and q_A estimation evolutions are affected by some spikes induced by the filter amplification of the measurement variations. In any case the average values of the estimated constraints perfectly center the required profiles. The $20th$ eigencurrent estimate starts at a wrong working point and then converges to the correct values after $\Delta t \approx 0.1\,s$. All the other estimation quantities are performed very close to the reconstructed ones.

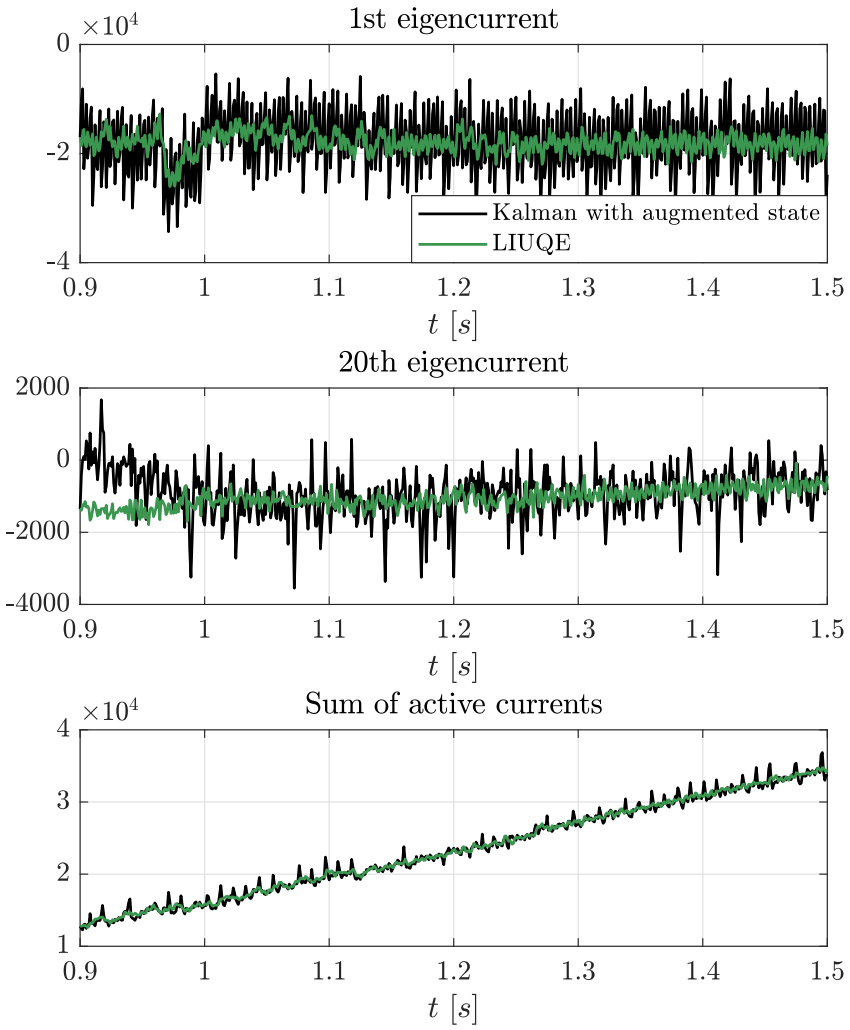

Figure 5.13: From top to bottom (1)-(3): slowest (1) and fastest (2) eigencurrents, sum of active currents (3)

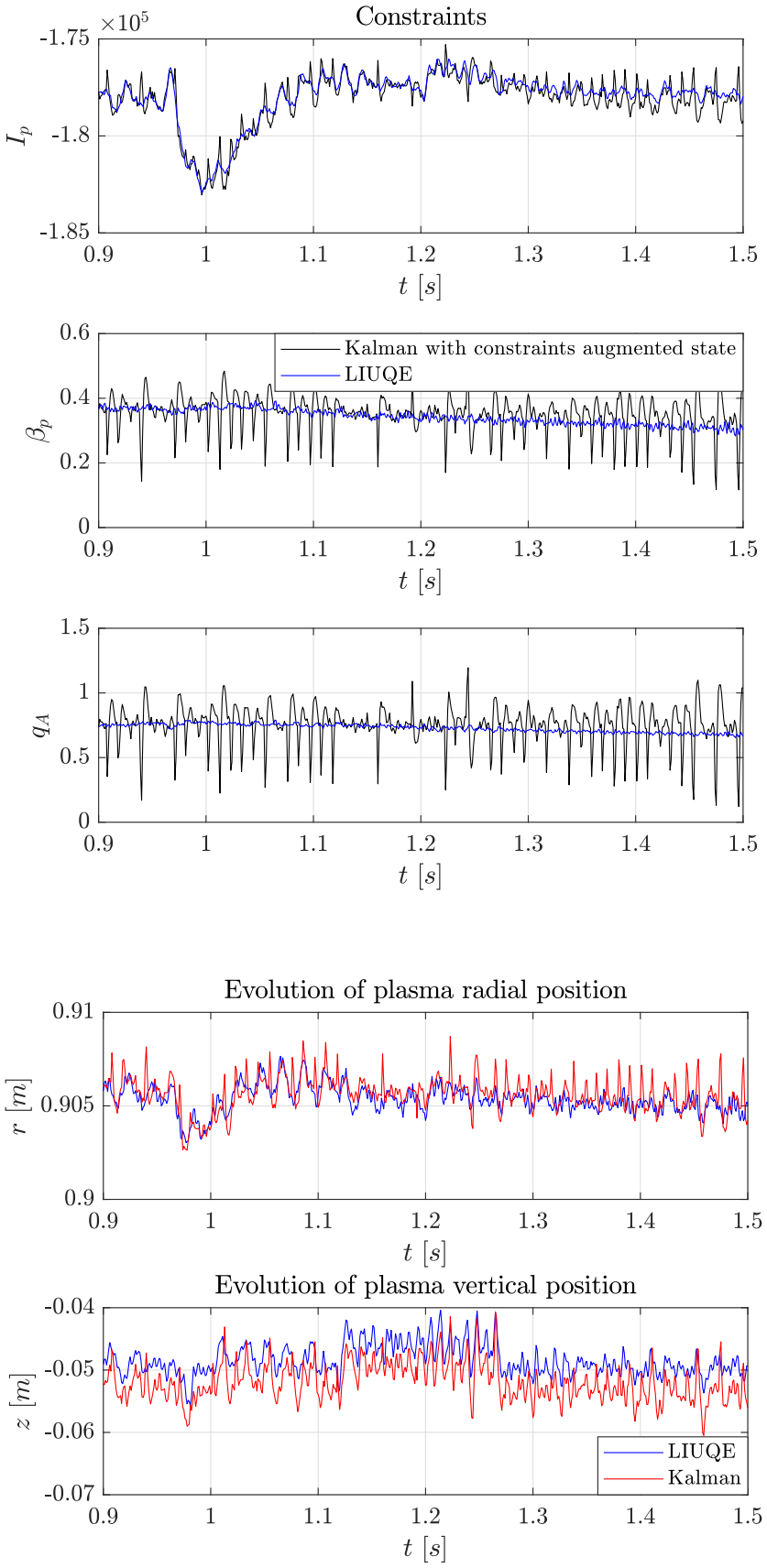

Figure 5.14: From top to bottom (1)-(5): I_p (1), β_p (2), q_A (3), radial (4) and vertical (5) plasma position

5.1.4 Error analysis

In this subsection a vertical position error analysis has been done. In table (5.1) are reported the means, the minima and the maxima errors in the z-position estimation with respect to LIUQE for all the shots taken into account. As we will see in (5.27), if we increment the number of vessel eigencurrents the estimation performance doesn't change too much if we adopt the same parameters in the covariance blocks design. This is due to the significative increase in the size of the augmented state of the system. In figures (5.15 , 5.16) the z-error evolutions of the shots presented in (5.1) are shown. We can see, as reported in figures (5.2 , 5.4), that the estimation of the z-position is diverging at the end of the interval of simulation, since at the end of the flat-top there is a fast increase in the β_p parameter, i.e. the plasma pressure is fastly changing. The mean values of the errors are in the order of $[mm]$ except for the limited shot in which the mean is of the order of tenths of a millimeter.

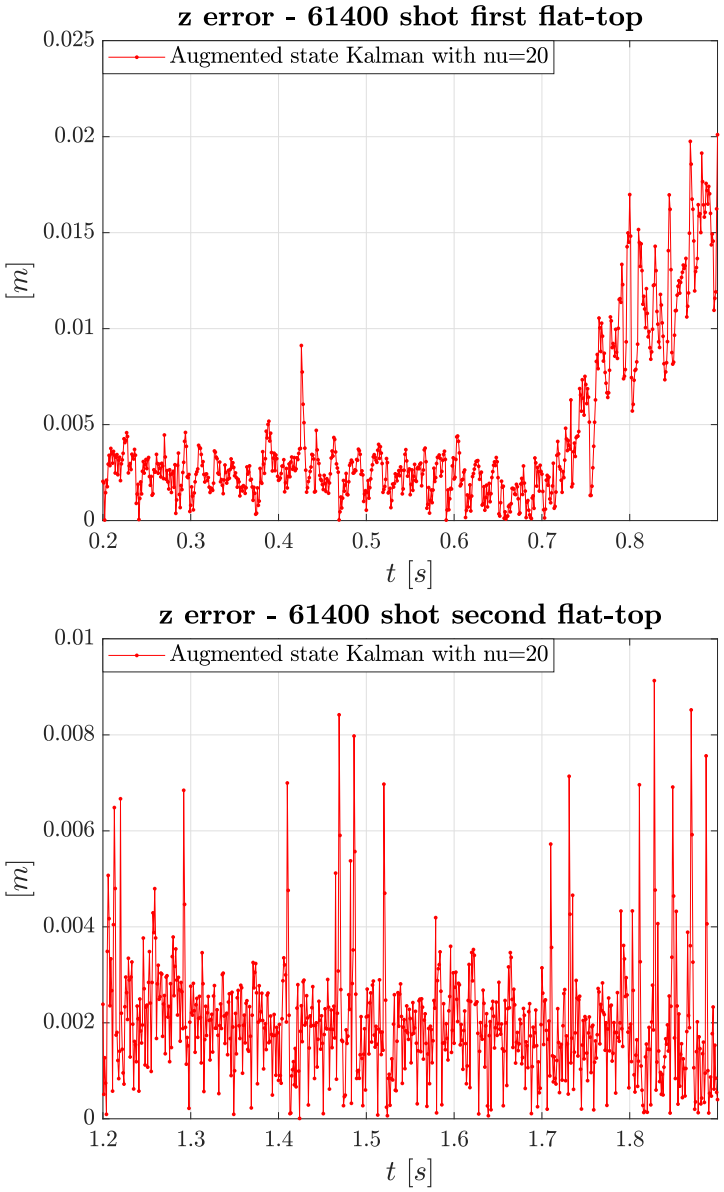

Figure 5.15: Diverted first and second flat-top z-error evolution

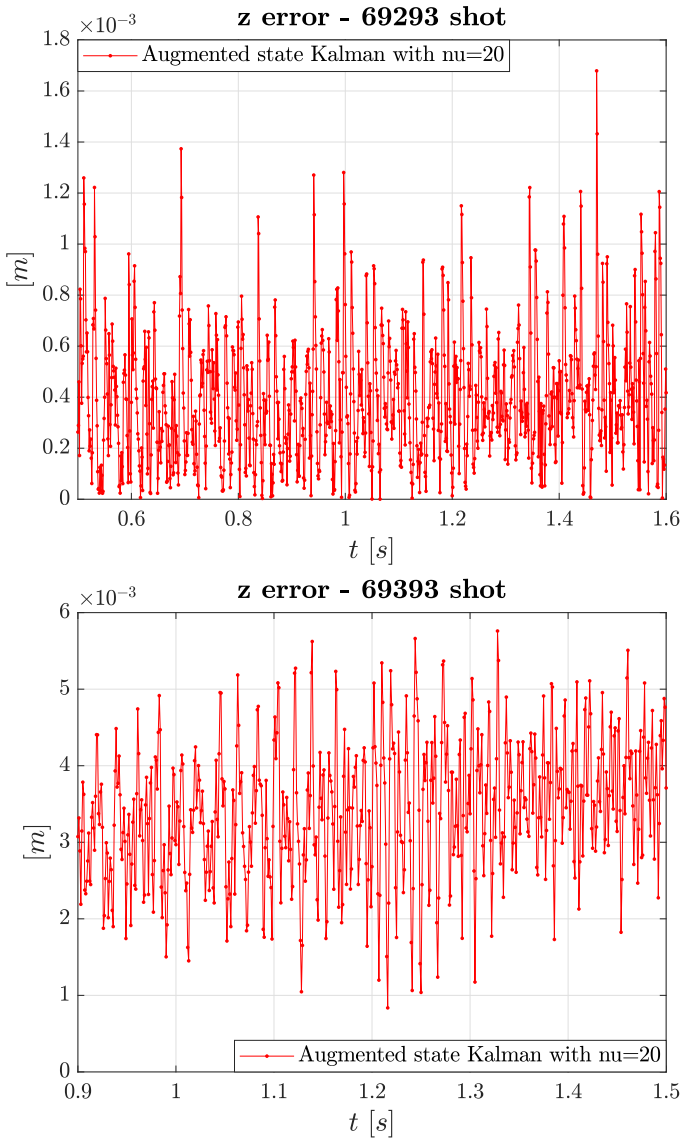

Figure 5.16: Limited and Negative Triangularity z-error evolution

The maximum values of the errors are still in the $[mm]$ range except for the diverted case, escpecially in the $1st$ flat-top where the error reaches the $[cm]$ range. As we can see in (5.15) the elongated shape of the plasma leads to a fast unstability the more we are far from the equilibrium. A solution should be to retrieve many close linearizations of FGE for high elongated plasmas. The minimum values of the errors range from tenths of a millimeter (shot 69393) to tenths of a micrometer (shot 69293).

z-errors [mm]				
	61400 1st flat-top	**61400 2nd flat-top**	**69293**	**69393**
Mean of z-error	4.3	2.0	0.39794	3.4
Max of z-error	20.1	9.1	1.7	5.8
Min of z-error	0.025876	0.0074226	0.00050041	0.83672

Table 5.1: Table of z-errors for different shots in the $[mm]$ scale

5.2 Observers comparison in the frequency domain

In this section the open-loop performances of the Kalman Filter observer have been compared to the previous implemented observer's ones. This observer is called MGA[3] and it is based on a linear combination of measurements obtained by solving a linear least-squares problem, fitting a plasma current distribution on the plasma domain using *Finite Elements Method* (for further details we refer to [11] and [23]).

The control voltages to vertical position transfer functions have been shown and discussed in the frequency domain. The stress has been put at first on three specific coils: F4, G1 and E4. Then, due to the particular choice of the simulation interval, we have considered only slow coil F7 and fast coil G1 since they where the closest to the plasma under analysis and so their responses are more significant. As a remark, in **TCV** there is only one series connected fast coil circuit called G1, as we can see from figures (1.4 , 1.5).
First of all we have compared the V_a to zI_p frequency responses taken from FGESS[4] in *continuous time* and in *discrete time*. As we can see from the following *Bode diagrams* (5.17), the responses diverge only in close proximity to the *Nyquist frequency*. In order to reach a better understanding of the observer responses the sample time has been set at $T_s = 10^{-5}\, s$ in order to increase the *Nyquist frequency* of the system.

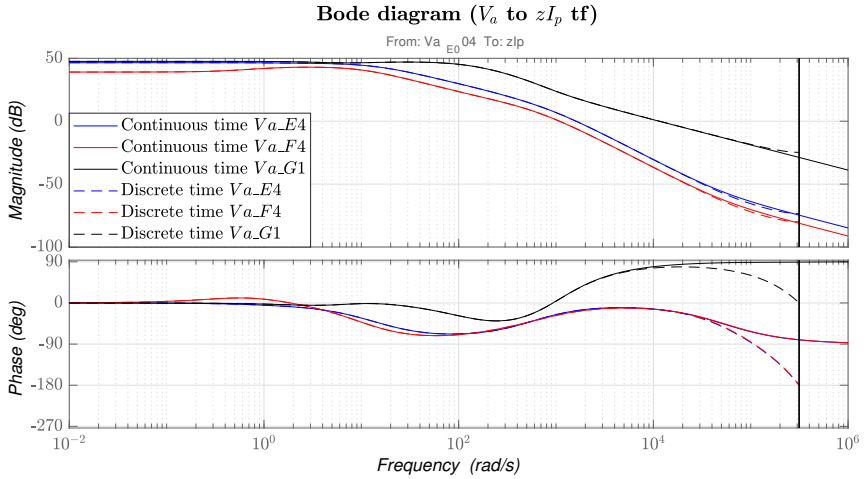

Figure 5.17: V_a to zI_p frequency responses in *continuous* and *discrete time* from FGESS, $T_s = 10^{-5}\, s$

Since until now the Kalman filter has been developed mainly in *discrete time*, this description has been retained for the next diagrams. Connecting properly the state spaces of the model given by FGESS with the state space model of the state augmented Kalman Filter given by KALSASS, the tranfer function of the Kalman Filter between the V_a input and the estimated $\hat{zI}_p$ output has been compared with the transfer function between the V_a input and the output zI_p of the model given by FGESS (5.19 , 5.20). As we can see in the next *Bode diagram* (5.18), it has been proven that the the Kalman Filter frequency response is exactly the same of the one of the model $\forall\ K \in \mathbb{R}^{n_x \times n_y}$, where in our case K is the Kalman gain given by the *Riccati equation*. The frequency analysis computations have been made taking into account a state with only external currents s.t. $n_x = n_e = n_a + n_u = 39$, and with external currents and constraints s.t. $n_x = n_e + n_c = 42$.

[3] It takes its name from the method on which it is based: MGA i.e *Measurements Green's Analysis*.
[4] This function computes the state-space model based on FGE linearization.

This result is detailed and proven in the following statement[5] .

Proposition 1. *Given the following state-space linear model of the system:*

$$\begin{cases} \dot{x} = A\,x + B\,u \\ y = C\,x \end{cases}$$

with $\mathcal{Y}(s) = \mathcal{L}\big(y(t)\big) = \mathcal{W}(s)\,\mathcal{U}(s) = \big[\,C\,(\,s\mathcal{I} - A\,)^{-1}B\,\big]\,\mathcal{U}(s)$ *and with* $n_x \triangleq \dim x$, $n_y \triangleq \dim y$, *and given the following state-space model of the observer:*

$$\begin{cases} \dot{\hat{x}} & = A\,\hat{x} + B\,u + K\,(\tilde{y} - C\,\hat{x}) = \\ & = (A - K\,C)\;\hat{x} + [B \;\; K]\;[u \;\; \tilde{y}]^T = \\ & = \tilde{A}\,\hat{x} + \tilde{B}\,\tilde{u} \\ \hat{y} & = C\,\hat{x} \end{cases}$$

if $\tilde{y} \equiv y$ [6] , *then* $\forall\, K \in \mathbb{R}^{n_x \times n_y}$ *we obtain that* $\hat{\mathcal{W}}(s) \equiv \mathcal{W}(s)$, *with tranfer function* $\hat{\mathcal{W}}(s) = \frac{\hat{\mathcal{Y}}(s)}{\hat{\mathcal{U}}(s)}$.

Proof. Since:

$$\dot{\hat{x}} = (A - K\,C)\;\hat{x} + [B \;\; K]\;[u \;\; \tilde{y}]^T$$

then:

$$\begin{aligned} \hat{\mathcal{Y}} &= \big[\,C\,(\,s\mathcal{I} - (A - K\,C)\,)^{-1}[B \;\; K]\,\big] \;\; [\mathcal{U} \;\; \tilde{\mathcal{Y}}]^T = \\ &= C\,(\,s\mathcal{I} - A + K\,C\,)^{-1}B\,\mathcal{U} + C\,(\,s\mathcal{I} - A + K\,C\,)^{-1}K\;\tilde{\mathcal{Y}} = \\ &= C\,(\,s\mathcal{I} - A + K\,C\,)^{-1}B\,\mathcal{U} + C\,(\,s\mathcal{I} - A + K\,C\,)^{-1}K\,\big[\,C\,(\,s\mathcal{I} - A\,)^{-1}B\,\big]\,\mathcal{U} = \\ &= \big[\,C\,(\,s\mathcal{I} - A + K\,C\,)^{-1}\,[\mathcal{I} + K\,C\,(\,s\mathcal{I} - A\,)^{-1}]\,\big]\,B\,\mathcal{U} \end{aligned}$$

The statement is proven *iff*:

$$C\,(\,s\mathcal{I} - A + K\,C\,)^{-1}\,[\mathcal{I} + K\,C\,(\,s\mathcal{I} - A\,)^{-1}]\,B = C\,(\,s\mathcal{I} - A\,)^{-1}B$$

If $K = \mathbb{O}$ it is trivially proven since:

$$C\,(\,s\mathcal{I} - A + \mathbb{O}\,C\,)^{-1}\,[\mathcal{I} + \mathbb{O}\,C\,(\,s\mathcal{I} - A\,)^{-1}]\,B = C\,(\,s\mathcal{I} - A\,)^{-1}B$$

If $K \neq \mathbb{O}$ the statement is proven if we impose that:

$$\begin{aligned} (\,s\mathcal{I} - A\,)^{-1} &= (\,s\mathcal{I} - A + K\,C\,)^{-1}\,[\mathcal{I} + K\,C\,(\,s\mathcal{I} - A\,)^{-1}] = \\ &= (\,s\mathcal{I} - A + K\,C\,)^{-1} + (\,s\mathcal{I} - A + K\,C\,)^{-1}\,K\,C\,(\,s\mathcal{I} - A\,)^{-1} \end{aligned}$$

If we multiply right-hand side and left-hand side by $(\,s\mathcal{I} - A\,)$ at right, we get:

$$\begin{aligned} \mathcal{I} &= (\,s\mathcal{I} - A + K\,C\,)^{-1}(\,s\mathcal{I} - A\,) + (\,s\mathcal{I} - A + K\,C\,)^{-1}\,K\,C = \\ &= (\,s\mathcal{I} - A + K\,C\,)^{-1}[\,s\mathcal{I} - A + K\,C\,] \end{aligned}$$

□

[5] The statement has been proven in *continuous time*.

[6] i.e. the second component of the input of the observer is exactly the output of the model.

Moreover since the transfer functions are equivalent $\forall\, C \in \mathbb{R}^{n_y \times n_x}$ this in particular implies that:

$$\frac{\hat{\mathcal{X}}(s)}{\hat{\mathcal{U}}(s)} = \frac{\mathcal{X}(s)}{\mathcal{U}(s)}$$

Therefore, since $zI_p = F\,x$ and $\hat{zI}_p = F\,\hat{x}$ [7] we obtain:

$$\frac{\hat{zI}_p(s)}{\hat{\mathcal{U}}(s)} = F\,\frac{\hat{\mathcal{X}}(s)}{\hat{\mathcal{U}}(s)} = F\,\frac{\mathcal{X}(s)}{\mathcal{U}(s)} = \frac{zI_p(s)}{\mathcal{U}(s)}$$

In order to graphically validate the previous statement the frequency responses of FGESS and of the Kalman filter are shown in figure (5.18). Only for these plots we have considered a generic interval of the flat-top zone of the shot 69393. In this case E4, F4 and G1 coils responses have been computed.

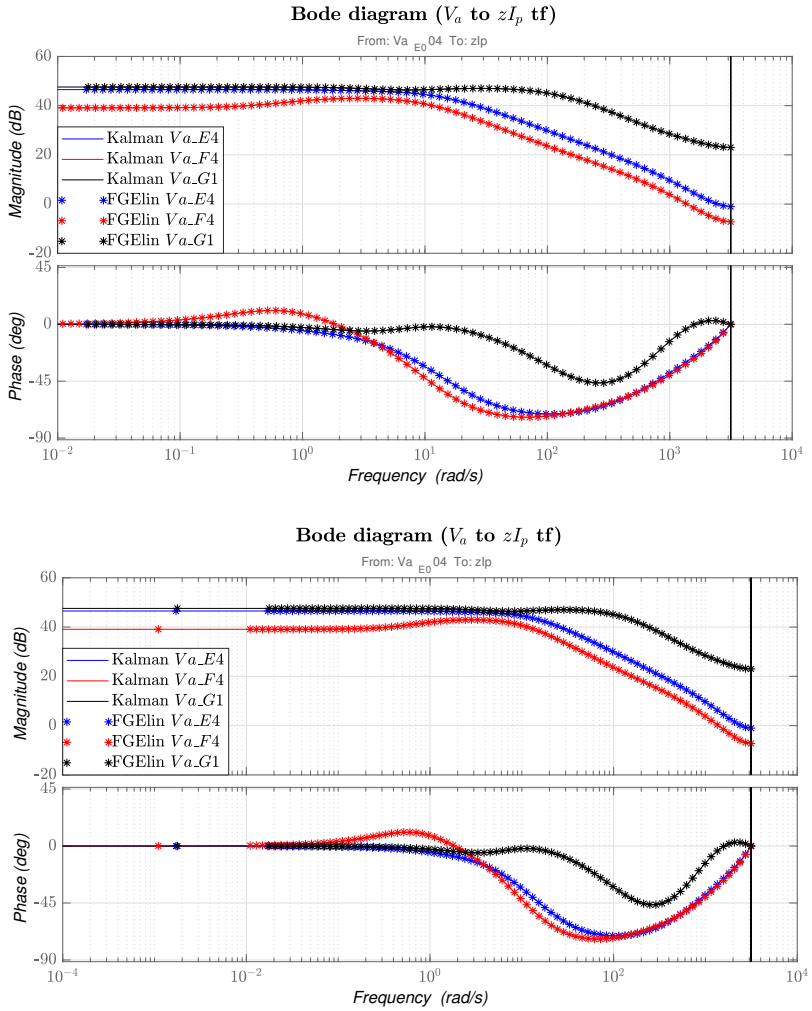

Figure 5.18: V_a to $z\hat{I}_p$ frequency responses in *discrete time* from FGESS and from the Kalman filter; From top to bottom (1-2): with $n_x = n_e$ (1) and with $n_x = n_e + n_c$ (2). We can see that the frequency responses of FGESS and of the Kalman filter are the same $\forall\, K$ and are not changing so much if the state is augmented

[7] If $x = I_e$ then $F = \frac{\partial zI_p}{\partial I_e}$, if $x = [I_e \;\; c]^T$ then $F = [\frac{\partial zI_p}{\partial I_e} \;\; \frac{\partial zI_p}{\partial c}]$.

As we can see, E-coils and F-coils have similar frequency responses both in the magnitude and in the phase diagram. On the other hand the frequency response of the fast coil G1 has a higher bandwidth and presents a bigger phase margin with respect to the slow coils. The reason of such a difference in the responses is that E and F-coils have a bigger inductance and therefore their response is affected by a higher time constant. Whereas, in the case of G-coils we have a bigger promptness due to the fact that these in-series wings have a smaller inductance and because these coils are placed inside the vacuum chamber and so the response is not affected by the attenuation and phase lag caused by the vessel's eddy-currents.
For the frequency analysis comparison of the observers (MGA and Kalman Filter) the simulation is carried on a subinterval of the second flat-top zone of shot 61400, i.e. $t \in [1.35\,,1.5]\,s$. Since in this time interval the plasma position is quite high, only fast coil G1 and slow F7 are considered, since they give the most significant contribution in vertical stabilization. The open-loop frequency responses of the MGA observer are computed in *continuous time* and then compared to FGESS and to the *discrete time* Kalman filter.

MGA estimator computes the plasma vertical position directly form a combination of measurements. It takes the measurements of I_a, B_m, Ψ_f and I_s which represents the vessel current of 38 segments relating to the 38 poloidal fluxes measuring the loop voltages. This quantities will be multiplied to a block of matrices I_{pzf}, I_{pzm}, I_{pza} and I_{pzv} giving the contributions on zI_p calculation [8]. In order to evaluate the frequency responses of MGA two methods have been developed to account for I_s. The first one, called MGA-T_{ius}, consists in a direct mapping from the vessel eigencurrent I_u passing directly from the plant (FGESS) to the 38-dimensional I_s current vector distributed as the poloidal flux loops, s.t $I_s = T_{ius}\, I_u$. In this case the influence of the first eigenmode on the global frequency response has been detailed. The second one, called MGA-$\dot{\Psi}_f$, (which is the most realistic, since I_u is not accessible and it is only predictable) consists in the computation of I_s directly from the knowledge of the *emf* $\dot{\Psi}_f$ s.t. $I_s = -\dot{\Psi}_f / R_s$, with R_s local vessel resistances matrix. In this case the computation has been done using a one-step derivator in *discrete time* or a *high pass filter* in *continuous time*. Since a perfect derivator in *continuous time* is a *not-causal system*, a good solution is to create an *HPF* as a *not strictly proper* tranfer function, and set an high *cut off frequency* f_c with respect to the simulation frequency (at least *Nyquist* one) so since $D = \frac{s}{1+\tau\, s}$ and $f_c = \frac{1}{\tau}$, the time constant τ has been set to $10^{-6}\, s$ in order to have a cut frequency at 1 *MHz*. The block diagrams describing the block connections in the two MGA approaces are shown in figures (5.19 , 5.20).

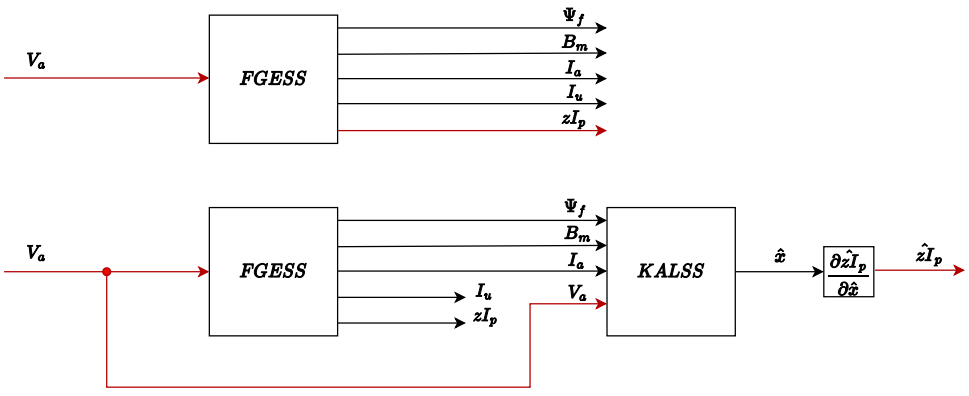

Figure 5.19: Block diagrams of FGESS and Kalman filter tranfer functions

[8] To have a detailed description on how these matrices have been computed we refer to [23].

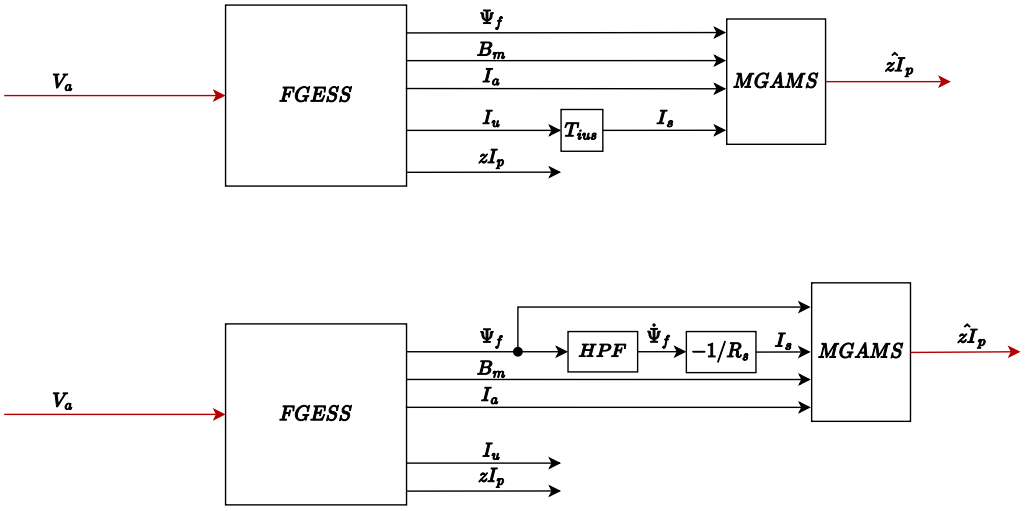

Figure 5.20: Block diagrams of MGA tranfer functions in the cases of (1) $I_s = T_{ius}\, I_u$ or (2) $I_s = -\dot{\Psi}_f / R_s$

In the next plots we compare the frequency results of MGA in the cases of considering only the slowest eigenmode with respect to the full vessel eigencurrent for the I_s contributions (5.21). The case with $n_u = 1$ represents the situation where one measurement of the loop voltage, together with an estimation of the global vessel resistance, is used to estimate the total vessel current, without taking any spatial dependencies into account.
On the other hand we have computed the Ψ_f-derivative for the I_s calculation (5.22) both in *discrete time* and in *continuous time*. The MGA results are compared to the *continuous time* FGESS responses, which are very close to the *discrete time* Kalman filter responses.

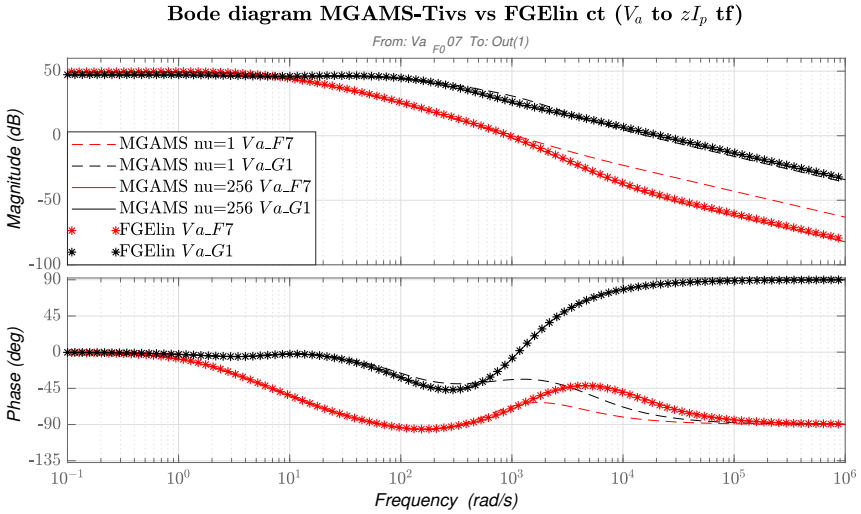

Figure 5.21: V_a to $\hat{zI}_p$ frequency responses in *continuous time* from FGESS and from the MGA-T_{ius} observer in the cases of $n_u = 1$ and $n_u = n_v = 256$

We can see that in the T_{ius}-case the frequency response of MGA with $n_u = 256$ is almost equivalent to the FGESS response. In (5.22) we see that the derivators produce almost the same responses in the *discrete* or continuous cases and the divergence occurs only in the proximity of the *Nyquist frequency*. As we will see in figures (5.25 , 5.26), these responses are very close to the ones of MGA-T_{ius} with $n_u = 1$.

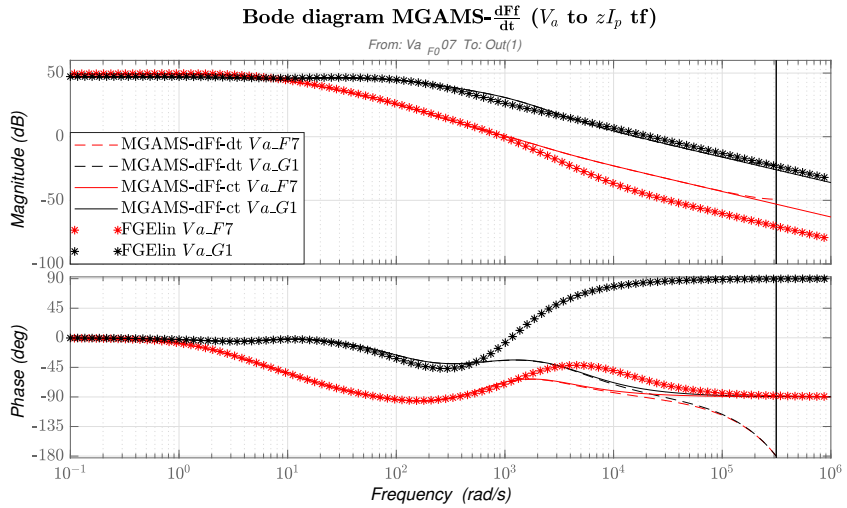

Figure 5.22: V_a to $z\hat{I}_p$ frequency responses in *continuous time* from FGESS and from the MGA-$\dot{\Psi}_f$ observer in the cases of *discrete time* derivator and *continuous time* derivator

Let's now present the frequency responses of the Kalman filter in *discrete time* considering the slow F7 coil and the fast G1 coil. We have considered the cases $n_u = 1; 20; 50; 100; 200; 256$: we can see from (5.23 , 5.24) that in the case $n_u = 256$ the frequency response is exactly equal to the *discrete time* FGESS, as expected. The phase margin grows up with the number of eigenmodes. In order to get the maximum efficiency, in feedback-control the optimal choice is to run the Kalman filter with $n_u = n_v = 256$ but for the $\frac{zI_p(s)}{V_a(s)}$ frequency responses it is sufficient to take to set $n_u \geq 50$ to augment the phase margin on F7 while to see significant improvements on G1 n_u should be close to n_v. In any case we have seen in Section (5.1) that the vertical position estimation is accurate, with errors in the *mm* range or lesser (see table (5.1)), even if we consider $n_u = 20$. Moreover, in figure (5.27) we can see in the error plot that we can obtain better performances if we consider a lower n_u since the augmented state will reduce its dimensionality.

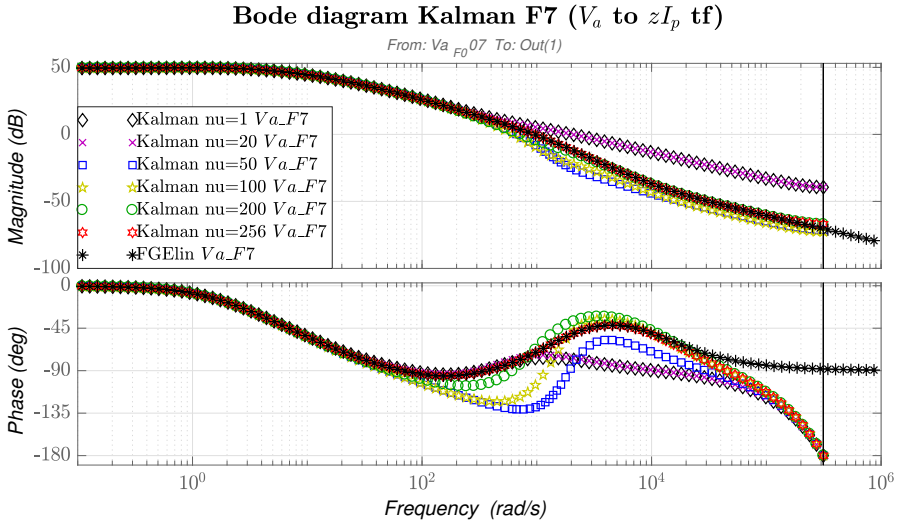

Figure 5.23: V_a to $z\hat{I}_p$ frequency responses of the Kalman filter in *discrete time* with increasing n_u, F7-coil

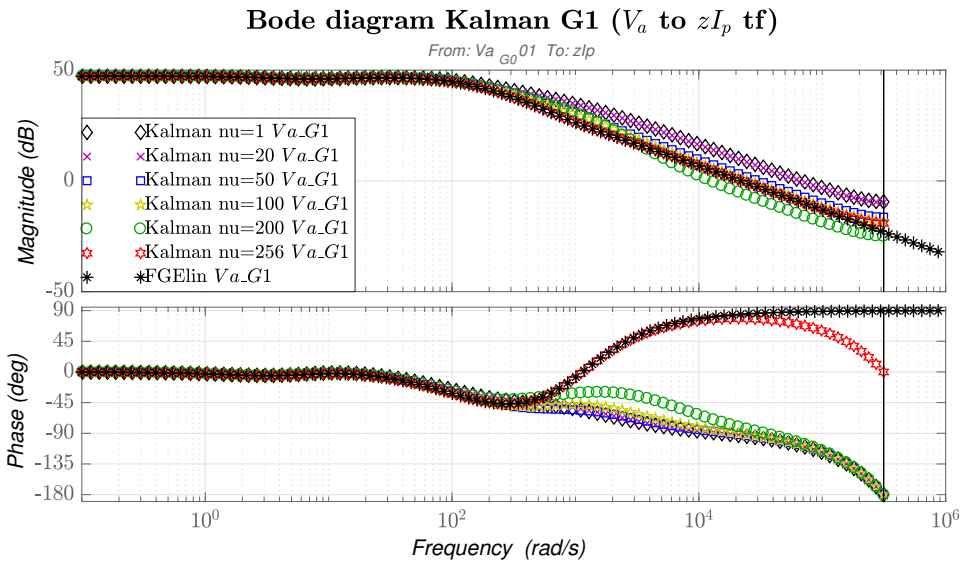

Figure 5.24: V_a to $z\hat{I}_p$ frequency responses of the Kalman filter in *discrete time* with increasing n_u, G1-coil

In the next plots shown in (5.25 , 5.26), the *Bode diagrams* of the MGA-T_{ius} with $n_u = 1$, and both *continuous time* and *discrete time* MGA-$\dot{\Psi}_f$ derivator blocks are compared to the Kalman filter case with $n_u = 1$ and to FGESS. We have already shown in (5.21) that the *continuous time* frequency response of FGESS is almost equivalent to the MGA-T_{ius} frequency response with $n_u = 256$. In figures (5.25 , 5.26), we can see that the MGA-T_{ius} response due to the slowest eigenmode ($n_u = 1$) has almost the same frequency response of the *continuous time* MGA-$\dot{\Psi}_f$ response using the *HPF* block, which considers 38 vessel currents.

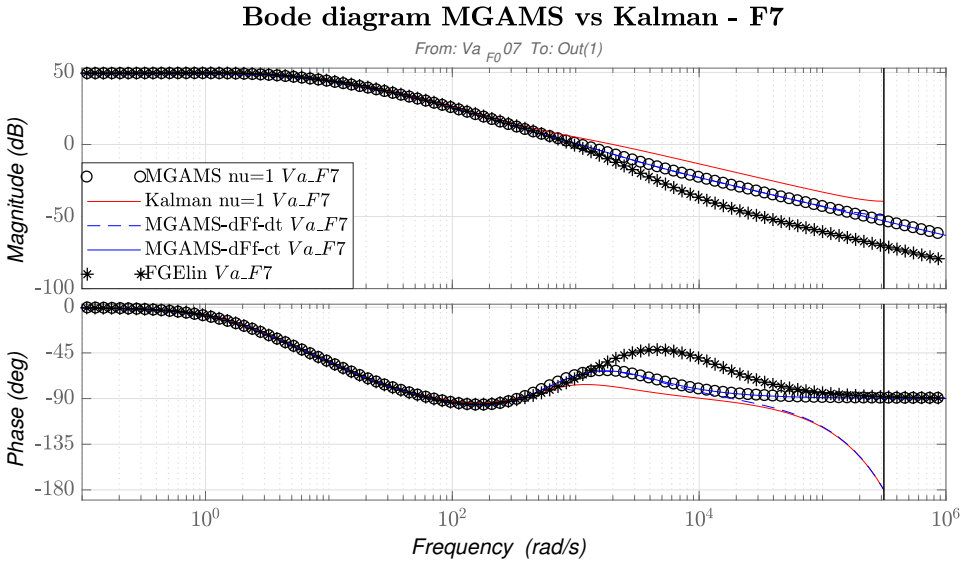

Figure 5.25: V_a to $z\hat{I}_p$ frequency responses of MGA and of the Kalman filter with $n_u = 1$, F7-coil

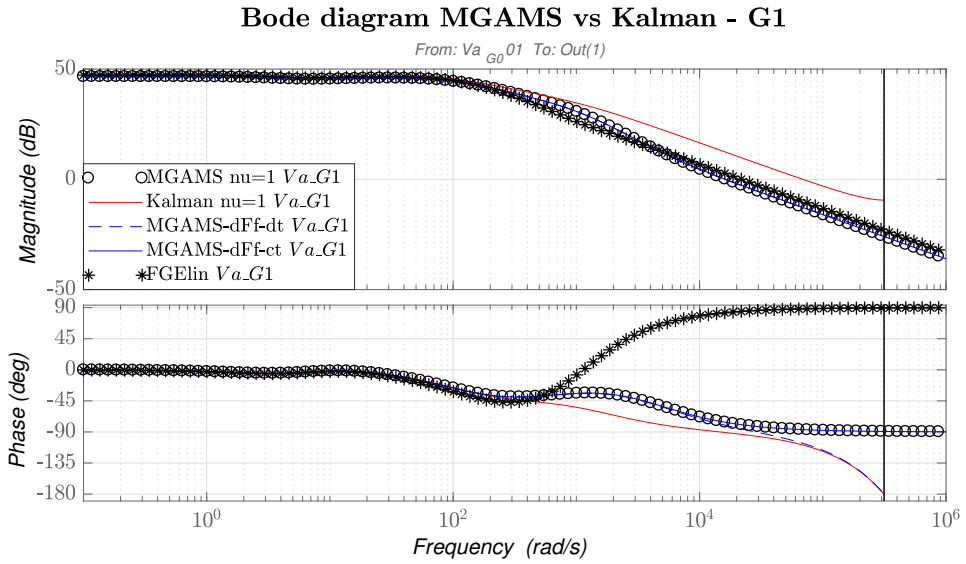

Figure 5.26: V_a to $z\hat{I}_p$ frequency responses of MGA and of the Kalman filter with $n_u = 1$, G1-coil

Moreover we can see that, since the real MGA takes directly the measurements of Ψ_f to determine I_s, the MGA observer has a lower margin phase [9] with respect to Kalman, which is exactly equivalent to FGESS and only diverges close to the *Nyquist frequency*. However, this improvement is reached when the Kalman filter works with $n_u = 256$ since in the $n_u = 1$ case the phase margin is lower in Kalman with respect to MGA.

In the last figure (5.27) the plasma vertical position estimation is shown using MGA (the implemented one i.e. MGA-$\dot{\Psi}_f$) or the full augmented state Kalman filter and it is compared to LIUQE. We have compared the cases in which the Kalman filter performs with $n_u = 20$ and $n_u = 256$. We have proven that even if the phase margin of the Kalman filter V_a to zI_p frequency response reduces when n_u reduces, for the vertical position estimation the estimates are better for the majority of the time instants if we consider $n_u = 20$ as we can see in the error plot. This is due to the fact that considering $n_u = 256$ means consider a covariance matrix Q of order $n_a + n_u + n_\varphi + n_{\Delta\Phi} = 19 + 256 + (19 + 256 + 3) + (19 + 256 + 3 + 19) = 850$ while if $n_u = 20$ we obtain $\dim Q = n_a + n_u + n_\varphi + n_{\Delta\Phi} = 142$. In this case we should put particular attention in the choice of the parameters in the blocks: tuning properly the covariances in the case with $n_u = 256$ should be more accurate than the case with $n_u = 20$ since the filter more degrees of freedom for the model design. In any case the results are very similar: we can see that MGA has a vertical distance error with low variance and a mean value approxilately around $3.5\,mm$, while in the Kalman filter the variance of the error is higher with maxima around $3\,mm$, minima in the order of tenths of a millimeter and mean value approximately around $2\,mm$ [10].

From the error analysis (5.1.4) and error plot (5.27) we can conclude that, for the vertical position estimation, the augmented state Kalman filter performs better than MGA in almost all the time instants regardless of the number of selected vessel eigencurrents. We have therefore validated the Kalman Filter method for vertical position and speed estimation in the **TCV** tokamak.

[9] These transfer functions can be easily stabilzed using a simple P-controller in the case of G-coils or using a PD-controller for the E and F-coils.

[10] The error plot is contained in a $1\,cm$ interval in the y-axis.

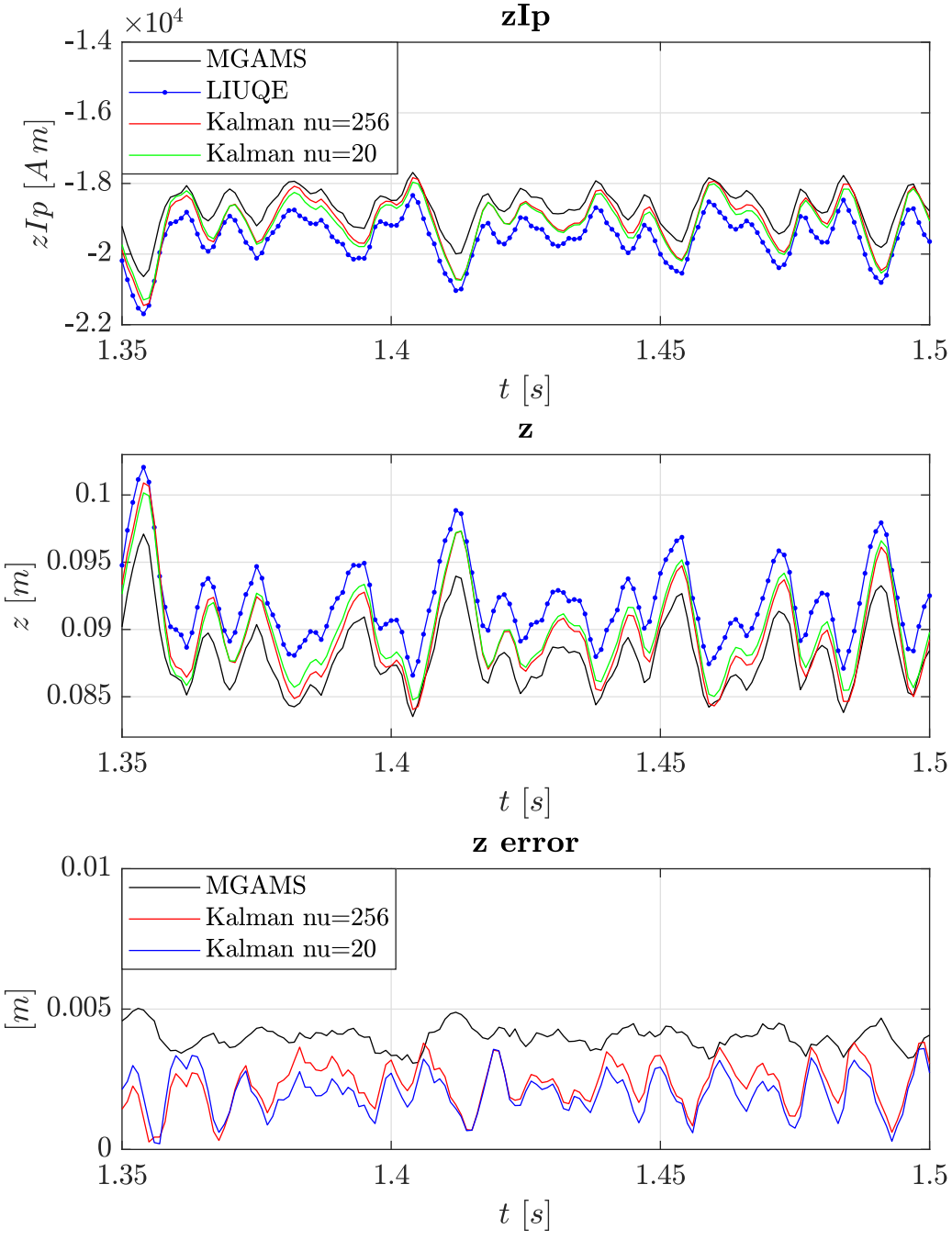

Figure 5.27: State augmented Kalman filter with $n_u = 256$ and $n_u = 20$, and MGA-$\dot{\Psi}_f$ estimates compared to LIUQE vertical position reconstruction, sample time $T_s = 10^{-3}\,s$, $n_\varphi = n_\xi + n_c = n_a + n_u + n_c \;\wedge\; n_{\Delta\Phi} = n_{\Delta\xi} + n_{\Delta c} + n_{\Delta V} = n_e + n_c + n_a$

Conclusions and Outlook

In this thesis a Kalman filter based observer has been designed. The open-loop simulations have been firstly carried onto a stable shot of **Anamak** and then brought onto unstable plasma configurations of already existing **TCV** shots. Statistical methods to test the correctness of the filter implementation have been developed. Moreover, the state has been augmented in order to recover some internal parameters of the plasma as well as particular unknown perturbations in the system. Finally, the open-loop frequency responses of the Kalman filter have been compared to the ones given by MGA observer. The Kalman filter is not decreasing the robustness of the responses and it is giving more accurate estimates with respect to the existing observer MGA, which allow to have a real-time understanding of the state of the system and of global plasma parameters. The next step will be the real-time implementation of the Kalman filter and its test on **TCV** shots. The filter should be coupled with a controller in order to be able to better perform with elongated unstable shots.

Improvements can be done if the filter will be set on multiple equilibria linearizations during the shot. To do so, a faster way of linearizing FGE should be found. The filter should be tested also on RZIP code [8] to decrease the time of the computations. An improved modeling and understanding of plasma physics would allow for a more accurate and detailed description of the system, in particular in covariance matrix tuning and avoiding the hypothesis of uncorrelation of the state components. More advanced stochastic descriptions of the system should be taken into account, especially considering cross-correlation between respectively active and vessel currents with their augmented pairs and trying to figure out the stochastic link between currents and constraints. *Current Diffusion Equation* must be add to avoid the assumption of constant I_p and so to make the Kalman filter ready also for ramp-up and slow-down phases [2]. Other possibilities can be tested as well, like *Particle filters* to avoid the Gaussian hypothesis on process noises and in the *posterior pdf*. Another approach, that would directly deal with the full non-linear system, can be considered. For this task an *Unscented Kalman filter* should be designed and, in order not to loose the real-time objective, tested on faster approximated non-linear solvers like for example RZIP.

Appendix A

Elements of Linear Estimation

The following Chapter will give the mathematical background used in this thesis: the probability concepts and the predicition theory have been mainly taken from [1] but also from [20] and [13]. The main structural features of linear systems for the asymptotic predictor theorems formulation have been taken from [9].

A.1 Concepts of Probability and Statistics

Definition 1. *The first element to consider is the set of all possible results of a phenomenum: these will be called* ***outcomes*** *and their set will be indicated with* ***S*** *(****Possibility space****).*

The set **S** should be both finite or infinite. We call **events** combinations of outcomes of **S**, they are substets of **S**.
An event A is verified if an outcome $s \in A \subseteq \mathbf{S}$.
If we call **F** the *set of all possible events*, **F** must respect:

1. if $A \in \mathbf{F}$ then $\bar{A} = \mathbf{S} - A \in \mathbf{F}$
2. if $A_i \in \mathbf{F}$, $i = 1, ..., N$, with N both finite or infinite, also

$$\bigcup_{i=1}^{N} A_i \in \mathbf{F}$$

Definition 2. *When a set* ***F*** *respects conditions* 1. *and* 2. *it is called a* σ*-algebra.*

From 1. and 2. we necessarily obtain that:

- $\emptyset \subseteq \mathbf{F}$
- $\mathbf{S} \subseteq \mathbf{F}$

Definition 3. *We call* ***probability*** *the function*

$$\begin{aligned} P\colon \boldsymbol{F} &\to [0,1] \subseteq \mathbb{R} \\ A &\mapsto P(A) \end{aligned}$$

The probability function has the following properties:

1. P(**S**)=1
2. given a family $\{A_i\}_i$ of events, $A_i \in \mathbf{F}$, $i = 1, ..., N$, with N both finite or infinite, s.t. $A_i \cap A_j = \emptyset$ for $i \neq j$ we must have that:

$$P\Big(\bigcup_{i=1}^{N} A_i\Big) = \sum_{i=1}^{N} P(A_i)$$

A random experiment C, also called *stochastic process*, is fully defined by our previous definitions, so we can write $C = \{\mathbf{S}, \mathbf{F}, P(\cdot)\}$.

Definition 4. *We call v real **aleatory variable** on experiment C the variable $v = \varphi(s)$, with $\varphi : \boldsymbol{S} \to \mathbb{R}$.*

Given a subset $V \subseteq \mathbb{R}$ we can define the probability that v belongs to V as $Prob\,(v \in V)$ and so $Prob\,(v \in V)$ represents the probability of the subset $K \subseteq \mathbf{S}$ of the outcomes s s.t $\varphi(s) \in V \ \forall\, s \in K$ [1]. From our previous definition of probability it is natural that $\varphi^{-1}(V) \in \mathbf{F}$, so the subset K is an event. If the last condition holds then:

$$Prob\,(v \in V) = P\,(\varphi^{-1}(V))$$

Definition 5. *If we take $q \in \mathbb{R}$ we call **probability distribution function (PDF)** of the aleatory variable v the function of q:*

$$F\,(q) = Prob\,(v \leq q) = P\,(\varphi^{-1}\,\big(\,\big]-\infty, q\big]\,\big)$$

In general F has the following properties:

- $F(-\infty) = 0$
- $F(+\infty) = 1$
- it is monotonic and not decreasing
- it is continous or at least discontinuous but a numerable number of discontinuity points (in these points the right limit of F is well defined)
- it is differentiable and the derivative is defined everywhere except in a null-measure set of points.

It contains the probabilistic informations of v such that:

$$P\,(a \leq v < b) = F\,(b^-) - F(\,a)$$

is the probability that v belongs to $[a, b] \in \mathbb{R}$.

Definition 6. *We define **probability density function (pdf)** the function of q:*

$$p\,(q) = \frac{dF\,(q)}{dq}$$

[1] To be more precise, the definition of real aleatory variable requires first the introduction of the σ-algebra $\mathcal{R}$ generated by the intervals $[a, b]$ of $\mathbb{R}$. $\mathcal{R}$ is the smallest σ-algebra containing intervals $[a, b]$ of $\mathbb{R}$. A real aleatory variable is an application from $\mathbf{S}$ to $\mathbb{R}$ s.t. $\varphi^{-1}(V) \in \mathbf{F}$, $\forall V \in \mathbb{R}$. These elements V of $\mathcal{R}$ are called *borelians*.

If we consider a point $q \in \mathbb{R}$ and an infinitesimal interval $[q, q+dq]$, then the area underneath the function p in this interval represents the probability that the aleatory variable v assumes values between q and $q + dq$:

$$p\,(q)\,dq = Prob\,(q \leq v < q + dq)$$

Definition 7. *We call* ***expected value*** *of an aleatory variable the function:*

$$\mu = \mathbb{E}\,[v] = \int_{-\infty}^{+\infty} q\,p(q)\,dq$$

If p is symmetric around q then $\mathbb{E}\,[v] = q$.

Definition 8. *We call* ***variance*** *of an aleatory variable the function:*

$$\sigma^2 = Var\,[v] = \int_{-\infty}^{+\infty} (q - \mathbb{E}\,[v])^2\,p(q)\,dq$$

In general the k-moment $m_k\,[v]$ of an aleatory variable is defined as:

$$m_k\,[v] = \int_{-\infty}^{+\infty} q^k\,p(q)\,dq$$

We easily obtain that:

- if $k = 0$ then $m_0\,[v] = 1$
- if $k = 1$ then $m_1\,[v] = \mathbb{E}\,[v]$
- if $k = 2$ then $m_2\,[v] = Var\,[v] + \Big(\mathbb{E}\,[v]\Big)^2$

If we consider a real aleatory variable v and a function $g\colon \mathbb{R} \to \mathbb{R}$ such that $w = g\,(v)$ is a new variable we can proove that w is a real aleatory variable too and its expected value can be predicted from the knowledge of the probability density p_v of v:

$$\mathbb{E}\,[w] = \int_{-\infty}^{+\infty} q\,p_w(q)\,dq = \int_{-\infty}^{+\infty} g\,(q)\,p_v(q)\,dq$$

The expected value is a linear operator, i.e. $\mathbb{E}\,[\alpha v_1 + \beta v_2] = \alpha\,\mathbb{E}\,[v_1] + \beta\,\mathbb{E}\,[v_2]$, in fact if the map g is linear, i.e. $w = \alpha\,v$, $\alpha \in \mathbb{R}$ we get

$$\mathbb{E}\,[w] = \mathbb{E}\,[\alpha\,v] = \int_{-\infty}^{+\infty} \alpha\,q\,p_v(q)\,dq = \alpha \int_{-\infty}^{+\infty} q\,p_v(q)\,dq = \alpha\,\mathbb{E}\,[v]$$

Definition 9. *The vector* $v = [v_1\ v_2\ ...\ v_n]^T$ *is called a* $\mathbb{R}$-***vector aleatory variable*** *if* $\exists\,\varphi\colon \boldsymbol{S} \to \mathbb{R}^n$ *s.t.* $\varphi^{-1}\,(v_1 \leq q_1, v_2 \leq q_2, ..., v_n \leq q_n) \in \boldsymbol{F}$, $\forall\,q = [q_1\ q_2\ ...\ q_n]^T \in \mathbb{R}^n$.

The function $F(q_1\ q_2\ ...\ q_n)$ is defined by:

$$F(q_1\ q_2\ ...\ q_n) = Prob\,(v_1 \leq q_1, v_2 \leq q_2, ..., v_n \leq q_n)\ ,\ q_i \in \mathbb{R}\ ,\ \forall\,i = 1, ..., n$$

All the inequalities must be verified at the same time[2] such that $F\colon \mathbb{R}^n \to [0, 1]$ is well defined and it is a multivariate distribution called *joint probability distribution.*

[2]There is a link between the *joint probability distribution* $F(q)$, $q \in \mathbb{R}^n$ and the *marginal probability distribution* $F_i(q_i)$ i.e. $F_i(q_i) = F(+\infty, +\infty, ..., q_i, ..., +\infty)$.

Definition 10. *We define* ***joint probability density*** *the function of* $q \in \mathbb{R}^n$*:*

$$p\left(q_1\ q_2\ ...\ q_n\right) = \frac{\partial^n F\left(q_1\ q_2\ ...\ q_n\right)}{\partial q_1 \partial q_2 ... \partial q_n}$$

Like in the univariate case the quantity $p\left(q_1\ q_2\ ...\ q_n\right) dq_1 dq_2 ... dq_n$ represents the probability that $q_i \leq v_i < q_i + dq_i$ holds $\forall\, i = 1, ..., n$ and so we obtain the link between marginal and joint probability density:

$$p_i\left(q_i\right) = \int_{-\infty}^{+\infty} ... \int_{-\infty}^{+\infty} p\left(q_1\ q_2\ ...\ q_n\right) dq_1 ... dq_{i-1} dq_{i+1} ... dq_n$$

Definition 11. *(**Expected value** in* $\mathbb{R}^n$*) If* $v = \left[v_1\ v_2\ ...\ v_n\right]^T$ *then*

$$\mathbb{E}\left[v\right] = \left[\mathbb{E}\left[v_1\right]\ \mathbb{E}\left[v_2\right]\ ...\ \mathbb{E}\left[v_n\right]\right]^T$$

Definition 12. *(**Covariance matrix**) If* $v = \left[v_1\ v_2\ ...\ v_n\right]^T$ *and* $q \in \mathbb{R}^n$ *then*

$$Cov\left[v\right] = \int_{\mathbb{R}^n} (q - \mathbb{E}\left[v\right])(q - \mathbb{E}\left[v\right])^T p(q)\, dq$$

Defining $w \triangleq q - \mathbb{E}\left[v\right]$ we obtain

$$Cov\left[v\right] = \mathbb{E}\left[w\, w^T\right]$$

with the following properties:

1. it is symmetric: $Cov_{ij}\left[v\right] = Cov_{ji}\left[v\right]$
2. it is positive semi-definite, in fact if we consider the quadratic form:

   $$x^T\, Cov\left[v\right] x = x^T\, \mathbb{E}\left[w\, w^T\right] x = \mathbb{E}\left[x^T\, w\, w^T\, x\right] = \mathbb{E}\left[x^T\, w\, (x^T\, w)^T\right] = \mathbb{E}\left[(x^T\, w)^2\right] \geq 0$$

   since $x \in \mathbb{R}^n$ is a constant for $\mathbb{E}\left[\cdot\right]$ and $x^T\, w \in \mathbb{R}$
3. the elements on the main diagonal are the variances of the univariate real aleatory variable v_i:

   $$Cov_{ii}\left[v\right] = Var\left[v_i\right]$$

   and the off diagonal terms represent the covariances of v_i and v_j:

   $$Cov_{ij}\left[v\right] = \mathbb{E}\left[\left(v_i - \mathbb{E}\left[v_i\right]\right)\left(v_j - \mathbb{E}\left[v_j\right]\right)\right]$$

4. $\mathbb{E}\left[v\, v^T\right] = Cov\left[v\right] + \mathbb{E}\left[v\right] \mathbb{E}\left[v^T\right]$

We see that if v is a White Noise aleatory signal its expected value is zero, and so:

$$Cov\left[v\right] = \mathbb{E}\left[v\, v^T\right]$$

Definition 13. *(**White noise**) A vector aleatory variable* w *is called* ***white noise*** *iff:*

$$\mu_w = \mathbb{E}\left[w\right] = 0$$
$$Cov\left[w\right] = \mathbb{E}\left[w\, w^T\right] = \sigma^2 \mathcal{I}$$

Definition 14. *(**White process**) An aleatory process $w(t)$, $t \in \mathbb{R}$ is white iff:*

$$\mu_w(t) = \mathbb{E}[w(t)] = 0$$
$$\mathbb{E}[w(t_1)\, w(t_2)] = \sigma^2\, \delta(t_1 - t_2)$$

with $\delta(t)$ Dirac's delta.

Definition 15. *If we consider a 2-vector aleatory variable $v = [v_1\ v_2]^T$ we call **correlation coefficient** the real number*

$$\rho = \frac{Cov_{12}[v]}{\sqrt{Cov_{11}[v]\, Cov_{22}[v]}} = \frac{\mathbb{E}\left[\left(v_1 - \mathbb{E}[v_1]\right)\left(v_2 - \mathbb{E}[v_2]\right)\right]}{\sqrt{Var[v_1]\, Var[v_2]}}$$

Since the covariance matrix is positive semi-definite, therefore

$$\left(\mathbb{E}\left[\left(v_1 - \mathbb{E}[v_1]\right)\left(v_2 - \mathbb{E}[v_2]\right)\right]\right)^2 \leq Var[v_1]\, Var[v_2]$$

so $\rho \in [-1, +1]$. We say that two variables are *uncorrelated* when $\rho = 0$,
i.e. $\mathbb{E}\left[\left(v_1 - \mathbb{E}[v_1]\right)\left(v_2 - \mathbb{E}[v_2]\right)\right] = 0$.

Theorem 1. *Necessary and sufficient condition to have uncorrelation between two aleatory variables v_1 and v_2 is that $\mathbb{E}[v_1\, v_2] = \mathbb{E}[v_1]\, \mathbb{E}[v_2]$*

Proof. Using linearity:

$$\begin{aligned}\mathbb{E}\left[\left(v_1 - \mathbb{E}[v_1]\right)\left(v_2 - \mathbb{E}[v_2]\right)\right] &= \mathbb{E}\left[v_1\, v_2 - v_1\, \mathbb{E}[v_2] - v_2\, \mathbb{E}[v_1] + \mathbb{E}[v_1]\, \mathbb{E}[v_2]\right] = \\ &= \mathbb{E}\left[v_1\, v_2\right] - 2\, \mathbb{E}\left[v_1\right] \mathbb{E}\left[v_2\right] + \mathbb{E}\left[v_1\right] \mathbb{E}\left[v_2\right] = \\ &= \mathbb{E}\left[v_1\, v_2\right] - \mathbb{E}\left[v_1\right] \mathbb{E}\left[v_2\right] = 0\end{aligned}$$

iff $\mathbb{E}[v_1\, v_2] = \mathbb{E}[v_1]\, \mathbb{E}[v_2]$. □

Definition 16. *If we consider a 2-vector aleatory variable $v = [v_1\ v_2]^T$ we say that their components are **stochastically independent** if $p_v(q_1\ q_2) = p_{v_1}(q_1)\, p_{v_2}(q_2)$.*

Theorem 2. *If two aleatory variables v_1 and v_2 are independent from each other, they are also uncorrelated.*

Proof. From the definition:

$$\mathbb{E}[v_1\, v_2] = \int_{-\infty}^{+\infty} \int_{-\infty}^{+\infty} q_1\, q_2\, p_{12}(q_1\, q_2)\, dq_1\, dq_2$$

For the independence of the variables:

$$\begin{aligned}\mathbb{E}[v_1\, v_2] &= \int_{-\infty}^{+\infty} \int_{-\infty}^{+\infty} q_1\, q_2\, p_{12}(q_1\, q_2)\, dq_1\, dq_2 = \\ &= \int_{-\infty}^{+\infty} q_1\, p_1(q_1)\, dq_1 \int_{-\infty}^{+\infty} q_2\, p_2(q_2)\, dq_2 = \mathbb{E}[v_1]\, \mathbb{E}[v_2]\end{aligned}$$

□

Definition 17. *We say that an aleatory variable is* ***normal*** *when its probability density follows a Gussian distribution i.e.:*

$$p\left(q\right) = \frac{1}{\sqrt{2\pi Var\left[v\right]}} \exp\Big(-\frac{\left(q - \mathbb{E}\left[v\right]\right)^2}{2Var\left[v\right]}\Big)$$

In this cases we write $v \sim \mathcal{N}\left(\mathbb{E}\left[v\right], Var\left[v\right]\right)$.

Theorem 3. *Gaussianity is conserved for linear transformations.*

Proof. We know that a normal variable v under the linear transformation $w = \alpha + \beta v$ is still an aleatory variable with:

$$\mathbb{E}\left[w\right] = \mathbb{E}\left[\alpha + \beta v\right] = \alpha + \beta\,\mathbb{E}\left[v\right]$$
$$Var\left[w\right] = Var[\left[\alpha + \beta v\right] = \beta^2\, Var\left[v\right]$$

so $w \sim \mathcal{N}\left(\mathbb{E}\left[w\right], Var\left[w\right]\right)$. □

If we take the linear transformation $w = (Var\left[v\right])^{-1}(v - \mathbb{E}\left[v\right])$ we obtain a *standard* normal variable s.t. $w \sim \mathcal{N}\left(0, 1\right)$.
If $v \in \mathbb{R}^n$, v is *normal* if its density probability is:

$$p\left(q\right) = \frac{1}{(2\pi)^{n/2}\sqrt{\det Cov\left[v\right]}} \exp\Big(-\frac{1}{2}(q - \mathbb{E}\left[v\right])^T (Cov\left[v\right])^{-1}(q - \mathbb{E}\left[v\right])\Big)$$

We say that a set of n aleatory variables is *jointly Gaussian* if the n-vector aleatory variable obtained putting in column the variables is *normal*. We have the following properties:

- if $v_1 ... v_n$ are *jointly Gaussian* then each v_i si *normal*
- if v_i is *normal* and independent $\forall\, i$ then $v = [v_1\ ...\ v_n]^T$ is *normal*
- if $v_1 ... v_n$ are *jointly Gaussian* and uncorrelated then they are also independent
- if $v \sim \mathcal{N}\left(\mu_v, Cov\left[v\right]\right)$ and $w = A\,v + b$, with $A \in \mathbb{R}^{m\times n}$ maximum rank, $b \in \mathbb{R}^m$, then $w \sim \mathcal{N}\left(\mu_w, Cov\left[w\right]\right)$ with $\mu_w = A\,\mu_v + b$ and $Cov\left[w\right] = A\,Cov\left[v\right]A^T$
- if *normal* scalar variables are *jointly Gaussian* then their linear combinations are *normal* scalar variables

Theorem 4. ***(Law of large numbers)*** *Given a set of independent aleatory variables* $\{v_i\}_i$ $i = 1, ..., N$, *if we define the* ***sample mean*** *as*

$$x_N = \frac{1}{N}\sum_{i=1}^{N} v_i$$

then:

$$\lim_{N\to\infty} x_N - \mathbb{E}\left[x_N\right] = 0$$

Theorem 5. ***(Central limit theorem)*** *Given a set of independent aleatory variables* $\{v_i\}_i$ $i = 1, ..., N$, *with the same probability distribution and with* $\mathbb{E}\left[v_i\right] = \mu$ *and* $Var\left[v_i\right] = \sigma^2$, *if we consider the* ***sample mean*** x_N *as defined in the previous theorem we have that* $\mathbb{E}\left[x_N\right] = \mu$ *and* $Var\left[x_N\right] = \sigma^2$. *If we define the* standard *variable of* x_N *as:*

$$y_N = \frac{\sqrt{N}\left(x_N - \mu\right)}{\sigma}$$

then:

$$\lim_{N\to\infty} y_N = v$$

with $v \sim \mathcal{N}(0,1)$

Definition 18. *(**Kolmogorov definition of conditional probability**) Given two events A and B from the σ-algebra $\boldsymbol{F}$, with the (unconditional) probability of B being greater than zero i.e. $P(B) > 0$, the (conditional) probability of A given B, $P(A \mid B)$ is the probability of A occurring if B has already happened. The conditional probability of A given B is the quotient of the probability of the joint intersection of events A and B, $P(A \cap B) = P(A, B)$ which represents the (joint) probability of A and B occurring together (not necessarily at the same time) and the probability of B:*

$$P(A \mid B) = \frac{P(A \cap B)}{P(B)}$$

Definition 19. *We call **likelihood** the joint probability of the observed data as a function of the parameters. Let X be an aleatory variable with probability density p depending on a parameter θ. We call likelihood the function:*

$$\mathcal{L}(\theta \mid x) = p_\theta(x) = P(X = x \mid \theta)$$

considered as a function of θ, given the outcome x of the aleatory variable X. The likelihood is equal to the probability that a particular outcome x is observed when the true value of the parameter is θ.

With no event (no data) $\mathcal{L}(\theta \mid x) = 1$, any non-trivial event will have a lower likelihood [10].

Theorem 6. *(**Bayes' theorem**) Given two events A and B with $P(B) \neq 0$ then:*

$$P(A \mid B) = \frac{P(B \mid A)\, P(A)}{P(B)}$$

with:

- $P(A \mid B)$ *is a **conditional probability**: the probability that the event A occurs by the assumption that B has already occured. It is also called the posterior probability of A given B*
- $P(B \mid A)$ *is a **conditional probability**: the probability that the event B occurs by the assumption that A has already occured. It can also be interpreted as the likelihood of A given a fixed B since $P(B \mid A) = \mathcal{L}(A \mid B)$*
- $P(A)$, $P(B)$ *are the probabilities of observing A and B respectively without any given conditions. They are marginal probabilities also called prior probabilities*

Proof. From the definition of conditional probability:

$$P(A \mid B) = \frac{P(A \cap B)}{P(B)}\ ,\ P(B) \neq 0$$
$$P(B \mid A) = \frac{P(B \cap A)}{P(A)}\ ,\ P(A) \neq 0$$

and since $P(A \cap B) = P(B \cap A)$. □

A.2 Bayes Estimation

Sometimes we have “a priori" informations about the unknown of an estimation problem. These informations can improve the estimation and compensate for random errors in the data. In Bayes estimation the unknown θ is seen as a vector aleatory variable. The density of probability of θ without any data (“a priori" density probability) summarises the “a priori" informations. A possible estimation is the expected value and the variance will be the “a priori" uncertainty. As data is received, the probability density is updated: this changes the expected value with respect to the “a priori" one and variance is expected to decrease. Formally there are two random experiments C_1 and C_2, C_1 generates θ and C_2 the data set d. The joint random experiment $C_1 \times C_2$ will generate the joint outcome vector $s = (s_1, s_2)$. A generic estimator is a function of data i.e. $\hat{\theta} = h(d)$, and the most it will be close to the vector aleatory variable θ to estimate the better it will be the estimation. If we take the following cost functional

$$J(h(d)) = \mathbb{E}\left[\|\theta - h(d)\|^2\right]$$

we call **optimum Bayes estimator** the function $h^o(\cdot)$ s.t.

$$J(h(d)) = \mathbb{E}\left[\|\theta - h^o(d)\|^2\right] \leq \mathbb{E}\left[\|\theta - h(d)\|^2\right] \ , \ \forall\, h(\cdot)$$

Proposition 1. *The **optimum Bayes estimator** which minimizes $J(h(\cdot))$ is:*

$$h^o = \mathbb{E}\left[\theta \mid d = x\right]$$

where x is the current variable for the data d. h^o is the expected value of θ conditioned to the fact that data have assumed the value x.

Proof. (Scalar case) In the expression:

$$\mathbb{E}\left[\|\theta - h(d)\|^2\right] = \mathbb{E}\left[\theta^2 - 2\theta\, h(d) + h(d)^2\right]$$

we define $g(d, \theta) = \theta^2 - 2\theta\, h(d) + h(d)^2$ s.t.:

$$\mathbb{E}\left[\|\theta - h(d)\|^2\right] = \mathbb{E}\left[g(d, \theta)\right] = \int_{x,y} g(x, y) p(x, y)\, dxdy$$

where x and y are the current variables for d and θ respectively, and $p(d, \theta)$ is the joint probability density of d and θ. From the definition of conditional probability it is automatic to get the following relation for the probability densities:

$$p(x, y) = p(y \mid x)\, p(x)$$

so:

$$\mathbb{E}\left[\|\theta - h(d)\|^2\right] = \int_{x,y} g(x, y) p(x, y)\, dxdy = \int_x \Big[\int_y g(x, y) p(y \mid x)\, dy \Big] p(x)\, dx$$

where:

$$\int_y g(x, y) p(y \mid x)\, dy = \mathbb{E}\left[g(d, \theta) \mid d = x\right]$$

Replacing $g(d, \theta)$ we obtain:

$$\mathbb{E}\left[g(d, \theta) \mid d = x\right] = \mathbb{E}\left[\theta^2 \mid d = x\right] - 2\mathbb{E}\left[h(d)\, \theta \mid d = x\right] + \mathbb{E}\left[h(d)^2 \mid d = x\right]$$

When $d = x$, $h(\cdot)$ is no longer a function of an aleatory variable and becomes a deterministic function. In such a case the expected value of $h(x)$ corresponds to $h(x)$ and we obtain:

$$\mathbb{E}\left[g(d,\theta) \mid d = x\right] = \mathbb{E}\left[\theta^2 \mid d = x\right] - 2\,h(x)\,\mathbb{E}\left[\theta \mid d = x\right] + h(x)^2$$

Adding and substracting $\mathbb{E}\left[\theta \mid d = x\right]^2$ we obtain:

$$\mathbb{E}\left[g(d,\theta) \mid d = x\right] = \left\|\mathbb{E}\left[\theta \mid d = x\right] - h(x)\right\|^2 + \mathbb{E}\left[\theta^2 \mid d = x\right] - \mathbb{E}\left[\theta \mid d = x\right]^2$$

therefore:

$$\begin{aligned}\mathbb{E}\left[\|\theta - h(d)\|^2\right] &= \int_x \Big[\, \left\|\mathbb{E}\left[\theta \mid d = x\right] - h(x)\right\|^2 + \mathbb{E}\left[\theta^2 \mid d = x\right] - \mathbb{E}\left[\theta \mid d = x\right]^2 \Big]\, p(x)\, dx = \\ &= \int_x \Big[\, \left\|\mathbb{E}\left[\theta \mid d = x\right] - h(x)\right\|^2 + Var\left[\theta \mid d = x\right] \Big]\, p(x)\, dx\end{aligned}$$

Finally, since $Var\left[\theta \mid d = x\right] \geq 0$ we get the minimum with:

$$h(x) = \mathbb{E}\left[\theta \mid d = x\right]$$

□

We will call *Bayes estimator* the function $\hat{\theta}(d) = h^o(d)$ and *Bayes estimation* the value $\hat{\theta}(x) = h^o(x)$ where x is the value of data d corrispondent to a particular outcome s.

If d and θ are *jointly Gaussian* i.e.:

$$\begin{pmatrix} d \\ \theta \end{pmatrix} \sim \mathcal{N}\left(\begin{pmatrix} 0 \\ 0 \end{pmatrix}, \begin{pmatrix} \lambda_{dd} & \lambda_{d\theta} \\ \lambda_{\theta d} & \lambda_{\theta\theta} \end{pmatrix}\right)$$

their *joint probability density* will be:

$$p\left(d,\theta\right) = K\,\exp\left(\frac{1}{2}\begin{pmatrix} d & \theta \end{pmatrix}\begin{pmatrix} \lambda_{dd} & \lambda_{d\theta} \\ \lambda_{\theta d} & \lambda_{\theta\theta} \end{pmatrix}^{-1}\begin{pmatrix} d \\ \theta \end{pmatrix}\right) = K\,\exp\left(-\frac{1}{2\lambda^2}\left(\frac{\lambda_{\theta\theta}}{\lambda_{dd}}d^2 - 2\frac{\lambda_{\theta d}}{\lambda_{dd}}d\theta + \theta^2\right)\right)$$

with $\lambda^2 = \lambda_{\theta\theta} - \frac{\lambda_{d\theta}^2}{\lambda_{dd}}$ and $K \in \mathbb{R}$.
The density probability of d is: $p\left(d\right) = K'\exp\left(-\frac{d^2}{2\lambda_{dd}}\right)$ so the density probility of θ conditioned by d is:

$$p\left(\theta \mid d\right) = \frac{p\left(d,\theta\right)}{p\left(d\right)} = \frac{K}{K'}\exp\left(-\frac{1}{2\lambda^2}\left(\theta - \frac{\lambda_{\theta d}}{\lambda_{dd}}d\right)^2\right)$$

so

$$p\left(\theta \mid d\right) \sim \mathcal{N}\left(\frac{\lambda_{\theta d}}{\lambda_{dd}}d, \lambda^2\right)$$

We can now calculate the Bayes estimator and evaluate its performances.
We obtain:

$$\hat{\theta}(x) = h^o(x) = \mathbb{E}\left[\theta \mid d = x\right] = \frac{\lambda_{\theta d}}{\lambda_{dd}}\,x$$

Since by hypothesis $\mathbb{E}[d] = 0$, then $\mathbb{E}[\hat{\theta}] = 0$ thus $\mathbb{E}[\theta - \hat{\theta}] = 0$.
Therefore:

$$\begin{aligned} Var[\theta - \hat{\theta}] = \mathbb{E}[(\theta - \hat{\theta})^2] = \mathbb{E}[(\theta - \frac{\lambda_{\theta d}}{\lambda_{dd}} d)^2] = \\ = \mathbb{E}[(\theta)^2] - 2\,\frac{\lambda_{\theta d}}{\lambda_{dd}}\,\mathbb{E}[\theta d] + \frac{\lambda_{\theta d}^2}{\lambda_{dd}^2}\,\mathbb{E}[d^2] = \\ = \lambda_{\theta\theta} - \frac{\lambda_{\theta d}^2}{\lambda_{dd}} = \lambda^2 \end{aligned}$$

If d and θ are vector aleatory variables and if their expected values are not null, i.e. $\mathbb{E}[d] = d_m$, $\mathbb{E}[\hat{\theta}] = \theta_m$, we can easily extend the formalism:

$$\begin{aligned} \hat{\theta} &= \theta_m + \Lambda_{\theta d}\,\Lambda_{dd}^{-1}\,(d - d_m) \\ Var[\theta - \hat{\theta}] &= \Lambda_{\theta\theta} - \Lambda_{\theta d}\,\Lambda_{dd}^{-1}\,\Lambda_{d\theta} \end{aligned}$$

In the absence of any measure ("a priori"), the only information available on the unknown is its expected value θ_m. In the posterior estimation to the expected value θ_m is added the quantity $\Lambda_{\theta d}\,\Lambda_{dd}^{-1}\,(d - d_m)$. Let's take $\dim d = \dim \theta = n$. If $\Lambda_{\theta d} = \mathbb{O}_{\dim\theta \times \dim d} = \mathbb{O}_{n\times n}$ the knowledge of d does not alter the "a priori" estimation since $d - d_m$ and $\theta - \theta_m$ are uncorrelated and so it is not provided any additional information on the unknown. Otherwise if $\Lambda_{\theta d} \neq \mathbb{O}_{n\times n}$ there is a relation between θ and d and therefore an improvement in the estimation. If $\Lambda_{\theta d}$ is positive definite this means that the components of the vectors $d - d_m$ and $\theta - \theta_m$ have on average opposite sign so if $[d - d_m]_k > 0$ then $[\theta - \theta_m]_k < 0$. Morover, supposing $\Lambda_{\theta d}$ fixed, and having defined the standard matrix 2-norm, high value of $\|\Lambda_{dd}\|_2$ means that the data is affected by considerable unceranty, and is therefore unreliable. In the evaluation of the unknown, a big value of $\|\Lambda_{dd}\|_2$ gives less weight to the information provided by the data.
For the variance discussion, let's take the scalar case for simplicity:

$$Var[\theta - \hat{\theta}] = \lambda_{\theta\theta} - \frac{\lambda_{\theta d}^2}{\lambda_{dd}} = \lambda_{\theta\theta}\left(1 - \frac{\lambda_{\theta d}^2}{\lambda_{\theta\theta}\,\lambda_{dd}}\right)$$

and remembering that the correlation coefficient is:

$$\rho = \frac{\lambda_{\theta d}}{\sqrt{\lambda_{\theta\theta}\,\lambda_{dd}}} \in [-1, +1]$$

we obtain:

$$Var[\theta - \hat{\theta}] = \lambda_{\theta\theta}\left(1 - \rho^2\right)$$

Since $|\rho| \leq 1$ the *posterior variance* is always inferior or at least equal to the "a priori" variance $\lambda_{\theta\theta}$. If $\rho = 0$ the "a priori" and the *posterior variances* coincide.

A.2.1 Geometrical interpretation of Bayes Estimation

The following results can be applied in a deeper formalism into *Hilbert space* L^2 thanks to *Riesz representation theorem*. The scalar case is considered for first.
Let's consider the set $\mathbb{H}$ of all 1-vector aleatory variables with null expected value i.e. $v \in \mathbb{H} \Rightarrow \mathbb{E}[v] = 0$. Since $\mathbb{H}$ is closed to linear combinations of its elements it is has a structure of vector space, i.e. if $v_1(s)$, $v_2(s) \in \mathbb{H}$ then $\alpha\,v_1(s) + \beta\,v_2(s) \in \mathbb{H}$, with $\alpha, \beta \in \mathbb{R}$, $\forall\, s$ outcome. The "zero" element of $\mathbb{H}$ is the variable s.t. the set of outcomes s for which

the corresponding variable cancels out is an event with probability equal to 1. Such a variable has zero variance. We can equip $\mathbb{H}$ with an internal product so defined:

$$\langle v_1, v_2 \rangle = \mathbb{E}[v_1 v_2] = Cov[v_1 v_2]$$

Therefore:

$$\begin{aligned}
&\langle v_1, v_2 \rangle = \langle v_2, v_1 \rangle \\
&\langle v, v \rangle = Var[v] \geq 0 \\
&\langle v, v \rangle = 0 \iff v \sim \mathcal{N}(0, 0) \\
&\langle \alpha v_1 + \beta v_2, v_3 \rangle = \alpha \langle v_1, v_3 \rangle + \beta \langle v_2, v_3 \rangle
\end{aligned}$$

We can then introduce the induced norm:

$$\|v\| = \sqrt{\langle v, v \rangle} = \sqrt{Var[v]} = \sigma$$

thus:

$$\cos\varphi = \frac{\langle v_1, v_2 \rangle}{\|v_1\| \, \|v_2\|} = \frac{\mathbb{E}[v_1 \, v_2]}{\sigma_1 \, \sigma_2} = \rho$$

In such a case two vectors of $\mathbb{H}$ will be *orthogonal* iff their corresponding aleatory variables are *independent*. They will be aligned when $\rho = 1$ and opposite when $\rho = -1$.
If $\lambda_{11} = Var[v_1]$ and $\lambda_{12} = Cov[v_1 v_2]$ then from Bayes we have that:

$$\begin{aligned}
\mathbb{E}[v_2 \mid v_1] = \frac{\lambda_{12}}{\lambda_{11}} v_1 = \frac{\mathbb{E}[v_1 v_2]}{Var[v_1]} v_1 = \frac{\langle v_1, v_2 \rangle}{\|v_1\|^2} v_1 = \\
= \|v_2\| \frac{\langle v_1, v_2 \rangle}{\|v_1\| \, \|v_2\|} \frac{v_1}{\|v_1\|} = \|v_2\| \cos\varphi \frac{v_1}{\|v_1\|}
\end{aligned}$$

So if $v_1 = d$ and $v_2 = \theta$ the conditional expected value $\hat{\theta}(d) = \mathbb{E}[\theta \mid d]$ is the *projection* of θ on d.

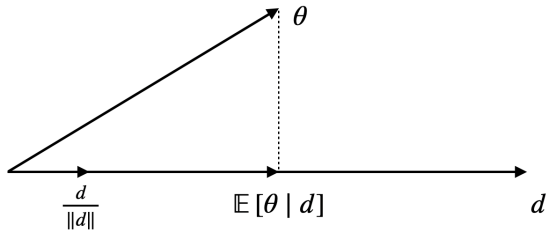

The posterior variance of estimation error of θ known d is the length of $\theta - \mathbb{E}[\theta \mid d]$. Using *Pitagora's formula* we obtain:

$$Var[\theta - \mathbb{E}[\theta \mid d]] = \|\theta\|^2 - \|\mathbb{E}[\theta \mid d]\|^2 = \lambda_{\theta\theta} - \lambda_{d\theta}^2 / \lambda_{dd}$$

where $\lambda_{\theta\theta} = Var[\theta]$ is the "a priori" variance.
If we consider n-vector aleatory variables the vector space structure of $\mathbb{H}$ is conserved since $v_k \in \mathbb{H} \Rightarrow \mathbb{E}[v] = \mathbb{O}_{n\times 1}$, $\forall\, k = 1, ..., n$. In this case if we take two vector aleatory variables v and w with null expected value we can generate the subspace $V(v) = \text{span}\{v\}$ from the components of v that are elements of $\mathbb{H}$. It's easy to proove that $\mathbb{E}[w \mid v]$ is a vector with $\dim \mathbb{E}[w \mid v] = \dim v$ in which the $k - th$-component is the aleatory variable of $\mathbb{H}$ obtained from the projection of the $k - th$-component of w on $V(v)$. The difference vector $w - \mathbb{E}[w \mid v]$ is orthogonal to the subspace $V(v)$.

A.3 Kalman Filter

Let's take the following discrete LTI dynamical system:

$$\begin{cases} x(t+1) &= F\,x(t) + w(t) \\ y(t) &= H\,x(t) + v(t) \end{cases} \quad , \qquad t \in \mathbb{Z}$$

where the state $x(t) = [x_1(t) \dots x_n(t)]^T \in \mathbb{R}^n$ and the output $y(t) = [y_1(t) \dots y_p(t)]^T \in \mathbb{R}^p$. F and H are deterministic matrices while the disturbances $w(t) \in \mathbb{R}^n$ and $v(t) \in \mathbb{R}^p$ are described in a probabilistic way assuming them uncorrelated and white noise Gaussian signals. Indicating with $Q \in \mathbb{R}^{n\times n}$ and $R \in \mathbb{R}^{p\times p}$ the coviariance matrices of these signals we can write $w \sim \mathcal{N}(0, Q)$ and $v \sim \mathcal{N}(0, R)$. In particular:

$$\begin{aligned} &\mathbb{E}[w(t)] = 0\ ,\ \forall\, t \\ &\mathbb{E}[v(t)] = 0\ ,\ \forall\, t \\ &\mathbb{E}[w(i)\,w^T(j)] = 0\ ,\ \forall\, j \neq i \\ &\mathbb{E}[v(i)\,v^T(j)] = 0\ ,\ \forall\, j \neq i \\ &\mathbb{E}[w(i)\,v^T(j)] = 0\ ,\ \forall\, j, i \end{aligned}$$

Another element of uncertainty is the initial state $x(t_0)$, $t_0 \in \mathbb{Z}$. The problem we want to face is the estimation of the state at time $N+k$, $k, N \in \mathbb{Z}$ from the observations of the ouput until the instant N. The solution of the problem in case $k = 1$ (*one-step prediction*) will be derived for first. From this solution the problem of *multi-step prediction* ($k > 1$) and *filtering* ($k = 0$) will be easier to solve.
$x(t)$ and $y(t)$ are vector aleatory variables since $w(t)$ and $v(t)$ are described in a probabilistic way. The problem can be seen as a Bayes estimation problem with $\theta = x(t)$ and $d = [y(N)\ y(N-1)\ \dots\ y(t_0)]^T$, therefore:

$$\begin{aligned} \hat{x}\,(N+k \mid N) &= \mathbb{E}[x\,(N+k) \mid y(N)\,,\, y(N-1)\,,\, \dots\,,\, y(t_0)] = \\ &= x\,(N+k)_m + \Lambda_{x(N+k)\,d}\,\Lambda_{dd}^{-1}\,(d - d_m) \end{aligned}$$

where $x\,(N+k)_m = \mathbb{E}[x\,(N+k)]$ and $d_m = \mathbb{E}[d]$. Λ_{dd} is the covariance matrix of d and $\Lambda_{x(N+k)\,d}$ is the unknown-data covariance matrix. Since the disturbances have null expected value and are Gaussian, the state and the output will have null expected value and will be Gaussian too, so:

$$\hat{x}\,(N+k \mid N) = \Lambda_{x(N+k)\,d}\,\Lambda_{dd}^{-1}\,d$$

is the *optimum Bayes estimator* of the state.
Let's find now a recursive formulation for the estimation, that is essential for real-time data processing.

A.3.1 Recursive Bayes Estimator and Innovation

Let's consider the scalar case for first. Furthermore let's take $d = [d(N)\ d(t_0)]^T = [d(2)\ d(1)]^T$ s.t.:

$$\begin{pmatrix} \theta \\ d(1) \\ d(2) \end{pmatrix} \sim \mathcal{N}\Big(\begin{pmatrix} 0 \\ 0 \\ 0 \end{pmatrix}, \begin{pmatrix} \lambda_{\theta\theta} & \lambda_{\theta 1} & \lambda_{\theta 2} \\ \lambda_{1\theta} & \lambda_{11} & \lambda_{12} \\ \lambda_{2\theta} & \lambda_{21} & \lambda_{22} \end{pmatrix} \Big)$$

where $\lambda_{ij} = \mathbb{E}[i\,j]$. The *optimum Bayes estimation* of θ given $d(1)$ is:

$$\mathbb{E}[\theta \mid d(1)] = \frac{\lambda_{\theta 1}}{\lambda_{11}}\,d(1)$$

while the *optimum Bayes estimation* of θ given $d(1)$ and $d(2)$ is:

$$\mathbb{E}\left[\theta \mid d(1), d(2)\right] = \begin{pmatrix} \lambda_{\theta 1} & \lambda_{\theta 2} \end{pmatrix} \begin{pmatrix} \lambda_{11} & \lambda_{12} \\ \lambda_{21} & \lambda_{22} \end{pmatrix}^{-1} \begin{pmatrix} d(1) \\ d(2) \end{pmatrix}, \quad \lambda_{12} = \lambda_{21}$$

If we define $\lambda^2 = \lambda_{22} - \frac{\lambda_{12}^2}{\lambda_{11}}$ then we get:

$$\begin{aligned}
\mathbb{E}\left[\theta \mid d(1), d(2)\right] &= \frac{1}{\lambda_{11}\lambda^2}\left(-\lambda_{\theta 1}\lambda_{21} + \lambda_{\theta 2}\lambda_{11}\right) d(2) + \frac{1}{\lambda_{11}\lambda^2}\left(\lambda_{\theta 1}\lambda_{22} + \lambda_{\theta 2}\lambda_{12}\right) d(1) = \\
&= \frac{1}{\lambda^2}\left(\lambda_{\theta 2} - \lambda_{\theta 1}\frac{\lambda_{12}}{\lambda_{11}}\right) d(2) + \frac{1}{\lambda^2}\left(\lambda_{\theta 1}\frac{\lambda_{22}}{\lambda_{11}} - \lambda_{\theta 2}\frac{\lambda_{12}}{\lambda_{11}} - \lambda^2\frac{\lambda_{\theta 1}}{\lambda_{11}}\right) d(1) + \frac{\lambda_{\theta 1}}{\lambda_{11}} d(1) = \\
&= \frac{\lambda_{\theta 1}}{\lambda_{11}} d(1) + \frac{1}{\lambda^2}\left(\lambda_{\theta 2} - \lambda_{\theta 1}\frac{\lambda_{12}}{\lambda_{11}}\right)\left[d(2) - \frac{\lambda_{12}}{\lambda_{11}} d(1)\right]
\end{aligned}$$

Definition 1. ***(Innovation)*** *Given two aleatory variables $d(1)$ and $d(2)$, we call innovation of $d(2)$ with respect to $d(1)$ the quantity:*

$$e = d(2) - \mathbb{E}\left[d(2) \mid d(1)\right] = d(2) - \frac{\lambda_{12}}{\lambda_{11}} d(1)$$

The main properties of e are the following:

1. $\mathbb{E}\left[e\right] = 0$
2. $\lambda_{ee} = Var\left[e\right] = \mathbb{E}\left[(d(2) - \frac{\lambda_{12}}{\lambda_{11}} d(1))^2\right] = \lambda^2$
3. $\lambda_{\theta e} = \mathbb{E}\left[\theta\,(d(2) - \frac{\lambda_{12}}{\lambda_{11}} d(1))\right] = \lambda_{\theta 2} - \lambda_{\theta 1}\frac{\lambda_{12}}{\lambda_{11}}$
4. $\lambda_{1e} = \mathbb{E}\left[(d(1)\,(d(2) - \frac{\lambda_{12}}{\lambda_{11}} d(1))\right] = \lambda_{12} - \lambda_{11}\frac{\lambda_{12}}{\lambda_{11}} = 0$

Thanks to these definitions we obtain:

$$\begin{aligned}
\mathbb{E}\left[\theta \mid d(1), d(2)\right] &= \frac{\lambda_{\theta 1}}{\lambda_{11}} d(1) + \frac{1}{\lambda^2}\left(\lambda_{\theta 2} - \lambda_{\theta 1}\frac{\lambda_{12}}{\lambda_{11}}\right)\left[d(2) - \frac{\lambda_{12}}{\lambda_{11}} d(1)\right] = \\
&= \frac{\lambda_{\theta 1}}{\lambda_{11}} d(1) + \frac{\lambda_{\theta e}}{\lambda_{ee}} e = \mathbb{E}\left[\theta \mid d(1)\right] + \mathbb{E}\left[\theta \mid e\right]
\end{aligned}$$

If $d(1)$ and $d(2)$ are uncorrelated then $\mathbb{E}\left[d(2) \mid d(1)\right] = 0$ and so $e = d(2)$. In this case we get:

$$\mathbb{E}\left[\theta \mid d(1), d(2)\right] = \mathbb{E}\left[\theta \mid d(1)\right] + \mathbb{E}\left[\theta \mid d(2)\right]$$

The *optimum Bayes estimation* from $d(1)$ and e is thus obtained by:

$$\mathbb{E}\left[\theta \mid d(1), e\right] = \begin{pmatrix} \lambda_{\theta 1} & \lambda_{\theta 2} \end{pmatrix} \begin{pmatrix} \lambda_{11} & \lambda_{1e} \\ \lambda_{e1} & \lambda_{ee} \end{pmatrix}^{-1} \begin{pmatrix} d(1) \\ e \end{pmatrix} = \mathbb{E}\left[\theta \mid d(1)\right] + \mathbb{E}\left[\theta \mid e\right]$$

since, from 1. and 3., $d(1)$ and e are uncorrelated. We observe that the estimation from $d(1)$ and e is equal to the estimation from $d(1)$ and $d(2)$:

$$\mathbb{E}\left[\theta \mid d(1), d(2)\right] = \mathbb{E}\left[\theta \mid d(1), e\right]$$

Innovation represents the part of $d(2)$ that cannot be predicted from $d(1)$.
Generalising to the multivariate case let's take:

$$\begin{pmatrix} \theta \\ d(1) \\ d(2) \end{pmatrix} \sim \mathcal{N}\left(\begin{pmatrix} \theta_m \\ d(1)_m \\ d(2)_m \end{pmatrix}, \begin{pmatrix} \Lambda_{\theta\theta} & \Lambda_{\theta 1} & \Lambda_{\theta 2} \\ \Lambda_{1\theta} & \Lambda_{11} & \Lambda_{12} \\ \Lambda_{2\theta} & \Lambda_{21} & \Lambda_{22} \end{pmatrix}\right)$$

In this case defining

$$e = d(2) - \mathbb{E}\left[d(2) \mid d(1)\right] = d(2) - \Lambda_{21}\Lambda_{11}^{-1}\, d(1)$$

we obtain:

$$\begin{aligned}\mathbb{E}\left[\theta \mid d(1), d(2)\right] &= \theta_m + \Lambda_{\theta 1}\Lambda_{11}^{-1}\left(d(1) - d(1)_m\right) + \Lambda_{\theta e}\Lambda_{ee}^{-1}\, e = \\ &= \mathbb{E}\left[\theta \mid d(1)\right] + \mathbb{E}\left[\theta \mid e\right] - \theta_m\end{aligned}$$

All the properties of e in the scalar case are valid in the multivariate case too.
It is possible to give a geometrical interpretation of the recursive Bayes estimation, where every aleatory variable is a vector of a normed vector space $\mathbb{H}$ and the estimation of θ from d is the projection of the vector θ on d. If we consider θ, $d(1)$ and $d(2)$ with null expected value and jointly Gaussian they belong to $\mathbb{H}$. If we consider the subspace $\mathbb{H}[d(1), d(2)] = \text{span}\{d(1), d(2)\}$ the *optimum Bayes estimation* of $d(2)$ from $d(1)$ is the projection of $d(2)$ on $d(1)$. The innovation e belongs to $\mathbb{H}\left[d(1), d(2)\right]$ and it is orthogonal to $d(1)$ since it is given by the difference between $d(2)$ and the projection of $d(2)$ on $d(1)$. The *optimum Bayes estimation* of θ from $d(1)$ is the projection of θ on $d(1)$ and the *optimum Bayes estimation* of θ from e is the projection of θ on e. Since:

$$\langle e, d(1)\rangle = 0$$

then:

$$\langle \mathbb{E}\left[\theta \mid d(1)\right], \mathbb{E}\left[\theta \mid e\right]\rangle = 0$$

and so:

$$\mathbb{E}\left[\theta \mid d(1), d(2)\right] = \mathbb{E}\left[\theta \mid d(1)\right] + \mathbb{E}\left[\theta \mid e\right]$$

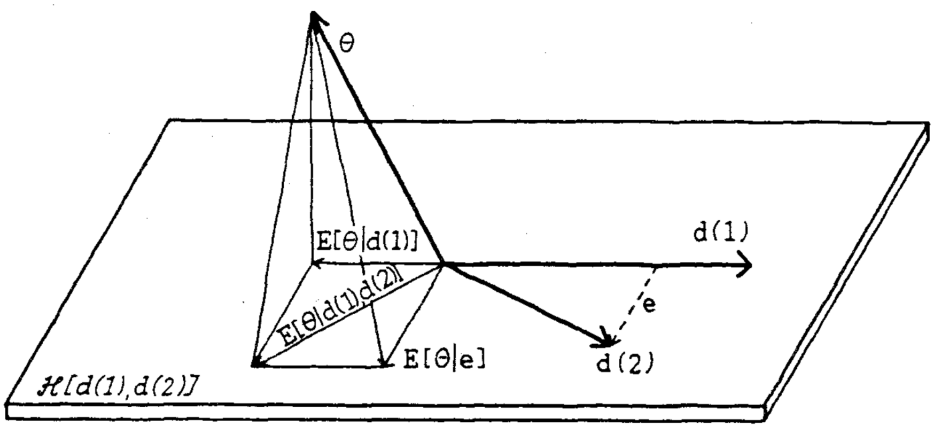

(From [1])

A.3.2 One-step Kalman Predictor

In the one-step state prediction problem at time $N+1$, the data consists of the observations of the output y from instant $t_0 = 1$ to instant N s.t.:

$$y^N = [y(N)^T\, y(N-1)^T ...\, y(1)^T]^T$$

In the vector space $\mathbb{H}$ of the aleatory variables, the components of y^N generate a subspace $\mathbb{H}[y^N] = \text{span}\{y^N\}$ called *subspace of the past.*
The innovation of $y(N+1)$ with respect to y^N is defined as:

$$e(N+1) = y(N+1) - \mathbb{E}[y(N+1) \mid y^N]$$

with $\dim e(N+1) = p$.
Since $\mathbb{E}[y(N+1) \mid y^N]$ is the projection of $y(N+1)$ on $\mathbb{H}[y^N]$, the innovation is orthogonal to the subspace $\mathbb{H}[y^N]$. We say that the innovation is *orthogonal to the past.*

Definition 2. *(**State prediction error**) We call state prediction error the quantity:*

$$\begin{aligned}\nu(N+1) &= x(N+1) - \mathbb{E}[x(N+1) \mid y^N] = \\ &= x(N+1) - \hat{x}(N+1 \mid N)\end{aligned}$$

We have that $\dim \nu(N+1) = n$ and the state predictor error is orthogonal to the past.

The *optimum one-step prediction of the output* is given by:

$$\hat{y}(N+1 \mid N) = \mathbb{E}[y(N+1) \mid y^N]$$

and using the state-space equation of the ouput we get:

$$\begin{aligned}\hat{y}(N+1 \mid N) &= \mathbb{E}[H\,x(N+1) + v(N+1) \mid y^N] = \\ &= H\,\mathbb{E}[x(N+1) \mid y^N] + \mathbb{E}[v(N+1) \mid y^N] = \\ &= H\,\mathbb{E}[x(N+1) \mid y^N]\end{aligned}$$

since from state-space equations $y^N = f(w^{N-1}, x(1), v^N)$ and since v^N is independent of $v(N+1)$ because $v(t)$ is a white noise, we have that $v(N+1)$ is independent of y^N and so $\mathbb{E}[v(N+1) \mid y^N] = \mathbb{E}[v(N+1)] = 0$.

Proposition 2. *The **recursive expression of state prediction** is given by:*

$$\hat{x}(N+1 \mid N) = F\,\hat{x}(N \mid N-1) + K(N)\,e(N)$$

with:

$$K(N) = [F\,P(N)\,H^T]\,[H\,P(N)\,H^T + R]^{-1}$$

and

$$P(N) = \mathbb{E}[\,\nu(N)\,\nu(N)]^T] = Var[\nu(N)]$$

Proof.

$$\begin{aligned}\hat{x}(N+1 \mid N) &= \mathbb{E}[x(N+1) \mid y^N] = \\ &= \mathbb{E}[x(N+1) \mid y^{N-1}, y(N)] = \\ &= \mathbb{E}[x(N+1) \mid y^{N-1}] + \mathbb{E}[x(N+1) \mid e(N)]\end{aligned}$$

with $e(N)$ innovation of $y(N)$ with respect to y^{N-1}.

1. $\mathbb{E}[x(N+1) \mid y^{N-1}] = \mathbb{E}[F\,x(N) + w(N) \mid y^{N-1}] =$
   $= F\,\mathbb{E}[x(N) \mid y^{N-1}] + \mathbb{E}[w(N) \mid y^{N-1}] = F\,\mathbb{E}[x(N) \mid y^{N-1}] = F\,\hat{x}(N \mid N-1)$

2. $\mathbb{E}[x(N+1) \mid e(N)] = \Lambda_{x(N+1)\,e(N)}\,\Lambda^{-1}_{e(N)\,e(N)}\,e(N)$

- Calculation of the covariance matrix $\Lambda_{x(N+1)\,e(N)}$:

$$\begin{aligned}
\Lambda_{x(N+1)\,e(N)} &= \mathbb{E}[x(N+1)\,e(N)^T] = \\
&= \mathbb{E}[x(N+1)\,[y(N) - \hat{y}(N \mid N-1)]^T] = \\
&= \mathbb{E}[x(N+1)\,[H\,(x(N) - \hat{x}(N \mid N-1)) + v(N)]^T] = \\
&= \mathbb{E}[\,[F\,x(N) + w(N)]\,[H\,(x(N) - \hat{x}(N \mid N-1)) + v(N)]^T] = \\
&= F\,\mathbb{E}[\,x(N)\,[(x(N) - \hat{x}(N \mid N-1))]^T]\,H^T + F\,\mathbb{E}[\,x(N)\,v(N)^T] + \\
&\quad + \mathbb{E}[w(N)\,[H\,(x(N) - \hat{x}(N \mid N-1)) + v(N)]^T]
\end{aligned}$$

$x(N)$ and $v(N)$ are independent since $v(t)$ is independent of $w(t)$ and initial data. Therefore the expected value of their product is equal to the product of the expected values and it is null since $v(N)$ is a white noise, thus $F\,\mathbb{E}[\,x(N)\,v(N)^T] = 0$. Morover, the third term of the last equation is:

$$\begin{aligned}
&\mathbb{E}[w(N)\,[H\,(x(N) - \hat{x}(N \mid N-1)) + v(N)]^T] = \\
&\mathbb{E}[w(N)\,x(N)^T]\,H^T - \mathbb{E}[w(N)\,\hat{x}(N \mid N-1)^T]\,H^T + \mathbb{E}[w(N)\,v(N)^T] = 0
\end{aligned}$$

for the properties of the white noises w and v.
Thus:

$$\begin{aligned}
\Lambda_{x(N+1)\,e(N)} &= F\,\mathbb{E}[\,x(N)\,[(x(N) - \hat{x}(N \mid N-1))]^T]\,H^T + F\,\mathbb{E}[\,x(N)\,v(N)^T] + \\
&\quad + \mathbb{E}[w(N)\,[H\,(x(N) - \hat{x}(N \mid N-1)) + v(N)]^T] = \\
&= F\,\mathbb{E}[\,x(N)\,[(x(N) - \hat{x}(N \mid N-1))]^T]\,H^T = \\
&= F\,\mathbb{E}[\,[x(N) - \hat{x}(N \mid N-1)]\,[(x(N) - \hat{x}(N \mid N-1))]^T]\,H^T + \\
&\quad + F\,\mathbb{E}[\,\hat{x}(N \mid N-1)\,[(x(N) - \hat{x}(N \mid N-1))]^T]\,H^T = \\
&= F\,\mathbb{E}[\,\nu(N)\,\nu(N)]^T]\,H^T + F\,\mathbb{E}[\,\hat{x}(N \mid N-1)\,\nu(N)^T]\,H^T
\end{aligned}$$

Now, since the state predictor error is orthogonal to the past $\nu(N)$ is orthogonal to $\mathbb{H}[y^{N-1}] = \text{span}\{y^{N-1}\}$. $\nu(N)$ is thus orthogonal to $\hat{x}(N \mid N-1)$ since the predictor $\hat{x}(N \mid N-1) \in \mathbb{H}[y^{N-1}]$ is based to data of the past until $N-1$ and so we have $\mathbb{E}[\,\hat{x}(N \mid N-1)\,\nu(N)^T] = 0$. Finally, calling $P(N) = \mathbb{E}[\,\nu(N)\,\nu(N)]^T] = Var[\nu(N)]$ the variance matrix of the state predictor error, we obtain:

$$\Lambda_{x(N+1)\,e(N)} = F\,P(N)\,H^T$$

- Calculation of the variance matrix of the innovation $\Lambda_{e(N)\,e(N)}$:

$$\begin{aligned}
\Lambda_{e(N)\,e(N)} &= \mathbb{E}[\,e(N)\,e(N)^T] = \\
&= H\,\mathbb{E}[\,\nu(N)\,\nu(N)^T]\,H^T + R + H\,\mathbb{E}[\,\nu(N)\,v(N)^T] + \mathbb{E}[\,v(N)\,\nu(N)^T]\,H^T
\end{aligned}$$

directly from the definitions of e and ν. With a similar calculation as for $\Lambda_{x(N+1)\,e(N)}$ we can proove that the last two terms of the equation are null so we obtain:

$$\Lambda_{e(N)\,e(N)} = H\,P(N)\,H^T + R$$

The recursive expression of state prediction is then:

$$\begin{aligned}\hat{x}(N+1 \mid N) &= \mathbb{E}\left[x(N+1) \mid y^{N-1}\right] + \mathbb{E}\left[x(N+1) \mid e(N)\right] = \\ &= F\,\hat{x}(N \mid N-1) + \Lambda_{x(N+1)\,e(N)}\,\Lambda^{-1}_{e(N)\,e(N)}\,e(N) = \\ &= F\,\hat{x}(N \mid N-1) + \left[F\,P(N)\,H^T\right]\left[H\,P(N)\,H^T + R\right]^{-1} e(N)\end{aligned}$$

Therefore, defining[3]:

$$K(N) = \left[F\,P(N)\,H^T\right]\left[H\,P(N)\,H^T + R\right]^{-1}$$

we get:

$$\hat{x}(N+1 \mid N) = F\,\hat{x}(N \mid N-1) + K(N)\,e(N)$$

□

A.3.2.1 Riccati Equation

There is a recursive way to calculate the variance matrix of the state predictor error $P(N) \in \mathbb{R}^{n \times n}$. Since:

$$\begin{aligned}\nu(N+1) &= x(N+1) - \mathbb{E}\left[x(N+1) \mid y^N\right] = \\ &= F\,x(N) + w(N) - F\,\hat{x}(N \mid N-1) - K(N)\,e(N) = \\ &= F\,\nu(N) + w(N) - K(N)\,e(N) = \\ &= F\,\nu(N) + w(N) - K(N)\left(H\left(x(N) - \hat{x}(N \mid N-1)\right) + v(N)\right) = \\ &= \left[F - K(N)\,H\right]\nu(N) + w(N) - K(N)\,v(N)\end{aligned}$$

we can compute:

$$\begin{aligned}P(N+1) &= Var\left[\nu(N+1)\right] = \mathbb{E}\left[\,\nu(N+1)\,\nu(N+1)\right]^T] = \\ &= \mathbb{E}\left[\,\left[F - K(N)\,H\right]\nu(N)\,\nu(N)^T\left[F - K(N)\,H\right]^T\right] + \\ &+ \mathbb{E}\left[\,w(N)\,w(N)^T\right] + \\ &+ \mathbb{E}\left[\,K(N)\,v(N)\,v(N)^T\,K(N)^T\right] + \\ &+ \mathbb{E}\left[\,\left[F - K(N)\,H\right]\nu(N)\,w(N)^T\right] - \\ &- \mathbb{E}\left[\,\left[F - K(N)\,H\right]\nu(N)\,v(N)^T\,K(N)^T\right] - \\ &- \mathbb{E}\left[\,w\,v(N)^T\,K(N)^T\right] + \\ &+ \mathbb{E}\left[\,w\,\nu(N)^T\left[F - K(N)\,H\right]^T\right] - \\ &- \mathbb{E}\left[\,K(N)\,v(N)\,\nu(N)^T\left[F - K(N)\,H\right]^T\right]\end{aligned}$$

We can proove that the last five addenda of the last equation are null, therefore:

$$\begin{aligned}P(N+1) &= \mathbb{E}\left[\,\left[F - K(N)\,H\right]\nu(N)\,\nu(N)^T\left[F - K(N)\,H\right]^T\right] + \\ &+ \mathbb{E}\left[\,w(N)\,w(N)^T\right] + \\ &+ \mathbb{E}\left[\,K(N)\,v(N)\,v(N)^T\,K(N)^T\right] = \\ &= \left[F - K(N)\,H\right]P(N)\left[F - K(N)\,H\right]^T + Q + K(N)\,R\,K(N)^T\end{aligned}$$

[3] $K(N)$ is well defined because $H\,P(N)\,H^T + R$ is symmetric and positive definite and so invertible, since $H\,P(N)\,H^T$ is symmetric and positive semi-definite and R is symmetric and assumed positive definite.

And since:

$$\begin{aligned}&[F - K(N)\,H]\,P(N)\,[F - K(N)\,H]^T + Q + K(N)\,R\,K(N)^T = \\ &= \; F\,P(N)\,F^T - K(N)\,H\,P(N)\,F^T - F\,P(N)\,H^T\,K(N)^T + \\ &+ \; K(N)\,H\,P(N)\,H^T K(N)^T + Q + K(N)\,R\,K(N)^T\end{aligned}$$

Morover, if we sum together the fourth and the sixth addenda and then we collect $K(N)$ both left and right, we obtain:

$$K(N)\,H\,P(N)\,H^T\,K(N)^T + K(N)\,R\,K(N)^T = K(N)\,[H\,P(N)\,H^T + R]\,K(N)^T$$

and using the definition of $K(N)$ on the first $K(N)$ of the last equation:

$$K(N) = [F\,P(N)\,H^T]\,[H\,P(N)\,H^T + R]^{-1}$$

we get:

$$K(N)\,[H\,P(N)\,H^T + R]\,K(N)^T = F\,P(N)\,H^T\,K(N)^T$$

and so the sum of the fourth and the sixth addenda cancels out with the third addendum. We can finally derive four equivalent formulations of the recursive variance matrix of the state predictor error:

$$\begin{aligned}P(N+1) &= F\,P(N)\,F^T - K(N)\,H\,P(N)\,F^T + Q = \\ &= F\,P(N)\,F^T - [F\,P(N)\,H^T]\,[H\,P(N)\,H^T + R]^{-1}\,H\,P(N)\,F^T + Q = \\ &= F\,P(N)\,F^T - K(N)\,[H\,P(N)\,H^T + R]\,K(N)^T + Q\end{aligned}$$

By means of this matrix equation, called the *Riccati Equation*[4], the variance matrix of the state prediction error can be updated. This matrix $P(N+1)$ is symmetric and positive semi-definite if the equation is initialized with a symmetric and positive semi-definite matrix.

Initialization: With the hypothesis that $t_0 = 1$ and using the multivariate *posterior variance* of the Bayes estimator, if we call $\theta = x(2)$, $\hat{\theta} = \hat{x}(2 \mid 1)$ and $d = y(1)$ we obtain:

$$\begin{aligned}P(2) &= Var\,[x(2) - \hat{x}(2 \mid 1)] = Var\,[\nu(2)] = \\ &= \mathbb{E}\,[\,[x(2) - \hat{x}(2 \mid 1)]\,[x(2) - \hat{x}(2 \mid 1)]^T] = \\ &= \Lambda_{x(2)\,x(2)} - \Lambda_{x(2)\,y(1)}\,\Lambda^{-1}_{y(1)\,y(1)}\,\Lambda_{y(1)\,x(2)}\end{aligned}$$

If we define $P_1 = Var\,[x(1)]$ the variance matrix of the initial state, we obtain of course a symmetric and positive semi-definite initializing matrix, so from:

$$\begin{cases}\Lambda_{x(2)\,x(2)} &= \mathbb{E}\,[\,[F\,x(1) + w(1)]\,[F\,x(1) + w(1)]^T] = F\,P_1\,F^T + Q \\ \Lambda_{x(2)\,y(1)} &= F\,P_1\,H^T \\ \Lambda_{y(1)\,y(1)} &= H\,P_1\,H^T + R \\ \Lambda_{y(1)\,x(2)} &= H\,P_1\,F^T\end{cases}$$

we obtain:

$$P(2) = F\,P_1\,F^T + Q - F\,P_1\,H^T\,[H\,P_1\,H^T + R]^{-1}\,H\,P_1\,F^T$$

In conclusion the initialisation can be put at the at time 1 if we impose $P(1) = P_1$. This result can be interpreted by holding that at instant 1, when you do not have past output

[4]It will often be called with the acronym DRE (Difference Riccati Equation).

measurements, the optimum prediction of the state $\hat{x}(1 \mid 0)$ coincides with the expected value of the variable $x(1)$, which is null. In the absence of information, the most reasonable prediction is the expected value, consequently the state prediction error $\nu(1)$ coincides with $x(1)$ whose variance is precisely P_1.
Concerning the initialization of the recursive expression of state prediction we have that :

$$\begin{aligned}\hat{x}(2 \mid 1) = \mathbb{E}\left[x(2) \mid y(1)\right] = \Lambda_{x(2)y(1)}\, \Lambda^{-1}_{y(1)y(1)}\, y(1) = \\ = F\, P_1\, H^T \left[H\, P_1\, H^T\right]^{-1} y(1)\end{aligned}$$

since $e(1) = y(1)$. In conclusion the initialisation can be put at time 1 if we impose $\hat{x}(1 \mid 0) = 0$ [5].

It is shown below the block diagram of the optimum one-step Kalman predictor:

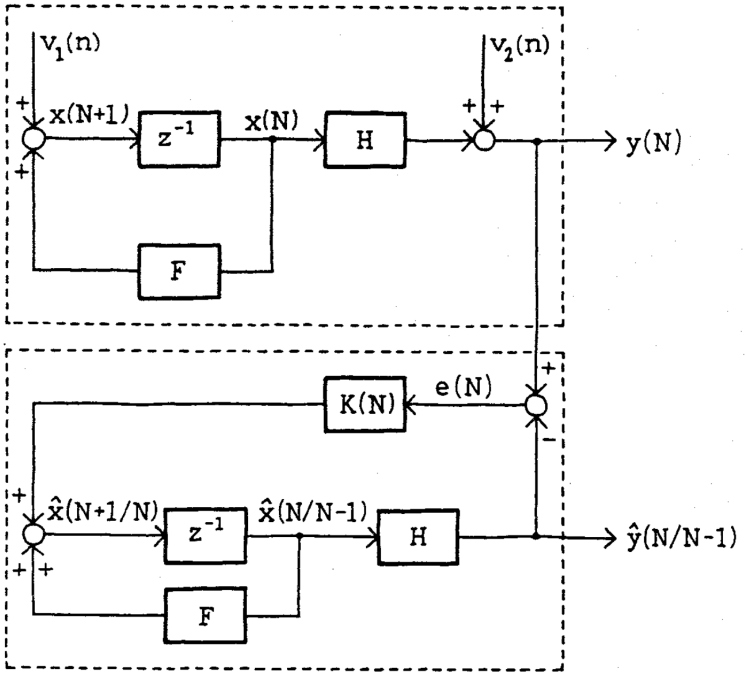

In this block diagram $v_1(n) = w(n)$ and $v_2(n) = v(n)$, (From [1])

A.3.2.2 Time-varying systems with exogenous input

We can generalize the previous theory to time-varying linear systems with *exogenous*[6] input $u(t)$ and with correlated disturbances between state and output. We consider the following discrete dynamical system:

$$\begin{cases} x(t+1) & = F(t)\, x(t) + G(t)\, u(t) + w(t) \\ y(t) & = H(t)\, x(t) + v(t) \quad , \qquad t \in \mathbb{Z} \end{cases}$$

[5] If the initial condition is $\mathbb{E}\left[x(1)\right] = x_1$ then $\hat{x}(1 \mid 0) = x_1$.
[6] i.e. a variable with a completely known trend

where, if $\delta(t)$ indicates the Kronecker delta and $V_{12} = Cov\,[w\,v]$, we obtain the following properties for $w(t)$ and $v(t)$:

$$\begin{aligned}
&\mathbb{E}\,[w(t)] = 0\ ,\ \forall\, t\\
&\mathbb{E}\,[v(t)] = 0\ ,\ \forall\, t\\
&\mathbb{E}\,[w(t_1)\,w^T(t_2)] = Q(t_1)\,\delta(t_2 - t_1)\\
&\mathbb{E}\,[v(t_1)\,v^T(t_2)] = R(t_1)\,\delta(t_2 - t_1)\\
&\mathbb{E}\,[w(t_1)\,v^T(t_2)] = V_{12}(t_1)\,\delta(t_2 - t_1)
\end{aligned}$$

with the hypothesis that $R(t) = Var\,[v(t)]$ is positive definite $\forall\, t \in \mathbb{Z}$. The initial condition $x(t_0) = x(1)$ is probablistically described as follows:

$$\begin{aligned}
&\mathbb{E}\,[x(1)] = x_1(t)\\
&\mathbb{E}\,[[x(1) - x_1(t)]\,[x(1) - x_1(t)]^T] = P_1
\end{aligned}$$

with the assumption that the disturbances and the initial condition are jointly Gaussian and uncorrelated, i.e.:

$$\mathbb{E}\,[v_i(t)\,[x(1) - x_1(t)]^T] = 0\ ,\ \forall\, i = 1, 2$$

In this case the equations for the Kalman one-step predictor are the following:

$$\begin{cases}
\hat{x}(N+1 \mid N) &= F(N)\,\hat{x}(N \mid N-1) + G(N)\,u(N) + K(N)\,e(N)\\
\hat{y}(N+1 \mid N) &= H(N)\,\hat{x}(N+1 \mid N)\\
e(N) &= y(N) - \hat{y}(N \mid N-1)
\end{cases}$$

where the Kalman gain is:

$$K(N) = [F(N)\,P(N)\,H(N)^T + V_{12}(N)]\,[H(N)\,P(N)\,H(N)^T + R(N)]^{-1}$$

and $P(N)$ solves the DRE:

$$P(N+1) = F(N)\,P(N)\,F(N)^T - K(N)\,[H(N)\,P(N)\,H(N)^T + R(N)]\,K(N)^T + Q(N)$$

The initializations are then:

$$\begin{aligned}
&\hat{x}(1 \mid 0) = x_1\\
&P(1) = P_1
\end{aligned}$$

A.3.3 Multi-step Kalman Predictor and Optimum Kalman Filter

Let's for first consider the following discrete LTI dynamical sistem:

$$\begin{cases}
x(t+1) &= F\,x(t) + w(t)\\
y(t) &= H\,x(t) + v(t)
\end{cases}\quad ,\qquad t \in \mathbb{Z}$$

where $w(t)$ and $v(t)$ are white noises eventually correlated, i.e.:

$$\mathbb{E}\,[v_i(t_1)\,v_j^T(t_2)] = V_{ij}\,\delta(t_2 - t_1) \qquad i, j = 1, 2$$

The multi-step predictor of the state in $k > 1$ steps, with $k \in \mathbb{Z}$, has the task of estimating the aleatory variable $x(N+k)$ from the data up to N, that is from the observation of $y(N), y(N-1), ...$ The optimal predictor $\hat{x}(N+k \mid N)$ will be given by:

$$\hat{x}(N+k \mid N) = \mathbb{E}\,[x(N+k) \mid y^N]$$

and since $x(N+k) = F\,x(N+k-1)+w(N+k-1)$ and since $w(N+k-1)$ is uncorrelated to y^N [7], we have that:

$$\hat{x}(N+k \mid N) = F\,\hat{x}(N+k-1 \mid N) = F^{k-1}\,\hat{x}(N+1 \mid N)$$

Furthermore, since $v(N+k)$ is uncorrelated to y^N the optimum k-step prediction of the output is:

$$\hat{y}(N+k \mid N) = H\,\hat{x}(N+k \mid N)$$

With regard to filtering, that is the problem of estimating $x(N)$ from the data $y(N), y(N-1), \ldots$, it is necessary to reset the calculation of the estimation:

$$\begin{aligned}\hat{x}(N \mid N) &= \mathbb{E}\left[x(N) \mid y^N\right] = \mathbb{E}\left[x(N) \mid y^{N-1}, y^N\right] = \\ &= \mathbb{E}\left[x(N) \mid y^{N-1}\right] + \mathbb{E}\left[x(N) \mid e(N)\right] = \\ &= \hat{x}(N \mid N-1) + \Lambda_{x(N)e(N)}\,\Lambda^{-1}_{e(N)e(N)}\,e(N)\end{aligned}$$

The variance matrix of the innovation $\Lambda_{e(N)e(N)}$ had already been calculated, while for the coviariance matrix $\Lambda_{x(N)e(N)}$ the calculation is similar to the one done for $\Lambda_{x(N+1)e(N)}$ and gives rise to:

$$\Lambda_{x(N)e(N)} = P(N)\,H^T$$

where, as usual, $P(N)$ is the variance matrix of the one-step prediction error of the state. Therefore:

$$\hat{x}(N \mid N) = \hat{x}(N \mid N-1) + K_0(N)\,e(N)$$

with $K_0(N)$ **Kalman filter gain** defined by:

$$K_0(N) = P(N)\,H^T\left[H\,P(N)\,H^T + R\right]^{-1}$$

Morover, if F is invertible and disturbances $w(t)$ and $v(t)$ are uncorrelated, we obtain that $\mathbb{E}\left[w(N) \mid y^N\right] = 0$ and so:

$$\begin{aligned}\hat{x}(N+1 \mid N) &= \mathbb{E}\left[F\,x(N) + w(N) \mid y^N\right] = \\ &= F\,\hat{x}(N \mid N) + \mathbb{E}\left[w(N) \mid y^N\right] = F\,\hat{x}(N \mid N)\end{aligned}$$

thus:

$$\hat{x}(N \mid N) = F^{-1}\,\hat{x}(N+1 \mid N)$$

Definition 3. *(**Variance matrix of filter error**) The variance matrix of filter error $x(N) - \hat{x}(N \mid N)$ is easily obtained from the variance matrix $P(N)$ of the prediction error. We have:*

$$Var\left[x(N) - \hat{x}(N \mid N)\right] = P(N) - P(N)\,H^T\left[H\,P(N)\,H^T + R\right]^{-1}H\,P(N)$$

We can hence give an alternative formulation of the DRE:

$$P(N+1) = F\,Var\left[x(N) - \hat{x}(N \mid N)\right]F^T + Q$$

[7] The vector of data y^N depends on $w(t)$ until $t = N-1$ and on $v(t)$ until $t = N$.

A.3.3.1 Asymptotic Predictor

On our previous LTI dynamical system we will suppose that the disturbances $w(t)$ and $v(t)$ are independent and their variance matrices are constant in time. We note that, despite the time invariance of the system, the predictor is time variant since the gain $K(N)$ is not constant as it depends on the solution of the Riccati equation. The prediction problem can be solved in a sub-optimal way, with an invariant predictor, whenever the following condition holds:

$$\lim_{N\to\infty} K(N) = \bar{K}$$

$\bar{K}$ is called *steady-state gain* and the corresponding predictor is called *asymptotic predictor*. Since:

$$K(N) = F\,P(N)\,H^T\,[H\,P(N)\,H^T + R]^{-1}$$

the convergence of $K(N)$ is ensured if the solution of the Riccati equation converges asymptotically, i.e.:

$$\lim_{N\to\infty} P(N) = \bar{P}$$

with positive semi-definite limit matrix $\bar{P}$ [8]. If we initialize the DRE with $\bar{P}$, the solution will be $\bar{P}$, indeed defining $P = P(N+1) = P(N)$ we obtain:

$$P = F\,P\,F^T - F\,P\,H^T\,[H\,P\,H^T + R]^{-1}\,H\,P\,F^T + Q$$

that is an algebraic equation called **Algebraic Riccati Equation** (ARE) with matrix unknown. $\bar{P}$ is the positive semi-defined solution of ARE from which we obtain the *steady-state predictor gain*[9]:

$$\bar{K} = F\,\bar{P}\,H^T\,[H\,\bar{P}\,H^T + R]^{-1}$$

Remember that the solution of the Riccati Equation is the variance matrix of the state prediction error. The convergence of this matrix indicates the predictor's ability to provide predictions of state variables with a limited probabilistic error.
Morover, since:

$$\begin{aligned}\hat{x}(N+1 \mid N) &= F\,\hat{x}(N \mid N-1) + \bar{K}\,e(N) = \\ &= F\,\hat{x}(N \mid N-1) + \bar{K}\,[y(N) - \hat{y}(N \mid N-1)] = \\ &= F\,\hat{x}(N \mid N-1) + \bar{K}\,[y(N) - H\,\hat{x}(N \mid N-1)] = \\ &= [F - \bar{K}\,H]\,\hat{x}(N \mid N-1) + \bar{K}\,y(N)\end{aligned}$$

the stability of the *asymptotic predictor* depends on the eigenvalues of the matrix:

$$[F - \bar{K}\,H] = F - F\,\bar{P}\,H^T\,[H\,\bar{P}\,H^T + R]^{-1}\,H$$

From the *Schur's condition* the *asymptotic predictor* is stable *iff* the eigenvalues are strictly inside the complex circle of radius 1.

A.3.3.2 Asymptotic stability

If we consider the solution of the state equation of the mechanism of generation of data

$$x(t+1) = F\,x(t) + w(t)$$

[8] The limit of a succession of positive semi-definite matrices is a positive semi-definite matrix.
[9] The *steady-state filter gain* is simply given by $K_\infty = F^{-1}\,\bar{K}$.

it is a sequence of aleatory variables, i.e. a *stochastic process*. If we apply the expected value operator we get:

$$\mathbb{E}\left[x(t+1)\right] = F\,\mathbb{E}\left[x(t)\right]$$

therefore:

$$\mathbb{E}\left[x(1)\right] = x_1 \;\rightarrow\; \mathbb{E}\left[x(2)\right] = F\,x_1 \;\rightarrow\; \mathbb{E}\left[x(3)\right] = F^2\,x_1 \;\rightarrow\; \mathbb{E}\left[x(4)\right] = F^3\,x_1 \;...$$

If the system is stable the eigenvalues of the powers of F become smaller and smaller as the exponent grows. F^k tends to zero with k. Therefore $\mathbb{E}\left[x(t)\right]$ also tends to zero $\forall\, x_1$. Morover if $F^k = \mathbb{O}_{n\times n}$ with finite $k \in \mathbb{Z}$ then F is a nilpotent matrix and the system of generation of data is a *dead-beat stochastic process*. Let's consider the variance matrix of $x(t)$:

$$\begin{aligned} Var\left[x(t+1)\right] &= \mathbb{E}\left[\left[x(t+1) - \mathbb{E}\left[x(t+1)\right]\right]\left[x(t+1) - \mathbb{E}\left[x(t+1)\right]^T\right]\right] = \\ &= \mathbb{E}\left[\left[F\left[x(t) - \mathbb{E}\left[x(t)\right]\right] + w\right]\left[F\left[x(t) - \mathbb{E}\left[x(t)\right]\right] + w\right]^T\right] = \\ &= F\,\mathbb{E}\left[\left[x(t) - \mathbb{E}\left[x(t)\right]\right]\left[x(t) - \mathbb{E}\left[x(t)\right]\right]^T\right]F^T + Q \end{aligned}$$

since $w(t)$ is uncorrelated to the past as it is a white noise. We obtain the so called **Difference Lyapunov Equation** (DLE):

$$\begin{aligned} &Var\left[x(t+1)\right] = F\,Var\left[x(t)\right]F^T + Q = \\ &= \;\Lambda(t+1) = F\,\Lambda(t)\,F^T + Q \end{aligned}$$

therefore:

$$Var\left[x(1)\right] = P_1 \;\rightarrow\; Var\left[x(2)\right] = F\,P_1\,F^T + Q \;\rightarrow\; Var\left[x(3)\right] = F^2\,P_1\,[F^T]^2 + F\,Q\,F^T + Q \;...$$

and finally:

$$Var\left[x(t)\right] = \left[\mathcal{I} + F^2 + ... + F^{2(t-2)}\right]Q + F^{2(t-1)}\,P_1$$

If F is stable then the matrix sum converges and so $Var\left[x(t)\right]\ \forall\ P_1$. Hence, if we define $\bar{\Lambda}$ the asymptotic limit solution of the DLE, it will be the positive semi-definite solution of:

$$\Lambda = F\,\Lambda\,F^T + Q$$

that is called the **Algebraic Lyapunov Equation** (ALE).
Summarizing, if the system is asymptotically stable, the data generation mechanism produces a stochastic process with expected value and variance matrix both convergent, i.e. produces asymptotically a *stationary stochastic process*. If we use the optimum predictor instead of the trivial one (based on the expected value estimation) the prediction error will be smaller and, for all the above considerations, it is therefore reasonable to expect that the prediction error cannot have, in such circumstances, divergent variance. We will now give some important results of stability theory for linear systems and optimal control.

Theorem 7. ***(First DRE convergence theorem)*** *If the data generation mechanism is stable, then:*

1. *the solution of the Riccati Equation converges asymptotically to the same limit matrix* $\bar{P}$, $\forall$ *positive semi-definite matrix* P_1
2. *the asymptotic predictor is stable*

The stability of the data generation mechanism is a *sufficient condition* for predictor convergence but it is not a *necessary condition.*
Let's now refresh some important results from *System Theory* (proofs can be found in [9]):

Definition 4. *(**Indistinguishable states in the future**) Given a discrete state space model:*

$$\begin{cases} x(t+1) &= F\,x(t) + G\,u(t) \\ y(t) &= H\,x(t) \end{cases} \quad , \qquad t \in \mathbb{Z}$$

with $x \in \mathbb{R}^n$, $u \in \mathbb{R}^m$ and $y \in \mathbb{R}^p$, we say that two states x_1 and x_2 are indistinguishable in $[0,k] = \{0,1,...,k\}$ $k \geq 0$ if $\forall\, u(0), u(1), ..., u(k-1) \in \mathbb{R}^m$, calling $y_1(t)$ and $y_2(t)$ the outputs of the system given the input and the initial conditions $x(0) = x_1$ and $x(0) = x_2$ we obtain $y_1(t) = y_2(t)$ $\forall\, t \in [0,k]$. Since:

$$\begin{cases} y_1(t) &= y_{1l}(t) + y_{1f}(t) \\ y_2(t) &= y_{2l}(t) + y_{2f}(t) \end{cases} \quad , \qquad t \in \mathbb{Z}$$

and the forced responses coincide $y_{1f}(t) \equiv y_{2f}(t)$ since the input is the same we obtain that x_1 is indistinguishable from x_2 iff the free evolutions coincide $y_{1l}(t) = y_{2l}(t)$ i.e.:

$$H\,F^t\,x_1 = H\,F^t\,x_2 \quad \forall\, t \in [0,k]$$

We will then write $x_1 \sim x_2$[10].

Definition 5. *(**Observability**) A state $x_0 \in \mathbb{R}^n$ is called not observable in $[0,k]$ if $x_0 \sim 0$, i.e. iff $y_l(t) = 0$ $\forall t \in [0,k]$. Formally:*

$$[H \mid H\,F \mid ... \mid H\,F^k]^T\,x_0 = \mathcal{O}_k\,x_0 = [0 \mid 0 \mid ... \mid 0]^T$$

where $\mathcal{O}_k = [H \mid H\,F \mid ... \mid H\,F^k]^T$ is the k-steps observability matrix. Thus x_0 is not observable in $[0,k]$ iff $x_0 \in \ker \mathcal{O}_k \subseteq \mathbb{R}^n$. If $x_0 \in \ker \mathcal{O}_{k+1}$ then $x_0 \in \ker \mathcal{O}_k$ so $\ker \mathcal{O}_{k+1} \subseteq \ker \mathcal{O}_k$, thus:

$$\{\underline{0}\} \subseteq ... \subseteq \ker \mathcal{O}_k \subseteq ... \subseteq \ker \mathcal{O}_2 \subseteq \ker \mathcal{O}_1 \subseteq \ker \mathcal{O}_0 \subseteq \mathbb{R}^n$$

Morover, if $\ker \mathcal{O}_k = \ker \mathcal{O}_{k+1}$ then $\ker \mathcal{O}_{k+1} = \ker \mathcal{O}_{k+2}$[11].

Theorem 8. *(**First criterium for observability**) Defining the **observability matrix** $\mathcal{O} = [H \mid H\,F \mid ... \mid H\,F^k]^T$, we say that (F,H) is observable iff $\ker \mathcal{O} = \{\underline{0}\}$ i.e. iff $rank\,\mathcal{O} = n$.*

Theorem 9. *(**Popov-Belevitch-Hautus criterium for observability**) Given $F \in \mathbb{R}^{n\times n}$, $H \in \mathbb{R}^{p\times n}$, we say that (F,H) is observable iff $rank\,[\lambda\mathcal{I} - F \mid H]^T = n$ $\forall\, \lambda \in \mathbb{C}$, where $[\lambda\mathcal{I} - F \mid H]^T \in \mathbb{R}^{(n+p)\times n}$ is the **PBH matrix of observability**. If (F,H) is not observable the PBH matrix loses rank in correspondence to all and only the eigenvalues of the not observable subsystem.*

Theorem 10. *If (F,H) is observable, then the ARE admits at least one positive semi-definite solution.*

This final theorem suggests that even in the hypothesis that the pair (F,H) is observable, it may happen that the ARE admits more positive semi-definite solutions. A simple way of imposing that the ARE admits a single solution is to require that the noise that disturbs the state actually affects all the state variables.

[10] It's easy to proove that $\sim$ is an equivalence relation.
[11] This result can be proved using the *Cayley-Hamilton theorem.*

Definition 6. *(**Square root of a matrix**) Given the state equation:*

$$x(t+1) = F\,x(t) + w(t)$$

*with $w \sim \mathcal{N}(0, Q)$ n-vector aleatory variable, it is possible to define the **square root of the matrix** Q as the matrix G s.t. $G\,G^T = G\,\mathcal{I}\,G^T = Q$. The system equation is now:*

$$x(t+1) = F\,x(t) + G\,u(t)$$

with the following properties:

- *such as $w(t)$ also $u(t)$ is a white noise i.e. $\mathbb{E}\left[u(t_1)\,u^T(t_2)\right] = 0$ iff $t_1 \neq t_2$*
- *$Var\left[u(t)\right] = \mathcal{I}\ ,\ \forall\, t.$*

In order to characterize the action of the noise state $w(t)$ let's consider the equation of state in the convenient form:

$$x(t+1) = F\,x(t) + G\,u(t)$$

Making the assumption that the initial state at time $t_0 = 1$ is deterministically known and, for example, null:

$$x(1) = 0$$

then:

$$x(2) = G\,u(1)$$

By indicating with $u_1(t), u_2(t), ..., u_m(t)$ the elements of the vector $u(t)$ and by $g^1, g^2, ..., g^m$ the columns of G, we obtain:

$$x(2) = \sum_{i=1}^{m} u_i(1)\,g^i$$

The state $x(2)$ is therefore a linear combination of the columns of the matrix G. The coefficients of this combination are the elements of the aleatory vector $u(t)$. As evidenced by the variance matrix (the identity) of $u(t)$ these elements are uncorrelated aleatory variables with not null variance. Considering all possible values they can assume, $x(2)$ can describe all possible linear combinations of G-columns. We can thus conclude that noise at time 1 affects all states belonging to the set $[G]$. At time 3 we have that:

$$x(3) = F\,G\,u(1) + G\,u(2)$$

Taking into account that $u(t)$ is a white noise, $u(1)$ and $u(2)$ are uncorrelated. We can conclude saying that noise at times 1 and 2 affects only all states that can be obtained as linear combinations of the G-columns and FG-columns, i.e. all states belonging to the set $[G \mid F\,G]$. Iterating this reasoning, we can conclude that noise at instants $1, ..., k$ has influence on the set $[G \mid F\,G \mid ... \mid F^{k-1}\,G]$. We can proove that this set is a subset of the state space. Let's introduce the concept of reachability:

Definition 7. *(**Reachability**) Given a discrete state space model:*

$$\begin{cases} x(t+1) &= F\,x(t) + G\,u(t) \\ y(t) &= H\,x(t) \end{cases}, \qquad t \in \mathbb{Z}$$

with $x \in \mathbb{R}^n$, $u \in \mathbb{R}^m$ generic input vector and $y \in \mathbb{R}^p$, we say that a state x is reachable at time k if $\exists\, u(0), ..., u(k-1) \in \mathbb{R}^m$ that brings the state from $x(0) = 0$ to $x(k) = x_f$ i.e.

$$\begin{aligned} x_f = x(k) &= F^k\, x(0) + \sum_{t=0}^{k-1} F^{k-1-t}\, G\, u(t) = \sum_{t=0}^{k-1} F^{k-1-t}\, G\, u(t) = \\ &= [G \mid F\, G \mid ... \mid F^{k-1}\, G]\ [u(k-1)\ u(k-2)\ ...\ u(0)]^T = \\ &= \mathcal{R}_k\ [u(k-1)\ u(k-2)\ ...\ u(0)]^T \end{aligned}$$

where $\mathcal{R}_k = [G \mid F\, G \mid ... \mid F^{k-1}\, G]$ is the k-steps reachability matrix. Thus x is reachable at time k if $x \in Im\,\mathcal{R}_k$.

Theorem 11. *(**First criterium for reachability**) Since $Im\,\mathcal{R}_k \subseteq \mathbb{R}^n$ and $Im\,\mathcal{R}_k \subseteq Im\,\mathcal{R}_{k+1}$, and since:*

1. *if $Im\,\mathcal{R}_k = Im\,\mathcal{R}_{k+1}$ then $Im\,\mathcal{R}_k = Im\,\mathcal{R}_{k+t}\ \forall t \geq 0$*
2. *$\bar{k} = \min_k\{Im\,\mathcal{R}_k = Im\,\mathcal{R}_{k+1}\} \leq n$*

*then, defining the **reachability matrix** $\mathcal{R} = [G \mid F\, G \mid ... \mid F^{n-1}\, G]$, we say that (F, G) is reachable iff $rank\,\mathcal{R} = n$.*

Theorem 12. *(**Popov-Belevitch-Hautus criterium for reachability**) Given $F \in \mathbb{R}^{n\times n}$, $G \in \mathbb{R}^{n\times m}$, we say that (F, G) is reachable iff $rank\,[\lambda\,\mathcal{I} - F \mid G] = n\ \ \forall\, \lambda \in \mathbb{C}$, where $[\lambda\,\mathcal{I} - F \mid G] \in \mathbb{R}^{n\times(n+m)}$ is the **PBH matrix of reachability**. If (F, G) is not reachable the PBH matrix loses rank in correspondence to all and only the eigenvalues of the not reachable subsystem.*

If $\lambda \in \mathbb{C} \wedge \lambda \notin \Theta(F)$ then $\det\,[\lambda\,\mathcal{I} - F] \neq 0$ and so $\text{rank}\,[\lambda\,\mathcal{I} - F \mid G] = n$ since the first n columns of $[\lambda\,\mathcal{I} - F \mid G]$ are linearly independent, therefore the **PBH matrix** can loose rank only if $\lambda \in \mathbb{C} \wedge \lambda \in \Theta(F)$, where $\Theta(F)$ is the spectrum of F.

Corollary 1. *Necessary condition to get (F, G) reachable is that the inputs are linearly independent, i.e. $m \geq \boldsymbol{c}$ where $\boldsymbol{c} = \max_{i\in\{1,...,r\}} m_g(\lambda_i)$ is called **cyclicity index** of F, m is the number of columns of G, r is the number of different eigenvalues of F and $m_g(\lambda_i)$ is the geometrical molteplicity of the eigenvalue λ_i.*

In the case of feedback systems we have the following:

Proposition 3. *Given $F \in \mathbb{R}^{n\times n}$ and $G \in \mathbb{R}^{n\times m}$ then $\forall\, K \in \mathbb{R}^{m\times n}$ and $\forall\, i \in \mathbb{Z},\ i \geq 0$ we have that:*

$$Im\,[G \mid F\, G \mid ... \mid F^{i-1}\, G] = Im\,[G \mid (F + G\, K)\, G \mid ... \mid (F + G\, K)^{i-1}\, G]$$

Hence if $i = n$ we have that (F, G) is reachable iff $(F + G\, K, G)$ is reachable.

It is not difficult to prove that a pair (F, G) is reachable *iff* the pair (F, GG^T) is reachable. For this reason, in the context of the prediction or filtration problem, the hypothesis (F, G) reachable is also found in the literature in the equivalent statement (F, Q) reachable.

Theorem 13. *(**Second DRE convergence theorem**) If the data generation mechanism is such that the pair (F, H) is observable and, for a square root matrix G of the disturbance variance matrix Q influencing the state, the pair (F, G) is reachable, then:*

1. *the solution of the Riccati equation converges asymptotically to the same limit matrix $\bar{P}$, $\forall$ positive semi-definite initial condition $P(1)$*

2. *the limit matrix* $\bar{P}$ *is positive definite*
3. *the asymptotic predictor is stable*

Note that the reachability mentioned in the previous theorem is the reachability of the state from noise. Thus, if the equation of state is:

$$x(t+1) = F\,x(t) + B\,w(t) + G\,u(t)$$

where $w(t)$ is an exogenous variable, the recheability of the pair (F, B) has no influence on the problem of convergence of the Riccati equation. There exists a weacker formulation of the problem that uses the concepts of *stabilizability* and *detectability* instead of *reachability*[12] and *observability*. Since not all systems are reachable $\operatorname{Im}\mathcal{R} \subseteq \mathbb{R}^n$ we can decompose the state space $\mathbb{R}^n$ into two orthogonal subspaces:

$$\mathbb{R}^n = \operatorname{Im}\mathcal{R} \oplus \left(\operatorname{Im}\mathcal{R}\right)^{\perp}$$

where $\left(\operatorname{Im}\mathcal{R}\right)^{\perp}$ is the *not reachable subspace*.

Theorem 14. *(**Hautus Lemma for stabilizability**) Given* $F \in \mathbb{R}^{n\times n}$, $G \in \mathbb{R}^{n\times m}$ *the following assertions for a discrete LTI system are equivalent:*

1. *the pair* (F, G) *is stabilizable iff* $\exists\, K \in \mathbb{R}^{m\times n}$ *s.t.* $F + G\,K$ *is asymptotically stable*
2. *the pair* (F, G) *is reachable or otherwise, the matrix of the not reachable subsystem is asymptotically stable*
3. $rank[\lambda\,\mathcal{I} - F \mid G] = n\ ,\ \forall\,\lambda \in \mathbb{C}$ *s.t.* $|\lambda| \geq 1$.

Dually, we can derive similar considerations for the concepts of *detectability* and *observability*:

Theorem 15. *(**Hautus Lemma for detectability**) Given* $F \in \mathbb{R}^{n\times n}$, $H \in \mathbb{R}^{p\times n}$ *the following assertions for a discrete LTI system are equivalent:*

1. *the pair* (F, H) *is detectable iff* $\exists\, L \in \mathbb{R}^{n\times p}$ *s.t.* $F + L\,H$ *is asymptotically stable*
2. *the pair* (F, H) *is observable or otherwise, the matrix of the not observable subsystem is asymptotically stable*
3. $rank[\lambda\,\mathcal{I} - F \mid H]^T = n\ ,\ \forall\,\lambda \in \mathbb{C}$ *s.t.* $|\lambda| \geq 1$.

Theorem 16. *(**General DRE convergence theorem**) Let's take the following discrete LTI dynamical system:*

$$\begin{cases} x(t+1) & = F\,x(t) + w(t) \\ y(t) & = H\,x(t) + v(t) \end{cases} \quad , \qquad t \in \mathbb{Z}$$

with white noises $w \sim \mathcal{N}(0, Q)$ *and* $v \sim \mathcal{N}(0, R)$ *uncorrelated and with positive definite variance matrix* R *s.t.* $\det R \neq 0$[13]. *If the data generation mechanism is such that the pair* (F, H) *is detectable and, for a square root matrix* G *of the disturbance variance matrix* Q *influencing the state, the pair* (F, G) *is stabilizable, then:*

[12] Reachability implies *controllability*.

[13] If $\det R = 0$ we obtain a *singular case* in wich it is necessary to introduce pseudo-inverse matrices to solve both DRE and ARE.

1. *the solution of the Riccati equation converges asymptotically to the same limit matrix* $\bar{P}$, $\forall$ *positive semi-definite initial condition* $P(1)$
2. *the asymptotic predictor is stable*

When the two noises are correlated the convergence theorem no longer holds. Intuitively, this can be understood by observing that if $V_{12} \neq 0$ then it is possible to obtain information on the state of the system starting from the observation of the output even in the case of $H = \underline{0}$ i.e. even if the system is totally unobservable.
The estimation error variance matrix $Var\left[x(t) - \hat{x}(t \mid t)\right]$ converges *iff* the prediction error variance matrix $P(t) = Var\left[x(t) - \hat{x}(t \mid t-1)\right]$ converges.

Bibliography

[1] Sergio Bittanti. *Teoria della Predizione e del Filtraggio*. Pitagora Editrice, 2006.

[2] Francesco Carpanese. Development of free-boundary equilibrium and transport solvers for simulation and real-time interpretation of tokamak experiments. Technical report, EPFL, 2021.

[3] Federico Felici. Real-time control of tokamak plasmas: from control of physics to physics-based control. Technical report, EPFL, 2011.

[4] Federico Felici. Magnetic modeling and control of tokamaks - modeling pf coils and vacuum vessel, 2020.

[5] Federico Felici. Magnetic modeling and control of tokamaks - plasma current control and magnetic measurements, 2020.

[6] Federico Felici. Magnetic modeling and control of tokamaks - plasma position stability and control, 2020.

[7] Federico Felici, Marco De Baar, and Maarten Steinbuch. A dynamic state observer for real-time reconstruction of the tokamak plasma profile state and disturbances. In *2014 American Control Conference*, pages 4816–4823. IEEE, 2014.

[8] Federico Felici, Stefano Marchioni, and Francesco Carpanese. Rzip and fge linearisation. SPC, 2020.

[9] Ettore Fornasini and Giovanni Marchesini. *Appunti di Teoria dei Sistemi*. Libreria progetto, 2011.

[10] Martin Haugh. Mcmc and bayesian modeling. *IEOR E4703 Monte-Carlo Simulation, Columbia University*, 2017.

[11] F Hofmann, JB Lister, W Anton, S Barry, R Behn, S Bernel, G Besson, F Buhlmann, R Chavan, M Corboz, et al. Creation and control of variably shaped plasmas in tcv. *Plasma Physics and Controlled Fusion*, 36(12B):B277, 1994.

[12] Ferdinand Hofmann. Fbt-a free-boundary tokamak equilibrium code for highly elongated and shaped plasmas. *Computer Physics Communications*, 48(2):207–221, 1988.

[13] Thomas Kailath, Ali H Sayed, and Babak Hassibi. *Linear Estimation*. Number BOOK. Prentice Hall, 2000.

[14] Kyril Kaufmann. Design of a kalman filter for tokamak equilibrium state estimation. Technical report, EPFL, 2021.

[15] Inc.. Mathworks. Chi-square inverse cumulative distribution function. `https://ch.mathworks.com/help/stats/chi2inv.html`.

[16] Inc.. Mathworks. *Control System Toolbox: For Use with MATLAB: Computation Visualization Programming*. MathWorks, 2000.

[17] Antoine Merle. Session 5a - mhd equilibrium in control, 2020.

[18] J-M Moret, F Buhlmann, D Fasel, F Hofmann, and G Tonetti. Magnetic measurements on the tcv tokamak. *Review of scientific instruments*, 69(6):2333–2348, 1998.

[19] J-M Moret, BP Duval, HB Le, S Coda, F Felici, and H Reimerdes. Tokamak equilibrium reconstruction code liuqe and its real time implementation. *Fusion Engineering and Design*, 91:1–15, 2015.

[20] Giorgio Picci. *Filtraggio statistico (Wiener, Levison, Kalman) e applicazioni*. Libreria Progetto, 2007.

[21] O Sauter and S Yu Medvedev. Tokamak coordinate conventions: Cocos. *Computer Physics Communications*, 184(2):293–302, 2013.

[22] Dan Simon. *Optimal State Estimation: Kalman, H infinity, and nonlinear approaches*. John Wiley & Sons, 2006.

[23] EPFL SPC. Vertical control in mgams. `https://spcwiki.epfl.ch/wiki/Vertical_control_in_MGAMS`.

[24] Robert Tye. Improvement of diamagnetic measurement on the tcv. Technical report, 2006.

[25] ML Walker and DA Humphreys. Valid coordinate systems for linearized plasma shape response models in tokamaks. *Fusion Science and Technology*, 50(4):473–489, 2006.